European Commission

radiation protection 106

Technical recommendations
on
measurements of
external environmental gamma radiation doses

A report of EURADOS Working Group 12

"Environmental radiation monitoring"

Edited by

I.M.G. Thompson, L. Bøtter-Jensen, S. Deme

F. Pernicka, and J.C. Sáez-Vergara.

EURADOS report 1999

A great deal of additional information on the European Union is available on the Internet.
It can be accessed through the Europa server (http://europa.eu.int).

Cataloguing data can be found at the end of this publication.

Luxembourg: Office for Official Publications of the European Communities, 1999

ISBN 92-828-7811-2

Printed in Italy

PRINTED ON WHITE CHLORINE-FREE PAPER

PREFACE

The European Radiation Dosimetry Group (EURADOS), in co-operation with Directorates General XI and XII of the European Commission, decided in 1994 to establish a Working Group to be concerned with the measurement of external environmental gamma radiation doses.

EURADOS Working Group 12 to report on "The measurement of external environmental gamma radiation doses" was composed of eighteen scientists nominated by virtue of their involvement and expertise in this field of study and their knowledge of radiation measurements in the environment.

The primary reason for the establishment of the Working Group was to prepare recommendations on the calibration of instruments and passive dosemeters used for measurement of environmental doses and on the interpretation of monitoring data to ensure harmonisation of dose measurements within Europe.

EURADOS is an independent scientific society established in 1981 to stimulate and improve co-operation on radiation dosimetry research and related topics within the European Union. The joint publications, the recommendations made and protocols developed are based on the scientific expertise of its members and should therefore provide a good scientific basis for the harmonisation of standards and procedures within the European Union.

The joint work of EURADOS Working Group 12 was supported by the European Commission, in particular by the Radiation Protection Unit of Directorate General XI, Environment, Nuclear Safety and Civil Protection and the Nuclear Fission and Radiation Protection Unit of Directorate General XII, Science, Research and Development, as part of an action group within the Joint Concerted Action No. FI4P-CT-96-0061 of the three organisations EURADOS, European Late Effects Project Group, EULEP and the International Union of Radioecolgy, UIR.

Stephen Kaiser	Hans Forsström	Günther Dietze
Head of Unit Radiation Protection Directorate General XI	Head of Unit Nuclear Fission and Radiation Protection Directorate General XII	Chairman EURADOS

EURADOS Working Group 12 "Environmental Radiation Monitoring"

I. M. G. Thompson[1] (Chairman), L. Bøtter-Jensen[2], P. Bilski[3], B. Burgkhardt[4], J. David[5], A. Delgado[6], S. Deme[7], G. Klemic[8], U. Lauterbach[9], D. McClure[10], S. Neumaier[11],. Olko[12], M. Osvay [13], F. Pernicka[14], W. Pessara[15], J. Shobe[16], G. Strachotinski[17], J.C. Sàez-Vergara[18], and T. Williams[19].

(1) Farthings Cottage, Pinfarthings, Amberley, Stroud, Glos GL5 5JH, England.

(2) Risø National Laboratory, DK-4000, Roskilde, Denmark

(3) Institute of Nuclear Physics, Health Physics Laboratory, UL Radzikowskiego 153, Krakow, 31-342,Poland

(4) Forschungszentrum, Karlsruhe GmbH, Hauptabteilung,Postfach 3640, 76021 Karlsruhe, Germany

(5) GSF-Foschungszentrum fur Unwett und Gesundheit GmbH, Ingelstradter Landstrasse,1,D-85758 Oberschleissheim, Germany

(6) Radiation Dosimetry Unit, IMA, E-28040 Madrid, Spain

(7) Atomic Energy Research Institute, PO Box 49, H-1525, Budapest, Hungary

(8) Radiation Physics Division, US DOE, Environmental Measurements Laboratory, 376 Hudson Street, New York,NY 10014-3621, USA.

(9) Physikalisch Technische Bundesanstalt, PO Box 3345, D-38023 Braunschweig, Germany

(10) NRPB, Chilton, Didcot, Oxon, OX11 ORQ, England.

(11) Physikalisch Technische Bundesanstalt, PO Box 3345, D-38023 Braunschweig, Germany

(12) Institute of Nuclear Physics, Health Physics Laboratory, UL Radzikowskiego 152, Krakow, 31-342,Poland

(13) Institute of Isotopes, Hungarian Academy of Sciences, PO Box 77, H-1525, Hungary.

(14) Nuclear Physics Institute, Radiation Dosimetry Department, 180 86 Prague, Czech Republic.

(15) Physikalisch Technische Bundesanstalt, PO Box 3345, D-38023 Braunschweig, Germany

(16) Building 245/RoomC229, US Dept. of commerce, NIST, Gaithersburg, Maryland 20899, USA.

(17) Retired from:-Österreichesches Forschungszentrum Seibersdorf Gmbh, A-2444 Seibersdorf, Wien

(18) CIEMAT,Radiation Dosimetry Unit, IMA,,Av., Complutense 22,E-28040, Madrid, Spain.

(19) Building 62, Division of Radiation Science and Acoustics,National Physical Laboratory, Teddington, Middx Tw11 OLW, England

CONTENTS

		Page Nos.
1.	INTRODUCTION	1
2.	NATURE AND VARIABILITY OF NATURAL ENVIRONMENTAL RADIATION IN EUROPE	3
3.	MEASUREMENTS QUANTITIES	10
4.	DETECTOR CHARACTERISTICS	15
	4.1 Active Detectors	15
	4.1.1 General	15
	4.1.2 Geiger-Müller counters	15
	4.1.3 Ionisation chambers	18
	4.1.4 Scintillation detectors	21
	4.1.5 Proportional counters	24
	4.1.6 Electronic dosemeters	26
	4.1.7 Summary of active detectors	27
	4.2 Passive Detectors	28
	4.2.1 General	28
	4.2.2 Thermoluminescent detectors (TLD)	33
	4.2.2.1 Lithium fluoride	36
	4.2.2.2 Calcium fluoride	38
	4.2.2.3 Calcium sulphate	39
	4.2.2.4 Aluminium oxide	40
	4.2.3 Photoluminescent detectors (PLD)	41
	4.2.4 Optically stimulated luminescence detectors (OSLD)	42
5.	DETERMINATION OF PROPERTIES OF INSTRUMENTS	43
	5.1 General	43
	5.2 Active Detectors	45
	5.2.1 Energy dependence of the response	47
	5.2.2 Dose rate dependence of the response	47
	5.2.3 Directional dependence of the response	48
	5.2.4 Internal background	48
	5.2.5 Cosmic ray response	48

5.3 Passive Detectors 49
5.3.1 Dose evaluation 49
5.3.2 Permanent properties 53
5.3.2.1 General features: sensitivity, dose range, linearity and lower detection level 53
5.3.2.2 Reproducibility and repeatability 55
5.3.2.3 Photon energy and angular dependence of the response 57
5.3.2.4 LET dependence: cosmic response and interferences from other radiation 59
5.3.3 Changing properties 61
5.3.3.1 Background signal: residual dose, zero dose readout and self-dose 61
5.3.3.2 Transit dose 63
5.3.3.3 Long term stability: temperature, light, humidity 67
6. CALIBRATION 71
6.1 General 71
6.2 Reference Instrument Method 71
6.3 Certificated Source Method 75
6.3.1 Free field technique 77
6.3.2 Monte Carlo calculations of the air kerma rate for open field geometries 79
6.4 Traceability 86
7. SPECTROMETERS 88
7.1 General 88
7.2 Detectors 89
7.2.1 Scintillation detectors 89
7.2.2 Semiconductor detectors 90
7.3 Signal Processing 92
7.3.1 Basic electronics 92
7.3.2 Computer aided instrumentation 95

7.4 Analysis of Pulse Height Spectra 96
7.4.1 Full-energy peak method 96
7.4.2 Energy band method 100
7.4.3 Total spectrum energy method 101
7.4.4 Spectrum unfolding 102
7.5 Detector Response Function and Response Matrix 105
7.5.1 Components of response function 105
7.5.2 Determination of response function and response matrix 107
8. INTERCOMPARISONS 109
8.1 Source of Data 109
8.2 EML Data 110
8.3 Data from International Intercomparisons of Environmental Dosemeters 111
8.4 CEC Intercomparisons 112
8.4.1 Intercomparisons 1984 to 1991 112
8.4.2 CEC intercomparisons 1994 118
8.4.2.1 Intercomparison experiments at Risø 118
8.4.2.2 Intercomparison experiments at PTB 120
9. MEASUREMENTS OF ENVIRONMENTAL FIELDS AND INTERPRETATION OF RESULTS 124
9.1 Introduction 124
9.2 Type of Measurement 126
9.2.1 Spot check 126
9.2.2 Monitoring and early warning 127
9.2.3 Mapping 129
9.3 Ancillary Equipment 136
9.4 Interpretation of Results 139
9.4.1 Primary data evaluation 140
9.4.2 Detection of man-made radiation 141
9.5 Example of Measurements 145
9.5.1 Measurement of natural radiation using pressurized ionisation chambers 145
9.5.2 Measurements of external photon air kerma rate in the vicinity of nuclear power stations 145

9.5.3 Mobile laboratories 147
9.5.4 Measurement of dose with TL dosemeters 151
9.5.5 Early warning systems 155
10. UNCERTAINTY ANALYSIS FOR ENVIRONMENTAL RADIATION MONITORING 159
10.1 General 159
10.2 Definitions 160
10.3 Procedure for Uncertainty Analysis, Passive Detectors 161
10.3.1 Write out y as a function of x_1 and determine the contributory variances 162
10.3.2 Evaluate the standard uncertainty, $u(x_i)$ 162
10.3.2.1 Uncertainty of the dosemeter response, $u(x_1)$ 162
10.3.2.2 Uncertainty of the packaging correction, $u(x_2)$ 163
10.3.2.3 Uncertainty of the storage control response, $u(x_3)$ 163
10.3.2.4 Uncertainty of the calibration factor, $u(x_4)$ 163
10.3.2.5 Uncertainty of the fading factor, $u(x_5)$ 164
10.3.3 The combined standard uncertainty 164
10.3.4 The expanded uncertainty 165
10.4 Example Calibration of Active Detector 166
10.5 Estimate of Uncertainty of Calibration of Active Detector 168
10.6 Estimate of Uncertainty of Field Measurements with Passive and Active Detectors 171
11. CONCLUSIONS 174
12. REFERENCES 177

1. INTRODUCTION

During the past decade there has been considerable interest in the levels of radiation to which the general public is exposed, both from natural causes but particularly since the Three Mile Island and Chernobyl accidents to that arising from man-made operations.

The fraction of the background dose rate to man from environmental gamma radiation is very variable and depends on factors such as the radioactivity of the local rock and soil, the nature of building materials and the construction of buildings in which people live and work. Dose rates to man from natural environmental gamma radiation therefore exhibit considerable geographical variation; they may be very much lower in areas of sedimentary rock compared with areas of igneous rock, and may be an order of magnitude higher in some parts of the world. The quantity now most commonly used for measurements made with the objective of monitoring radiation levels in the environment to determine long term changes in these levels is air kerma. The natural environmental gamma ray air kerma rate varies with time, and this in itself makes it difficult to specify the exact air kerma rate at a particular site; it cannot be regarded as a fixed, invariable quantity.

The measurement of the air kerma rate from photon radiation in the neighbourhood of a nuclear installation is an essential part of any environmental measurement programme that is necessary to demonstrate that members of the public are not exposed to unacceptable levels of radiation arising from the operation of the installation.

The contribution to the environmental air kerma rate from a nuclear installation that has to be measured is normally smaller than that from the natural radiation. The natural radiation comprises cosmic radiation from the outer space and terrestrial radiation from the rocks and soil. The photon energy spectrum is complex, with ^{40}K, ^{238}U and its daughter products and ^{232}Th and its daughter products all contributing to the terrestrial air kerma rate. Likewise the composition of the cosmic radiation is complex with about 25% of the cosmic air kerma rate being produced from soft radiation from electrons and photons, and the remaining 75% being produced from a hard component, mostly from mu mesons. The interpretation of measurements is made more difficult since the natural air kerma rate can be significantly different from one location to another, and vary with time at any fixed location. The magnitude of these variations may often exceed the air kerma rate arising from an installation.

To ensure that measurements can be made with sufficient accuracy it is necessary to determine the response of the monitoring equipment to cosmic radiation, to the terrestrial radiation and to take into account the inherent background signal due to electrical noise and radioactivity within the monitor itself. Calibration also poses problems since it is usually not possible to use a calibration facility within which the dose rate is low enough to permit calibration at the levels to be measured. Advice on these problems can be found in the BCRU Publication [GIB93].

Severe radiation accidents at nuclear facilities within any country have safety and political consequences of varying severity in other countries. Following the 1986 Chernobyl reactor accident large and expensive radiation monitoring systems were set up in many countries as part of the improvement to their nuclear emergency management. Many local government organisations that previously had little or no interest in radiation measurements now undertake environmental dose measurements using both active and passive detectors.

To help improve the quality and accuracy of environmental radiation measurements within Europe, the Commission of the European Communities (CEC) sponsored intercomparison experiments during the past ten years under four different study contracts [CEC89 and CEC90].

The purpose of this Technical Report is to disseminate the considerable experience and expertise gained by the participants during the ten year CEC intercomparison programme. Practical advice is given on all aspects of environmental photon dose monitoring. The report starts by describing the nature and variability of environmental gamma radiation within Europe and then discusses the quantities that should be used for measurements. The characteristics and performance of both passive and active detectors as well as of spectrometry systems are discussed. Type testing and calibration methods are recommended which will enable the response of the monitoring equipment to the different radiation components to be properly determined. Techniques for assessing the uncertainties associated with both calibration and measurements are described. Examples are given of the early warning systems installed within European countries.

It is hoped that this report will assist in the harmonisation of environmental photon dose measurements within Europe and the rest of the world.

2. NATURE AND VARIABILITY OF NATURAL ENVIRONMENTAL RADIATION IN EUROPE

Natural radiation cannot be avoided by any of the population of the world. It comes from space, from the earth, from air, water and food, and from other natural sources. The estimated per caput annual effective dose equivalent from external irradiation of natural sources in areas of normal background is shown in Table 2.1.

Table 2.1: Estimated per caput annual effective dose equivalent from external irradiation of natural sources in areas of normal background, [UNSC88].

Source of irradiation	Annual effective dose equivalent (μSv)
Cosmic rays	
Ionizing component	300
Neutron component	55
Primordial radionuclides	
^{40}K	150
^{238}U series (^{226}Ra)	100
^{232}Th series (^{228}Ra)	160
Total (rounded)	800

Cosmic rays come from space and from the sun. Those from space are fairly constant in number, but those from the sun increase during solar flares. The number of cosmic rays entering the earth's atmosphere is affected by the earth's magnetic field: more enter near the poles where the magnetic field is highest than near the equator, so exposure decreases with decreasing latitude. As they penetrate the atmosphere, cosmic rays undergo complex interactions and are gradually absorbed, so that exposure also decreases with decreasing altitude as well as with increasing pressure (see Table 2.2.), [LOW66]. These data represent maximum values, associated with minimum solar activity. Minimum values may be a few percent lower at sea level and perhaps 10% lower at the highest altitudes considered.

Table 2.2: Absolute cosmic-ray intensities expressed as equivalent kerma rates for 50° N geomagnetic latitude [LOW66].

Pressure (hPa)	Altitude[1] (m)	Kerma rate[2] (nGy h^{-1})
1013	0	31.8
981	277	33.8
932	707	38.0
883	1158	43.9
834	1615	52.8
785	2112	65.0
735	2627	82.9
686	3170	109.1
637	3750	~140
588	4359	~184

1) Based on U.S. standard atmosphere, [LOW66].

2) These values have been calculated from exposure rate values using W/e=33.97 J/C and 1 μR h^{-1} = 8.764 nGy h^{-1} The data represent maximum values, associated with minimum solar activity. Minimum values may be a few percent lower at sea level and perhaps 10% lower at the highest altitudes considered

The majority of the Europe's population lives at altitudes close to sea level. In the UNSCEAR 1982 Report, [UNSC82] the absorbed dose rate in outdoor air from the ionizing component of cosmic rays was estimated to be 32 nGy h^{-1}; this value is taken to be numerically equal to the effective dose equivalent. Indoors, the doses are somewhat lower because of the shielding effect of building structures. Dose rates measured at the centre of various levels of a 12-storey building showed a fairly smooth decline with depth (Table 2.3).

Table 2.3: Absorbed dose rates in air due to ionizing component of cosmic radiation in the centre of a 12-storey building [UNSC88]

Level	Dose rate ($nGy\ h^{-1}$)	Transmission Factor
Roof	31.4	1
12	20.2	0.64
10	20.0	0.64
8	18.1	0.58
5	17.4	0.55
4	13.7	0.44
2	11.5	0.37
Basement	8.6	0.27

The variation with altitude and latitude of the neutron component is similar to that of ionizing component. At sea level the neutron fluence rate is about 0.008 $cm^{-2}\ s^{-1}$, the estimated dose equivalent rate is 2.4 $nSv\ h^{-1}$.

Many materials in the earth's crust are radioactive because they contain small amounts of the uranium and thorium naturally active species and potassium. The levels of radioactivity depend on the type of rock or soil: it is high in granites, low in some sedimentary rocks and intermediate in soils. Average activity mass concentrations of ^{40}K, ^{238}U and ^{232}Th and absorbed dose rates in air 1 m above the ground surface due to these concentrations are given in Table 2.4. These data are typical for the world but the data for Europe would be more or less the same. Estimates of outdoor absorbed dose rate in air from terrestrial radiation sources 1 m above the ground level obtained in large scale surveys for several European countries are given in Table 2.5. The table gives the dose rate per unit activity mass concentration in soil, i.e. the conversion coefficients connecting the radionuclide concentration in the soil and the resulting dose rate. The indoor terrestrial gamma radiation absorbed dose rates in air at the same sites are usually 1.2 times higher then the outdoor values [AMA92].

Table 2.4: Average activity mass concentrations of ^{40}K, ^{238}U and ^{232}Th and absorbed dose rates in air 1 m above the ground surface due to these concentrations, [UNSC88].

Radionuclide or decay series	Dose rate per unit activity mass concentration in soil ($nGy\ h^{-1}$ per $Bq\ kg^{-1}$) (wet weight)	Average activity mass concentration in soil [a/] ($Bq\ kg^{-1}$) (wet weight)	Absorbed dose rate in air [a/] ($nGy\ h^{-1}$)
^{40}K	0.043	370 (100 – 700)	16 (4 – 30)
^{238}U	0.427	25 (10 - 50)	11 (4 - 21)
^{232}Th	0.662	25 (7 - 50)	17 (5 - 33)

[a/] The typical ranges are given in parentheses

Table 2.5: Estimates of outdoor absorbed dose rate in air from terrestrial radiation sources 1 m above the ground level obtained in European large scale surveys, [UNSC88].

Country	Year reported	Number of Measurements	Absorbed dose rate in air ($nGy\ h^{-1}$)	
			Average	Range
Austria	1980	>1000	43	20 – 150
Belgium	1987	272	43	13 – 58
Czech Republic [a)]	1973	143	74	26 – 166
Denmark	1980	14 sites	38	17 – 52
Finland	1980	-	65	-
France	1985	5142	68	10 – 250
Germany (GDR)	1969	1005	85	24 – 270
Germany (FRG)	1978	24739	53	4 – 350
Hungary	1987	123 sites	55	20 – 130
Iceland	1982	-	28	11 – 83
Ireland	1980	264	42	4 – 180
Italy	1972	1365	57	7 – 500
Netherlands	1985	1049	32	10 – 60
Norway	1977	234	73	20 – 1200
Poland	1980	352 sites	37	15 – 90
Portugal, [b)]	1991	-	85	9 – 230
Romania	1979	2372	81	32 – 210
Slovakia [c)]	1977	139	72	54 – 103
Spain, [d)]	1991	1053	44	25 – 82
Sweden	1979	-	80	18 – 4000
Switzerland	1964	-	60	-
United Kingdom	1984	1400	40	4 – 100

a) [SPU73], b) [AMA92], c) [SPU77] and d) [QUI92]

The penetrating gamma rays emitted by the rocks irradiate the whole body more or less uniformly. Since most building materials are extracted from the earth, they are also radioactive, and human beings are exposed whilst being indoors as well as when outdoors. Doses are affected by the geology of the area and the structure of the buildings: they are higher in dwellings constructed from masonry than in timber dwellings.

Photons from primordial radionuclides usually make up the most significant terrestrial component. Because of weapons test in the 1950's and 60's a small world-wise contribution from ^{137}Cs may now be considered part of the radiation background. Due to the Chernobyl accident in 1986, large areas of Europe are contaminated with ^{137}Cs and a decreasing fraction of ^{134}Cs.

It is important to note that though most of the flux (~ 70%) of a typical environmental spectrum is due to gammas of energy less than 500 keV, these low energy photon components do not contribute as much to the absorbed dose in air as do the higher energy photons. Most of the total dose (~ 70%) is from photons with energies greater than 500 keV. This is a similar situation for man-made radiation, (See Figure 2.1).

When evaluating variations of dose rate with time it is important to take into account that the total dose rate from environmental radiation is not constant over the course of a day or from one day to the next. Some of the natural temporal variations are associated with diurnal temperature changes and the accompanying atmospheric turbulence. Radon gas exhaled from soil during the night stays near the surface of the earth while the air is cold, with the gamma emitting progeny causing an increase in the radiation background level during this time. As the air is warmed by the sun during the day, vertical diffusion reduces the radon concentration and the ground level radiation decreases.

Precipitation also plays a major role in natural variations in the background radiation. For example, rain or snow can scavenge airborne radon progeny causing an increase in radiation levels for several hours. Subsequently wet ground or snow deposited on or in the soil surface attenuates the terrestrial component causing radiation levels to drop below the previous baseline after the precipitation stops, the levels gradually increase as the ground dries. Other possible natural variations are related to seasonal influences in the exhalation rate of radon from the ground, such as frozen soil allowing less of the gas to escape, or changes in the cosmic ray component with atmospheric pressure and solar cycle, (See Figure 2.2). Snow cover is more effective at attenuation than an equivalent rainfall because it remains on the surface instead of draining immediately into the soil. A seasonal pattern of outdoor air kerma rate occurs, therefore, in regions subject to significant snowfall. Sievert and Hultquist [SIE52] have shown that a 20 cm depth of snow reduces the environmental gamma-ray air kerma rate by 26% for a snow density of 0.1 g cm^{-3}, and by 58% for a snow density of 0.4 g cm^{-3}.

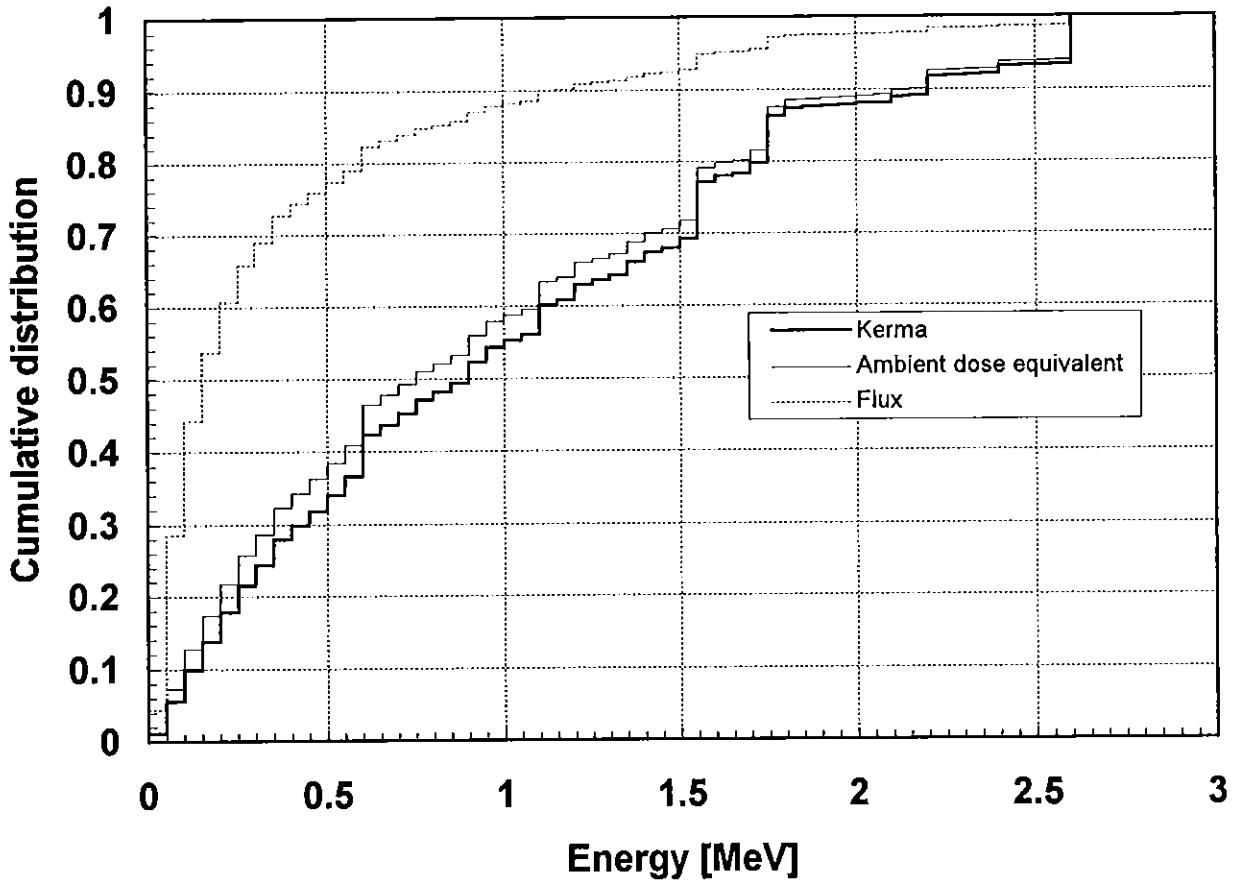

Figure 2.1: Accumulative distributions of terrestrial photon flux, air kerma and ambient dose equivalent at 1 metre height above the ground, [PER96].

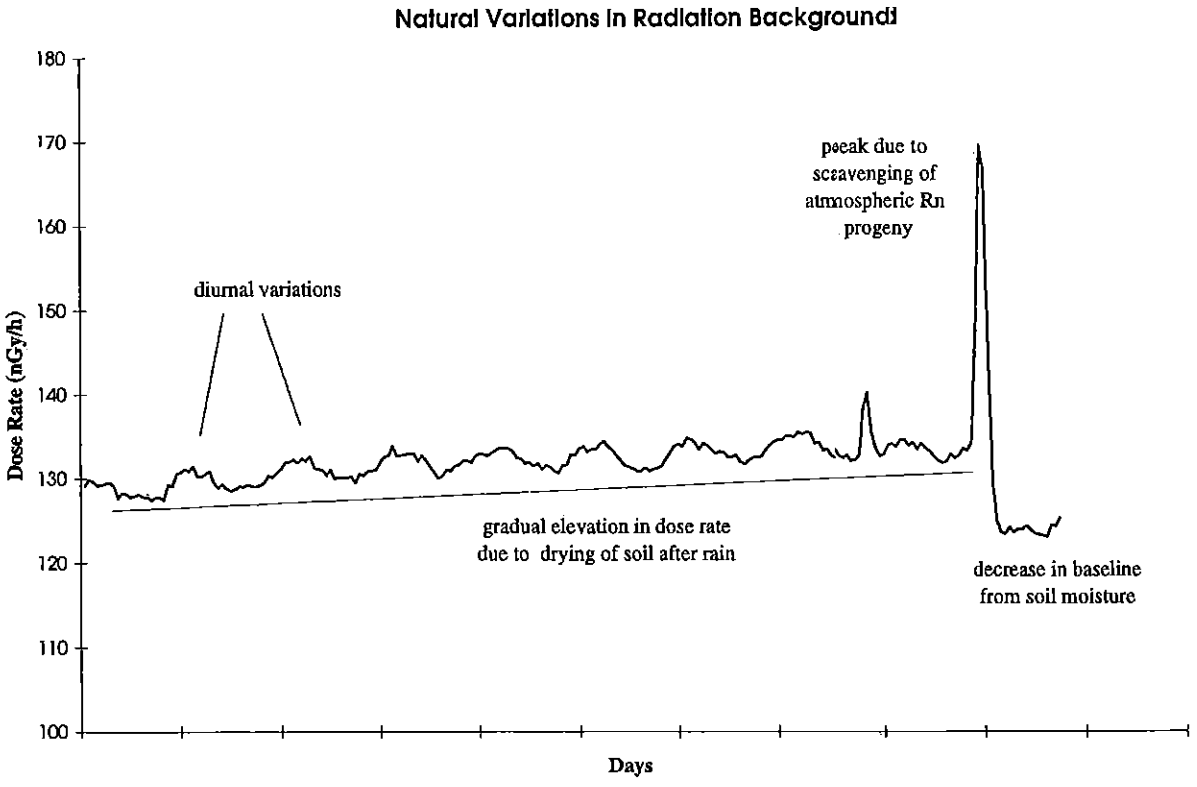

Figure2.2: Typical short-term variations observed in the outdoor exposure rate, [HUF94].

3. MEASUREMENT QUANTITIES

In the past environmental photon and cosmic radiation levels have usually been measured in terms of the quantity exposure rate and in units of $\mu R\ h^{-1}$. From the start of 1986 members of the European Community were required to report all radiation measurements in terms of S.I. units. As the S.I. units for exposure, the coulomb per kilogram has an unsuitable magnitude e.g. 10 $\mu R = 2.58 \times 10^{-9}$ C kg^{-1}, the results of environmental photon radiation levels are now frequently reported for the quantity air kerma rate, in S.I. units of nGy h^{-1}. During the past ten years, therefore, measurements of environmental gamma radiation have usually been made in terms of air kerma rate in air the detector being placed at a standard height of 1 m above the ground.

At the point of measurement, the absorbed dose rate to the body, or to any organ in the body, will not be the same as the instrument indication, partly because of the numeral difference between air kerma to the air and the absorbed dose to tissue, and partly because of the attenuation and scattering of the radiation by the body. There is however no difference between the numerical values of absorbed dose rate to tissue and dose equivalent rate, because a quality factor of unity applies for environmental gamma radiation.

However, the operational quantity now recommended by the ICRU [ICRU85] for area monitoring is ambient dose equivalent (or in some circumstances directional dose equivalent) and the unit is the sievert (Sv). Thus depending upon the purpose of the measurement either air kerma or ambient dose equivalent should be used for measurements of external environmental gamma radiation doses.

Where the measurements are made over long time periods in order to demonstrate whether changes in the radiation environment have occurred, air kerma is preferred since its numerical value for a fixed radiation field has and will remain constant. This can only be true for a physical quantity like air kerma since any dose equivalent quantity can change its numerical value for a fixed radiation field as new biological data becomes available to change those humanly judged factors, Q, N and W_T.

Many measurements of environmental gamma radiation are made for comparison with limits designed to restrict to acceptable levels the radiation risks to people not occupationally exposed. Acceptability is often judged not only in relation to legal limits but also in relation to natural background levels of radiation. The quantity recommended by ICRP [ICRP87] for control and

limitation of doses to people is effective dose. However, effective dose is not a measurable quantity so one has to measure either the ambient dose equivalent or the air kerma and apply an appropriate correction or conversion factor to calculate the effective dose.

In 1989, the British Committee on Radiation Units (BCRU), [BCRU89], recommended that:

1. If measurements are made with the objective of monitoring radiation levels in the environment to elucidate long-term changes in these levels, then air kerma should be used.

2. If the objective is to give an indication that levels from man made sources are acceptable within specified limits for the exposure of people, then ambient dose equivalent should be used. It should be noted that radiation risks to individuals are best expressed by the quantity effective dose equivalent. If this latter quantity is to be assessed, it may be necessary to obtain details of the quality of the environmental radiation that cannot be described adequately by simple measurements of either air kerma or ambient dose equivalent.

3. If both the above objectives pertain, the measurements should record both air kerma and ambient dose equivalent.

A further consideration in deciding which measurement quantity is best to use is the radiation field to which members of the public are exposed. Apart from during a nuclear emergency, at the locations at which measurements are made the natural radiation is by far the largest contribution. This natural radiation comprises cosmic radiation from outer space and terrestrial radiation from rocks and soil. The complex cosmic radiation field irradiates the person from above, whilst the irradiation from the ground occurs equally around the person's body. Any plume irradiation or ground contamination is equally isotropic and even for these few cases where direct radiation from the station occurs, e.g. 6 MeV photons, the person never remains facing in one direction only. For all these irradiations we can assume that the person is being irradiated rotationally isotropic in the horizontal plane (ROT).

Now if air kerma is selected the monitoring instrument's detector will have an isotopic response. To convert the air kerma reading to whole body dose equivalent a conversion factor of 0.87 Sv/Gy is applicable for isotropic environmental gamma radiation, [ASH79], or 0.86 for the ratio of effective dose to air kerma, [CLA93].

If ambient dose equivalent is selected for monitoring the detector will again have an isotropic response. From Fig. 1 of ICRU Report 39, we can obtain the required conversion coefficient from ambient dose equivalent to effective dose equivalent. Although this statement from ICRU refers to the effective dose equivalent it is still applicable to the estimation of effective dose since for radiation protection purposes the numerical values of the effective dose are very close to those for the effective dose equivalent. For isotropic radiation and a typical natural terrestrial radiation the ratio of effective dose equivalent to ambient dose equivalent is 0.6. That is to say a measurement of the ambient dose equivalent will over-estimate the effective dose equivalent by a factor of 1.67. This has been recognised by ICRU in Report 39, they say "If the over-estimation of H_E by H*(10) is unacceptable for photons at low energies, or for near isotropic radiation fields, more complex measurements will be needed". Thus no matter whether air kerma or ambient dose equivalent is used, neither will provide a proper measure of the dose equivalent to a member of the public, but will require the application of a conversion coefficient. Air kerma measurements results in a numerical over-estimation of dose equivalent by a factor of 1.15, [ASH79] and [CLA93] and ambient dose equivalent over-estimates by a factor of 1.67.

One further point, is that for on-site measurements, the over-estimation in effective dose from a measurement of ambient dose equivalent is acceptable since the doses to individuals are all subsequently measured by their personal dosemeters. For example, an area is monitored in ambient dose equivalent and gives say 1 Sv h^{-1}. A person working in such an area for 1 hour is then assumed to receive an effective dose of less than 1 Sv, but the dose to that person is taken as that from their personal dosemeter not that from the monitoring instrument. For off-site persons, i.e. members of the public, no personal dosemeters are worn hence measurements in terms of the ambient dose equivalent would lead to significant over-estimations unless the appropriate conversion coefficient was applied.

Conversion factors for monoenergetic photons from air kerma to effective dose E/K_a, from air-kerma to ambient dose equivalent, H*(10)/Ka and from ambient dose equivalent to effective dose E/H*(10) are given in Table 3.1 and Figure 3.1 [ICRP77]. The ratio of $H^*(10)/K_a$ varies significantly with photon energy being 1.74 at 60 keV and 1.21 at 660 keV. Thus it cannot be assumed that a radiation monitoring instrument designed to measure the air kerma will also be satisfactory for measurements of the ambient dose equivalent; this is discussed more fully in Section 4.1.

Table 3.1: Quotients $H^*(10)/K_a$, E/K_a and $E/H^*(10)$ for monoenergetic photon radiation. The values were calculated using the approximate formula stated in Section 5.2.2 and used in ICRU Report 47 [ICRU92] (with the exception of the values for $H^*(10)/K_a$ below 20 keV)

Photon energy In keV	**$H^*(10)/K_a$**	**E/K_a**	**$E/H^*(10)$**
10	0.01	0.01	1.00
15	0.26	0.04	0.15
20	0.61	0.12	0.20
30	1.10	0.42	0.38
40	1.47	0.79	0.53
50	1.67	1.11	0.66
60	1.74	1.31	0.75
80	1.72	1.43	0.83
100	1.65	1.39	0.84
150	1.49	1.26	0.85
200	1.40	1.18	0.84
300	1.31	1.09	0.83
400	1.26	1.06	0.84
500	1.23	1.04	0.85
600	1.21	1.02	0.84
800	1.19	1.01	0.85
1000	1.17	1.00	0.85
1500	1.15	1.00	0.86
2000	1.14	0.99	0.87
6000	1.11	0.99	0.89

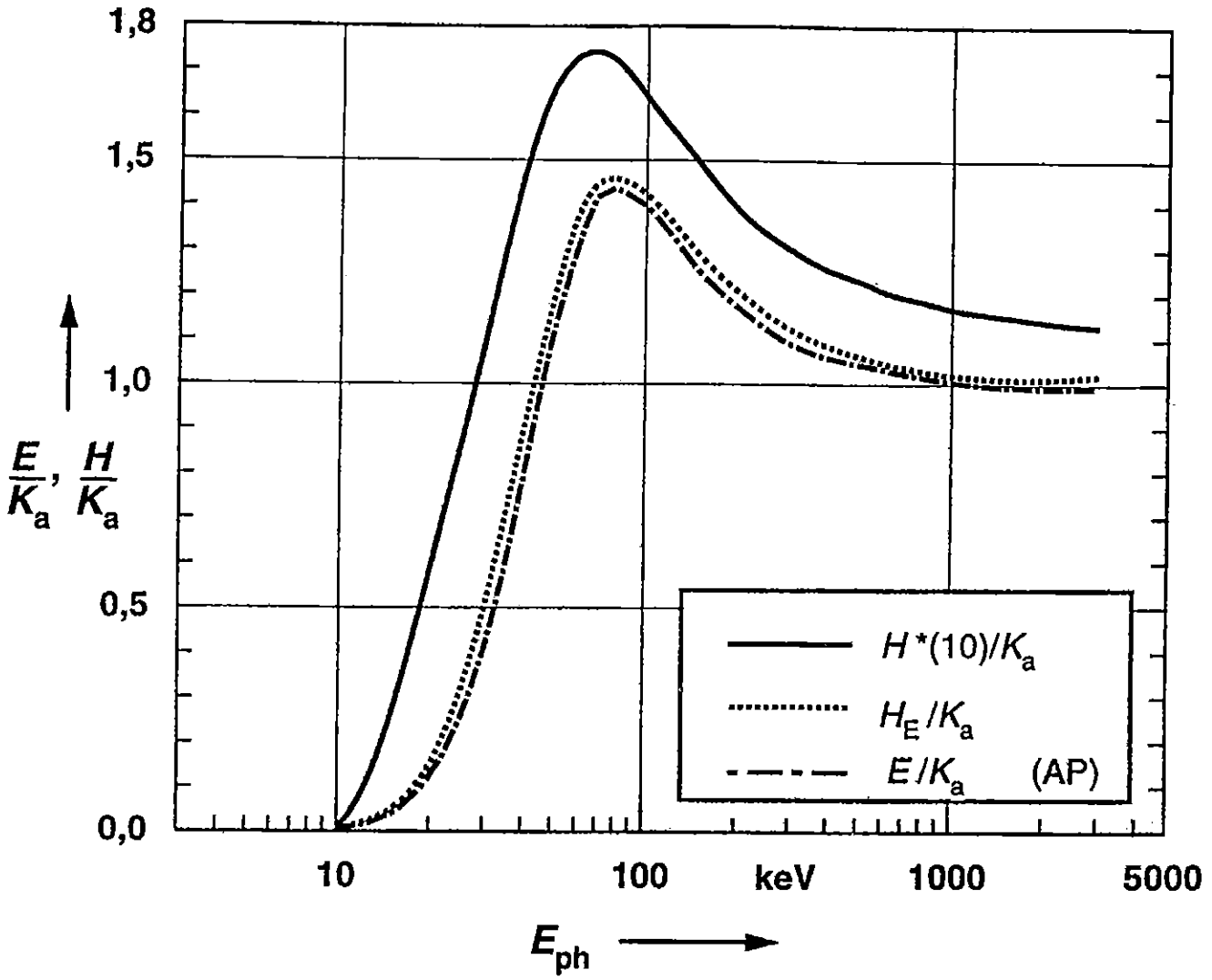

Figure 3.1:

Comparison of (K_a: air kerma) with :- the quantity for area monitoring, $H^*(10)$, with the effective dose equivalent, H_E, and with the effective dose E for monoenergetic photon radiation, E_{ph}. The values of H_E and E are valid for whole-body exposure from the front (AP, anterior-posterior); the values of the effective dose are smaller for other irradiation geometries of the whole body, [ICRU92].

4. DETECTOR CHARACTERISTICS

4.1 Active Detectors

4.1.1 General

This section provides information on the characteristics of environmental monitoring systems using a variety of different types of active radiation detector to measure air kerma rates. Systems that measure the radiation spectrum or which estimate the air kerma rate from their measured spectra are described in Chapter 7. Whilst many of the characteristics are a direct function of the detectors themselves, others will be attributable to the electronics required for the specific type of detector. Often the requirements of the detector will dictate a particular electronic system which will itself dictate the characteristics of the system as a whole.

The data presented in this section is largely based upon experience of currently available environmental monitoring systems. The radiological characteristics and suitability for field use of some of these instruments have been examined and discussed in publications, [GIB93] and [CLA93]. All the active detectors are used in monitoring instruments which can be designed to measure either the ambient dose equivalent or the air kerma.

4.1.2. Geiger-Müller counters

Geiger-Müller, (GM), counters measure the product of the fluence rate of the radiation and the interaction probability with the counter walls. Hence their response per unit dose is higher at low photon energies. To overcome this an energy compensating filter is fitted to the GM counter and they are now one of the most widely used detectors for environmental monitoring. The compensation filters, however, absorbs the lowest energy photons and so their response falls off very rapidly below energies of approximately 50 keV. However, this is of little significance for the majority of environmental monitoring applications. The photon energy dependence of a GM counter frequently used for environmental measurements is shown in figure 4.1.1. The response is shown for both ambient dose equivalent and for air kerma and for both quantities the response has been normalized to unity for a ^{137}Cs source.

GM based systems have a variety of features which make them well suited as both portable environmental monitoring systems or fixed installed systems.

Because the electronic signal from the detector is significantly large the electronics necessary for this type of detector are relatively simple and uncomplicated. A direct consequence of this is that GM based systems are considerably smaller and lighter than their counterparts which use ionisation chambers or scintillators. In addition GM based systems are considerably less expensive. They also have excellent battery life, and because none of the electronic parameters are particularly critical, any changes in response due to temperature or other environmental conditions have little or no effect on the overall performance of the system.

The internal background of a GM counter is caused by traces of radioactivity in its components, chiefly from the metal or glass walls of the detector as well as from its anode. The internal count rate can be a significant fraction of the count rate from the environmental photon radiation.

The internal background of a GM counter, its inherent response, can be determined either from measurements made down a deep mine (see section 5.2.4) or by using the coincidence technique described in the BCRU Guide, [GIB93].

The cosmic ray response can be determined either from measurements made at sea or on a lake, or by calculation or by coincidence technique, [GIB93]. Since the efficiency for counting cosmic radiation is 100% then the count rate for a cylindrical GM detector is dependent upon its cross-sectional area. For a cylindrical counter, the side area is normally much larger than the top end area, so the cosmic-ray response is least when the axis of the detector is vertical. This means that provided they are orientated vertically, they also have good polar response characteristics for environmental photon radiation fields.

The sensitivity of GM detectors is generally not as high as that of high pressure ion chambers or scintillators, although it is more than adequate for environmental monitoring purposes.
Typical characteristics of the GM counter type whose energy response was shown in figure 4.1.1 are as follows:

- Response to ^{137}Cs, 0.02 counts s^{-1} per nGy h^{-1}.
- Response to cosmic radiation, 0.03 counts s^{-1} per nGy h^{-1}.
- Inherent response, ~ 0.2 counts s^{-1}.

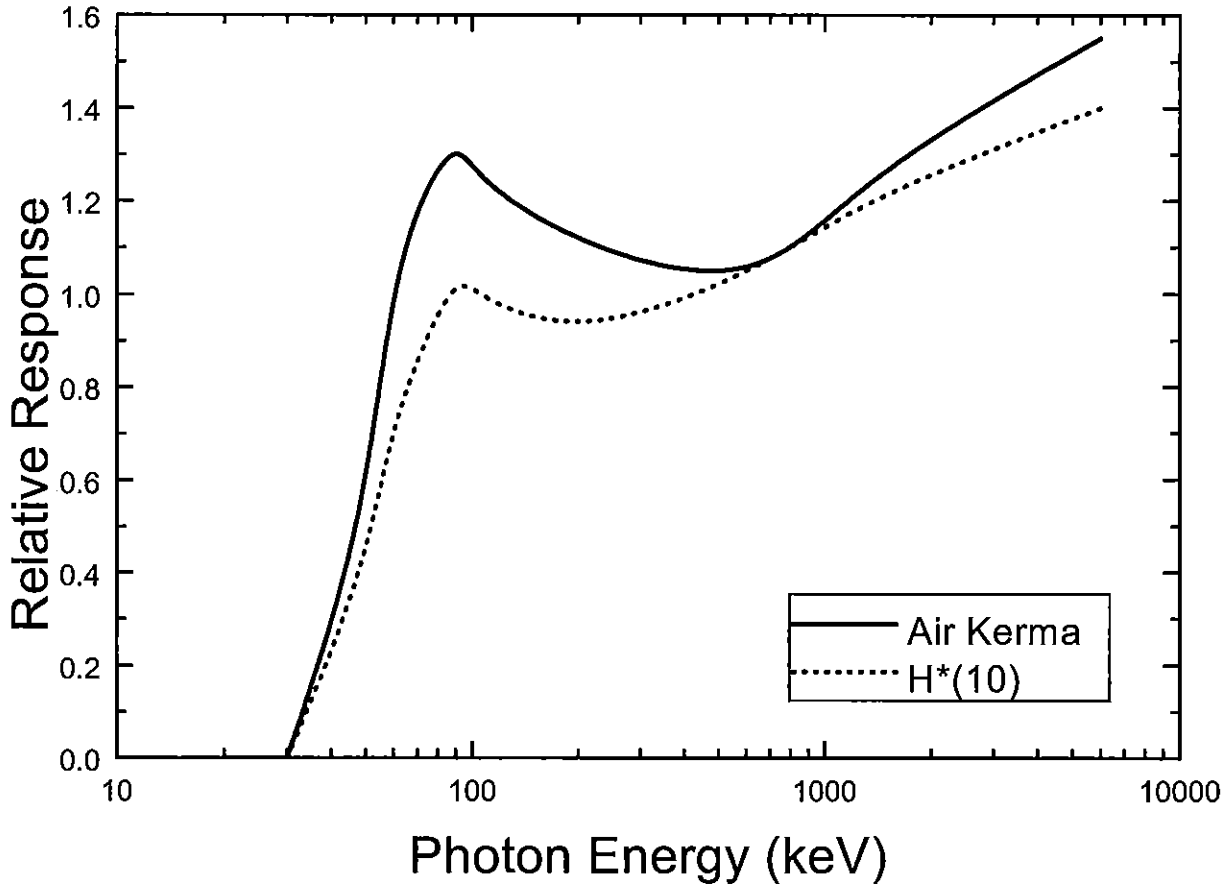

Figure 4.1.1: Energy dependence of Geiger-Müller counter

4.1.3. Ionisation chambers

Ionisation measurements of gamma-ray air kerma rates should be made under conditions of electron equilibrium. In ionisation chambers at atmospheric pressure, the air-equivalent or tissue-equivalent walls provide most of the secondary ionising electrons. In high pressure ionisation chambers, the walls play a lesser part because a large fraction of the ionisation arises from gamma-ray absorption in the high pressure gas.

Air filled ionisation chambers with approximately air-equivalent walls have been used as the commonest form of dosemeter. The volume of ionisation chambers associated with radiation protection instruments, however, are not large enough to make satisfactory measurements at environmental air kerma rates and resort must be made to large chambers at atmospheric pressure or to high pressure ionisation chambers.

A frequently used portable high pressure ionisation chamber is that of Shambon [SHA63] which has a volume of 8 litres filled with argon at 30 atmospheres. The energy response characteristics of high pressure ionisation chambers is constrained by their construction, depending chiefly on their wall material and thickness. They have relatively thick walls of high Z material for both the measurement of air kerma and ambient dose equivalent (Figure 4.1.2) which produces a dramatic fall off in response at energies below approximately 80 keV. As in the case of the GM, this is of little significance in the environmental monitoring application.

The detector geometry of typical systems is usually either spherical or cylindrical and this results in good polar response characteristics.

Internal radioactive contamination from alpha radiation can produce a significant inherent response which can be minimized by using a dense electron attaching gas (freon) to enhance columnar recombination in the alpha particle tracks. In high pressure chambers, the pressure and the addition of an electron attaching gas such as oxygen will increase the recombination in the alpha particle tracks. Measurements of the inherent response made down the laboratory situated in a deep mine, UDO, give readings of between 0.48 and 1.13 nGy h^{-1} for commercial high pressure chambers, [CEC90].

The cosmic ray response can be determined from measurements made at sea or on a lake. Most high pressure ionisation chambers have an approximately equal sensitivity to cosmic and to terrestrial photon radiation.

The advantages offered by a high pressure ionisation chamber are good sensitivity (provided they are of sufficient volume and high pressure) and good environmental stability, i.e. their response is unaffected by variations in temperature, pressure and humidity. The ionisation current produced at environmental levels are, however, small even in large volume chambers, typically 10^{-13} A. Care must be taken to reduce leakage currents and the polarising voltage should be kept very constant. Although the ionisation chamber is environmentally stable the measuring system should be tested to ensure that it is not subject to changes due to variations in temperature, pressure and humidity. The power requirements are such that typical systems will operate for over a week without requiring replacement batteries.

High pressure ionisation chamber systems are generally large and bulky. This makes them more suited to installed applications rather than portable ones. As an example, a typical system like the Reuter Stokes RSS112, weights approximately 19 kg and has a volume of some 40 litres.

Monitoring systems based on high pressure ionisation chambers are generally very expensive, although a significant proportion of the cost often relates to the process electronics and data storage facilities provided.

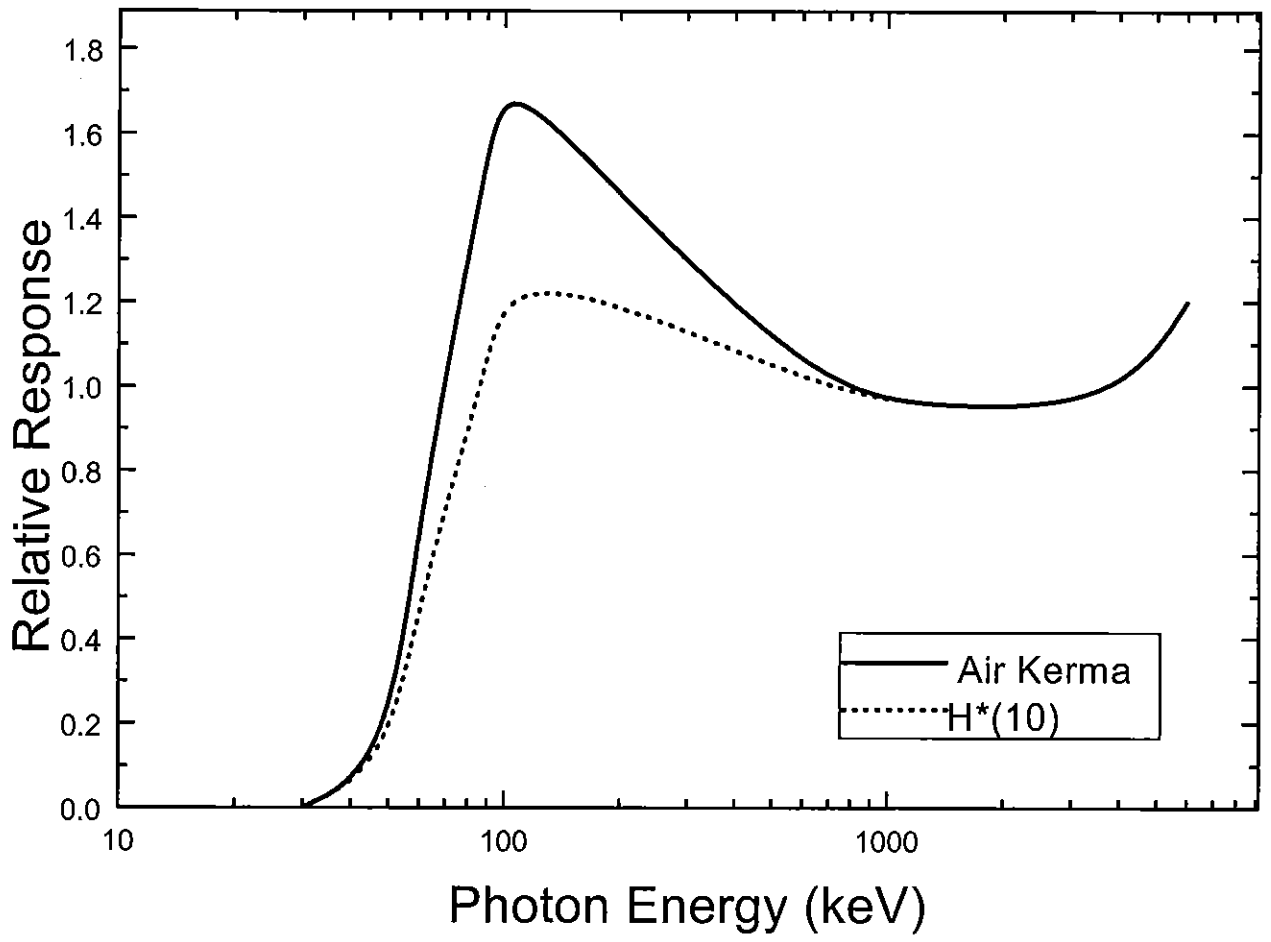

Figure 4.1.2. Energy dependence of high pressure ionisation chamber

4.1.4. Scintillation detectors

Scintillation detectors are frequently used for environmental dose rate measurements. As the detector has a much higher density than gas filled ionisation chambers a significantly smaller detector gives comparable sensitivity but this saving in size is offset by the size of the photomultiplier that has to be used.

The scintillation detector based systems used for environmental monitoring usually employ organic, plastic scintillators. Inorganic scintillators such as NaI(Tl) offer a higher sensitivity but are unsuitable for dosimetric measurements, because their effective atomic number is greater than that of air they significantly over-respond at photon energies between 30 keV and 600 keV (see Figure 4.1.3). Inorganic scintillators have not only a short-term fading fluorescence but also a long term phosphorescence. If they are irradiated at high air kerma rate prior to being used for environmental measurements the retained luminescence can lead to falsely high readings. However, NaI systems are used to good effect where the purpose of the monitoring is more of a screening exercise aimed at identifying affected areas, rather than making quantitative dose rate measurements. The use of scintillators for spectrometric measurements is described in Chapter 7.

Organic scintillators are more suited for air kerma rate measurements, particularly for energies above 100 keV, since their mass energy absorption coefficient corresponds approximately to that of air. Below 100 keV the response falls off rapidly with decreasing photon energy but by coating the scintillator with a thin layer of high atomic number material such as ZnS, the air-equivalent response can be extended down to 20 keV. At low photon energies the fluorescent light is produced solely in this ZnS layer whereas above 100 keV the gamma- and X-radiation penetrates the ZnS layer and the light is produced chiefly in the thick organic scintillator.

Homogeneous incorporation of the ZnS within the plastic scintillator is restricted to small detectors since low energy photons will not penetrate to the ZnS within the inner layers of a large Crystal. Kolb and Lauterbach [KOL74] developed a ZnS (Ag)-loaded anthracene detector, which is approximately air-equivalent from 20 keV to 2 MeV (Figure 4.1.4). A more recent evaluation by McClure, [McC87], of the Automess Szintomat (type 6134), based upon a plastic scintillator (type NE 120) with a ZnS (Hg) layer shows a poorer energy response on the most sensitive range.

The energy response characteristics of plastic scintillator based systems are generally superior to those employing GM or high pressure ionisation chamber detectors. However, this superiority is only

significant at low photon energies, i.e., below approximately 60 keV and as such does not represent a significant advantage for the application of environmental monitoring. Nonetheless scintillator based systems are often chosen for this characteristic alone.

Because it is easy to fabricate the scintillator in whatever shape is required, the polar response characteristics of scintillator based systems are generally satisfactory.

In scintillation detectors the dark current of the photomultiplier tube limits the lowest air kerma rate that can be measured. Low noise photomultiplier tubes should always be used, and operated so that the optimum ratio of signal to dark current is obtained. This can be achieved by careful selection of the operating voltage or by employing a cooling device. The inherent response if the MAB 500 Scintillator measured at the UDO laboratory [CEC90] was found to be between 5 to 10.5 nGy h^{-1}.

Inherent activity of the detector material can impose a limitation on the sensitivity. The major contribution is ^{40}K activity in the scintillator and in the glass of the photomultiplier; this can be reduced by means of special potassium free scintillators and photomultiplier tubes, and by using mountings with quartz windows. Aluminum should be avoided for the scintillator mounting and electrolytically purified copper or magnesium, which has low inherent activity, should be used instead.

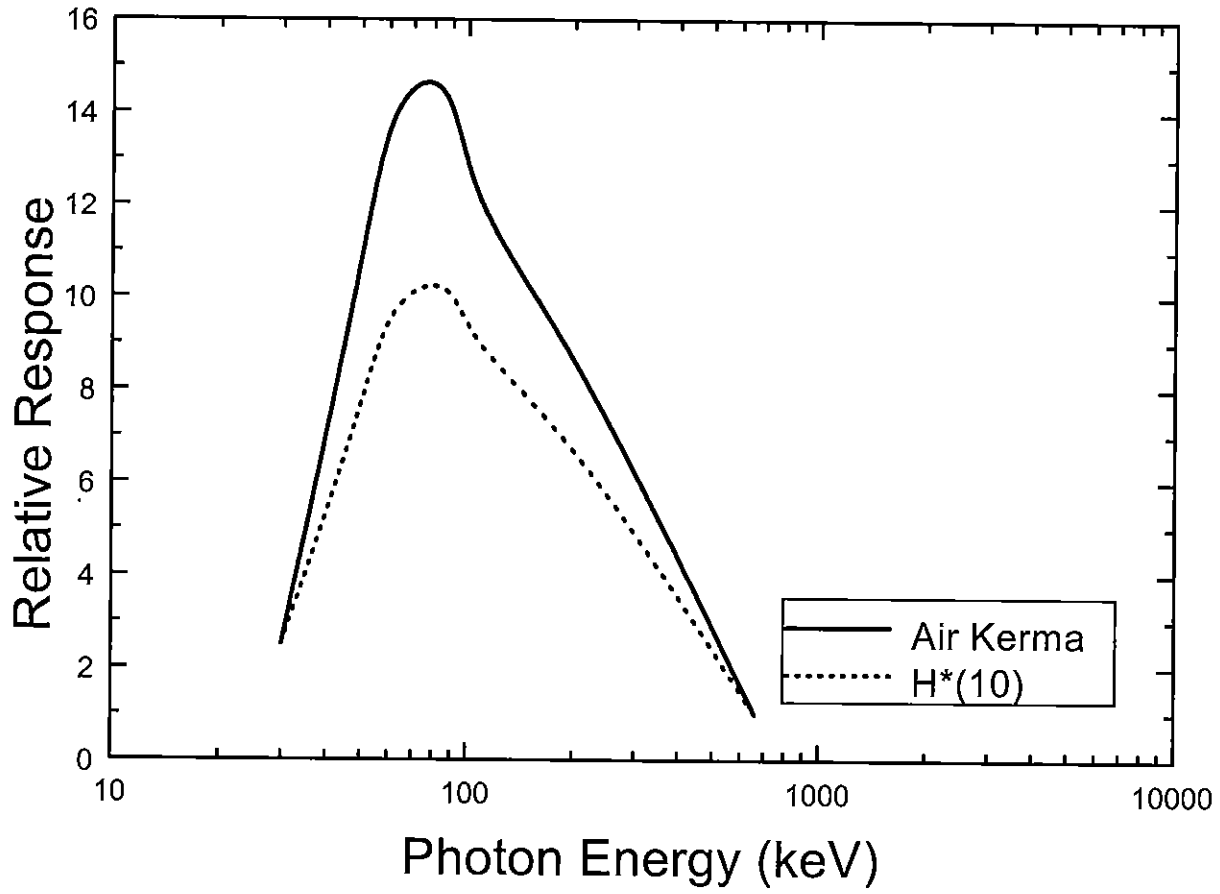

Figure 4.1.3: Energy dependence of Na(I) scintillator

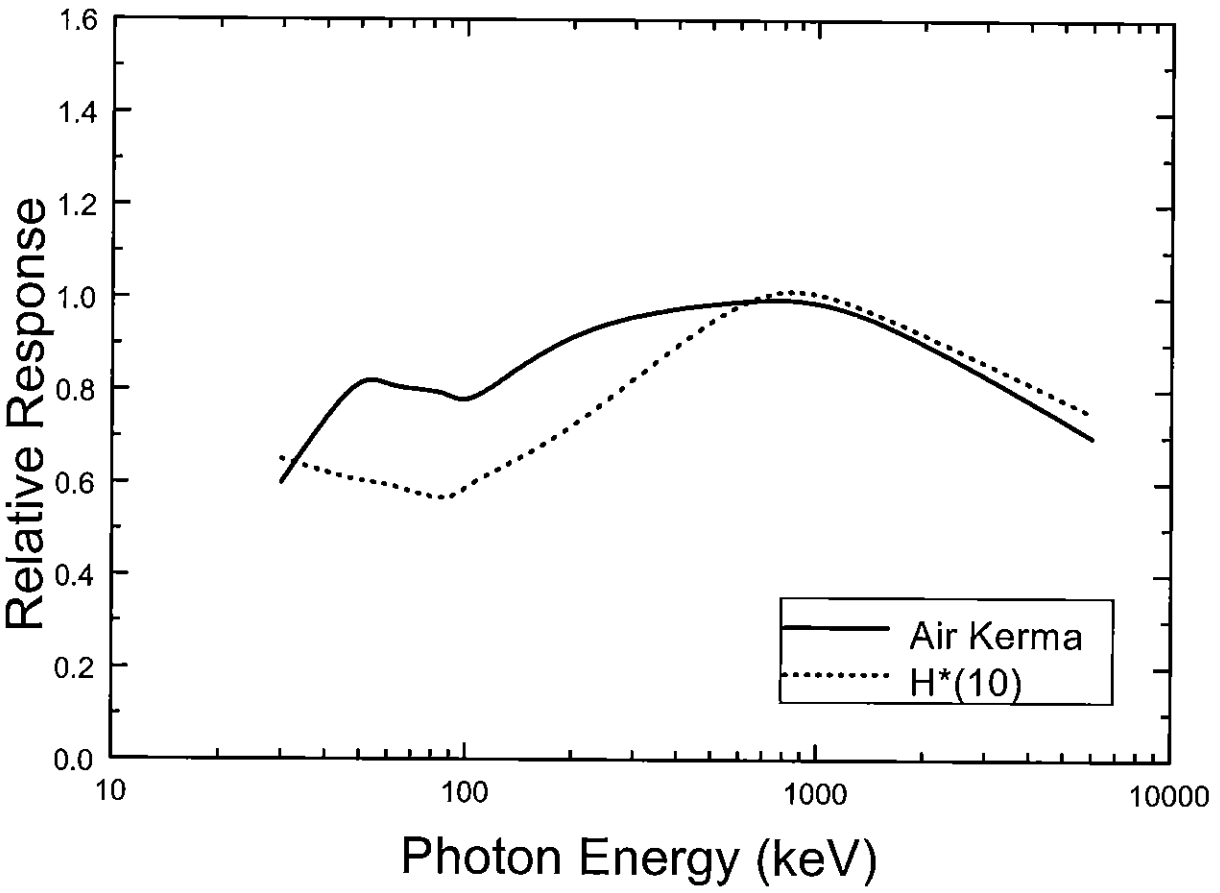

Figure 4.1.4: Energy dependence of plastic ZnS(Ag) scintillator

The major drawbacks of scintillator based monitoring systems are all related to the associated electronics. The gain of a scintillation detector (scintillator and photo multiplier tape) is proportional to the high voltage applied across the PM tube dynode chain. This means that the HV supply has to be highly stable, the photomultiplier amplification changes by approximately 0.7% per degree Celsius. Because of the conditions in which environmental monitoring systems are used, this has to be maintained over a wide range of temperatures and temperatures gradients and this is difficult to achieve. As a result, scintillator based systems generally have inferior temperature characteristics compared with GM and ionisation chamber based systems. The associated electronic systems are relatively complex, certainly compared to GM detector systems, and hence are more expensive. They also have greater power demands than other systems and as such cannot be operated continuously for long periods of time without replacing or charging the batteries.

Once again, because of the complexity, scintillator based systems are generally heavier and more cumbersome than GM based systems.

4.1.5. Proportional counters

The energy compensated proportional counter is the detector type sometimes used for environmental monitoring. The proportional counter has similar energy response characteristics to GM counters. They are normally used with energy dependence compensation, and have no significant response to photon radiation below energies of approximately 50 keV. However, this is of little significance for the majority of environmental monitoring applications.

Proportional counter based systems have a variety of features which make them well suited both as portable and as fixed environmental monitoring systems.

The electronic signal from the detector is proportional to the energy imparted in the sensitive volume of the counter and therefore the energy dependence compensation is possible using proper signal processing electronics, taking into account the amplitude of the signal and/or by using energy dependence compensating filter combination. The proportional counter can be used in different modes. The simplest one is the counting mode. In this case the response of the proportional counter is similar to the response of the GM counter but with a much more wider count rate range. Another possibility is the ionization chamber mode, i.e. summing of the amplitudes of the impulses.

The output signal is proportional to the dose rate, without correction for energy dependence which is due to the non air-equivalent detector wall. The most sophisticated mode is the weighted signal processing. In this case the weighting factor is a function of the pulse height. Using this method the required energy dependence (e.g. air kerma, or ambient dose equivalent) can be obtain with high sensitivity and a wide energy range.

Other advantages are the low background of the detector, its short dead time and the extremely wide measuring range. A direct consequence of these is that proportional counter based systems use only a single detector for measurement of environmental dose rate from the normal background up to the high dose rates encountered during nuclear accident, i.e. from 10 $\mu Gy\ h^{-1}$ to 10 $Gy\ h^{-1}$, which is six orders of magnitude.

The electronic parameters are particularly critical, any shifts due to temperature or other environmental conditions should be carefully compensated for. Due to the requirements to have high stability of the signal processing electronics and high voltage power supply the proportional counter based systems are considerably more sophisticated and expensive than for other detector types. Usually they have shorter battery life than the simpler GM counter based systems.

The internal background and the cosmic radiation response of a proportional counter is similar to that of a GM counter of the same size.

The physical shape of the majority of proportional counters used for environmental monitoring are high aspect ratio cylinders. This means that provided they are orientated correctly i.e. vertically, they have good polar response characteristics for environmental radiation fields.

The sensitivity of proportional counter depends on its sensitive volume, the sensitivity of the large volume proportional counter is therefore as high as that of high pressure ion chambers or scintillators, it is fully adequate for environmental monitoring purposes.

The proportional counter do not use any quenching gas, the lifetime of a high quality proportional counter is therefore practically unlimited.

4.1.6. Electronic dosemeters

The commercially available electronic dosemeters are designed to be worn on the person and to measure the quantity personal dose equivalent, $H_p(10)$. Their use for free-field environmental measurements is non standard, but they were included in the recent CEC intercomparison at Risø (see Chapter 8, [BØT95]), to see if they could be used for such measurements. Since the electronic dosemeters have their displays in units of Sieverts the Risø calibration results shown in Table 4.1 give the responses in terms of the ratio of the indicated values to the reference values in air kerma rate from the calibration sources and have been normalised to the response to ^{226}Ra. These latter values are given in Table 4.1 in parenthesis and the subsequent field intercomparison results given in Tables 8.5 in Chapter8 have been normalised to air kerma units.

Most electronic dose meters use either GM. counters or solid state devices for their detectors. Those with GM. detectors have similar energy responses to those given in Section 4.1.2. At the present time very little data exists on the air kerma response of electronic dosemeters having solid state detectors.

Table 4.1: Results of free field source calibration with electronic dosemeters

Dosemeter Type	Ra-226 Response	Co-60 Response	Cs-137 Response
Alnor RAD 101S	1.260	1.247 (0.990)	1.196 (0.949)
Alnor RAD 101S	-	1.209	1.150
Alnor RAD 101S	1.276	1.239 (0.971)	1.174 (0.920)
Alnor RAD 101S	1.309	1.310 (1.001)	1.237 (0.945)
Siemens EPD	1.123	1.070 (0.952)	1.205 (1.073)
Siemens EPD	1.094	1.050 (0.960)	1.170 (1.069)
Siemens EPD	1.136	Failed	Failed
Siemens EPD	1.103	1.049 (0.951)	1.189 (1.078)
Stephens Gamma Com	1.403	1.442 (1.028)	1.263 (0.900)
Stephens Gamma Com	1.241	1.230 (0.991)	1.159 (0.934)
Aloka Type PDM 102	1.136	1.097 (0.966)	1.204 (1.060)
Aloka Type ADM 102	0.859	0.778 (0.906)	0.921 (1.072)
Bristol Bleeper	1.358	1.364 (1.004)	1.260 (0.928)
Bristol Bleeper	1.381	1.375 (0.996)	1.252 (0.907)
Appleford	1.098	1.098 (1.000)	1.035 (0.943)
Appleford	0.977	0.962 (0.985)	0.916 (0.938)
SAIC PD1[1)]	1.163	1.069 (0.919)	1.146 (0.985)
SAIC PD1[1)]	1.142	1.068 (0.935)	1.180 (1.033)
SAIC PD2	1.052	1.071 (1.018)	1.203 (1.144)
Merlin DMC 90	1.173	1.170 (0.997)	1.320 (1.125)
FAG FH 41D-1	1.235	1.206 (0.977)	1.184 (0.959)

1) Dosemeter display in units, mR, of exposure.

NOTE: The values given in parenthesis are the responses normalised to the response from Ra-226.

The intercomparison results demonstrate that electronic dosemeter measurements of environmental radiation obviously require careful interpretation due to either the dosemeters' high cosmic responses or to their high inherent responses. Nevertheless it is encouraging that the estimates of the terrestrial air kerma rate give close agreement with that measured by active doseratemeters and TLDs. Compared to TLDs electronic dosemeters have the advantage that they can be directly read out *in situ*. They are thus very suitable for measurements during emergencies where the dosemeters can be read out *in situ* at frequent intervals.

4.1.7 Summary of active detectors

Table 4.2 summarises the main characteristics of the different types of active radiation detectors. Electronic dosemeters mostly use Geiger-Müller detectors and their characteristics are given in the table.

Table 4.2: Summary of active detectors.

Properties	**Geiger-Müller Counter**	**High Pressure Ionisation Chamber**	**Plastic Scintillator**	**Proportional Counter**
Radiation Sensitivity	Low	High	Low	High
Dose Rate Range (mGy h^{-1})	10^{-5} – 100 (7 decades)	10^{-5} –1 (6 decades)	10^{-5} –1 (6 decades)	10^{-5} –10000 (9 decades)
Inherent Background	High	Very Low	Low	Low
Photon Energy Response	Satisfactory	Good	Good	Adjustable
Cosmic Response	Differs from photon response	Correct	Correct	Differs from photon response
Angular Response	Good	Very Good	Satisfactory	Good
Operational Size and Weight	Small and Light	Bulky and Heavy	Bulky and Heavy	Small and Light
Detector Lifetime	Long	Long	Medium	Very long
Electronics	Simple	Sensitive	Complex	Sensitive
Battery Life	Long (months)	Medium (< 1 week)	Low (2 – 3 days)	Low (2 – 3 days)
Environmental Robustness	Good	Good	Poor	Poor
Price	Low	Very High	High	High

4.2. Passive Detectors

4.2.1. General

Passive detectors have obvious advantages for environmental measurements because they are small, cheap and have a wide measuring range and they also do not require *in situ* electronics or power supply. Passive detectors provide measurements of the dose integrated during a time interval (days to months), so that only an averaged dose rate for this period can be estimated. The routine procedure for a passive detector monitoring system involves three main steps: preparation of the detectors, field exposure and readout, [PIE83].

The necessity of a delayed process to obtain the data seems to be an important disadvantage for passive detectors, but they have some benefits that show during their use in environmental monitoring, e.g., the measurement of a field with dose rates highly fluctuating due to rapid changes in the weather conditions modifying the plume direction. In this case, the real impact on the environment and population could be better appreciated by measuring integrated doses in a large number of points distributed near the facility.

In the use of passive detectors, dose integration and dose evaluation are separate processes. Thus, a specific procedure in the laboratory is necessary to read the signal stored in the detectors. Then, the calibration factor and other corrections are applied to calculate the integrated dose. This procedure permits to assess the systematical uncertainties and to improve the statistical uncertainty using redundant detectors.

Usually the passive detector Laboratory is far from the control area, making it necessary to take into account the environmental transit doses. The estimates of the transit dose is normally done using an additional batch of detectors (Transit dosemeters) that will be kept during the exposure time of the field dosemeters in a storage jig with a low and known radiation level.

From this consideration, a minimum integration time has to be defined in the implementation of an environmental passive detector network. This interval may range between one day to one year, depending on the purpose of the measurement and the technical capabilities of the passive system. One to three months exposures are the most commonly employed periods for short term environmental

monitoring. Long term monitoring for one year is also frequently performed in order to determine annual doses and their variability.

A passive radiation detector Laboratory is commonly referred as the System, i.e., the equipment and procedures used for assessing the evaluated value. The system consists essentially of the following elements:

- Detector, a passive device with one physical property (such as the emitted light or optical density when processed) which can be directly related to a radiological quantity.
- Dosemeters, combination of detectors and suitable holder where the detectors are located during the exposure. The holder not only protects the detectors from the external agents (water, dust, contaminants) but it also provides adequate conditions for charge particle equilibrium.
- Reader, an instrument which is used to process the detectors after the exposure to ionizing radiation and to measure how much quantity of the sensible physical property is obtained.
- Additional equipment for performing ancillary processes such as annealing or cleaning: oven, ultrasonic cleaner, vacuum tweezers, irradiators.
- Documented procedures for converting the proper operation of the dosimetric system.

There are many types of passive detectors that are being employed in environmental monitoring. Solid state effects such as the photographic effect, track generation or luminescence have been applied in the developing of suitable detectors. In addition, other types of passive detectors (electret ion chamber, bubble detectors) are also being recently implemented in practice. However, the most widely employed environmental passive systems are based on luminescence detectors such as thermoluminescent (TLD), photoluminescents (PLD) or optically stimulated luminescence detectors (OSLD). Luminescence phenomena are named after the type of radiation used to excite or to stimulate the light emission.

Extensive and detailed descriptions of different passive systems are given in the literature, [OBE81, HOR84, McK95]. A continuous update of this information can also be found in the Proceedings of the International Conference on Solid State Dosimetry, [GOL93 and PET96].

Thermoluminescence detectors are available in different forms such as chips, rods, disks, cubes, powder, glass bulb or special cards including several detectors. The size of TL detectors is really small (usually not larger than 4 mm) and their indications can be considered as point readouts in the radiation field.

Photoluminescence detectors are in general larger than Tl-detectors. Typical dimensions of commercially available glasses are for instance 8.5 mm x 8.5 mm x 1.5 mm or 16 mm x16 mm x 1.5 mm. On the other hand normally only one detector is used in a badge. In some dosimetry systems the only detector can be scanned providing information like a multi TL-detector dosimeter.

The passive detectors are usually employed in groups of several individual detectors, allocated in a suitable holder or mini-phantom. As the size of the holder is small, very similar irradiation conditions can be expected for all the detectors. The holder must provide the adequate filtration to obtain charged particle equilibrium for the detected radiation quality. Normally, the holder is also designed to protect the detectors against dirtiness, liquids or light. Obviously, this point is particularly important in environmental monitoring.

In order to correct the energy response of the used phosphor, some passive detector holders contain different plastic and metallic filters. Angular and energy response of a dosemeter may be influenced by its design, specially by energy compensation filter in the holder. Moreover, some designs emanate from personal dosemeters combining several phosphors and filtration to get different response on the detectors and, using an adequate algorithm, to calculate the contribution of different photon energy components to the readout (discriminating dosemeters). This can be an important feature because normally the natural radiation spectrum is often unknown. Special holders can be necessary in some environmental applications such as high energy photon fields. In order to characterise the response of the TLD badge in these radiation fields, the implementation of specific categories in the type testing programmes could be convenient.

The quality and design of the new generation of passive detector readers have provided high quality instruments with good long term electronic stability, high sensitivity and range of measurement, compatibility with external computers and reliable heating systems. In some laboratories, the reader employed for personal dosimetry purposes is the same as for environmental measurements. In general, this is an acceptable situation because the strict quality control programs required for personal dosimetry systems are also adequate for environmental monitoring.

Different types of heating systems are now available on TLD readers: ohmic heating (planchet, hot finger), hot gas (linear, constant) and optical heating. Some TLD reader designs need to use an inert gas (usually nitrogen) for a better readout when low signals are detected and reduce infrared component

from the metallic parts. In general, all the actual TLD readers are appropriate to be used in environmental monitoring, and a major automation during the pellets (chip, rod) readout should be recommendable for the future.

The light emitted from the luminescent detectors when they are being processed is normally collected using a photomultiplier assembly which provides a signal to be processed in an adequate device (photon counting or pico-ammeter). The integrated current during the readout time is a good estimate of the total light emitted by the detector and, therefore, it can be directly related to the amount of ionizing radiation which was absorbed within the detector. When the relationship between heating time and heating temperature is known, i.e. linear, it is possible to obtain the glow curve as the instantaneous signal at the photomultiplier as a function of the temperature during the readout. When the heating profile is unknown or complex, a pseudo-glow curve from the detector will be still useful.

In environmental monitoring, TLD's are very often employed near the lower detection limit and thus environmental doses have to be evaluated working on signals from the detector presenting neither a very convenient signal to noise ratio nor TL to background ratios. In these conditions, conventional TL procedures that integrate all the light during the readout may not provide results with adequate quality. Evaluation methods based on the analysis of the glow curve features have demonstrated significant improvement in the TLD performance, especially for the measurement of very low doses. These methods can recognise anomalous readouts produced by contaminated dosemeters, defective readouts or dirtiness in the reader. Thus, it is possible to establish rejection criteria based on the shape of the glow curve that with the conventional method would be impossible. Another advantage of glow curve analysis (GCA) is its capability for estimating background contributions individually and in the same readout which produces the dosimetric signal. The conventional method is normally based in separate measurements of the dark current and the zero dose reading from another group of dosemeters, being in many cases more complicated and inaccurate than GCA. Even this technique is still not in common use, recently developed GCA computer programs allow for practical implementation of this method for environmental monitoring.

In contrast to TLD systems there are only a few PLD systems commercially available and only one manufacturer offers systems which makes use of the modern UV pulsed laser technique. In this reader a nitrogen gas laser is used for the UV light-excitation of the glass. The time dependent fluorescence light intensity is integrated in two different periods, subtracting the radiation independent long term component from the radiation induced short term component. For improvement of the

random uncertainty usually 20 laser pulses within one second are used for each readout. Within a second light path a photo diode permits to correct fluctuations of the laser pulse intensity. Optical filters in front of the multiplier reduce the intrinsic PL intensity. Automatic glass scanning may be carried out optionally by two movable diaphragms, a horizontal one in the fluorescence light path and a vertical one in the UV light path in order to estimate the effective photon energy and to give some information about the radiation incidence.

Prior to use, passive detectors must be annealed in order to eliminate any signal due to previous exposures and to optimise the detector properties. In the case of PLD annealing is carried out at 400°C for 1 hour.

TLD reader anneal is a suitable procedure but practical considerations make it only appropriate when only a few detectors are involved. However, the use of automatic TLD readers permits to consider the reader anneal as useful for a great number of readouts. On the other hand, TLD annealing in an oven permits the simultaneous and homogeneous anneal of a large detector number and it can be suitable for medium-large scale laboratories. It should be necessary not only to check the temperatures and heating times for each anneal but also to test the homogeneity in the oven. Thus, computerised ovens are strongly recommended. Attention has to be equally given to the reproducibility of the cool down stage as for some materials the final sensitivity also depends upon this stage. Oven anneal strongly influences the glow curve shape and induces a reduction on the sensitivity of dosemeters, when compared with reader annealed detectors. This effect is proportional to the rate of cooling of the dosemeters, which is normally lower using oven anneal. In general, oven anneal provides better reproducibility and long term stability properties.

It is important to mention the special care that should be taken in using all the materials and objects related with the environmental passive system, including detectors, holders and shielding for low dose stations. Contamination checks and low counting methods are recommended to test any residual radioactivity that could affect the measurements. Tweezers should be used when pellets are employed. Special attention must be paid in the storage of the pellets trying to keep an identification system if individual corrections are performed for each detector. The maintenance and the cleanliness of the mechanical, electronics and optical parts of the reader are also important. Therefore, the laboratory must be kept tidy and neat all the time.

4.2.2. Thermoluminescent detectors (TLD)

Thermoluminescence (TL) is the light emission occurring during heating of the solid state detector that has already absorbed some energy from incident ionizing radiation upon the detector. Thermoluminescent materials (also called phosphors) are able to store part of the incoming energy from ionizing radiation with sufficient stability. Impurities intentionally added (doping material) to a host lattice create new energy levels within the band gap between the valence and conduction bands. These new levels act as traps for charge carriers (electrons/holes) created during the material irradiation, preventing the prompt recombination.

When the irradiated phosphor is heated up to an adequate temperature (200-400°C), the trapped charges will receive enough energy to be liberated and cause recombination processes with optical light emission, restoring the phosphor to the pre-irradiation condition. In fact, one of the most important TLD advantages is its reusability, which permits for correction of sensitivity for the each individual detector and the recording of its history.

A wide variety of dielectric materials exhibiting TL included rocks, minerals, artificial inorganic single crystals and polycrystalline solids, glasses and ceramics, organic compounds such as polymers, certain biological materials. Most studied materials are those that are used in radiation dosimetry applications.

Several varieties of calcium fluoride and calcium sulphate are used World wide. These materials show a high sensitivity that permits the detection of doses below 10 μGy. However, due to the high effective atomic number ($Z>15$), they also present a significant over-response at low photon energies (<50 keV) when usual environmental quantities are measured (kerma in air, ambient dose equivalent). In case of necessity this effect can be corrected using adequate filters over the TL detectors. Furthermore, TL multi-detector designs can provide not only the dose but also information on the photon energy distribution of the radiation field and sometimes the mean photon energy of the radiation field.

Materials with an effective atomic number similar to soft tissue such as lithium fluoride or lithium borate have an inherently good response to measure absorbed doses in tissue, water or air. Although these phosphors show lower sensitivities than the previous group, LiF:Mg,Ti is probably the

TL material more used in TLD environmental networks and it is commonly used for reference measurements.

In the last ten years, near tissue-equivalent phosphors with high sensitivity have been developed in different laboratories (LiF:Mg,Cu,P in China and Poland; α-Al_2O_3:C in Russia). These materials are very promising in their environmental applications, and several groups are now working in their complete characterisation and implementation in the routine monitoring programmes.

Figure 4.2.1 shows which TLD are used in practical environmental monitoring. Data are from the Eleventh International Intercomparison of Environmental Dosemeters, organised by the U.S. Department of Energy and which was held at the Idaho National Engineering Laboratory (USA) during 1996 and with more than 120 participants from 20 countries, [KLE99].

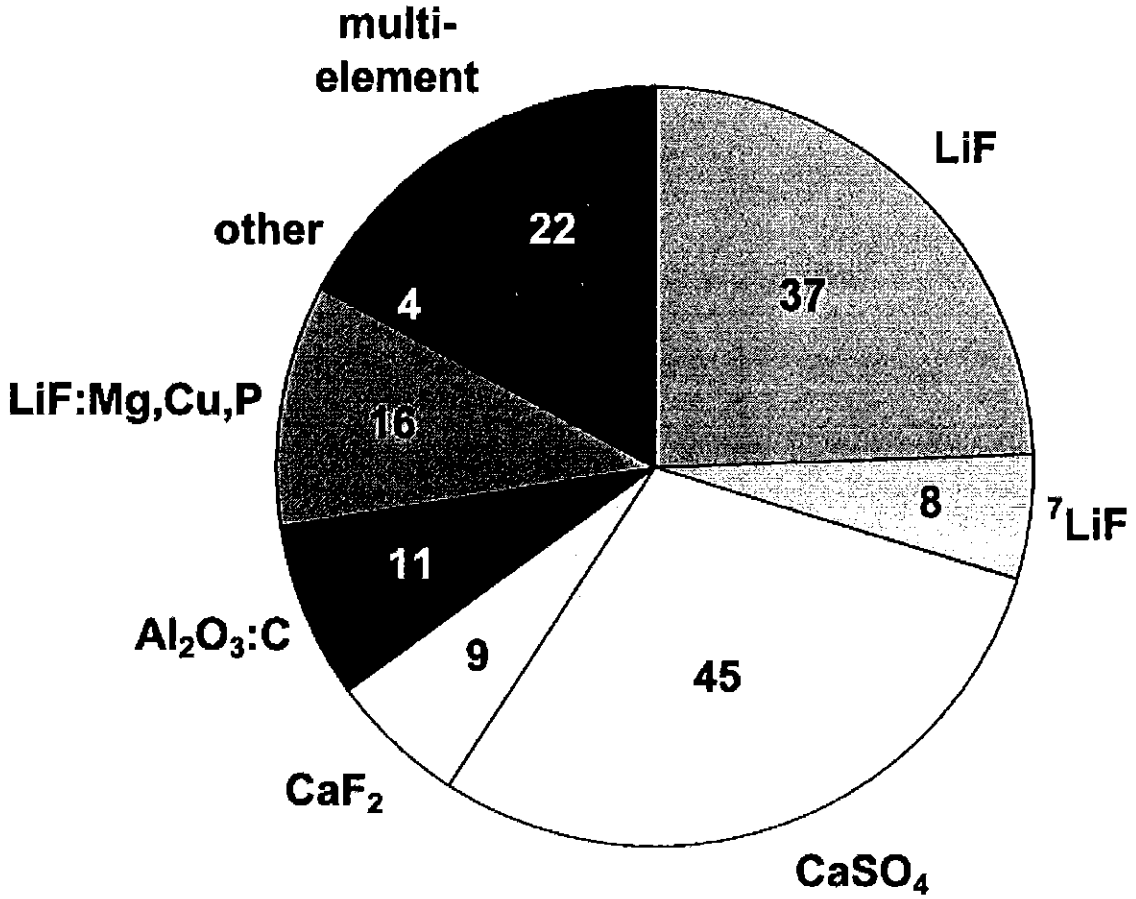

Figure. 4.2.1: TL materials commonly employed for environmental monitoring. Dosemeter material submittted to the 11th International Intercomparison of Environmental Dosemeters, [KLE99]. The numerical values are the total numbers of dosemeters of each material used during the intercomparison.

Table 4.3: TL material characteristics,[McK95].

Material	**LiF**		**$Li_2B_4O_7$**	**CaF_2**		**$CaSO_4$**		**Al_2O_3**
Dopants	Ti,Mg	Mg,Cu,P	Cu	Mn	Dy	Dy	Tm	C
Zeff	8.2		7.4	16.3		15.3		10.2
Energy Response 30keV/1.25 MeV	1.3	1.0	0.9	15	15	12	12	2.9
Fading (dark)	Low	Low	Low	High	High	Low	Low	Low
Light Sensitivity	Low	Low	High	Low	Low	Low	Low	High
Main peak (°C)	210	215	200	260	200 240	220	220	185
Sensitivity relative to TLD-100	1	30	2	5	15	15	15	40
Minimum Measurable Dose (μGy)	10	0.5	1	10	1	1	1	0.5
Thermal Treatments (OVEN)								
* Pre-Exposure	1 h 400°C + 2 h 100°C	10 min 240°C	30 min 300°C	10 min 400°C	1 h 400°C	1 h 400°C	1 h 400°C	None
* Post-Exposure	10 min 100°C	10 min 130°C	5 min 100°C	None	10 min 115°C	10 min 120°C	10min 120°C	None
Readout Cycle								
* Maximum Temperature	300-400°C	240°C	350°C	400°C	400°C	350-400°C	350-400°C	350-400°C
* Heating rate	Independent	Independent	Independent	Independent	Independent	Independent	Independent	< 5°C/s

Table 4.3 summarises the relevant characteristics of the most commonly used TL phosphors in environmental monitoring. The suggested thermal treatments and readout profile are based on recent publications which offer detailed discussions about this subject.

4.2.2.1. Lithium fluoride

The phosphor LiF:Mg,Ti (Z=8.2) is probably the widest used phosphor in dosimetry. It was developed in the 1940s and it is usually mentioned as the reference phosphor against which the newer materials are assessed. Nowadays, the material is available in numerous forms, being employed from powder to multi-chips cards.

LiF:Mg,Ti shows a complex glow curve, which depends on detector treatment, reading procedure, radiation type, dose level, etc. The "dosimetric peak" is at about 230°C and many studies have been performed to optimize its characteristics such as thermal fading, stability, sensitivity or linearity. As a result of this, many procedures have been proposed for the annealing, readout and handling, and the performance of the TLD system depends highly on the practical procedures implemented (Figure 4.2.2).

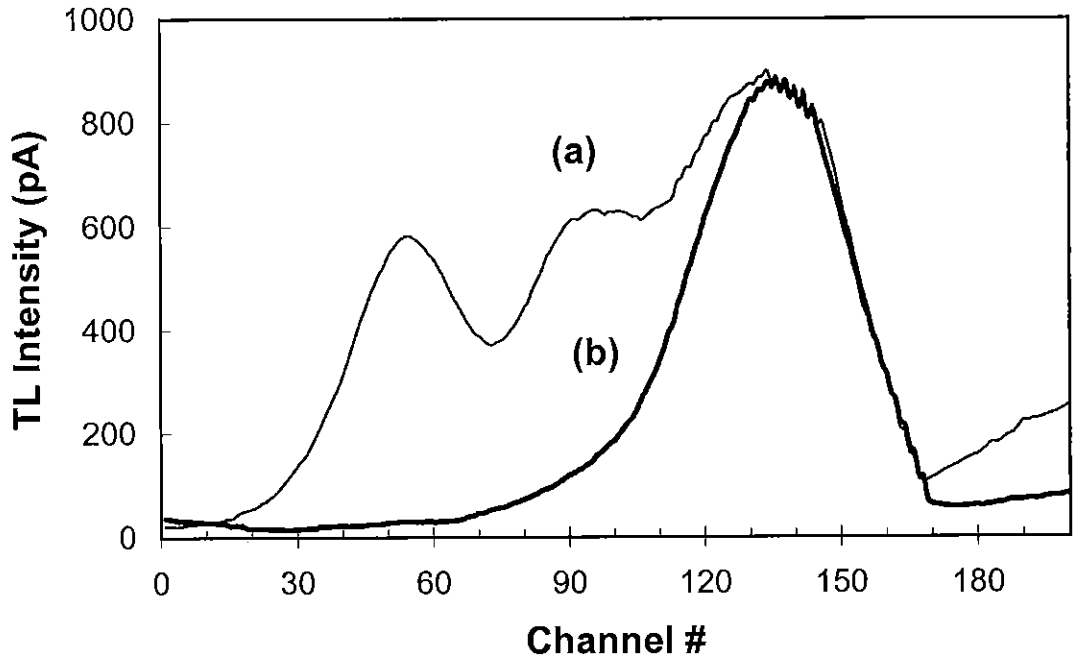

Figure 4.2.2: Glow curve from a LiF:Mg, Ti detector as obtained in a planchet reader (linear heating 7°C/s). Imparted dose: 40 μGy.
(a) Reader anneal
(b) Oven anneal: 1 hour 400°C + 2 hours 100°C before exposure and 10 min 100°C before readout.

One of the techniques commonly employed for the study of LiF:Mg,Ti is the numerical glow curve analysis, GCA. This approach has permitted not only to understand some basic aspects of thermoluminescence, but also to provide a better dose assessment, [DEL90].

The three-dopants lithium fluoride variety LiF:Mg,Cu,P can be considered as the most promising TL materials for some dosimetric uses. It combines relevant advantages of the traditional LiF:Mg,Ti (dosimetric peak stability, negligible influence from light or moisture) with properties such as hypersensitivity and low self-dose, [ZHA93]. A detectable threshold dose as low as 60 nGy can be achieved using this phosphor. Therefore, its use in environmental monitoring is very interesting. However, the material also shows under-response for low energy photons for the radiation quantities air kerma or ambient dose equivalent, [OLK93].

The LiF:Mg,Cu,P glow curve is more simple than the curve of LiF:Mg,Ti, with an enlarged main peak around 245°C and 2-3 low temperature peaks (Figure 4.2.3). There are 1-2 high temperature peaks which might be responsible for the high residual dose obtained in several applications.

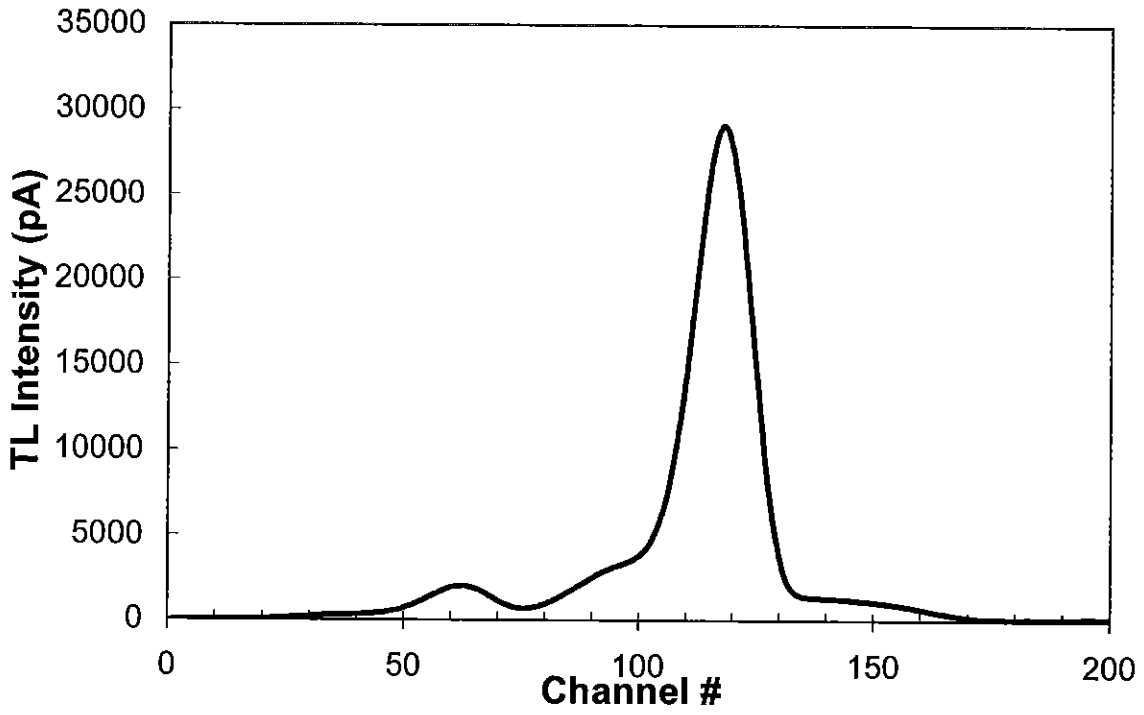

Figure. 4.2.3: Glow curve from a LiF:Mg, Cu,P detector as obtained in a planchet reader (linear heating 7°C/s). Imparted dose: 40 μGy.

Some studies on the reduction of the residual dose have shown that there is a practical temperature limit around 240°C. If the detectors are heated above this value, a decrease in sensitivity and a greater dispersion have been reported. Thus, special care must be considered when adjusting the thermal treatments and readout cycle using this phosphor, [PIT90 and SAE96a].

4.2.2.2. Calcium fluoride

Calcium fluoride doped with manganese, dysprosium or thulium, are highly sensitive but non tissue-equivalent phosphor (Z=16). These phosphors demonstrate highly complicated glow-curves, composed of several peaks (Figure 4.2.4). Even the single glow curve offered by CaF_2:Mn (TLD-400) is in fact a superposition of several peaks very close together to each other. The other calcium fluoride phosphors show complicated glow curves structures containing up to six different peaks in the range 100-300°C. Moreover, some of these peaks are LET dependent and a detailed interpretation based on the glow curve analysis can be necessary in order to obtain reliable results.

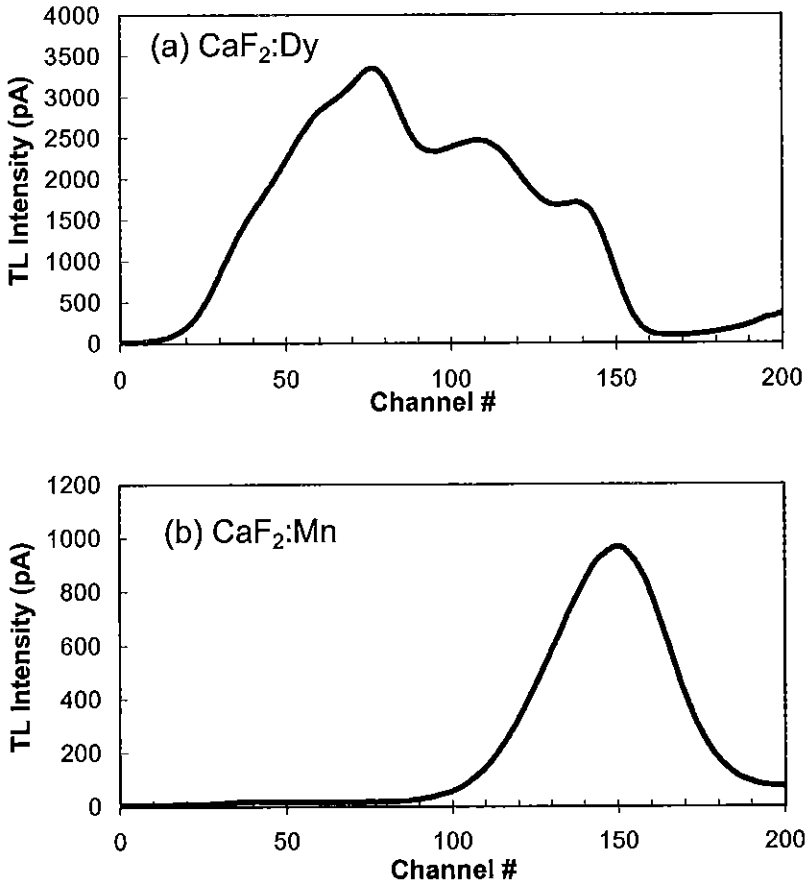

Figure. 4.2.4: Glow curve from calcium fluoride detectors as obtained in a planchet reader (linear heating 7°C/s). Imparted dose: 40 μGy. (a) CaF_2:Dy (b) CaF_2:Mn

4.2.2.3. Calcium sulphate

Calcium sulphate is another high sensitive phosphor but it is not tissue-equivalent (Z=15). Several dopants have been employed to optimise thermal fading and light sensitivity. Nowadays calcium sulphate doped with dysprosium (Harshaw TLD-900) or thulium (Panasonic) are widely used in environmental measurements.

The glow curve from calcium sulphate shows one wide dosimetric peak about 280°C, and one or two low temperature peaks ranging in 80-120°C (Figure 4.2.5). In order to eliminate this contribution and to reduce thermal fading, a pre-readout anneal to 100-120°C can be carried out.

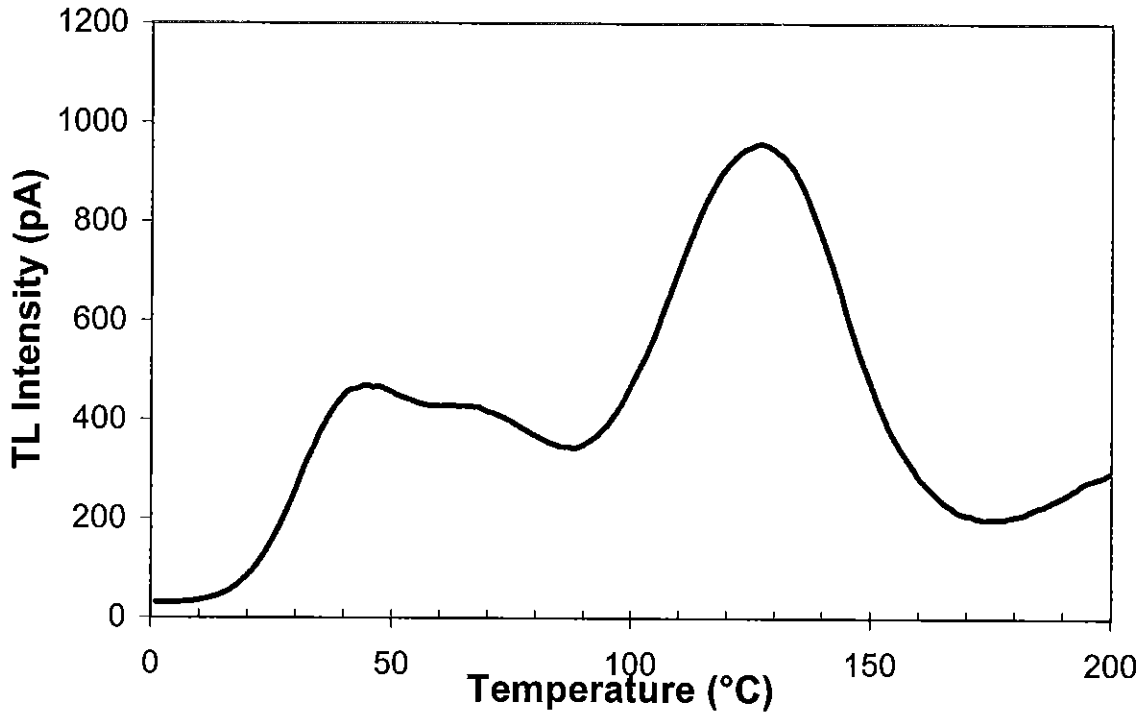

Figure. 4.2.5: Glow curve from a $CaSO_4$:Dy detector as obtained in a planchet reader (linear heating 7°C/s). Imparted dose: 40 μGy.

4.2.2.4. Aluminium oxide

The history of alumina detectors as a radiation dosemeter looks back to the 1950s, when a large number of materials were investigated. Some natural alumina crystal were found to be more favourable than lithium fluoride. Several kind of alumina detectors are now available, characterised by large measuring range, convenient glow curve and optimal emission spectrum.

Much effort is devoted to studying the properties of α-Al_2O_3:C, which was developed in Russia during the late 1980s, [AKS90]. It is a hypersensitive phosphor (up to 40 times higher sensitivity than LiF:Mg,Ti) with a moderate over-response to low energy photons (Z=10.2).

The phosphor shows a very simple glow curve, with only one wide peak about 210°C (Figure 4.2.6). The glow curve can be significantly altered depending on the heating rate during readout, inducing important reduction on the sensitivity when the heating rate is increased.

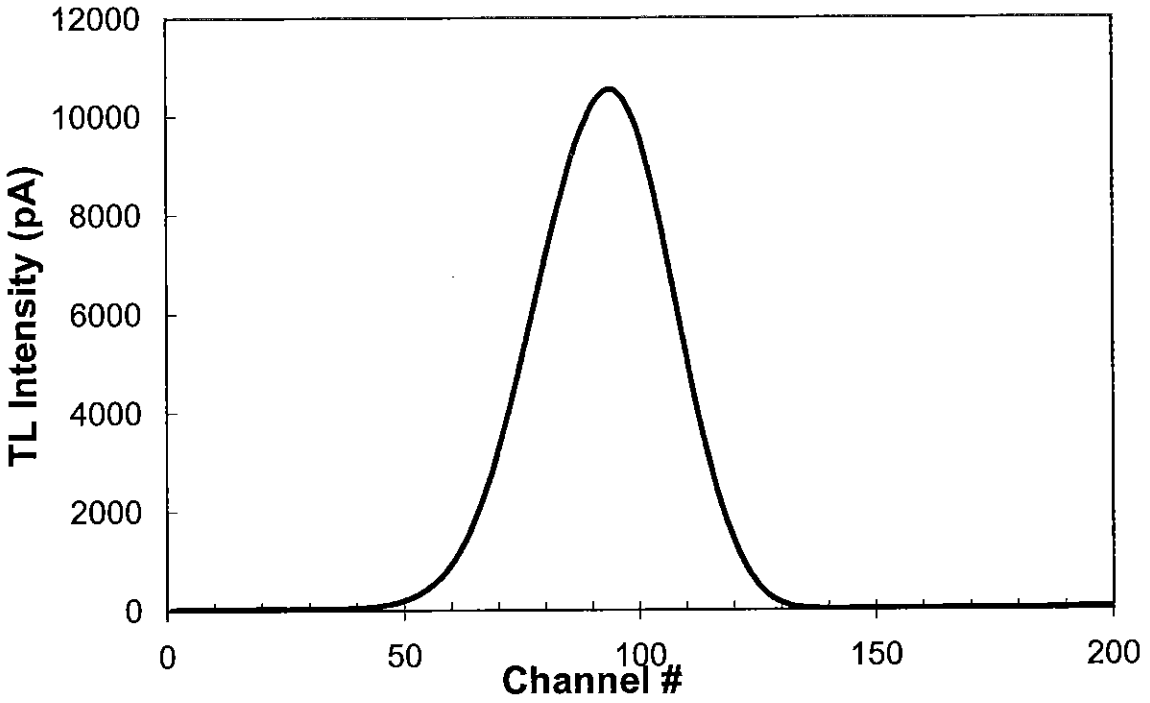

Figure.4.2.6: Glow curve from an Al_2O_3:C detector as obtained in a planchet reader (linear heating 7°C/s). Imparted dose: 40 μGy.

Excellent reproducibility and negligible thermal fading (<3% a year) has been reported for aluminium oxide. The most important disadvantage of this material is its light sensitivity. Light

induced fading up to 40% and noticeable background increase have been reported when the detectors are illuminated with 300 lux (white light) for 5 hours.

4.2.3. Photoluminescent detectors (PLD)

Photoluminescent dosimetry is based on the formation of fluorescence centres in silver activated phosphate glass dosimeters (PLD). When exposed to UV-light, radiation induced PL fluorescence light is emitted, the intensity of which is proportional to the absorbed dose. The dose information is very stable and does not get lost during readout, which therefore may be repeated at any time during accumulation.

Since 1965 glass dosimeters in a spherical tin capsule for energy compensation have been applied in large scale use for environmental monitoring in Germany. During readout the glasses have been excited by a mercury UV-lamp. Because of the intrinsic pre-dose of more than 1 mGy exposure periods of at least six months have been necessary.

The new generation of PLD systems make use of the low-Z glass in a flat capsule with a small energy compensation filter and during readout a pulsed UV-laser excitation. This readout technique allows to separate individually the intrinsic pre-dose from the radiation induced reading by utilising different decay times of the two reading components, resulting in a pre-dose of a few μGy with a standard deviation ±1 μGy. Readers with fully automatic readout are commercially available now and, a commercial system has received the PTB pattern approval both as an individual and as an area dosemeter, [BUR96a and BUR96b].

The essential advantages of this type of glass dosimeters in environmental monitoring are the low internally subtracted pre-dose, the long-term stability of the PL, which is insensitive to ambient influences like temperature and humidity and results in low fading without any temperature treatment before readout, the good batch homogeneity, the possibility of re-read or dose accumulation, the high reproducibility of the one element detector reading and the ability to indicate photon energy during fully automatic readout.

4.2.4 Optically stimulated luminescence detectors (OSLD).

Rather than heating a dosemeter (TL) some materials exhibit optically stimulated luminescence (OSL) when they are exposed to a particular light spectrum. Such detectors are Al_2O_3:C single crystals which have been used as OSL dosemeters for rapid assessment of environmental photon dose rates. It has been shown that Al_2O_3:C Possess higher OSL sensitivity than TL sensitivity. In TL measurements thermal quenching is a major problem that crucially depends on the heating rate used and, therefore, the all-optical nature of the OSL procedure is an obvious advantage as it obviates the necessity to heat the material and thereby avoiding destruction of the luminescence signal.

The OSL stimulation spectrum, i.e. OSL versus stimulation wavelength of Al_2O_3:C shows a smooth broad stimulation resonance peaking around 500 nm and thus very suitable for, for example, using a filtered halogen lamp producing a broad wavelength band from 420-550 nm as the stimulation light source. The OSL signal from Al_2O_3:C is typified by a bright rapidly decaying curve. Fig. 4.2.7.a. shows OSL decay curves from Al_2O_3:C dosemeters exposed over 15 and 72 hours to the natural environmental radiation. Fig. 4.2.7.B. sows the response of Al_2O_3:C to short term exposures to the environmental background radiation compared to that of a high pressure ionisation chamber, [BØT96 and BØT97].

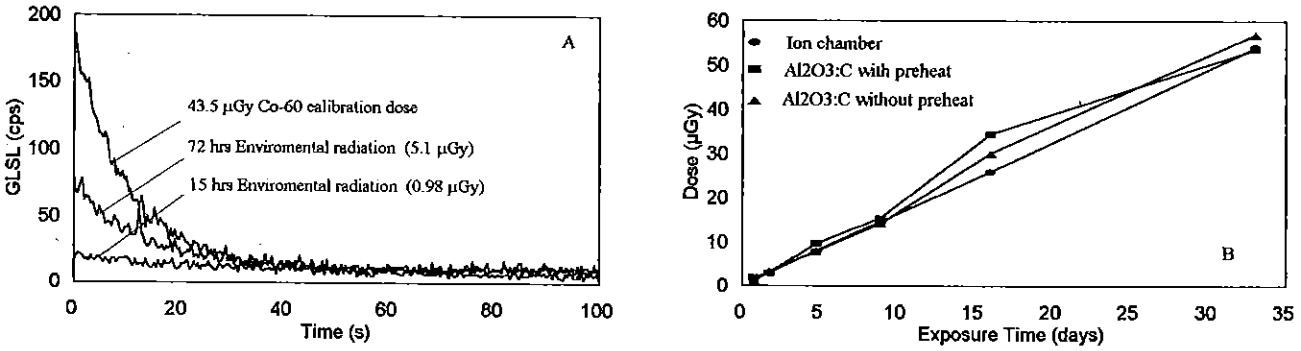

Figure 4.2.7 A OSL decay curves from Al_2O_3:C dosemeters exposed over 15 and 72 hours to the natural environmental radiation representing integrated doses of 0.98 and 5.10 µGy, respectively, compared to that from a 44 µGy ^{60}Co gamma calibration dose.

Figure 4.2.7.B Short-term OSL measurements of the natural environmental photon radiation using Al_2O_3:C (with and without preheat 100°C/30 s applied prior to readout) carried out over different time periods ranging from 1 to 33 days compared with data obtained by continuously monitoring high pressure ionisation chamber (Reuter Stokes RS-111).

5. DETERMINATION OF PROPERTIES OF INSTRUMENTS

5.1. General

The general relationship between the reading of an instrument, $M_{Total,}$ at a discrete photon energy, E, the response, r, of the instrument to the radiation field, the kerma rate, $\dot{K}$, in the field and the background reading, R_i, due to the electronic noise, leakage currents and/or inherent radioactivity of the instrument is given by:

$$M_{Total} = r\,\dot{K} + R_i \qquad (5\text{-}1)$$

But this relationship is only valid for a radiation field with monoenergetic photons or particles and for normal incidence of the photons. The response r can be dependent on the parameters listed below:

- Photon (particle) energy E
- Kerma rate, $\dot{K}$
- Incidence direction of photons, φ
- Ambient temperature, T
- Air pressure, p
- Humidity, h.

Therefore the response r is given by the functional relationship:

$$r = f(E,\dot{K}, \varphi, T,p,h) \qquad (5\text{-}2)$$

In a situation where the photons have an energy distribution, as in the environmental radiation field, the kerma rate depends on the spectral distribution of the fluence rate in this field or lastly on the photon energy

$$\dot{K} = g(E) \qquad (5\text{-}3)$$

The contribution of photons in an energy interval dE to the reading dM_{Total} is then given by

$$dM_{Total}/dE = g_E\,(E) f_e\,(E,g(E), \varphi, T,p,h) \qquad (5\text{-}4)$$

The equation for the instrument's reading in a radiation field with photon energies between E_1 and E_2 must be written as :-

$$M_{Total} = \int_{E_1}^{E_2} g(E) f(E, g(E), \varphi, T, p, h) dE + R_i \qquad (5\text{-}5)$$

Where R_i is the inherent background reading.

This equation shows the very complex relationship between a reading M_{Total} of an instrument, the properties of the detector, represented by r and the kerma rate g(E) in a field with an energy distribution of the photons or ionising particles.

For the determination of the instrument's response r for photons or particles with a discrete energy equation (5-1) can be used taking into account the listed parameters. If this response r is not dependent on the energy this value is also valid for measurements in radiation fields with photons or particles of various energies.

For the determination of the response the parameters should be selected within the range of the later operation of the detector (kerma rate, incidence direction of the photons, ambient temperature, air pressure and humidity).

In a situation where the kerma rate $\dot{K}_s$ in the field of an artificial source is of the same order as the kerma rates $\dot{K}_t$ in the terrestrial radiation field and $\dot{K}_c$ in the cosmic environmental field the relationship between the reading, the responses r_c, r_t and r_a to these components and the kerma rates can be formally written as:

$$M_{Total} = [\, r_c(\dot{K}_c) + r_t(\dot{K}_t) + r_a(\dot{K}_a)] \qquad (5\text{-}6)$$

But if the response is dependent on the energy each term of this equation contributing to the reading of the kerma rate must be replaced by equation (5-5).

In this case a much more sophisticated evaluation of the response to this complex radiation field is necessary. This is illustrated in Section 9.4.2. But the knowledge of the detector responses to the components in this field and of the inherent background is indispensable for the correct evaluation of such measurements.

5.2. Active Detectors

The methods for the determination of the essential properties of environmental dose rate meters are described in the IEC standard "Portable, transportable or installed equipment to measure X or gamma radiation for environmental monitoring IEC 61017 Part 1 Ratemeters" [IEC91a] and "IEC 61017 Part 2 Integrating assemblies," [IEC94]. It is recommended to use the test procedures given in these standards for the determination of the instrument's properties listed below. Table 5-1 lists the radiological, environmental and electrical specifications in the two IEC 61017 standards, Part 1 and Part 2.

The functional relationship of these characteristics between the influence quantity and the instrument's response is needed for a precise evaluation and interpretation of environmental measurements.

These determinations should not replace qualification tests according to the IEC standard.

Table 5.1: Radiological, environmental and electrical specifications for "Portable, transportable or installed equipment to measure X or gamma radiation for environmental monitoring, Part 1 Ratemeters", [IEC91a] and Part 2 Integrating assemblies, [IEC94].

Characteristic under test or influence quantity	**Range of values of influence quantity**	**Limits of variation of indication**
Relative intrinsic error	Effective range of measurement	± 15%
Radiation energy Photon	50 keV to 1.5 MeV	± 30%
Photon	6 MeV	± 50%
Beta	E_{max} = 2.27 MeV	< 2%
Angle of incidence – Photon 662 keV [1]	0° to ± 120°	± 20%
60 keV [1]	0° to ± 90°	± 30%
	± 90° to±120°	± 50%
662 keV and 60 keV [2]	All angles	± 20%
662 keV [3]	0° to ± 60°	± 20%
60 keV [3]	0° to ± 45°	± 30%
	± 45° to ±60°	± 50%
Retention of reading	1 hour	± 2%
Air kerma rate dependence	10 nGy h^{-1} to10 mGy h^{-1}	<± 15%
Overload	10 times range maxima	Indication > full scale
Power supply voltage –		
Primary batteries	After 40 h intermittent use	± 10%
Secondary batteries	After 12 h continuous use	± 10%
AC mains (if applicable)	88% to 110% of operating voltage	± 10%
	57 Hz to 61 Hz or 47 Hz to 51 Hz	± 10%
Ambient temperature	-10°C to + 40°C	± 20%
	-25°C to + 55°C	± 50%
Relative humidity	40% to 90% at + 35°C	± 10%
Mechanical shocks	300 m s^{-2}	Operates within specifications
Electromagnetic field of external origin	Stated by manufacturer	Stated by manufacturer
Magnetic field of external origin	Stated by manufacturer	Stated by manufacturer

1) For detector axis of symmetry along calibration direction axis.

2) For detector axis normal to calibration direction axis.

3) Plane perpendicular to detector axis normal to calibration direction axis.

5.2.1. Energy dependence of the response

For the determination within the photon energy range of the intended use the procedures given in chapter VII Sub-clause 7.2.2 of the IEC standard should be used. The energy requirements of this IEC standard are that the instrument's energy dependence should be within ±30% from 50 keV to 1.5 MeV and within ±50% at 6 MeV.

The response should be determined using the following reference radiations:

- filtered X-rays 60, 87, 109, 149, 185 and 211 keV, low air kerma rate series. (see ISO standard 4037/Part 1), [ISO96]
- gamma radiations from ^{241}Am (59.5 keV), ^{137}Cs (662 keV) and ^{60}Co (1.17 and 1.33 MeV), [ISO96].

If the energy response is required below 60 keV then radiations from the filtered X-rays of 8, 17, 26 ,30 , and 48 keV from the low air kerma rate series of the ISO standard 4037/ Part 1, [ISO96], should be used.

If the instrument is to be used to measure environmental air kerma rates in the area surrounding a nuclear power station producing radiation up to 9 MeV, it will also be necessary to determine the response up to this energy, [ISO96].

The conditions for the production of these ISO radiations are given in [ISO96]. The requirements for the standardisation of the reference radiation fields are given in ISO standard 4037/ Part 2, [ISO97] and the techniques for calibrating the instrument in the reference radiation fields are given in ISO standard 4037/ Part 3, [ISO99].

5.2.2. Kerma rate dependence of the response

The procedures for the determination of relative intrinsic error are given in Sub-clause 7.1.2, of [IEC91a] and [IEC94], it is recommended to use the method in the paragraph "Type test".

For an instrument to comply with this standard the relative intrinsic error shall be within ±15% over the whole effective range of the instrument, this excludes any uncertainty associated with the determination of the calibration air kerma rate. Chapter 6 gives recommendations on the calibration methods to be used for the low rates applicable to environmental instruments.

5.2.3. Directional dependence of the response

It is recommended to use the procedures for the determination of the variation of the response with angle of incidence as given in IEC 61071-1, Sub-clause 7.3.2, [IEC91a]. This standard has many requirements for directional response but one of the main requirements is that the instrument's response to Cs ^{137} (662 keV) should be within ± 20% for angles from 0^0 to $\pm 120^0$

5.2.4. Internal background

The contribution R_i to the reading arises from any internal radioactive contamination or from the electronic noise of the instrument.

R_i can be observed as the reading in a radiation-free environment, i.e. one, which is shielded against the cosmic and the terrestrial radiation. The cosmic radiation is effectively eliminated at a depth of 600m below ground in a mine.

The remaining terrestrial contribution from the local rocks can virtually be eliminated within a shielding of 10 cm selected lead with low inherent radioactivity or in a pure rock salt area where the contamination of ^{40}K is very low, e.g. 2-3 Bq kg^{-1} yields an air kerma rate of about 0.6 nGy h^{-1}, [CEC89 and CEC90].

5.2.5. Cosmic ray response, r_c

The response of an instrument to the complex field of cosmic radiation can be determined in a pure cosmic radiation field. This is approximately realised on a fresh water lake or at sea where the water depth is at least 5 m depth and at a distance of about 1km from the flat land in order to eliminate

the terrestrial radiation. The vessel on which the measurements are performed has to be constructed from materials of low inherent radioactivity.

The reference values for the cosmic radiation are given as a function of the geographical position, the altitude above sea level, the air pressure and temperature, the seasonal variation and the periodic variation with the solar cycle are given in the following references [UNSC77 and GIB93].

The cosmic ray response, r_c, is the ratio of a reading of a dose rate meter calibrated in air kerma rate to a reference value of the air kerma rate for the cosmic radiation, $R_c / \dot{K}_c$.

This response is only valid for cosmic radiation fields of the same composition. The composition varies for example with the altitude above sea level, so that new determinations of the responses are required for different altitudes.

The contribution of the internal background, R_i, has to be subtracted from the reading R_c before calculating the response.

5.3 Passive Detectors

5.3.1. Dose evaluation

Passive environmental monitoring systems provide an indirect method to estimate the amount of ionizing radiation which had reached the detector. As a result of the proper operation of the system, measurements of emitted light from every detector are obtained, which must be converted to the adequate estimate of the radiation quantity. This process can be summarised as follows:

$$D = [M\ N\ ICF\ F_{ad}\ F(E,\Omega)] - Dt - SD \qquad (5\text{-}7)$$

D = field dose

M = detector readout, non radiation induced component subtracted

N = calibration factor

ICF = individual correction factor (ICF=1 for batch calibration)

F_{ad} = fading correction factor

$F(E,\Omega)$ = energy and angular response correction factors

D_t = transit dose

SD= self-dose correction

The calibration factor N enables to convert the detector readout M (normally expressed in units of electric charge or counts) to the desired radiological quantity. The irradiation of a calibration batch should be performed at least once a year in a Meteorological Laboratory which would be traceable to a Primary or Secondary Radiation Metrology Laboratory. The proper conditions for calibration include free in air geometry and a collimated field from a source. The calibration procedure should include calculation of N and its uncertainty using adequate methods. In order to check that N remains stable, a pseudo-calibration batch irradiated at an auxiliary irradiation facility should be used for each monitoring period.

Batch homogeneity from the manufacturers is one important parameter that affects the standard deviation from sample to sample. Most of the manufacturers provide detector batches with relative standard deviation in the range 5-10%. This value needs to be improved when accurate measurements are required, but generally the detector price increases with better batch homogeneity. To overcome this problem the use of an individual correction factor ICF for each detector is highly recommended. Using ICFs not only improves reproducibility (from 5% to 1-2%), but also provides a valuable quality control tool which permits to monitor the real capability of each detector during its lifetime. The calculation of ICFs implies several irradiations (3 to 5 times) of a large number of detectors (at least 50), in order to compute the single detector relative sensitivity within the batch and the repeatability of each detector. A simple irradiation device such as self-contained panoramic irradiator or turntable irradiator should be adequate for this purpose because the only requirement is a homogenous irradiation of the batch.

The calibration procedure for glass dosemeters is in some aspects more easy and reliable, because an ICF is not necessary, the calibration glass for the absolute calibration can be used at least for three months and any instabilities of the dosimetry system during readout is controlled by a built-in glass, which is automatically re-measured after 20 readouts of routine glasses.

A fading correction factor F_{ad} should be applied when the fading cannot be reduced sufficiently by physical methods. The fading correction factor F_{ad} is defined as the ratio of the response of the calibration detectors to the response of the fading control detectors after subtraction the background component, having in mind that this factor includes all long-term influences on the dosemeter component (see Section 5.3.3.3.).

The photon energy and angular responses correcting factor $F(E,\Omega)$ takes into account the response for a more typical radiation energy and direction found in the field than used for the calibration (see Section 5.3.2.3).

Passive detectors need to be prepared, packed, transported to the field site and, after the field exposure, returned to the laboratory for the readout. Therefore, the detectors receive not only the dose in the field, but also undesired doses during these procedures. The transit dose D_t is a measure of this additional contribution and it should be subtracted from the field readouts (see Section 5.3.3.2.).

Finally, self-dose SD should be also considered. Sources for self-dose are intrinsic to the detector (radioactive traces) and radioactive compounds in the holder material, specially metallic filters (see Section 5.3.3.1.).

In summary, the proper dose evaluation for a passive monitoring system involves many parameters. Some of them can be considered as permanent properties because they are independent of changing aspects during the monitoring period. These parameters are normally determined during type testing and they provide the performances and features of the system. The criteria and procedures for environmental radiation monitoring systems using passive dosemeters are described in some international standards [IEC91b], including tests for linearity, batch homogeneity, reproducibility, detection threshold, photon energy response, angular response and stability,(Table 5.2).

The second type of parameters are related to operational system tasks which can be affected by unstable or out-of-control factors from one monitoring period to the next period. Therefore, the changing properties are far from remaining as a constant and they need to be determined in every monitored period.

Table 5.2: Performance requirements for environmental TLD systems with minimum period of use of seven days E(7 d) and thirty days (30 d), [IEC91b].

Pereformance characteristic	**Range of values of influence quantity**	**Performance requirements**
Batch homogeneity	Reference dose is ten times the required detection threshold limit: E(7 d): 0.10 mSv; E(30 d): 0.30 mSv	< 30%
Reproducibility	Reference dose: E(7 d): 0.05 mSv; E(30d): 0.20 mSv	< 7.5%
Linearity	Dose range: E(7 d): 10μSv-100 mSv E(30d): 30 μSv-100 mSv	< 10%
Stability of dosemeters under various climatic conditions	30 d standard test conditions 90 d standard test conditions 30 d at 50°C, 65% relative humidity 30 d at 20°C, 90% relative humidity	< 5% < 10% <20% < 20%
Detection threshold	Standard test conditions	E(7 d): <10 μSv E(30 d): <30 μSv
Self-irradiation	30 d storage under standard test conditions	<30 μSv
Residual signal	Previous dose of 10 mSv Response dose level of 0.20 mSv	Detection threshold not exceeded and change in response lower than 10%
Effect of light exposure on the dosemeter	Light exposure of 1000 $W.m^{-2}$ for 24 hours and one week	Detection threshold not exceeded and change in response lower than 10% when compared to dark storage
Photon energy response	Photon energy range: 30 keV 30 keV-80 keV 80 keV-3.0 MeV	Difference from true value: <30% Less than factor of 2 <30%
Isotropy (photons)	Gamma sources (^{137}Cs or ^{60}Co) and rotational geometry on the three axis centered at the dosemeter	<15%

Recent European references recommend that the overall standard uncertainty of the field dose measurement should not exceed 25%. This value includes all unknown relevant influence parameters within the rated range of use and is valid for the whole measuring range. It can be reduced if some influence parameters are known, like energy and direction of the radiation field, and can be corrected. No detailed minimum requirements are given here for the parameters like energy and angular response, linearity, reproducibility, long term stability of the dosemeter, short term stability of the reader, temperature, humidity and light influence. But the influence of the single parameters may not exceed certain limits in order to approach the overall standard uncertainty. It is also recommended that an additional dose contribution of 100 μGy within a year can be detected in comparison with a field reference group which per definition has not seen this contribution.

5.3.2. Permanent properties

5.3.2.1. General features: sensitivity, dose range, linearity and lower detection level

The sensitivity of a luminescent detector is normally defined as the light detected signal per unit of imparted dose. However, this definition involves many instrumental aspects which make difficult the measurement and comparison of absolute sensitivities. For that reason, relative sensitivities to a reference material is often employed. For TLD, the 'standard' material is LiF:Mg,Ti. Relative sensitivities in Table 4.3 range from 1 to 40 depending upon the TL material. Moreover, the sensitivity of a given TL phosphor can be increased or reduced depending on the operational procedures (annealing, readout-cycle).

Passive dosemeters can be exposed in environmental fields for periods from a few hours to a few years but the most typical exposure time is usually between one and twelve months. While natural radiation dose-rates are in the range of 100 nGy/h, detectors must be capable to measure doses from a few hundred nGy to about 1 mGy. In places where elevated radiation levels are observed, measured doses could be from one to three orders of magnitude higher. However, at such doses, usually much below 1 Gy all TL detectors recommended for environmental monitoring should show no supralinear or sublinear response. For example, LiF:Mg,Ti pellets are known to show some supralinear with dose after gamma ray irradiation above 1.5 Gy and LiF:Mg,Cu,P are sublinear above 10 Gy. Therefore, high-dose non-linear dose response effects do not need to be considered in environmental monitoring.

As mentioned in Section 5.3.1, in spite of the excellent linearity of most of the passive systems in the usual environmental dose range, tests based on the results obtained from several groups of detectors irradiated at different doses should be used for the calibration of the system. A calibration graph (imparted dose versus readout) and regression analysis provide a more accurate estimation of the calibration factor N and the associated statistical error for the whole dose range of interest. In addition, the study of intercept permits to check if the zero dose subtraction method is correct

The lower limit of the dose range, D_{min}, for environmental dosemeter systems is defined here as the lowest dose, which can be measured with an overall uncertainty better than 25%. In order to compare the properties of dosimetry systems with respect to environmental monitoring D_{min} is a more representative parameter than the lower detection limit, which is usually based on the standard deviation of unirradiated detectors, ignoring not only the non-linearity of dose measurements in the low dose range but also other influence parameters like the energy and angular response. Consequently, some systems indicate an unrealistic low value of the lower detection limit, which is of no practical interest.

The D_{min} value depends on various parameters. Using the same passive system for environmental monitoring at different sites, the D_{min} value may differ if, for instance, for one site a correction of the field spectrum is possible or if normalised local doses are only of interest to measure small increases relative to an reference location.

One of the goals for passive environmental monitoring should be the capability to detect small increases in the usual obtained levels, which can be related with the operation of the facility or the plume income. For the passive systems it is not enough to be able to determine accurately this low dose level from a single and controlled irradiation. It must be a true difference, from the statistical point of view, among two successive quarterly measurements in order to decide if there is any real impact. This discriminating capability is generally related to the lower detection limit but in practice it is also related with the measured level. Therefore, very closely related to the lower detection limit is the minimum exposure period t_{min}, (see Section 5.3.3.2.) which must be defined also considering the expected dose rate to be monitored. The minimum exposure period is given by the ratio

$$t_{min} = D_{min} / D'_{nat} \qquad (5\text{-}8)$$

where D'_{nat} is the minimum expected dose rate in the environment. Accordingly, a minimum exposure period of one week (168 hours) is recommended for systems with D_{min}= 10 μGy. However, in certain types of environmental applications it is of importance to minimise the exposure time to a period shorter than 24 hours. Nowadays, measurements of doses below a few μGy became possible with the hypersensitive TL phosphors such as LiF:Mg,Cu,P and Al_2O_3.

5.3.2.2. Reproducibility and repeatability

Reproducibility is defined as the closeness of the agreement between the results of measurements of the same amount of a quantity (i.e., a given dose level), where the individual measurements are carried out changing conditions such as measuring instrument or detector, observer or location. On the other hand, repeatability is the closeness of the agreement between the results of successive measurements of the same measured (i.e., a given dose level) carried out subject to the same measuring conditions during a short period of time. Both features are dependant on the entire passive system characteristics because they imply aspects related with the detectors, reader, handling and procedures.

For type testing, the figure for the reproducibility of a passive dosimetric system is commonly estimated by the relative standard deviation obtained from a group of dosemeters (at least 10) irradiated to a dose which is in the range of the expected level in routine monitoring. An estimate of repeatability can be obtained by the relative standard deviation from a detector which has been prepared, irradiated and read during, at least, 10 consecutive cycles. Although the recommended maximum values for both properties are 7.5%, it is not difficult to reach figures below 5% without major efforts. For instance, the standard deviation at higher doses can be improved using ICF (see Section 5.3.3.3.).

The "Characteristic Curves" shown in Figure 5.1 are the graph of the relative standard deviation (coefficient of variation) for a group of at least ten detectors versus the imparted dose [PIE84]. The lower the dose level, the higher the relative standard deviation for the checked group. The graph can be also employed for the estimation of the lower detection limit.

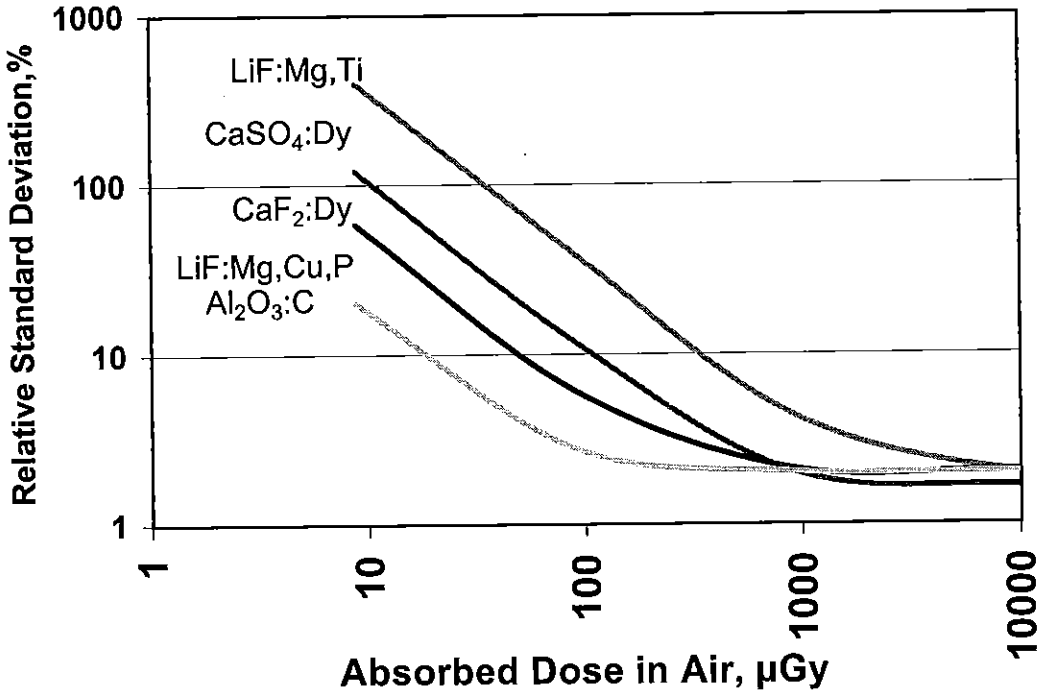

Figure. 5.1: The relative standard deviation (coefficient of variation) vs. exposure for different environmental dosimetry systems.(Adapted from Piesch [PIE84])

TLD and PLD phosphors show a very good repeatability within the readouts number (no changes observed for more than 100 readouts). However, some TLD materials such as LiF:Mg,Cu,P may present some problems (decrease in sensitivity) depending on handling conditions and thermal treatments. In this case, optimisation studies must be carried out.

Reproducibility and repeatability figures are often employed to express the uncertainty in the field measurements. However, if the results from badges irradiated under laboratory conditions are compared with field results at the same dose level, the field data will show, in general, a higher dispersion due to other error sources affecting the field dosemeters. Therefore, direct assessment of the uncertainty in the field measurement based on a reproducibility test might not be correct, being more adequate to carry out a complete error analysis which includes the different identified error sources and random uncertainties.

5.3.2.3. Photon energy and angular dependence of the response

Photon energy response of an ideal environmental dosemeter should correspond closely as possible the radiation quantity dependence on photon energy. Energy response function of a given dosemeter for ambient dose equivalent is different from that of air kerma due to photons scattered from ICRU sphere. This difference is most pronounced at photon energies about 80 keV.

As in the case of active instruments (see Section 5.2.1.), the photon energy response for passive systems should be determined using the adequate reference radiations [ISO96]. The photon energy and angular responses of a dosemeter are dependent upon the construction of the holder (thickness and atomic numbers of materials surrounding the detector), the atomic composition of the TL detector (effective atomic number, Z) and the intrinsic thermoluminescence efficiency of the detector. TL materials based on lithium fluoride such as LiF:Mg,Ti and LiF:Mg,Cu,P are almost perfectly tissue-equivalent with regard to photons (Z=8.2). LiF:Mg,Ti relative photon energy air kerma response is below 80 keV about 30-40% higher than that of LiF:Mg,Cu,P because of differences in both phosphors intrinsic sensitivity to low-LET photon induced secondary electrons (Figure 5.2). However, both characteristics are still so flat that LiF detectors can be applied for environmental monitoring in holders without compensation filters. If necessary, the H*(10) over response of LiF:Mg,Ti material in the energy range below 30 keV should be eliminated by covering the detector with a suitable filter (e.g. 1 mm Al).

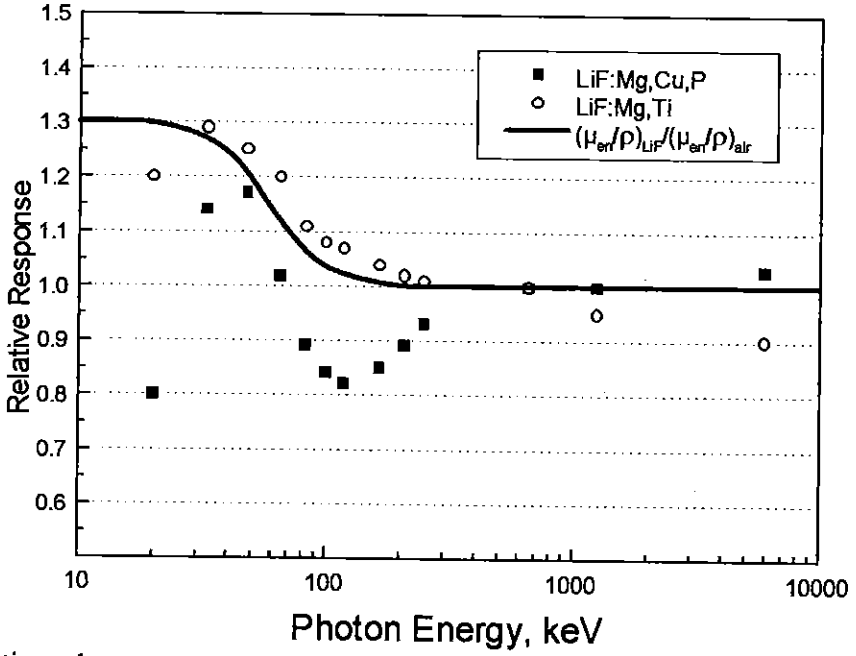

Figure. 5.2: Relative photon energy response of two varieties of lithium fluoride: LiF:Mg,Ti and LiF:Mg, Cu,P

High effective atomic number phosphors such as calcium sulphate or calcium fluoride show a high over response for photons of energies below 100 keV due to photoelectric effect on calcium atoms (Figure 5.3). This over response can be compensated by various metal filters of aluminium, steel, cooper, cadmium, tin and lead. However, the major disadvantage of this technique may be the considerable angular dependence. To overcome this undesired effect, special filtering techniques have been developed.

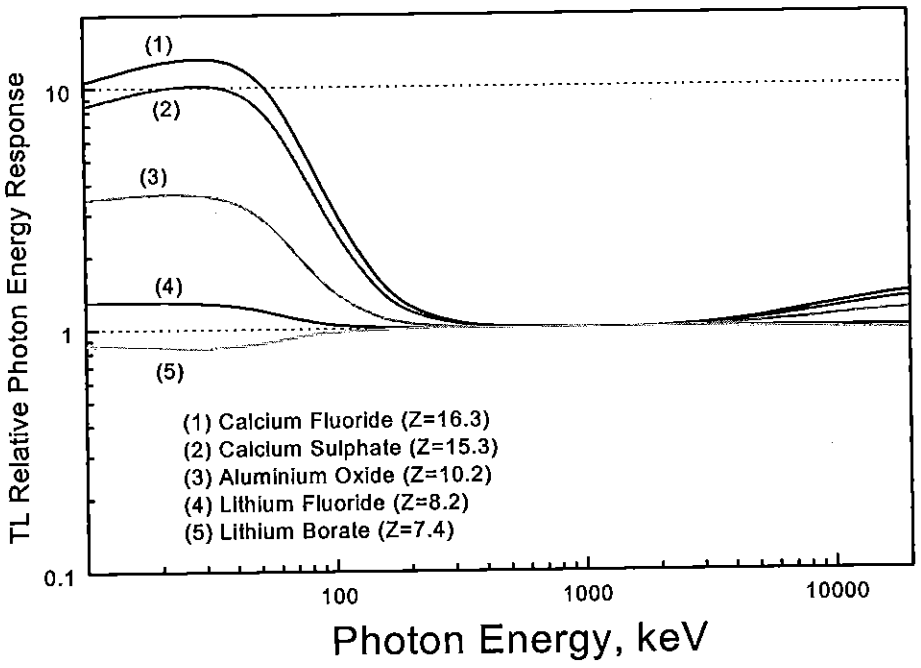

Fig. 5.3: Relative photon energy response of several TL materials having different effective atomic number(Z)

The response of the PLD personal dosemeter has been optimised by an energy compensation filter with respect to the personal monitoring radiation quantity Hp(10), providing a calibration on a slab phantom. The same capsule has been successfully used also in environmental monitoring fieldsThe angular response of the flat glass dosemeter in environmental monitoring is improved by arranging two dosemeters rectangular to each other.

High energy photons (>4 MeV) response must also be considered, specially for the holder design. At these high photon energies, at least 2000 mg cm^{-2} may be needed to provide charged particles equilibrium, but the recommended environmental quantity H*(10) is defined under 1000 mg cm^{-2} of tissue-equivalent material. Some build-up experiments have shown that in general usual environmental passive systems offer acceptable response (±10%) at high photon energies when compared to their ^{137}Cs or ^{60}Co response, [SAE96b].

While isotropic response is required for environmental dosemeters, photon energy response depends on the radiological quantity to be measured. Hence, two separated tests are usually required to characterise these properties. Nevertheless, both of them can be closely related specially if there are additional filters for energy compensation. Therefore, it is recommended to study the data obtained from both tests in order to judge more correctly the true features of the dosemeter.

Actual international recommendations are widely permissive in these topics (±20% for TLD & RPL, +100% for film). However, efforts in the optimisation of the angular and photon energy responses in the environmental dosemeters are encouraged. Even the extension of the energy range up to 6-7 MeV might be suggested, considering the presence of high energy photons in the vicinity of some nuclear and medical facilities.

5.3.2.4. LET dependence: cosmic response and interferences from other radiations

Response of TL detectors per unit absorbed dose usually strongly decreases with an increase of radiation linear energy transfer (LET), [BIL94] This effect has to be taken into account particularly when radiation field in environment is different than that used for calibration of dosemeters.

In a natural radiation environment, cosmic ray exposure contributes usually in about 10-50% to a total dose rate. Cosmic rays at ground level are mostly 80% muons, which can generate high-energy (up to GeV) secondary electrons. In contrast, irradiation of TL dosemeters with ^{60}Co or ^{137}Cs gamma rays results in secondary electrons within energy range of several hundreds of keV. Hence, e.g. LiF TL detectors, calibrated against gamma radiation in air, registers 0.85 of muon produced ionization, [O'BR78]. This effect is additionally modified by an intrinsic LET dependence of differently doped detectors i.e. LiF:Mg,Cu,P detectors show about 10% higher response for low-LET cosmic rays as LiF:Mg,Ti, [OLK94].

For the experimental estimation of the response to cosmic rays the passive detectors are exposed on the surface of a sufficient deep and extended lake, i.e. minimum about 4 m depth and 25 m from the flat land, [BUD96.]. The practical problem here is to find a location for a longer exposure period, which ensures a lower uncertainty. In a recent long-term experiment, pre-irradiated and unirradiated PLD and different TLD were exposed on the surface of a lake in a floating support for 550 days. Fading, self-dose, and transit dose correction were done carefully. Assuming a reference cosmic rate of 289 μGy per year at the lake altitude the relative response to cosmic rays was found to be 0.82 and 0.84 for the LiF:Mg,Ti and CaF_2:Dy detectors and 0.91 and 0.95 for the phosphate glass and LiF:Mg,Cu,P detectors. The LET response of the two detector groups are discussed as the reason for the different response to cosmic rays. In an European intercomparison some of these results are confirmed. For comparison of environmental dose results of different solid state and active dosimetry systems the response to cosmic rays should be taken into account.

For environmental radiation monitoring of gamma doses around nuclear facilities it is of importance to use TL detectors with a low sensitivity for neutrons. The large variety of TL materials makes it possible to meet this requirement. As neutron radiation is always accompanied by gamma photons, neutron monitors contain two dosemeters of different sensitivities to neutrons and gamma photons. *e.g.,* LiF:Mg,Ti detectors with the natural Li isotope composition can overestimate evaluated gamma doses in radiation fields with a thermal neutron contribution. Therefore application of LiF detectors with ^{7}Li, which has a very low cross-section for (n,alpha) reaction with thermal neutrons, is recommended. Another possibility is using the peak 6 at 250°C-280°C generated by high LET radiation on LiF:Mg,Ti with ^{6}Li isotope. High-sensitive for gamma-rays LiF:Mg,Cu,P detectors are insensitive for high-LET alpha particles, produced in Li(n,alpha) reactions.
Therefore, LiF:Mg,Cu,P with natural Li isotope composition could be, for most cases, easily used for environmental monitoring also around nuclear facilities. Finally, some TL materials such as CaF_2:Tm show complex glow curves which single peaks exhibit different LET sensitivity. Therefore, this is another possibility for mixed field environmental dosimetry.

5.3.3. Changing properties

5.3.3.1. Background signal: residual dose, zero dose readout and self-dose

The readout of fresh annealed detectors contains the uncompleted annealed contribution of the past exposures, the so called residual dose, and the non-radiation induced zero dose from the detector and from the reader, for instance photomultiplier dark current and planchet light emission. In addition, during exposure the self-dose due to radionuclide contamination in the detector and mainly in the holder and capsule may contribute an undesired dose contribution. Light effects before readout may also increase the zero reading. All these contributions have to be determined carefully and subtracted from the total readout at the end of the exposure period.

The question of background signals is one of the points that glow curve analysis techniques can help to simplify. The different evolution with temperature during readout of the true TL signals and the background signals is employed by these techniques to separate both contributions. This is made in the same readout from which the dosimetric information is obtained. This procedure estimates the real background contribution to the TL measurement, individually for each dosemeter and avoiding the use of zero doses dosimeters or second readings. Nevertheless, these computerised analysis methods have only been developed up to now, for specific materials and heating methods (LiF:Mg,Ti, ohmic heating) and are not generally available.

PLD systems using the pulsed UV laser readout technique are able to measure the non-radiation induced zero dose for subtraction individually within each readout cycle. Fresh annealed glasses indicate a nominal value of 30±1 μGy.

TLD show negligible residual dose values even after frequent repeated use as long as the pre-exposure does not exceed 1 Gy and an oven annealing at higher temperatures is applied.
After readout in automatic TLD systems using reader annealing the residual dose has to be carefully checked to recognise in time any increase. The detector holders of some systems allows the oven annealing occasionally for the restoration of the original zero dose. On the other hand, PLD accumulate the dose until the glasses are annealed at 400°C without leaving behind a residual dose.

The zero reading of TLD depends on several detector procedures and readout parameters like the annealing, the inert gas flow and temperature rate during readout, the method of glow curve analysis and setting of regions of interest, but also the multiplier temperature or cleanliness of the heating device. In general, the lower the TL signal the higher the influence of reader parameters on the dose results. Low sensitive materials and short exposure periods need more care to the reader properties. In a former intercomparison study the measured zero dose values covers a wide range from less than 1 μGy to more than 100 μGy. For many TLD systems the standard deviation of the zero dose of the single detector has found to be higher than that of the batch uniformity in the zero dose. In this case it is sufficient to subtract a mean value of the zero dose, which may be measured for each exposure period using a representative unirradiated control batch of detectors. An immediate second readout may not be representative for the individual zero dose to be subtracted from the actual readout.

The zero reading of PLD-systems is measured after annealing in general. A nominal value of 30 ± 2 μSv is then expected as a predose. The pulsed laser technique subtracts the intrinsic pre-dose by measuring the long term photoluminescense after each laser pulse (see 4.2.1).

The self dose - of TL and PL materials has been found to be negligible in general, [DEL95 and BUD96], but the contribution from the holders and capsules, especially if they contain metal filters, has to be checked at least in every new batch of dosemeters. Simple tests about the total self-dose rate affecting the dosemeters should be carried out for every production batch in order to assure that this level is negligible in the dosimetric system. The test could consist in the storage of a group of dosemeters during one monitoring period in a shielded place where the dose rate can be continuously measured with a reference instrument to confirm that the dose rate is low and constant. Typical values for self-dose are shown in Table 5.2.

Table 5.2: Measured self-dose values for different detectors and capsules

Detector	Capsule	Air kerma (μGy per year)
^{7}LiF:Mg,Ti	PE holder	< 0.3
LiF:Mg,Cu,P	Plastic holder	7.0 ± 0.5
$Li_2B_4O_7$:Cu	Plastic 2mm	29 ± 3
$CaSO_4$:Tm	Lead 0.7mm	4 ± 1
CaF_2:Dy	Tin sphere	29 ± 2
Glass SC-1	Tin/Plastic	9.5 ± 0.5

The sensitivity of some TL materials such as Al_2O_3:C or lithium borate can be significantly reduced by visible light leaks, which also affect dramatically the background signal of unirradiated detectors. In this case, the holder must be specifically designed to avoid any incident light on the detectors during the exposure. Moreover, special care must be implemented during the handling and readout processes to minimise this effect.

5.3.3.2. Transit dose

The transit dose D_t is the sum of accumulated dose contributions in the transit period $t_t = t_e - t_m$, which is defined as the difference between the exposure period t_e (period from detector annealing to detector readout) and monitoring period t_m (period during which the detectors are installed in the field location). Therefore it is not restricted to the period of mailing or transport exclusively. Figure 5.4 shows the different contributions during routine exposure of an environmental passive detector, [DIN95]. The contribution of D_t to the overall uncertainty of the environmental dose measurement may be effectively reduced by keeping the transit period t_t small in comparison to the monitoring period t_m and the dose rate low (use of shielding whenever possible).

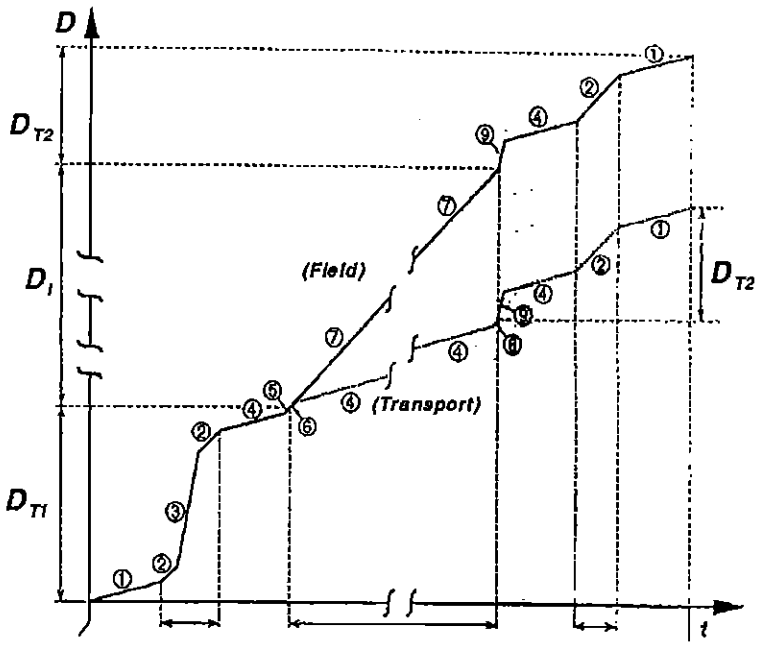

(1) Storage in the shielding of the Dosimetry Service
(2) Transport without undesired exposure by an artificial source
(3) Transport with undesired exposure by an artificial source
(4) Storage in the shielding of the Plant Service for environmental monitoring
(5) Transport from the Plant Service to the location
(6) Transport back of the Transport dosemeters T to the shielding of the Plant Service
(7) Accumulation of the environmental dose at the location No. i
(8) Transport of the Transport dosemeters T from the shielding of the Plant Service to the location No. i
(9) Transport from the location No. i to the Plant Service with undesired exposure by an artificial source

Figure. 5.4: Dose accumulation of the Field dosemeters (F_i) and Transport dosemeters (T). D_i is the environmental dose at the location No. i. The sum of D_{T1} and D_{T2} is the transport dose including all contributions during the handling of the dosemeters, (Adapted from DIN [DIN95]).

Provided that in a first approximation the natural dose rate $\dot{D}_{nat}$ is constant during the transit period, $\dot{D}_t$ is given by

$$\dot{D}_t = t_t \times \dot{D}_{nat} \qquad (5\text{-}9)$$

Unfortunately, frequently it is not possible to assume a constant value for $\dot{D}_{nat}$ and the transit period sometimes can extend more than one week. Therefore, a suitable procedure for proper transit dose subtraction is needed. In principal, four methods are used in practice to determine the transit dose:

(A) A portable shield is used, in which a control dosemeter set is stored during the complete exposure period t_e. The field dosimeters are taken off only during the monitoring period t_m at the monitored site for exposure in the environment. Additional undesired exposure is negligible and the transit dose D_t is given by the mean dose Dm of the control dosemeter set in the shielding

$$D_t = (1-t_m/t_e)\times Dm \qquad (5\text{-}10)$$

(B) A control dosemeter set is sent from the lab to the site, where it is stored in a shield during the monitoring period t_m while the field dosemeters are exposed. After return all dosemeters are readout simultaneously. The control dosemeters give the dose Dm. Provided that the dose rate $\dot{D}_{sh}$ in the shield had been measured with the solid state dosemeters in the past and $\dot{D}_{sh}$ is considered to be constant, then the transit dose D_t is given by

$$D_t = Dm - t_m \times \dot{D}_{sh} \qquad (5\text{-}11)$$

If an electronic dosemeter (ED) or an active dose-rate meter is used to find out the dose-rate in the shield, then the correction factor k for the correction of the mean response of the passive detectors in comparison to that of the ED or active device in the fields of interest, for instance in the lab or in the shield, should be used.

$$\dot{D}_{sh}\,(\text{passive}) = k(\text{ED or active}) \times \dot{D}_{sh}\,(\text{ED or active}) \qquad (5\text{-}12)$$

k takes into account the energy dependence and response to cosmic rays for the different dosimetry systems.

(C) Here shields are only used for short time storage during the transit period t_t to reduce the transit dose. An expected transit dose D_t(expected) is estimated on the basis of representative dose rates $\dot{D}_{ti}$ in corresponding intervals t_i determined in the past using passive detectors or electronic dosemeters with the correction factor k_i respectively.

$$D_t\,(\text{expected}) = \Sigma_i\, k_i\, t_i\, \dot{D}_{ti}\,(\text{ED}) \qquad (5\text{-}13)$$

For surface mail the $\dot{D}_{tLAB}$(expected) value and the k_{LAB} factor will represent approximately the unknown dose rate. For air mail a dose rate $\dot{D}_{tFLIGHT}$ of about 1.5 μGy/h and k_{shield} may be assumed for the short interval flight in high flight altitudes. For the remaining interval surface mail conditions should be considered.

Especially during the transport of the dosemeters an undesired exposure cannot be excluded. It is suggested to use ED during the transport, which can be readout immediately after arrival. By comparing the difference between the measured and the expected dose, undesired dose contributions may be detected. But the subtraction of the so measured undesired dose from the local dose values might fail to correct effectively, because a homogeneous undesired exposure cannot be assumed in the most cases. Therefore the dose contribution exceeding the expected dose is compared with the minimum environmental dose measured at any location with the passive detectors during the monitoring period. If the condition

$$D_{mail}(ED) \times k_{mail} - D_{mail}(expected) > 0.05 \times D(location) \qquad (5\text{-}14)$$

is fulfilled, the value of the difference should be taken into consideration for an increase of the overall uncertainty of environmental dose measurement at this time.

(D) In the case there is no shielding at the site to be monitored and no ED available then it is useful to send the control dosemeter to the site together with the field dosemeters for the forthcoming monitoring period and to send them back immediately with the exchanged field dosimeters of the past monitoring period and evaluate them together with the latter dosemeters. If the reading is higher than expected then it can be found out by the results of the field dosimeter of the last monitoring period whether the contribution comes from the way to or the way from the site. In the second case the field dosimeter of the running monitoring period could be exchanged once more.

5.3.3.3. Long-term stability: temperature, light, humidity

Long-term instabilities are considered here as any changes in the response as well as in the readout after exposure due to light, humidity and temperature.

Humidity and light effects during exposure in the environment can be avoided by using suitable protective capsules and pouches. The expected humidity inside sealed dosemeters does not affect seriously the common TLD and PLD with the exception of $Li_2B_4O_7$ TLD. The possible influence of the laboratory illumination during readout for some detector types (for instance Al_2O_3) may be eliminated by special handling procedures (for instance yellow light filters). Some automatic TLD readers and the PLD system omit such effects and reduce the special cleaning maintenance by opening and closing the capsule detector holder inside the dark chamber in the reader.

The effect of the temperature, which results mostly in the reduction of the readout, is called fading. Fading rate is not a constant for a given material and temperature but it depends strongly on the temperature treatment before exposure as well as readout, [DeP80]. On the other hand, a suitable annealing procedure can be applied in order to reduce fading physically and/or fading correction factors may be established for the reduction of the remaining fading analytically.

Strictly speaking, phosphor stability can be affected by two kinds of phenomena: some affecting the trapped charges (decrease in the signal obtained, i.e., usual fading factor), some affecting the phosphor trap system (increase or decrease in the measured signal, i.e., sensitivity changes). However, very often in practice only trapped charges leakage seems to be considered, assuming a perfect stability of the trap structure in the phosphor. In principle the LiF:Mg,Ti peaks 4(180-200°C) and 5 (210-225°C) are of dosimetric importance due to their stability over several years. However, the fading properties of LiF:Mg,Ti reflects its complex glow curve structure. In fact, both unexposed and exposed detectors indicate a change in response and fading, respectively, which is different also for the main glow peaks. The other usual TL materials show negligible change in response when remaining unexposed, [BUR84].

Fading experiments [BUR78] have shown, that generally temperature treatment in an oven before readout is much more effective than a pre-readout at a lower temperature in the reader.
The fading of CaF_2:Dy material, for instance, is almost negligible for environmental monitoring after an overnight post-exposure annealing at 100°C. As a consequence, the lack in the low temperature glow peaks results in a lost of sensitivity by a factor of 4, which is still a factor 5 higher than that of LiF:Mg,Ti. Usually a temperature treatment of less than one hour at about 100°C in an oven is applied for fading reduction.

PLD systems are only slightly affected by the temperature in environmental monitoring. During irradiation the low temperature dependence of 0.1%/°C may be balanced after about 20 days storage at room temperature. Build-up has not to be taken into account after a waiting time of 5 days or a temperature treatment of 35°C/24 h. Fading of glass dosimeters is negligible. Earlier experiments indicated a long term fading of -2% after 8 years of storage at 30°C.

For short-term exposure periods up to some months, the repeated estimation of fading correction factors might be necessary for each exposure period individually due to the unpredictable short-term changes in temperature. On the other hand, if the condition of annealing before and after exposure, the storage condition of calibration detectors and field detectors and the readout procedure is not changed, then a long-term fading correction factor may be applied as found in Figure 5.5 for instance.

Locations of a country wide survey with different climatic conditions need an individual fading correction factor. Therefore, some detectors in the dosemeter can be intended to be irradiated in a moment during the exposure time to check the fading factor. However, the fading correction factor is of the same importance (weight) as the calibration factor and should therefore be based on a sufficient number of detectors. Thus, the number of control dosemeters in this case may exceed the number of field badges. In order to reduce the number of control dosemeters, the fading correction factor found at one reference location of representative climatic conditions should be applied for all locations at least at one site, probably for different sites. Instead of a single reference location, selected locations (for instance, sunny and shadowed) or randomly found locations should be used for the estimation of an average reliable fading correction factor.

The estimation of the fading correction factor F_{ad} (see Section 5.3.1) will be explained here using the results of a ten years fading experiment with LiF:Mg.Ti detectors (Figure 5.5).

The experiment was done over 20 half yearly monitoring periods, namely during 10 periods from November to April (winter season) and further 10 during May to October (summer season). For each season, two separate batches of 10 dosemeters were irradiated to 25 mGy with ^{137}Cs photons, one batch at the beginning of the monitoring period (i.e. 180 days before readout) and the second batch like the calibration dosemeters (2 days before readout). The calibration batch was stored in a suitable shielding during the field monitoring period. The Figure5.5 demonstrates the effect of the long-term climatic changes over 10 years (<1%), the influence of the irradiation at the beginning or the end of the monitoring period (3% lower for those dosemeters irradiated at the end of the field exposure) and the effect of the different climatic conditions in the summer and winter season on dosemeter reading (4% lower for the summer season dosemeters).

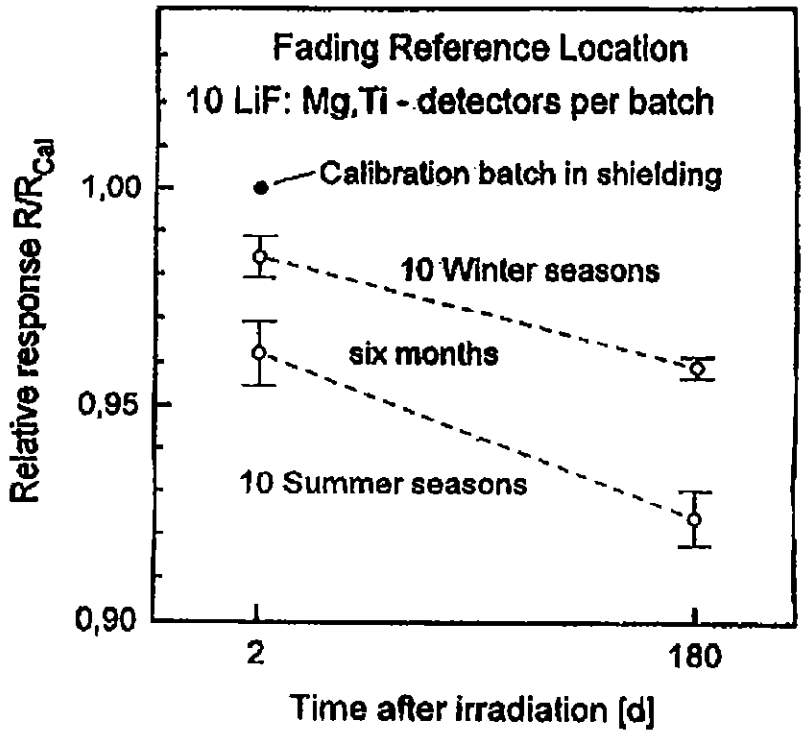

Figure. 5.5: Long term fading at an open air reference location. The graph shows the mean relative ratio R(open air)/R(shield) for batches of LiF:Mg,Ti detectors which were exposed for six months and irradiated two days before readout (182nd day after annealing of detectors)

From these results some recommendations can be derived for the estimation of the fading correction factor:

- The fading control dosemeters should be irradiated with half the calibration dose at the beginning and with half at the end of the monitoring period, in order to simulate a continuous irradiation of the natural background than is done with a single irradiation at the beginning or at the end of the monitoring period. In practice, continuous irradiation in a constant open air field of an artificial source cannot easily be offered and it also may be inconvenient to irradiate the fading detectors at any time during the monitoring period.

- The fading control dosemeters should be exposed together with some field dosemeters in the field at some selected or randomly found locations, which are representative for the climatic conditions, resulting in a typical mean fading correction factor for the monitored site.

The use of pre-irradiated and post-irradiated fading control dosemeters is not recommended for glass dosemeters because the fading is negligible.

6 CALIBRATION

6.1 General

Since the air kerma rates used for calibration may be of the same order of magnitude as the natural background, special considerations have to be taken into account. At background levels the inherent background reading of the instrument being calibrated may be comparable, or even exceed, the background level and so it should therefore be known and taken into account.

An environmental radiation monitoring instrument is calibrated by placing its detectors in a radiation field of known air kerma rate and comparing the instrument reading with this air kerma rate. The air kerma rate can be determined in two ways, either by using an instrument whose calibration is traceable to national standards or by using a radioactive source whose activity has been certified and from which the air kerma rate at the point of test is calculated, taking into account the air attenuation and the influence of scattered photons, [IAEA98].

The air kerma rate used for calibrations with national standards is normally several orders of magnitude greater than those used with environmental instruments in the field. It may therefore be necessary to use more than one instrument in the calibration chain to transfer the calibration to air kerma rates more suitable to environmental detectors. It is important to consider how the response of each instrument varies with air kerma rate and if necessary to correct for the effect. A secondary standard instrument designed for protection level measurements which can be calibrated directly against the primary standard can be used at kerma rates down to about 200 nGy h^{-1}. If the environmental radiation monitoring instrument and the secondary standard instrument have no significant air kerma rate dependence and can both be used at this kerma rate with sufficient resolution then it will not be necessary to introduce an intermediate instrument.

6.2 Reference Instrument Method

In this method the air kerma rate at the point of test is measured using a secondary standard reference instrument.

The radiation source can be used with or without a collimating system. The air kerma rate at distance from a radiation source is made up of the sum of several components.

1. The direct radiation from the source.
2. Radiation scattered from the surroundings of the calibration facility.
3. Radiation scattered by the surrounding air, sometimes referred to as "build-up in air".
4. The natural environmental photon radiation from the calibration facility.
5. The internal background of the instrument, including leakage.
6. Cosmic radiation.

A background reading of the reference instrument shall be taken without the source present and will contain the contributions from the environment, internal background and cosmic radiation. For the purpose of the calibration no measurements of these individual contributions are necessary. Section 6.4 gives further details of the method for measuring the scatter correction.

The reference instrument is placed at the point of test and the air kerma rate as measured by the reference instrument is given by:

$$\dot{K}_a = (K_r \times k_r \times R_r) - B_r \qquad (6\text{-}1)$$

where $\dot{K}_a$ = Air kerma rate due to direct and scattered radiation from the source.

k_r = Reference instrument range calibration factor.

K_r = Reference instrument energy calibration factor

R_r = Reference instrument reading due to direct and scattered radiation corrected for air air density if necessary

B_r = Background reading determined by the reference instrument which includes contributions from internal background of the instrument, environmental radiation from thecalibration facility and cosmic radiation.

The detector to be calibrated is then placed with its reference point at the same point of test and the calibration factor N_{INST} is given by:

$$N_{INST} = \dot{K}_a \ (M_i - B_i)^{-1} \qquad (6\text{-}2)$$

where:- M_i = Instrument reading due to direct and scattered radiation, corrected for air density if necessary.

N_{INST} = Detector calibration factor.

B_i = Instrument background reading.

With this technique it should be noted that the contribution from scattered radiation is not determined separately or corrected for. For a well designed collimated system the scattered radiation should not exceed a few percent compared to the direct radiation so its effect upon the calibration can be neglected. For uncollimated radiation it can also be neglected provided a low scatter facility is used and source to detector distances do not exceed 120 cm.

Alternatively the readings of both the reference instrument and the instrument being calibrated can be made for just the direct radiation by using a shadow-shield calibration method, Figures 6.1a and 6.1b.

The advantage of this method is that the response of the instrument to be calibrated and the reference instrument to the scattered radiation can be corrected for. In this method double the number of measurements has to be taken, namely with and without an individually shaped lead shield, for each instrument design. With this technique the source-to-detector distance must be sufficiently large to ensure a nearly parallel beam of uniform intensity over the entire detector volume.

The detector response with no shield present is the ambient background (A) plus radiation from the source; the latter comprises primary gamma rays (p) and room scatter (s).

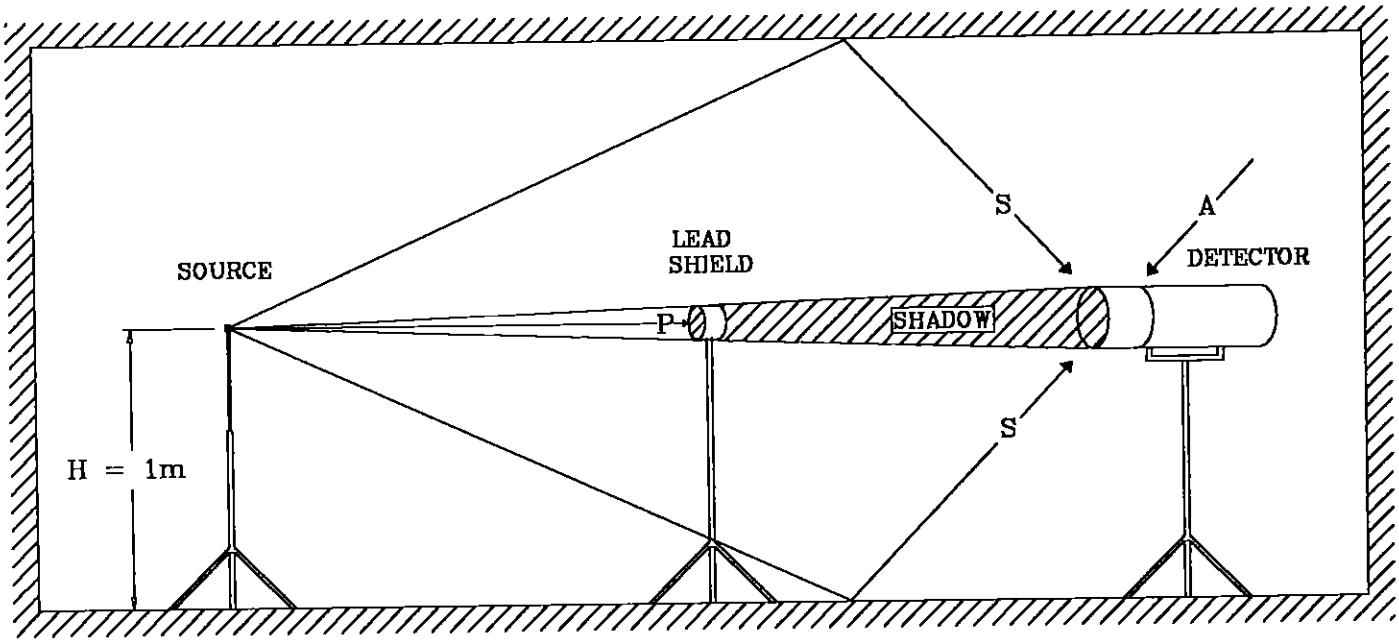

Figure 6.1a: Shadow-shield calibration set-up. (P) primary beam, (A) ambient radiation, (S) room scatter component.

If the direct air kerma rate value has been certificated or calculated for a distance of 100 cm, the primary beam air kerma rates, $\dot{K}_d$ at other distances d from the source can be calculated from the relationship:

$$\dot{K}_d = \dot{K}_{100} \{100/d\}^2 e^{-\mu(d-100)} k_d \qquad (6\text{-}3)$$

where $\dot{K}_{100}$ is the air kerma rate at 100 cm distance according to the source certificate or calculated as described in Section 6.3, μ the linear attenuation coefficient for the radiation in air, d the distance in cm between detector and source, and k_d the source decay-correction factor, if applicable. Values of the linear attenuation coefficient, μ; for ^{137}Cs $\mu = 9.28 \times 10^{-5}$ cm^{-1}, for ^{60}Co $\mu = 6.8 \times 10^{-5}$ cm^{-1} and $\mu = 7.5 \times 10^{-5}$ (average) cm^{-1} for ^{226}Ra, [BØT85].

To determine the responses from the components A and S, a lead shield thick enough to absorb the primary gamma rays, (P), should be placed between the source and detector so as to "shadow-shield" the primary beam. The difference between the readings with and without the shield, yields the response from the primary beam.

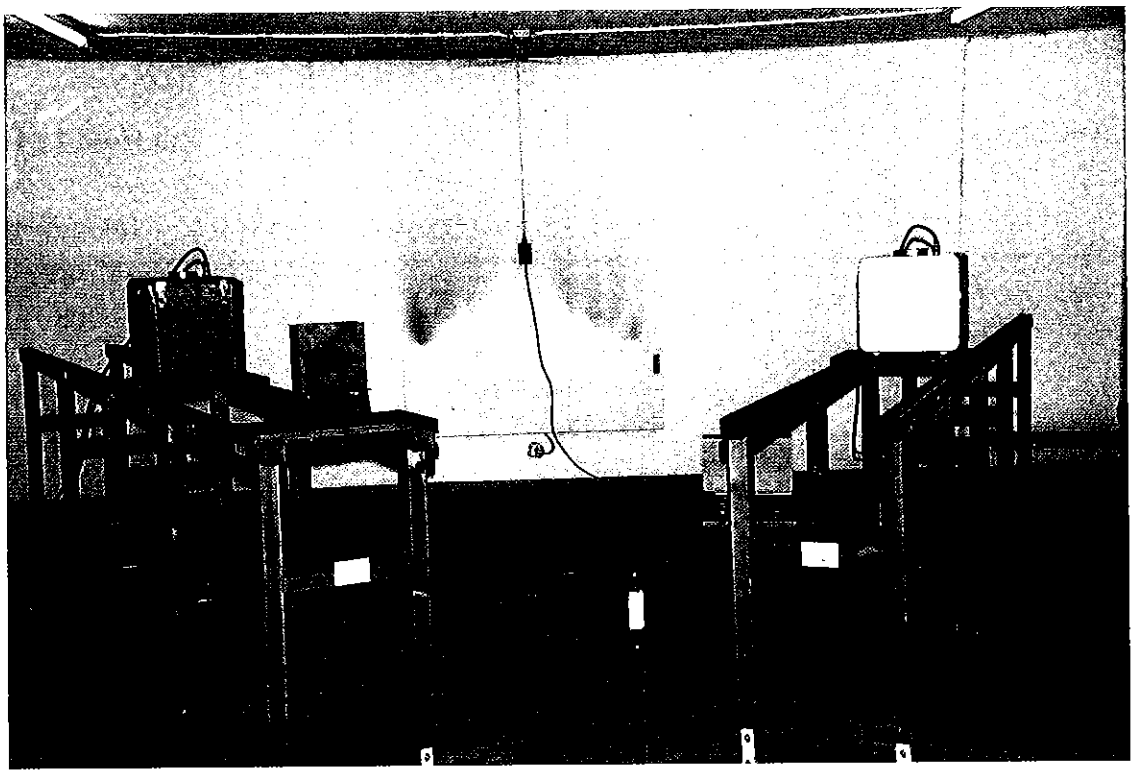

Figure 6.1b: The shadow-shield calibration facility at the Risø National Laboratory.

6.3 Certificated Source Method

In this technique the air kerma rates at the points of test are calculated from the actual certificated activity of the source, given by the manufacturer or from a calibration performed at a secondary laboratory, taking into account the air attenuation and the influence of scattered photons, [BØT82 and BØT89].

As with the reference instrument method the source can be used collimated or uncollimated.

Factors for calculating the air kerma rate from the certificated activity for the calibration sources of ^{60}Co, ^{137}Cs and ^{241}Am are given in column 4 of Table 6-1.

Table 6.1: Radionuclides used for ISO reference gamma radiations, [ISO96].

Radioactive Nuclide	**Gamma-ray Energy (keV)**	**Half-life (years)**	**Air kerma rate at 1 m from 1 MBq(1) (nGy h^{-1})**
^{60}Co	1173.3 1332.5	5.272	308
^{137}Cs	661.6	30.3	79
^{241}Am	59.54	432	3.0

Note (1) The air kerma rates are for unshielded point sources and are therefore given only as a guide.

It is interesting to note that, as shown in Figure 6.2, the spectrum from a ^{226}Ra source is similar to that of natural environmental gamma radiation. Although not specified as an ISO reference radiation, nevertheless ^{226}Ra is a useful reference source to use for calibrating instruments whose variation of response with energy is small. No correction is then necessary for energy dependence.

If an uncollimated calibration set-up is installed indoors scattered photons from the floor, the walls and the ceiling contribute to the radiation field from the uncollimated point source. All of these photons have lower energies than the unscattered primary photons.

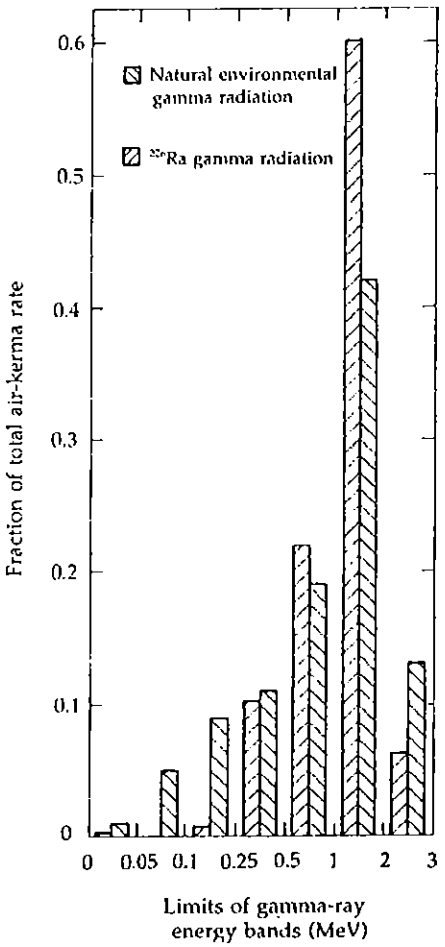

Figure 6.2: Comparison of the gamma-ray energy spectra from a ^{226}Ra source and natural environmental radiation, calculated from Beck, [BEC72a].

6.3.1 Free field technique

A calibration set-up with an uncollimated point source outdoors on flat ground, called the free-field technique, Figure 6.3a and 6.3b, has the advantage that by using large source-to-detector distances many instruments can be placed in circles around the source and thus be calibrated at the same time. With this method the air kerma rate is calculated from the source activity and corrections are applied for scattered photons from the ground and the air and for air attenuation (Section 6.2). Measurements of the radiation fields may also be made with a secondary standard instrument.

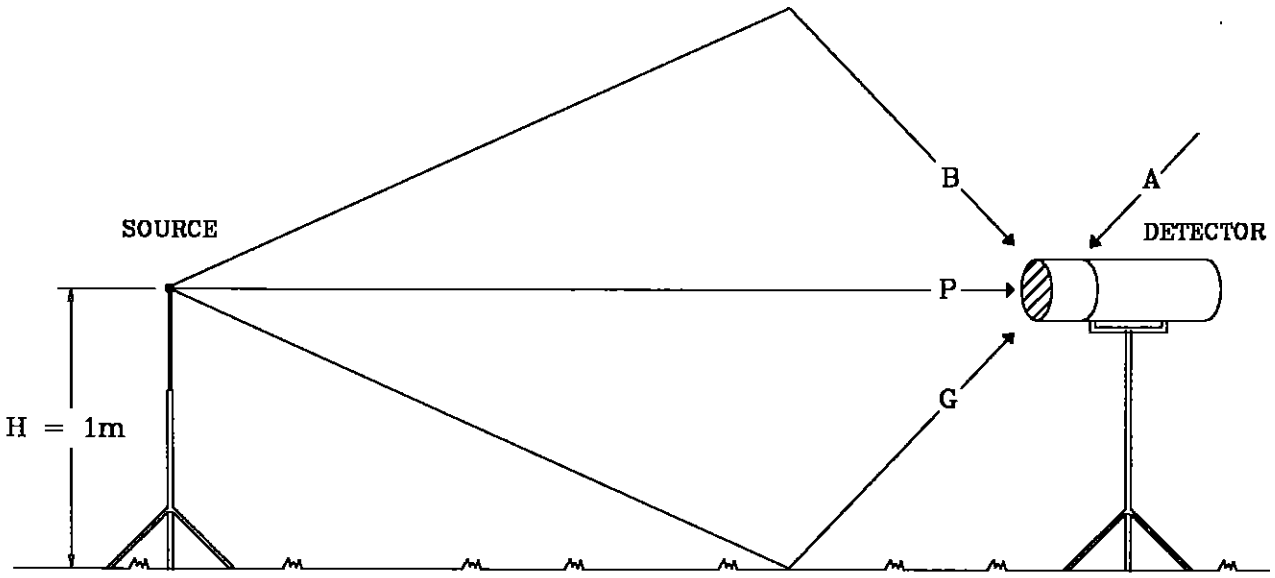

Figure 6.3a: Free-field calibration set-up. (P) primary beam, (A) ambient radiation, (B) build-up in air, (G) ground albedo.

Figure 6.3b: The free-field calibration site at Risø.

The radiation components to be considered are the ambient background (A), the primary beam from the source (P), the scattered component from the ground surface (G) and the build-up in air (B).

If the direct air kerma rate value has been certificated or calculated for a distance of 100cm the primary beam air kerma rates, $\dot{K}_d$ at other distances d from the sources can be calculated from the relationship:

$$\dot{K}_d = \dot{K}_{100} \ (100/d)^2 e^{-\mu(d-100)} k_d \qquad (6\text{-}4)$$

where $\dot{K}_{100}$ is the air kerma rate at 100 cm. distance according to the source certificate (for ^{226}Ra using an air kerma rate constant of 7.23 mGy $m^2 h^{-1} g^{-1}$), μ the linear attenuation coefficient for the radiation in air, d the distance in cm between detector and source, and k_d the source decay-correction factor, if applicable.

6.3.2. Monte Carlo calculations of the air kerma rate for open free-field geometries

The MCNP code has been used to calculate the air kerma rate from sources of ^{137}Cs, ^{60}Co and ^{226}Ra in different source-to-detector distances in a free-field geometry on a flat ground (open field). The elemental compositions of soil, air and source material which are needed for thses calculations can be extended to more complex geometries including buildings, trees etc., [BØT92].

At the detector point the air kerma rate, $\dot{K}$, has three components: the uncollided kerma rate, $\dot{K}_{uncol}$, from photons emerging from the source; the scattered kerma rate from the ground, $\dot{K}_{ground}$, originating from photons leaving the ground surface into the detector point after one or more scattering reactions in the air/ground media; and finally the scattered kerma rate from air, $\dot{K}_{air}$, originating from photons leaving the air into the detector point after one or more scattering reactions in the air/ground media. From special features in the MCNP code regarding photon importance and photon energy distribution it is possible to separate the scatter contributions from air and ground:

$$\dot{K} = \dot{K}_{uncol} + \dot{K}_{ground} + \dot{K}_{air} = \dot{K}_{uncol} + \dot{K}_{scatter} \qquad (6\text{-}5)$$

If the photon importance for the ground medium is set at zero, all photons which would be scattered from the ground and into the detector will be "killed". The remaining scatter component is therefore from single and multiple scattering in the air only. By subtracting this air scatter from the total scatter component the ground scatter component will emerge.

For a given radionuclide the energy distribution of the kerma rate from scattered photons at the detector point will depend on the measurement geometry, viz. the source-to-detector distance and the distance of the source-detector above the ground. Such a distribution is shown in Figure 6.4 for a ^{137}Cs source. The source-to-detector distance, d, is here 3 metres and both source and detector are elevated 1 metre above ground. The total scattered air kerma rate for this geometry has been calculated as: $\dot{K}_{scatter} = 0.12\ \dot{K}_{uncol}$ Consequently, the total kerma rate, $\dot{K}$, can be expressed by the uncollided kerma rate $\dot{K}_{uncol}$:

$$\dot{K} = \dot{K}_{uncol} + \dot{K}_{scatter} = 1.12\,\dot{K}_{uncol} \qquad (6\text{-}6)$$

which implies that uncollided photons contribute approximately 89% of the total kerma rate, K, and scattered photons contribute the remaining 11%. The energy distribution for the scattered photons is shown in Figure 6.4.

If the response of a given detector as a function of the photon energy, E, is r(E), the instrument response, r_{total}, to the total air kerma rate, $\dot{K}$, having a spectral distribution k(E), as shown in Figure 6.4, can be calculated as:

$$r_{total} = \Sigma^{n}_{i=1}\, k(E_i)\, r(E_i) \qquad (6\text{-}7).$$

where n is the number of photon energy intervals used in the spectral calculation.

In Figure 6.5 the ratio of total scattered to uncollided air kerma rate is shown for the three sources ^{137}Cs, ^{60}Co and ^{226}Ra as a function of the source-to-detector distance (d) and with the source and detector elevated 1 metre above ground.

The results shown in Figure 6.5 of the scattered air kerma rates have been separated into contributions from air and ground. For this work photons which scattered within the source material are counted as primary (unscattered) photons.

Detailed calculated values are shown in the Tables 6.2, 6.3 and 6.4, and graphically in Figures 6.6, 6.7 and 6.8 for a source to detector range of 0.5 to 50 metres. All the results are normalised to the uncollided kerma rate, $\dot{K}_{uncol}$.

Table 6.2: Relative scattered air kerma from the radionuclide ^{137}Cs in free-field calibration geometries as a function of source-to-detector distance. The source and detector are both placed one metre above ground. The statistical uncertainty of the calculated values is less than 2%.

Relative scattered air kerma rates in free-field calibration geometries $(\dot{K}_{scatter} / \dot{K}_{uncol}) \cdot 100\%$			
Distance (m)	**Radionuclide: ^{137}Cs**		
	Air	**Ground**	**Air + Ground**
0.5	0.28	0.68	0.96
1.0	0.97	2.28	3.25
2.0	1.66	6.43	8.09
3.0	2.44	9.61	1205
4.0	3.15	12.20	15.30
5.0	3.88	13.13	17.01
6.0	4.40	14.50	18.90
7.0	5.23	15.50	20.73
8.0	5.62	15.85	21.47
9.0	6.27	15.85	22.12
10.0	6.96	15.63	22.59
15.0	9.87	15.33	25.20
50.0	26.93	14.50	41.43

Table 6.3: Relative scattered air kerma rates from the radionuclide ^{60}Co in free-field calibration geometries as a function of source-detector distance. The source and detector are both placed one metre above ground. The statistical uncertainty of the calculated values is less than 2%.

Relative scattered air kerma rates in free-field calibration geometries $(\dot{K}_{scatter} / \dot{K}_{uncol}) \cdot 100\%$			
Distance (m)	**Radionuclide: ^{60}Co**		
	Air	**Ground**	**Air + Ground**
0.5	0.15	0.36	0.51
1.0	0.60	1.24	1.85
2.0	1.05	3.85	4.91
3.0	1.58	6.11	7.69
4.0	1.91	8.31	10.20
5.0	2.35	9.38	11.73
6.0	2.76	10.90	13.70
7.0	3.29	11.45	14.74
8.0	3.69	12.02	15.71
9.0	4.09	12.44	16.53
10.0	4.69	12.23	16.92
15.0	6.48	13.01	19.49
50.0	17.14	11.55	28.69

Table 6.4: Relative scattered air kerma rates from the radionuclide ^{226}Ra in free-field calibration geometries as a function of source-detector distance. The source and detector are both placed one metre above ground. The statistical uncertainty of the calculated values is less than 2%. The Υ-spectrum ^{226}Ra + daughters include 64 photon energies with photon yields exceeding 0.01%.

Relative scattered air kerma rates in free-field calibration geometries $(\dot{K}_{scatter} / \dot{K}_{uncol}) \cdot 100\%$			
Distance (m)	**Radionuclide: ^{226}Ra + daughters**		
	Air	**Ground**	**Air + Ground**
0.5	0.22	0.56	0.79
1.0	0.74	1.89	2.63
2.0	1.36	5.32	6.68
3.0	2.04	7.77	9.81
4.0	2.40	10.60	13.00
5.0	3.19	11.05	14.24
6.0	3.56	12.30	15.86
7.0	4.22	12.62	16.84
8.0	4.74	13.18	17.92
9.0	5.06	13.75	18.81
10.0	5.43	13.74	19.17
15.0	8.01	14.39	22.40
50.0	22.18	12.56	34.74

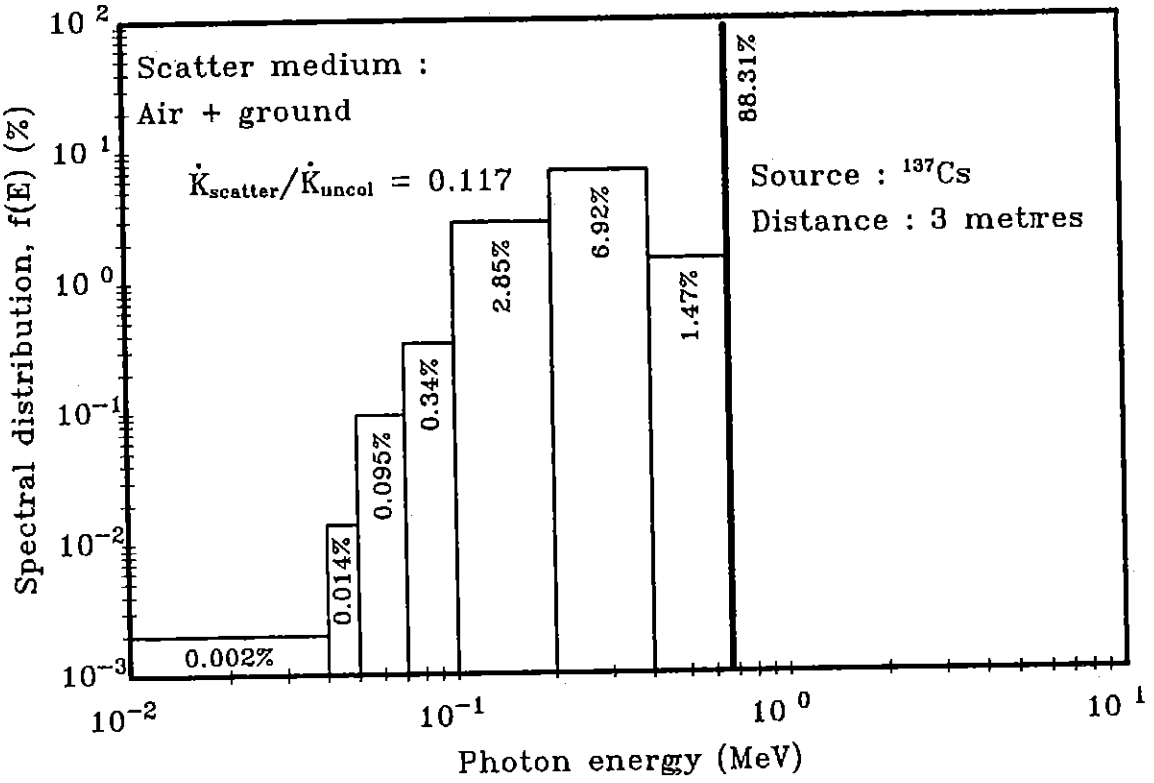

Figure 6.4: Energy distribution of the relative free-field air kerma rate from a ^{137}Cs source at a distance of 3 metres.

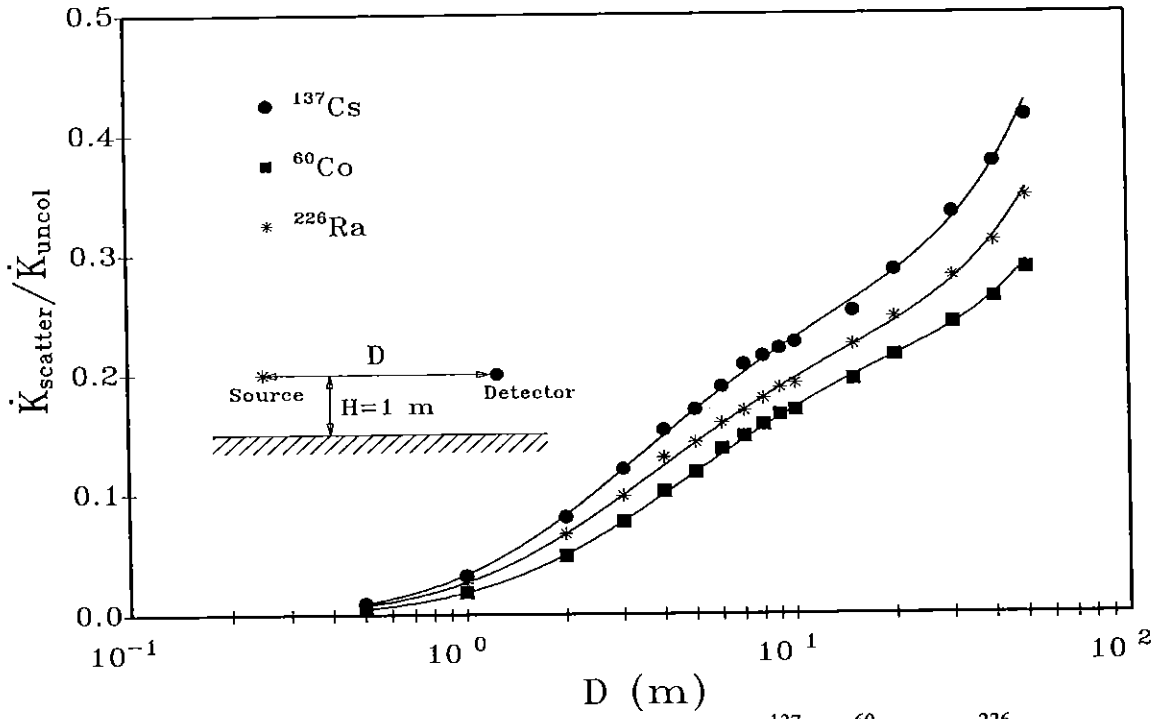

Figure 6.5: Relative scattered free-field air kerma rates from ^{137}Cs, ^{60}Co and ^{226}Ra sources as a function of distance.

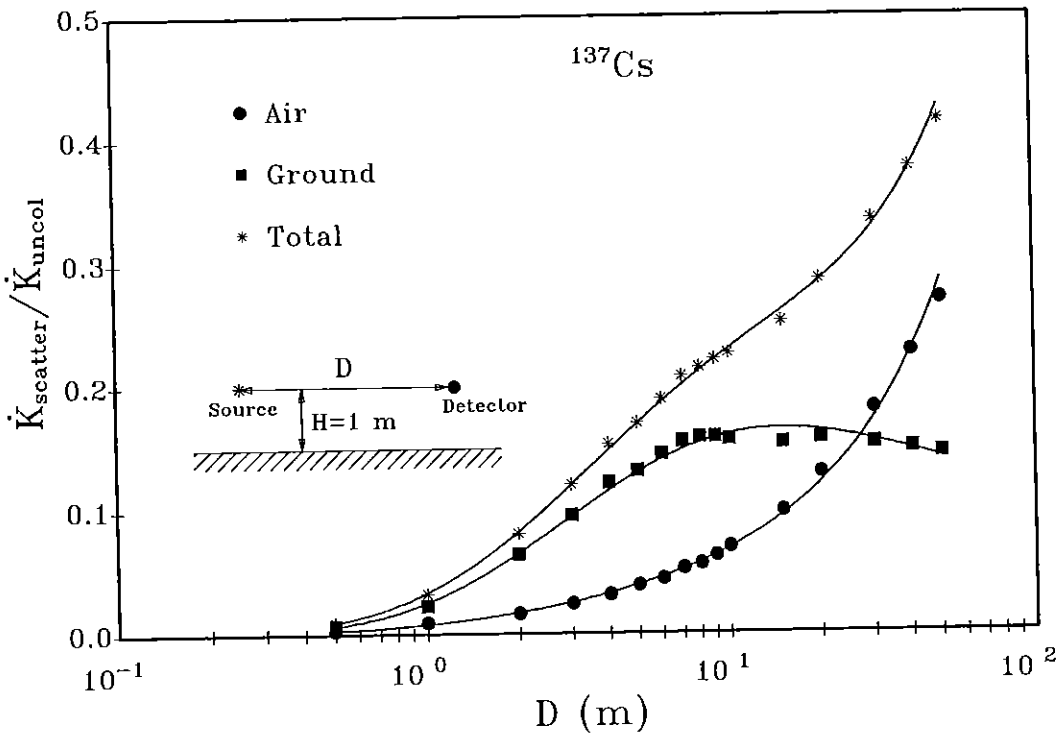

Figure 6.6: Relative scattered ground and air scattered air kerma rate component from a ^{137}Cs source as a function of distance.

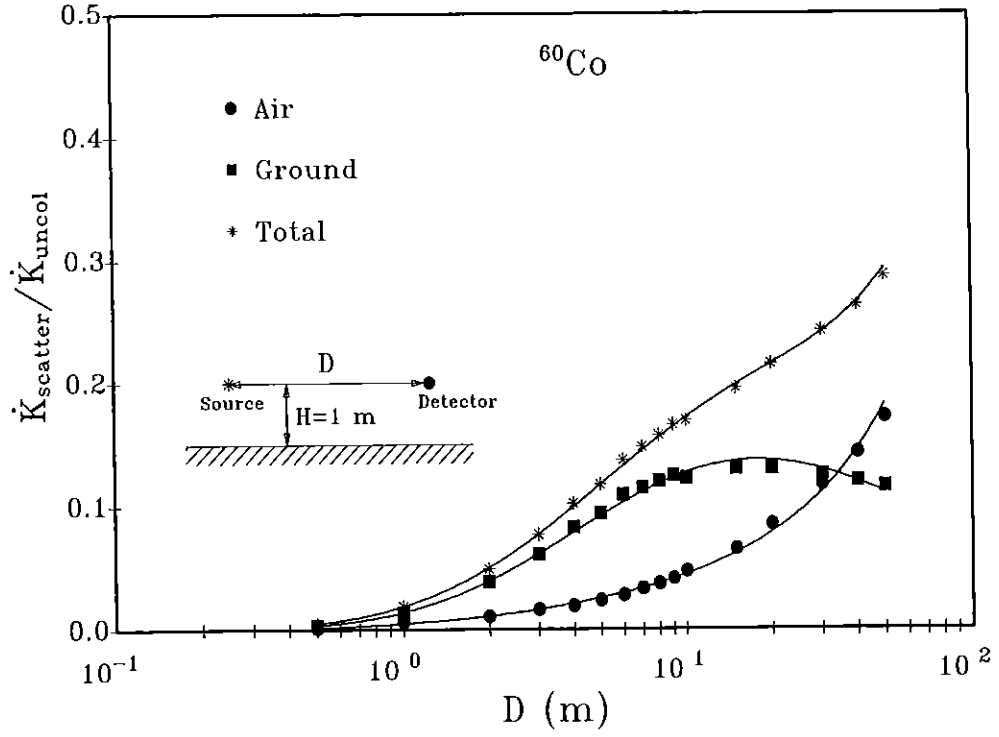

Figure 6.7: Relative scattered ground and air scattered air kerma rate components from a ^{60}Co source as a function of distance.

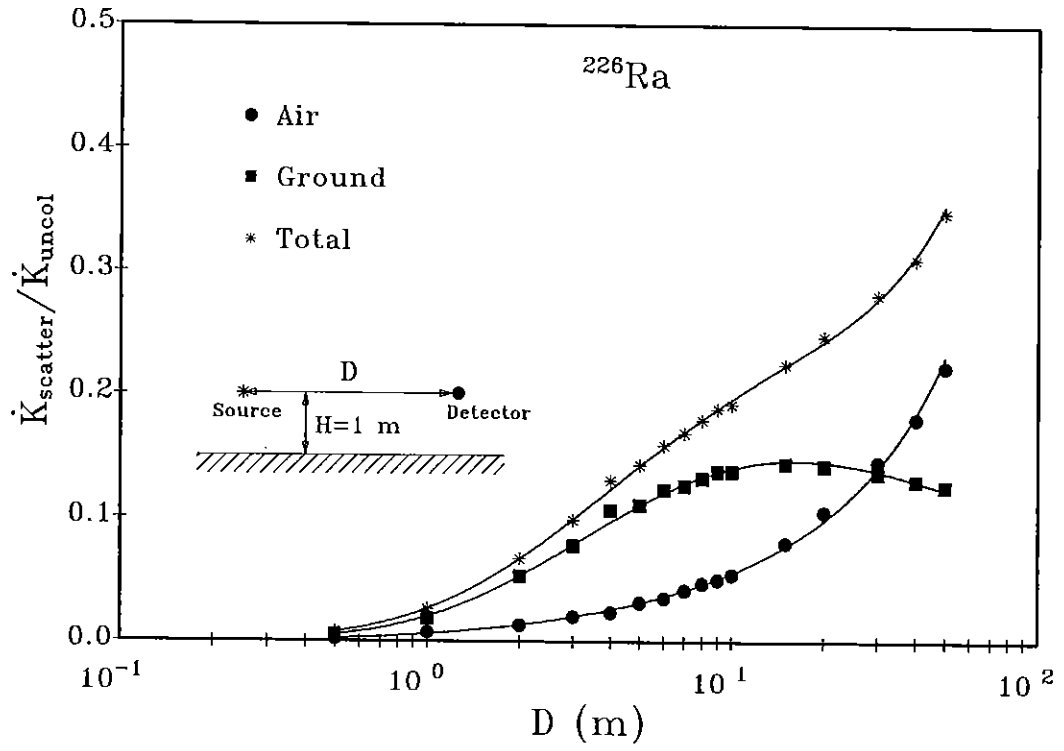

Figure 6.8: Relative scattered ground and air scattered air kerma rate components from a ^{226}Ra source as a function of distance.

6.4 Traceability

Traceability is the property of the result of a measurement or the value of a standard whereby it can be related to stated references, usually national or international standards, through an unbroken chain of comparisons all having stated uncertainties. In the field of ionising radiation primary standards are maintained by the Bureau International des Poids et Mesures (BIPM) and a number of primary standardising laboratories throughout the world. It is important that all measurements have a documented calibration chain to one of these primary laboratories.

An essential part of traceability is periodic calibration at suitable time intervals. The time interval between periodic calibrations should be within the acceptable period defined by national regulations within the country. Where no such regulations exist the time interval should be based on experience and on the availability of good records of performance of the instrument. Normally the calibration interval should not exceed 1 year.

Periodic calibrations using radioactive sources should be performed at air kerma rates between 0.01 $\mu Gy\ h^{-1}$ and 1 $\mu Gy\ h^{-1}$. These can be carried out by exposing the detector in specified calibration conditions to the reference gamma radiation from low activity ^{60}Co, ^{137}Cs or ^{226}Ra

sources. These low activity sources should have been calibrated by comparison with higher activity sources; a re-entrant ionisation chamber, e.g. the NPL secondary standard radionuclide calibrator, [WOO83], is suitable for this purpose. The output of these higher activity sources should have been measured in the same specified calibration conditions by a protection level secondary standard dosemeter. Alternatively a calibrated source can be used provided the air kerma rate is certified. In this way, traceability to national standards will have been achieved.

It is important that environmental dose rate measurements made in different countries can be compared with confidence; to maintain this confidence it is crucial that all measurements, whether with a source or calibrated instrument, are traceable to national standards.

7. SPECTROMETERS

7.1 General

Spectrometers were originally designed to be used in laboratories, for example for the analysis of environmental soil samples removed from a field site. About thirty years ago an analysis method was developed in which laboratory spectrometers were brought to the field for in situ gamma spectrometry. This technique has many advantages over soil sampling; large areas of ground can be covered by a single measurement thereby minimizing sampling errors and averaging out local inhomogeneities; results can be evaluated at the field site and much time and effort is saved in the collection and processing of soil samples. Continued improvements in detector portability and resolution have allowed this method to become more practical in recent years.

Other instruments described in this report are considered to be "single parameter" devices since they provide a measure of one quantity of the environmental radiation field, such as exposure or air kerma. Spectrometry systems may be considered "multiparameter" devices since they measure the energy and number of photons incident on the detector and can be used to identify the radionuclides present and to determine a number of useful radiological quantities. The determination of such quantities requires appropriate detector calibration and sophisticated data analysis. Only some of these techniques are presently available commercially, while the others require development and analysis on the part of the user. Concentration (activity per mass) or inventory (activity per unit area) of specific nuclides and their associated dose can be determined by using the Full Energy Peak Method which involves calibrating the detector and modelling the source distribution. For cases where the source distribution is unknown, the energy distribution of dose can be calculated by performing a Spectrum Unfolding after determining the detector's response function. A quick estimate of the total dose can be determined from the number of counts in the complete spectrum (Total Spectrum Energy Method) or for the case of a spectrum from natural terrestrial nuclides, in certain energy channels (Energy Band Method). All of these analysis techniques will be described in this chapter.

To take advantage of the full capabilities of spectrometers for in situ measurements requires the user to perform more sophisticated analyses than that needed for single parameter devices. Spectrometers also tend to be less easily portable and more expensive than single parameter devices. Despite these limitations and the relatively high cost of germanium detectors, the wealth of

information provided by a spectrometer makes it extremely valuable for complete analysis of the environmental gamma radiation field. This has been demonstrated in its extensive use for fallout studies and continued application to new problems in remediation.

7.2 Detectors

A spectrometry system consists of a detector plus an electronic chain for signal processing. For in situ measurements the detector must be efficient enough to be able to detect the low levels typical of environmental radiation in reasonable time intervals (usually 1 hour or less). This can be achieved by using detectors with a large volume or made of materials with a high atomic number. Two types of detectors are presently used for environmental gamma spectrometry: scintillation and semiconductor detectors.

7.2.1 Scintillation detectors

The scintillation method is one of the oldest methods used for radiation detection. The ideal material for manufacturing a scintillation detector should possess properties such as linear conversion efficiency, short decay time, good optical properties, etc. It is impossible for any scintillation material to fulfill all these requirements simultaneously. Thus one has to find a compromise among these and other factors, depending on a particular application. The discovery of NaI(Tl) in the early fifties started the era of modern scintillation spectrometry of gamma radiation.

One important parameter of any NaI(Tl) detector is the efficiency of energy transfer from incident radiation to the sensitive part of the detector. Different experimental and theoretical findings show that during the absorption of radiation and subsequent emission of light there is approximately one photon emitted for each electron-hole pair created in NaI (Tl), resulting in excellent scintillation efficiency for gamma radiation.

Another important parameter is the ratio of relative probabilities for photoelectric interactions and Compton scattering in the detector. The energy spectrum of environmental gamma radiation includes numerous peaks from different radionuclides present in the natural decay series and resulting from man-made activities. These full-energy peaks are "sitting" on the top of a continuous spectrum resulting from different interaction processes in air and the detector. Especially for low energy peaks to be detectable above the continuum, it is advantageous for the ratio of photoelectric to Compton effect in the detector to be large.

The high atomic number of NaI (Tl) results in favorable conditions for photoelectric interactions.

Energy resolution is an important factor for environmental applications where it may be necessary to distinguish closely spaced peaks. The typical resolution of a 3"x3" NaI(Tl) detector is 5-10%, depending on the energy of gamma radiation, [NUC80].

The response time of a scintillation detector is limited by the exponential decay process of its activator excited state. For NaI(Tl) this decay time is 230 ns, which is unfortunately too long for high counting rates. In most scintillators there are also other slower phosphorescence processes (decay time 150 μs) which compete with the exponential decay. These processes result in additional pulses which follow the main scintillation pulse. This undesirable effect also becomes more significant for high counting rates.

Another disadvantage of NaI(Tl) is its hydroscopic property which can cause crystal deterioration when exposed to air. This property results in the necessity to use an airtight packing of the crystal.

7.2.2 Semiconductor detectors

Semiconductor detectors were developed in the 1960's and have much better resolution than scintillation detectors. The most widely used semiconductor for gamma spectrometry is based on germanium. Since the energy required to produce one electron hole pair in Ge is low, (~ 3 eV) many such pairs contribute to each pulse so that statistical variations are small, allowing resolution on the order of 1 keV.

Early Ge detectors used lithium to compensate for impurities that could not be completely eliminated in crystal growth. These detectors require constant cooling with liquid nitrogen. In the 1980's high purity Ge (HPGe) detectors became available. HPGe detectors may be allowed to warm up when not in use making them preferable for field applications. They are maintained at liquid nitrogen temperatures while in use by means of a detector-cryostat-dewar assembly in a portable configuration, usually with a 1-5 litre dewar having a holding time typically of about 24 h. The part of the cryostat enclosing the sensitive part of the detector has a thinner "window" to reduce attenuation of incident gamma rays. This window is usually made of aluminum, a composite of carbon, or beryllium. beryllium tends to be brittle but has low attenuation for low energy photons, while aluminum is the most rugged.

Table 7.1: Typical spectrometry parameters for coaxial HPGe detectors[1)]

Parameter	Detector	
	p-type	n-type
Energy range (MeV)	0.040 – 10	0.003 - 10
Efficiency (%)	10 – 120	10 – 100
Resolution (keV) at 1.33MeV	1.75 - 2.30	1.80 - 2.70
FWTM/FWHM	1.90 - 2.00	1.90 - 2.30
Peak-to-Compton ratio	34 - 86:1	34 - 64:1

[1)] adopted from Canberra [CAN97] and EG&G [EGG97]

HPGe detectors are available in p-type or n-type, with the n-type detectors being more sensitive to low energy photons (less than 30 keV). This and some of the other features of germanium detectors that should be considered for particular applications are summarized in Table 7.1. The efficiency of germanium detectors is by convention expressed relative to the absolute efficiency of a 3"x3" NaI(Tl) crystal, and detectors with efficiency greater than 100% are now available. The quoted efficiency is that for 1.33 MeV photons from a ^{60}Co source situated 25 cm from the end cap, divided by 1.2×10^{-3} (the corresponding sodium iodide efficiency). The energy resolution is characterized by the peak full width at half maximum (FWHM), usually measured with a ^{60}Co source. The peak shape is expressed as the ratio of the full width at one-tenth maximum (FWTM) to the FWHM. This is a measure of the deviation of the peak from a gaussian shape and should be around 2 or less. The "peak-to Compton" ratio is a measure of the detectors ability to distinguish low energy peaks in the presence of high energy photons. A higher peak-to-Compton ratio means that there will be less Compton scatter from the high energy lines to interfere with low energy peaks of interest. It is expressed as the ratio of the 1.33MeV peak to the average Compton plateau between 1.040 and 1.096 MeV. The peak-to-Compton ratio is much higher for germanium detectors than for scintillation detectors.

The high resolution of germanium detectors usually makes them preferable to sodium iodide for most *in situ* spectrometry applications where the identification and quantification of sources is the goal. However, for some applications the lower cost and easier portability of the sodium iodide detector may make it advantageous. This could be the case for applications where it is known that there

are only natural emitters, or where expected contaminants have well separated gamma energies, or where liquid nitrogen is simply unavailable.

7.3 Signal Processing

Single events of energy deposition during interaction of ionising radiation in the detector result in the creation of pulses at the detector output. The amplitude of the pulse for the ideal detector is proportional to the energy deposited in the detector by an appropriate event. The pulses thus carry important information about the primary radiation. Prior to extracting this information the pulses have to be sorted out and transferred to a storage device where they are made available for a further analysis. This is made possible with to the help of different electronic units in the spectrometry chain. Principles of signal processing and necessary electronics are described for example by Knoll, [KNO79].

7.3.1 Basic electronics

Generally, there are two different types of pulses encountered in spectrometry measurements: linear and logic pulses. A linear pulse, through its amplitude and shape, carries information about the energy and sometimes the nature of radiation. On the other hand, the logic pulse in the spectrometry system is merely indicating the presence or absence of radiation. For practical reasons, pulse processing is divided into a few separate steps performed by appropriate electronic units. All spectrometry systems start with linear pulses and only later in a certain part of the spectrometry chain (pulse-height discriminators or ADC) are these transformed into logic pulses.

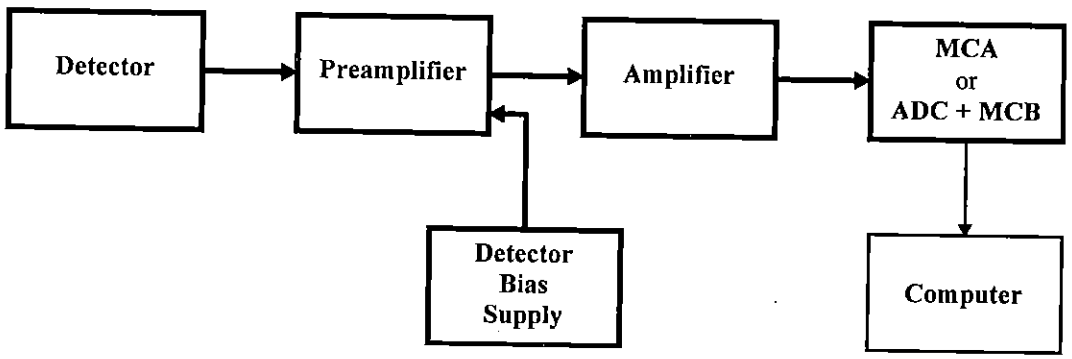

FIGURE 7.1: Block scheme of a HPGe spectrometry system.

The block scheme of a HPGe spectrometry system is shown in Figure 7.1. The pulses from this type of detector are unfortunately small and they have to be first amplified in a preamplifier and a linear amplifier before they can be further analysed. The main functions of the preamplifier are the conversion of collected charge into a voltage pulse, its amplification and shaping. The preamplifier here acts as an interface between the detector and pulse processing electronics. The most important requirement for a preamplifier is low noise. Charge sensitive preamplifiers with a FET transistor in the input stage are preferred for most spectrometry applications. Cooling of the FET reduces preamplifier noise so that its contribution to an overall uncertainty, usually expressed in terms of FWHM, is low. Another important source of preamplifier noise is its capacitive loading. This type of noise is caused mainly by the capacitance of the detector and connecting cables. To maximise the signal-to-noise ratio the preamplifier is usually mounted directly on the detector (a detector cryostat is also used to cool the FET). The constant component of noise level for zero input capacitance, expressed in FWHM of the response function, is for modern preamplifiers of the order of 500eV. This parameter may double for higher capacitance of practical detectors but it is still much less than the contribution from other sources.

Most radiation detectors require a dc high voltage for their operation. The high voltage supply for the spectrometry detector is provided by the detector bias supply. The high voltage may range from a few hundred volts to more than 4000 V depending on the detector. Besides a wide range of voltages for different detectors there are also different requirements as to the polarity, maximum current, stabilisation against drifts, etc. This is reflected in the different designs of bias supply for both scintillation and semiconductor detectors. An important feature of the preamplifier for the HPGe detector is a facility to shutdown the high voltage if sensors indicate a warm-up of the detector in order to minimise the risk of FET damage. For scintillation detectors the high voltage is supplied directly to the voltage divider of the photomultiplier. Therefore, the bias supply for these detectors is not connected to the preamplifier as in the case of the semiconductor detector.

Linear pulses at the preamplifier stage of the spectrometry system are called "linear tail pulses". They are generated at the output of a circuit with a large integrating time constant connected to the detector. The large time constant ensures that full charge collection is achieved. Such a circuit is represented by the preamplifier itself and the connecting cables. The resulting linear tail pulses are characteristic for their long tail compared with the leading edge. Typical decay time of the pulse is of the order of 50-100 μs compared to rise time 10-50 ns depending on the preamplifier. Amplitudes of these pulses are of the order of 0.1 mV, which is not large enough for counting and they have to be further amplified. However, the long tails would cause "pile-up" of signals, so that it is also necessary

to shape the pulses to reduce their time width. To achieve this the time constant of the circuit must be much less than the decay time of the tail pulse. Linear amplifiers with a shaping time constant typically 1.5-4 μs (faster shaping for NaI) are therefore used. The voltage gain of these amplifiers can be varied over a wide range and linear shaped pulses with amplitudes up to 10 V are produced at the output. Capabilities for pile-up rejection, pole-zero cancellation, base line restoration, etc., are presently available for most spectrometry amplifiers.

A unit that selects appropriate pulses and counts them is called an analyser. The single channel analyzer is the simplest device that can be used for spectrometry measurements but multi-channel analysers (MCA) are now more commonly used. In the MCA the shaped pulses are first selected according to their amplitudes. If the amplitude is within the selected "window" the pulse is converted into the logic pulse (a digit) by an analogue to digital converter (ADC) and the information about its amplitude is stored in a memory. Because the distortion of measured pulses occurs mostly in the ADC stage, this part must be optimized for high throughput, linearity of conversion and resolution. The 100 MHz Wilkinson type ADC's are used for environmental applications. In some cases, one MCA with a sufficient memory can be used with several ADC's working in a multiplex mode.

The measurement data is stored as a number of counts for each channel equal to the number of pulses with amplitude corresponding to the channel address. This is a basic function of any MCA. In an ideal case the number of counts in the channel will correspond to the number of events with a given energy deposition. The data stored in memory may be displayed. Beside the display, modern analysers also make provisions for simple data manipulation and evaluation functions. These include energy calibration, region of interest (ROI) definition, peak search, peak net area calculation, etc.

The widespread use of scintillation counting in radiation detection and especially spectrometry would be impossible without the availability of devices that convert the weak light output of a detector into a corresponding electrical signal. The photomultiplier (PM) tube as an extremely sensitive light detector accomplishes this task well. Generally, the PM tube detects light at the photocathode coupled to the electron multiplier consisting of dynodes each of them amplifies the incident electron current. As a result, current output proportional to light intensity is produced at the anode. A typical gain of a ten stage system is of the order of 10^7 but it can be higher for high-yield dynodes. Besides the dependence on a dynode material, the gain of the PM tube strongly depends on voltages applied to the dynodes and on their proper biasing. This is achieved by an external high voltage supply and a voltage divider. Because of this dependence, the HV source has to be stable without any ripple. For applications that require a battery supply, the HV source has to be optimised as tube currents, especially at the latter stages, can be high which results in a rapid

discharge of the battery. An indispensable part of any system using a PM tube is a photomultiplier base. This mechanical assembly is designed to accommodate not only a particular type of a PM tube but it contains a voltage divider and quite often also a preamplifier. Modern scintillation detection systems are constructed in compact packages called scinti-blocks or scinti-packs that house the detector, PM tube and necessary ancillary equipment (voltage divider, HV supply and preamplifier).

A great variety of PM tubes and bases are commercially available to suit particular applications. A low dark current and an anode pulse width are probably the most important parameters of the PM tubes for in situ spectrometry measurements. It is essential that they have a rugged construction as they have to withstand different environmental conditions that can negatively influence the measurement.

7.3.2 Computer aided instrumentation

Developments in computer technology have enabled the widespread application of computers in spectrometry systems. In some applications a stand alone computer is used to replace the memory part of the MCA together with a separate ADC and a multichannel buffer (MCB). The computer is used for the system control and data evaluation, and can be used while the MCB is busy collecting data. Portable versions of such systems are now available that use a notebook PC. Other systems use an ADC in the form of a plug-in card which is inserted into the PC. These systems are much cheaper, and though they are somewhat less accurate are quite useful for a number of spectrometry applications. Most computer based systems are also supported by a software designed for the spectra analysis and activity measurements. Standard options of these software packages include automatic peak search, deconvolution of peaks, calculation of peak parameters (position, FWHM, area, standard deviation), energy calibration, activity calculation, etc. It is good practice to check for the inclusion of the latest changes in nuclear data .in a nuclide library supplied with the software. While these standard spectra analysis options were designed for laboratory spectrometry, new commercial software packages specifically for *in situ* applications have recently become available for use with portable spectrometry systems.

The *in situ* gamma spectrometry technique using a germanium detector and the full energy peak method is commercially available as a hardware-software package from different manufacturers. They include detectors with calibration factors that have been estimated based on crystal dimensions or calculated using Monte Carlo techniques. Sodium iodide detectors are available with conversions to

dose rate, but the elaborate unfolding techniques described in 7.4.4 are not presently part of these packages.

7.4 Analysis of pulse height spectra

The first step in any spectrometry measurement is the collection and viewing of the differential pulse height distribution. This can be used to quickly determine basic features of a radiation field, such as the maximum energy of the spectrum or the presence or absence of a certain nuclide. For more quantitative information, evaluation of the pulse height distribution is the essential task of any spectrometry measurement.

Since most detectors used for spectrometry measurements are not spherically symmetrical the results will depend on the source geometry and on the mutual orientation of the detector and the source. Results will be different for the detector facing down or positioned horizontally, they will also depend on the source type (e.g. if the source is a radioactive cloud or soil). For simplicity, we will assume that the detector is placed 1 m above the flat surface and that it is facing downwards. Further, we will assume that the major source of radiation is in the ground. This is a standard geometry used for measurements of kerma rates from the terrestrial radiation. The treatment of other situations is very similar.

7.4.1 Full-energy peak method

This method is based on the assumption that the estimated peak area for energy E is proportional to the true peak area for that energy and thus to the fluence of unscattered primary photons. A calibration factor to convert from peak count rate to soil activity must be determined for the detector for appropriate energies. It consists of three terms, one depending only on the detector efficiency, another that depends only on the source distribution in the soil, and a third that folds together the angular response of the detector with the angular distribution of incident photons for a particular source distribution. This calibration equation (7-1) may be written so that it relates the full-energy count rate, $\dot{N}_f$, at energy, E, to the kerma rate, $\dot{K}_a$, from photons originating from the given radionuclide with energy, E, as

$$\dot{N}_f / \dot{K}_a = (\dot{N}_0 / \varphi)(\dot{N}_f / \dot{N}_0)(\varphi / \dot{K}_a) \qquad (7\text{-}1)$$

where $(\dot{N}_0 / \varphi)$ is the full-energy count rate per unit fluence rate of photons of energy, E, incident on the detector in normal direction to the detector face, $(\dot{N}_f / \dot{N}_0)$ is the correction factor reflecting

the angular dependence of the response, and $(\varphi / \dot{K}_a)$ is the fluence rate of unscattered photons with energy, E, at the detector position per unit kerma rate at that place from both scattered and unscattered photons originating from the source with the initial energy E.

The values of $(\dot{N}_0 / \varphi)$ for different energies, E, are obtained experimentally using a set of standardized point sources with appropriate energies. The source is positioned on the axis of the detector and at least 1m from the detector front face. The fluence rate at the detector position is calculated from the source certificate taking into account attenuation inside the source, its encapsulation and air. Any contribution to the peak from other sources is corrected by taking the background measurement without the source. Finally, the measured ratios are fitted using standard algorithms and values for other energies may be deduced from the fit. Attention has to be paid especially to the lower energies where individual characteristics of the detectors (their construction, dead layers, etc.) may influence their response.

Most of the detectors used for *in situ* spectrometry measurements are of cylindrical shape and are used "looking downward" with their axis perpendicular to the measured surface. Due to the axial symmetry of these detectors their response does not depend on the azimuthal angle. The angular correction factor $(\dot{N}_f / \dot{N}_0)$ for a given energy, E, can be determined as

$$\dot{N}_f / \dot{N}_0 = (2\pi / \varphi_T) \int_0^{\pi/2} \varphi(\theta)(\dot{N}_f(\theta) / \dot{N}_0) \sin\theta d\theta \qquad (7\text{-}2)$$

where, φ_T, is the total fluence rate of unscattered photons at the position of the detector and, θ, is its zenith angle with $\theta = 0$ corresponding to the downward direction. The ratio $(\dot{N}_f(\theta) / \dot{N}_0)$ represents the relative full-energy peak count rate of the detector per unit fluence rate at angle, θ, and (7-2) then describes a weighting procedure for $(\dot{N}_f(\theta) / \dot{N}_0)$ over the fluence rate distribution. The term $(\dot{N}_f(\theta) / \dot{N}_0)$ is detector dependent and for a cylindrical detector oriented vertically it depends on a ratio of the detector length (L) and diameter (D). Its variation is caused by the different effective surface of the detector for photons coming from directions with different, θ, that is more pronounced for L≠D. It can be determined experimentally in a similar way as $(\dot{N}_0 / \varphi)$. The angular correction factor $(\dot{N}_f / \dot{N}_0)$ can be calculated by numerical integration of (7-2) for different source distributions. The whole procedure is fully described in [EML92].

Calculations show [BEC72b] that for the source distributions generally encountered in the environment, more than 80% of unscattered photons reach the detector at angles $\theta = 30°$-$90°$ where

the response is more or less uniform. This has the effect that even for L/D≠1 the variation in $(\dot{N}_f / \dot{N}_0)$ is not so critical. Of course, this is not valid for lower energies where the individual characteristics of the detectors are more visible. Based on the experimental findings, Helfer and Miller [HEL88] published a set of calibration factors for different L/D ratio and the detector orientation in the field. Their uncertainty is estimated to be 10-15% for energies higher than 200 keV which is usually sufficient for most of practical applications.

The relative fluence rate of unscattered photons reaching the detector from the direction, θ, θ+$d\theta$ is $(\varphi(\theta)/\varphi_T)\sin(\theta)d\theta$. It depends on the actual distribution of the source in the soil. The distribution may change with time as nuclides penetrate into the soil or get washed away [JAC90]. To treat this problem an exponential distribution of the specific activity in the soil, $A_v(\xi)$, is assumed

$$A_v(\xi) = \rho(z) A_{m,0} \exp(-\xi / \beta) \tag{7-3}$$

where, ρ, is the soil density (g/cm^3), $A_{m,0}$, is the activity per unit mass at the surface (Bq/g), ξ and β are the mass per unit area and the relaxation mass per unit area in soil, both in g cm^{-2}. The mass per unit area, ξ, that is relevant for the attenuation is than defined as

$$\xi = \int_0^z \rho(z')dz' \tag{7-4}$$

where, z, is the linear depth in the soil (cm).

The last term, $(\varphi / \dot{K}_a)$, of equation (7-1) involves both unscattered and scattered photons that contribute to the kerma rate. It is found from transport calculations using the Monte Carlo method of electron-photon transport.

Table 7.2 gives the conversion coefficients $(\varphi / \dot{K}_a)$ for homogeneously distributed natural radionuclides. They can be used to calculate the actual kerma rates from the corresponding full-energy peak count rates. The values of (φ / A_v) are also given for calculation of the radionuclide specific activities. The conversion coefficients for other source arrangements can be derived in a similar way.

Table 7.2: Yield, unscattered photon fluence rate at 1m above ground per unit kerma rate [GIB93]and/or per unit activity per unit mass [SAI95] of natural radionuclides homogeneously distributed in the ground

Nuclide	Energy (keV)	Yield (s^{-1} Bq^{-1})	φK_a (m^{-2} s^{-1} per nGy h^{-1})	φA_v (m^{-2} s^{-1} per Bq kg^{-1})
Uranium series				
^{226}Ra	186.0	0.033	2.19	1.18
^{214}Pb	242.0	0.075	4.96	2.98
	295.1	0.192	13.90	8.28
	352.0	0.369	28.70	17.10
^{214}Bi	609.3	0.469	45.00	27.50
	665.4	0.0158	1.62	0.97
	768.4	0.0497	5.59	3.25
	934.0	0.0319	3.87	2.29
^{234m}Pa	1001.0	0.00845		0.63
^{214m}Bi	1120.3	0.155	20.10	12.20
	1238.1	0.061	8.21	5.07
	1377.7	0.041	7.12	3.61
	1402.0	0.0138		1.23
	1408.0	0.025	5.97	2.23
	1509.2	0.022	3.40	2.02
	1729.6	0.030	4.87	2.98
	1764.5	0.162	25.70	16.20
	1847.4	0.0216	3.78	2.22
	2118.5	0.0125		1.38
	2204.1	0.0524	9.30	5.92
	2447.7	0.0162	3.18	1.93
Thorium series				
^{228}Ac	209.0	0.0455	1.79	1.72
^{212}Pb	238.6	0.434	22.30	17.30
^{224}Ra	240.8	0.0397		1.58
^{228}Ac	338.4	0.120	6.71	5.47
	463.1	0.0464	2.83	2.41
^{208}Tl	510.6	0.0809	5.94	4.38
	583.0	0.306	19.70	17.60
^{212}Bi	727.3	0.0675	5.74	4.30
^{228}Ac	794.8	0.0484	3.69	3.22
^{208}Tl	860.3	0.0453	3.63	3.13
^{228}Ac	911.2	0.290	23.30	20.60
	964.6	0.0545		3.98
	969.0	0.175	18.90	12.80
	1588.2	0.0370	3.79	3.52
^{212}Bi	1620.7	0.0149		1.43
^{228}Ac	1630.5	0.0195		1.87
^{208}Tl	2614.4	0.359	51.40	44.20
Potassium				
^{40}K	1460.8	0.170	176.00	9.71

A major problem of in situ gamma spectrometry arises from the fact that certain assumptions are made about the source distribution and the associated attenuation of unscattered photons. Different methods have been proposed by several groups to improve this shortcoming. Generally, they fall into three distinct categories according to the effect they are based on. These are:

1) Methods which use the counts between the full-energy peak and the Compton edge to provide information on relative scatter and therefore the attenuation to indicate the source distribution [KAR90 and ZOM92].

2) Methods which compare results from low and high energy lines to check assumptions made about the source distributions since the attenuation of unscattered photons depends on their energy [SOW89, RYB92 and MIL84].

3) Methods which use soil coring to various depths in conjunction with *in situ* spectrometry measurements to determine the source distributions, [REG96].

Unfortunately, all of these methods have their limitations and there is a need for more studies although the second method seems to be promising. Recent developments in this field are reviewed in ICRU, [ICRU94].

7.4.2 Energy band method

The total dose from the natural terrestrial radionuclides can be quickly determined using the energy band analysis method. It is mostly used with the low resolution sodium iodide detector and for airborne surveys for the purpose of uranium or geological exploration. The combined effects of the detector finite resolution, scattering of radiation before it reaches the detector and a complex spectrum of sources encountered in the environment cause spectral interference between the different sources. As a result, if we select an energy band (window) characteristic for a certain nuclide, the registered number of counts will also include contributions from other windows. In the case of three windows (K, U and Th windows) we can write a set of equations which relate a vector of true counts, **N**, to the vector of measured counts, $\mathbf{N_1}$, as

$$\mathbf{N}_1 = \mathbf{F} \bullet \mathbf{N} \qquad (7\text{-}5)$$

where a 3x3 matrix, **F**, contains elements describing the interference between channels. We can find the true counts vector, **N**, as a solution of this equation using an inverse matrix

$$\mathbf{N}_1 = \mathbf{F}^{-1} \bullet \mathbf{N} \qquad (7\text{-}6)$$

With a proper calibration [LOV84 and GRA74] the stripped (true) counts may be related to activities of K, U and Th or their contributions into the kerma rate. IAEA [IAEA91] recommends the following window settings:

Potassium 1.37 - 1.57 MeV

Uranium 1.66 - 1.86 MeV

Thorium 2.41 - 2.81 MeV.

They also recommend corrections for influences from the sources not included in this equation (radon daughters, cosmic radiation).

Slightly different windows are recommended at EML [EML92]. They relate the measured energies (counts per window multiplied by mean photon energy corresponding to that window) in bands E_1 = 1.32-1.60 MeV, E_2 = 1.62-1.90 MeV, E_3 = 2.48-2.75 MeV and E_T (total) = 0.15-3.40 MeV to the exposure rates to be measured and give elements of matrix for a 3"x3" NaI(Tl) detector obtained from a regression analyses of the measured "known" spectra.

7.4.3 Total spectrum energy method

This method is based on the idea that the total number of counts in the entire spectrum is related to the total dose. It has primarily been used for sodium iodide detectors. The air kerma, $\dot{K}_a$ is equal to the integral

$$\dot{K}_a = \int_0^\infty (\mu_{tr} / \rho)\varphi(E)EdE \qquad (7\text{-}7)$$

where, $\varphi(E)EdE$, is the energy fluence between, E, and, $E+dE$. As, (μ_{tr}/ρ), is fairly constant over the energies from a few hundred to several MeV, the integral will be proportional to the total energy in this interval. With a proper calibration, an instrument based on this principle can be used to measure kerma or exposure rates from the environmental gamma sources. EML [EML92] prescribes the total spectrum energy window from 0.15 to 3.4 MeV. This is a range of energies covering most radionuclides that may occur in the environment.

While the total spectrum method can be useful for a quick analysis it does not give the relative contributions to the kerma rate (or exposure) from different sources and thus does not take advantage of the energy resolution of the spectrometer. This is probably its main disadvantage.

7.4.4 Spectra unfolding

The most complete analysis of in situ data is to "unfold" the measured spectrum. The measured spectrum is a distribution of pulse heights that is essentially a spectrum of absorption in the detector. What is desired is the incident spectrum. While the position of each channel is directly connected with the energy deposited in the detector, a count in the continuum could represent a photon partially absorbed in the detector or a fully absorbed photon that was already scattered in the environment. The incident spectrum has to be obtained from the measured spectrum by the process called deconvolution or spectrum unfolding. A review of this topic may be found in ICRU, [ICRU94].

Generally, spectrum unfolding requires solution of the Fredholm integral equation of the 1. type

$$N_1(h) = \int_0^\infty R(E,h)N(E)dE \tag{7-8}$$

where $N_1(h)$ is a measured pulse height distribution, $R(E,h)$ represents a response function of the system, and $N(E)$ is the spectrum of photons reaching the detector. The spectrum of primary photons is usually found in an approximate form as a solution of the matrix equation

$$\mathbf{N_1} = \mathbf{R} \bullet \mathbf{N} \tag{7-9}$$

where $\mathbf{N_1}$, $\mathbf{R}$ and $\mathbf{N}$ have a newly defined meaning. A vector, $\mathbf{N_1}$, is realized by the results of measurement, $\mathbf{N_{1i}}$ corresponds to the number of counts in the i-th channel of the multichannel analyzer, $\mathbf{R_{ij}}$ represents contribution into the i-th channel from photons in the j-th energy interval, and $\mathbf{N_j}$ is the number of original photons in the j-th energy interval. Here the response matrix, $\mathbf{R}$, is a discrete form of the response function.

A few general problems arise in the unfolding process. In many cases, especially in the case of scintillation detectors, the response matrix is ill conditioned. Uncertainties in the response matrix can be caused by the fact that both are calculated as well as measured response matrices are only approximations for the real situation. Errors in the matrix $\mathbf{R}$ become amplified when it is inverted.

Small variations in the measured spectrum due to experimental uncertainties can therefore lead to large errors in the calculated spectrum or possibly unphysical solutions.

Because of these effects, the exact solution of equation (7-9) generally cannot be obtained and we have to search for the solution using other methods. Scofield [SCO63] described a simple iterative technique known as the Scofield-Gold technique. The algorithm describing the i-th iteration step is

$$\mathbf{N}^{(i)} = \mathbf{R} \bullet \mathbf{N}^{(i)}$$

$$\mathbf{d}_j^{(i)} = \mathbf{N}_j^{(i)} / \mathbf{N}_{1j}^{(i)} \qquad (7\text{-}10)$$

$$\mathbf{N}_j^{(i+1)} = \mathbf{d}_j^{(i)} \bullet \mathbf{N}_1$$

where $\mathbf{d}_j^{(0)} = 1$ and first guess of $\mathbf{N}^{(1)}$ is the measured pulse height spectrum. The whole procedure was discussed by Clements [CLE72] and he suggests to premultiply the matrix equation (7-9) by, $\mathbf{R}^T$, a transpose matrix of **R**, and a diagonal weight matrix, **W**, with elements equal to the inverse of the variance for each channel

$$\mathbf{R}^T \bullet \mathbf{W} \bullet \mathbf{N}_1 = \mathbf{R}^T \bullet \mathbf{W} \bullet \mathbf{R} \bullet \mathbf{N} \qquad (7\text{-}11)$$

This resulted in a much better solution of equation (7-9) in the sense of a minimum χ^2.

Another advantage of the described premultiplication is in the potential to solve the overspecified matrix equation. This is the case when a vector, $\mathbf{N}_1$, has more elements than the vector, **N**. The response matrix, **R**, is not square so that it can not be inverted. The use of the transpose matrix, $\mathbf{R}^T$, eliminates this problem.

All iterative techniques give an estimation of the real spectrum only. Methods of a search for the optimum solution as well as criteria of convergence may differ. In principle, one can use any of the methods of modern numerical mathematics. On the other hand a good search in a sense of a convergence does not necessarily mean a good unfolding. In practice, solutions can oscillate, sometimes negative values result, and one part of the spectrum may give good agreement while another part does not. This may create false peaks in the unfolded spectrum, or resolution abilities of the system may decrease. This is more pronounced for NaI(Tl) detectors.

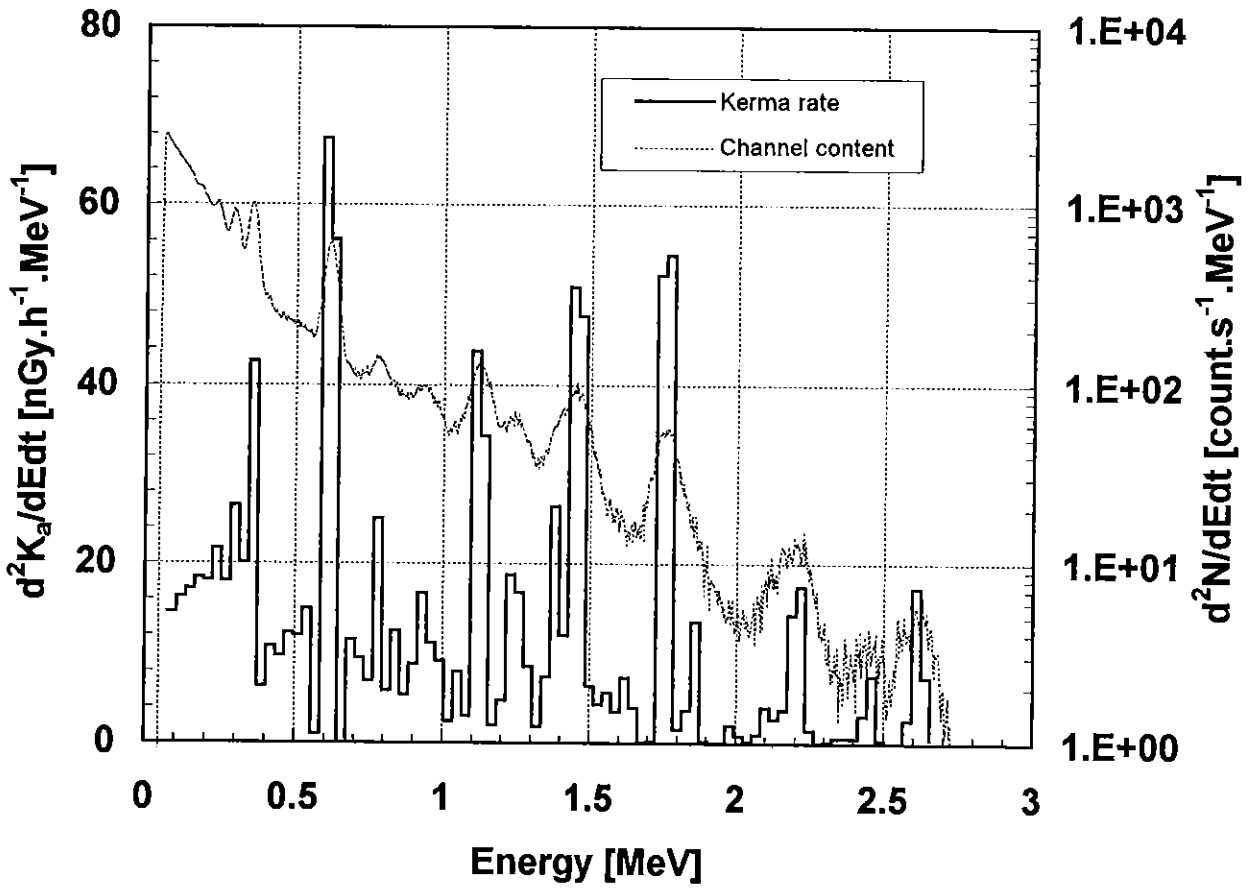

FIGURE 7.2: Measured pulse height and kerma rate energy distributions for ^{226}Ra source during free field calibration of a NaI(Tl) spectrometer

An example of the resolution ability of the practical NaI(Tl) spectrometry system is given in Figure 7.2. It shows a pulse height distribution and resulting kerma rate distribution for a ^{226}Ra source during a free-field calibration. A 3"x3" detector was used to collect data. The spectrum was unfolded using a response matrix with 30 keV energy bins. The unfolding procedure used was described by Kluson [KLU90]. One can clearly see a contribution into the kerma rate from different energies of the source as well as from natural radionuclides (^{40}K).

7.5. Detector Response Function and Response Matrix

In order to unfold a measured spectrum, the detector's response to incident radiation must first be determined. Out of the various ways photons can interact with a detector, the three most important interaction mechanisms are: photoelectric absorption, Compton scattering and pair production. Less significant processes like coherent scattering and nuclear reactions compete with the above processes but are usually not significant for detection of environmental radiation. More detailed descriptions of the interaction processes can be found in most dosimetry textbooks.

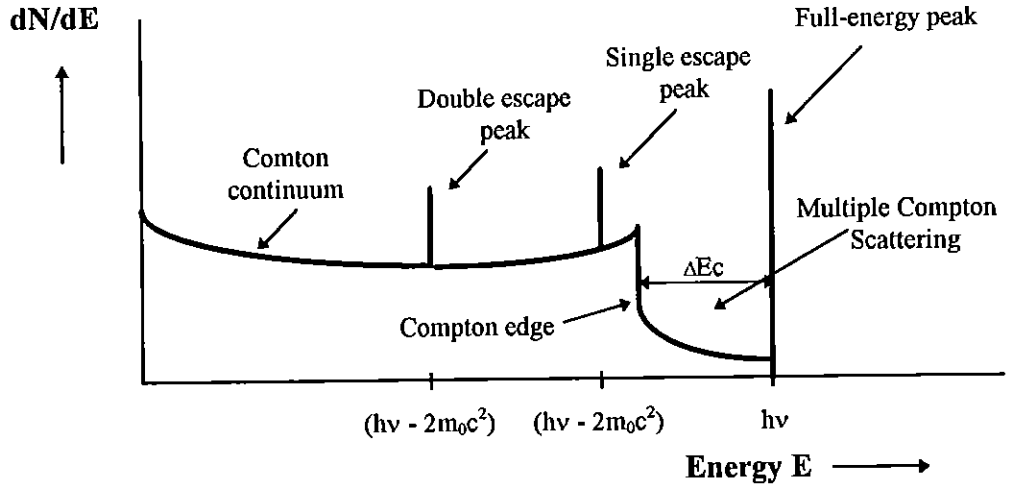

FIGURE 7.3: Typical response of an ideal detector to photons of energy hν.

A differential pulse height spectrum (pulse heights expressed in energy E) for a hypothetical detector with an ideal resolution is sketched in Figure 7.3. One can see a typical picture described by the above processes. Unfortunately, real detectors usually do not have an "ideal" resolution and the combined effects of interaction physics and detector construction also play a substantial part in formation of the final shape of the spectra.

7.5.1. Components of response function

In practice, the relation between the initial photon energies and resulting pulse heights is more complex than that illustrated in Figure 7.3 and is generally expressed by a functional dependence called the response function. The response function $R(E_0,h)$ may be written [BER72] as the convolution of the energy deposition function $D(E_0,E)$ and the resolution function $G(E,h)$

$$R(E_0,h) = \eta(E_0)\int_0^{E_0} D(E_0,E)G(E,h)dE \qquad (7\text{-}12)$$

where

$R(E_0,h)dh$ is the probability that a photon with energy E_0 will produce a pulse with a height between h and $h+dh$;

$\eta(E_0)$ is the probability that the incident photon will undergo at least one interaction in the detector;

$D(E_0,E)dE$ is the probability of an energy deposition between E and $E+dE$ in the case that a photon interacts in the detector;

$G(E,h)dh$ is the probability that an amount of energy E deposited in the detector will give rise to a pulse with a height between h and $h+dh$.

The response function is normalised so that the integral of $R(E_0,h)$ over all h equals to $\eta(E_0)$.

The resolution function $G(E,h)$ in this equation reflects the fact that an event with energy deposition E does not necessarily leads to creation of a pulse with a definite height h but rather a spectrum of pulses is observed for successive events. In other words it accounts for fluctuations in the detector response to a given energy deposition. It is a source of an imperfect (finite) resolution of the detector. Generally, there are different sources of fluctuations which influence the behavior of the whole system. Probably, the most important is the statistical nature of the counting process which cannot be fully eliminated and presents the permanent minimum source of signal distortion. Other, usually less significant sources have their origin in operational drifts and random noise in the measuring chain. They can be substantially reduced by a proper selection and adjustment of the instrumentation.

In the case where all processes are stochastic, the resolution function, $G(E,h)$, is described by the Gaussian

$$G(E,h) = \frac{1}{\sqrt{2\pi}\sigma(E)}\exp\{-\frac{[f(h)-E]^2}{2\sigma^2(E)}\} \qquad (7\text{-}13)$$

A standard deviation, $\sigma(E)$, can be expressed as $\sigma(E) = 0.425\ FWHM(E)$ or better as a resolution of the detector $R(E) = \sigma(E)/E$ which is a measurable parameter of the system.

This is a practical procedure which is used to determine the resolution function. A set of sources with different energies is used to measure the FWHM and the measured values are fitted by a power law function [KNO79]. This is a convenient form used for further calculations.

In practical spectrometry systems, besides the statistical sources of finite resolution there are also sources like noise, drift, etc., which contribute into the total, $FWHM_T$. We can write

$$FWHM_T^2 = FWHM_{noise}^2 + FWHM_{statistical}^2 + FWHM_{drift}^2 + \ldots \quad (7\text{-}14)$$

The procedure for experimental evaluation of the resolution, described before, that involves a measurement of *FWHM* is thus the measurement of the overall performance of the system for particular experimental conditions and settings of the electronic chain. A proper adjustment of the whole electronic chain has to be made if we want to use the value of the detector resolution obtained from a different experimental setup.

7.5.2. Determination of response function and response matrix

A detector response function as defined in 7.5.1 describes behaviour of the detector when irradiated by photons of single energy, E_0. It is essentially an orthogonal cut of the general response surface. A practical application of spectrometry methods involves the whole range of photon energies so that a number of such response functions for a given detector are needed. In principle, the detector response functions can be obtained experimentally, using a set of monoenergetic sources. The response function for the other energies can be deduced by different interpolation and extrapolation techniques. Elaborate procedures were described [BER72 and RAD87] that enable construction of response functions for photon energies important for the environmental spectrometry. A main disadvantage of this method is the presence of scattered radiation which disturbs the measurement. Miller [MIL84] proposed a shadow shield method which partially solves the problem.

Another approach is to perform Monte Carlo calculations. As this can be done for any energy, there is then no need to interpolate. The process of energy deposition in the detector is fully described by the energy deposition function, D (E_0, E). This function can be calculated using a Monte Carlo simulation that involves the full transport of photons and electrons. Its folding with the resolution function is an effective way to evaluate the response functions for different detectors. The method makes it possible to simulate those detector-to-source arrangements which would be hard to prove experimentally. An example of the Monte Carlo calculation of the response functions for a Bicron 3x3" NaI(Tl) detector and different energies of photons is given in Figure 7.4.

Recently, Fehrenbacher.[FEH96] made extensive calculations of response functions for semiconductor detectors used during *in situ* measurements. To some extent, Monte Carlo modeling can include the influence of individual detector characteristics like housing, dewar, etc. However, some characteristics such as thickness of the dead layer, exact positions of contacts, etc, are difficult to model as they are usually not known very well. This is most significant for low energy photons.

In practice, unfolding procedures involve the response matrices rather than the response functions. Any element, $\mathbf{R_{ij}}$, of the response matrix, $\mathbf{R}$, is expressing the probability that a photon with energy, E_j, will give rise to the pulse in the interval (h_{i-1}, h_i). It can be obtained by simple integration of (7-12) over the values of pulse heights. We can write

$$\mathbf{R}_{ij} = \int_{h_{i-1}}^{h_i} R(E_j, h)dh \,. \tag{7-15}$$

The pulse height intervals are related to the energy intervals (energy bins) through appropriate calibration. In principle, it is not necessary for the energy bins to be equidistant but it is a good practice to divide the whole energy scale into number of energy bins of the same width according to the required resolution and resolution properties of the detector.

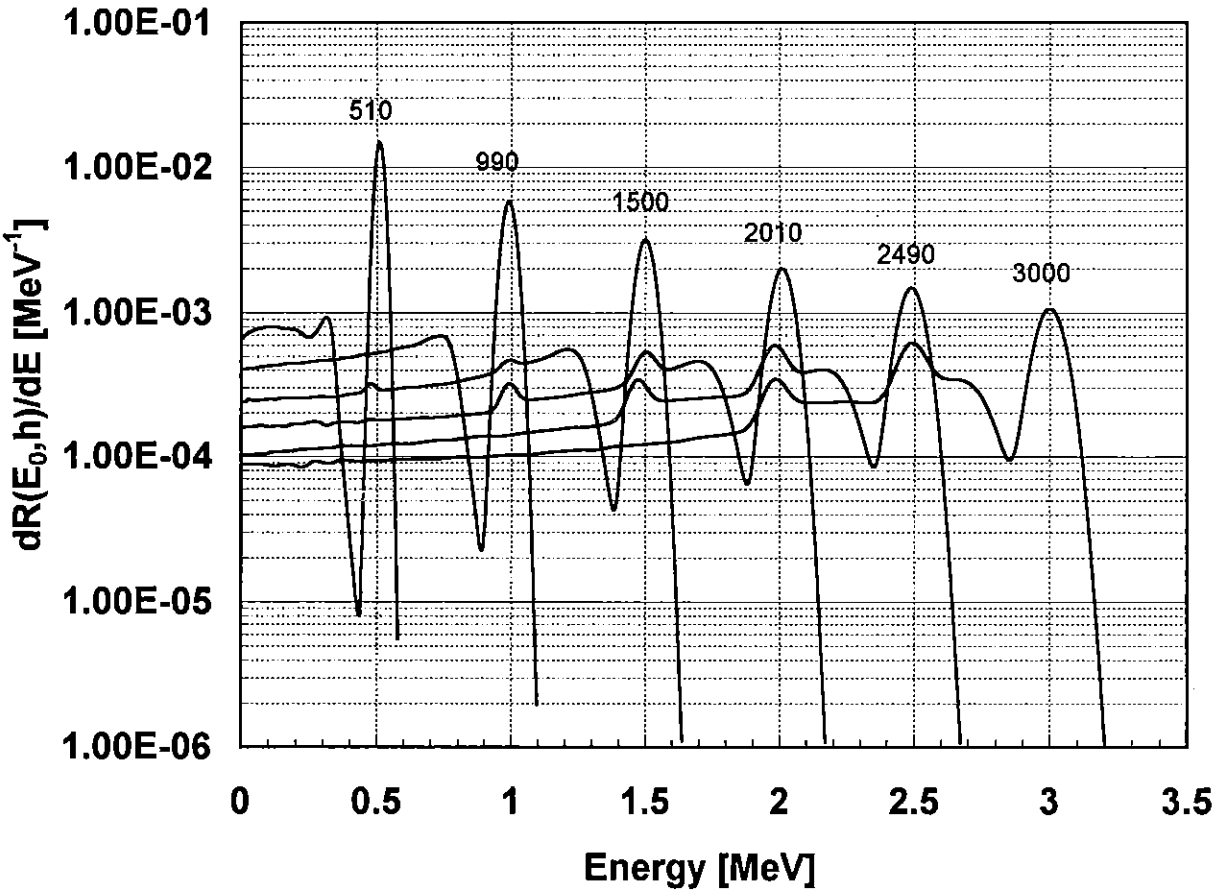

Fig. 7.4: Calculated response functions for a 3" x 3" Na(TI) detector for different energies of incident photons, [KLU90].

8. INTERCOMPARISONS

Networks of active and passive detectors have been established in many countries to monitor environmental radiation for potential increases due to nuclear facility accidents or weapons activity. Active detectors provide a record of temporal changes in the radiation level, but require occasional maintenance and can be too expensive to be left at multiple sites to adequately cover the area around a facility. Passive detectors provide only a measure of the total dose, but are a useful supplement to active monitors because they can be widely deployed over large areas since the individual dosemeters are inexpensive, small, and have no power requirements. Passive detectors have proved especially useful for long term measurements at sites that are not easily accessible for servicing instruments due to difficult environmental conditions. The most commonly used passive detector presently in use is the thermoluminescent dosimeter (TLD), with at least 17,000 in 26 countries around the world being monitored by TLDs.,[KLE99].Active detectors such as pressurized ionization chambers (PICs) compensated Geiger-Müller (GM) tubes are maintained at hundreds of locations, and in many cases are linked to a central computer which stores the data, [DeC96].

Because of their widespread use, TLDs have the potential to be the only detector on the scene of an accident during the initial stages. At the time of the Three Mile Island accident, the only field monitors in place both on and off site were TLDs and passive particulate and charcoal samplers, [HUL80]. It is therefore important to compare the results obtained with active and passive detectors where simultaneous measurements have been made. This section will review some representative data that allows comparison between both types of detectors in use for the measurement of environmental radiation.

8.1 Sources of Data

The U.S. Department of Energy Environmental Measurements Laboratory (EML) is one source of such data, with monthly TLD and PIC measurements having been made at an environmental testing station for the last 20 years. Another source is the International Intercomparisons of Environmental Dosemeters, in which many types of passive dosemeters submitted by participants from around the world are deployed simultaneously at a field site along with PICs, typically for about 3 months, [DeP86]. The CEC has sponsored European TLD intercomparisons, [McK85and DRI88] and other intercomparisons that have included many active instruments such as PICs, GM detectors and scintillators, as well as TLDs and new electronic dosemeters that are being tested for applications to environmental dosimetry, [BOT95].

8.2 EML Data

The Environmental Measurements Laboratory has maintained a field station for measuring natural environmental background conditions and testing field instruments since 1976, [KRE91]. The site is located in Chester N.J. in rural area with no local sources of pollution, a flat terrain, and soil that has been undisturbed for at least the last 30 years. This station has been equipped to measure radioactivity in surface air, chemical composition of precipitation, radon, meteorological data, and environmental radiation. For environmental radiation monitoring two of EML's pressurized ionization chambers, [DeC72 and VAN93], provide a continuous record of exposure rate, and up until 1990 monthly TLD measurements were made using ^{7}LiF TLDs, [CHI94]. (Since 1990 TLDs have been deployed on a quarterly schedule).

While the TLDs measure the total dose, a mean dose rate is obtained by dividing by the field deployment time. This can then be compared with the average dose rate measured by the PICs during the same time period. (This is an appropriate quantity for comparison since short term variations are then averaged over the deployment time). Monthly data from January 1987 through June of 1990 is shown in Figure 8.1.

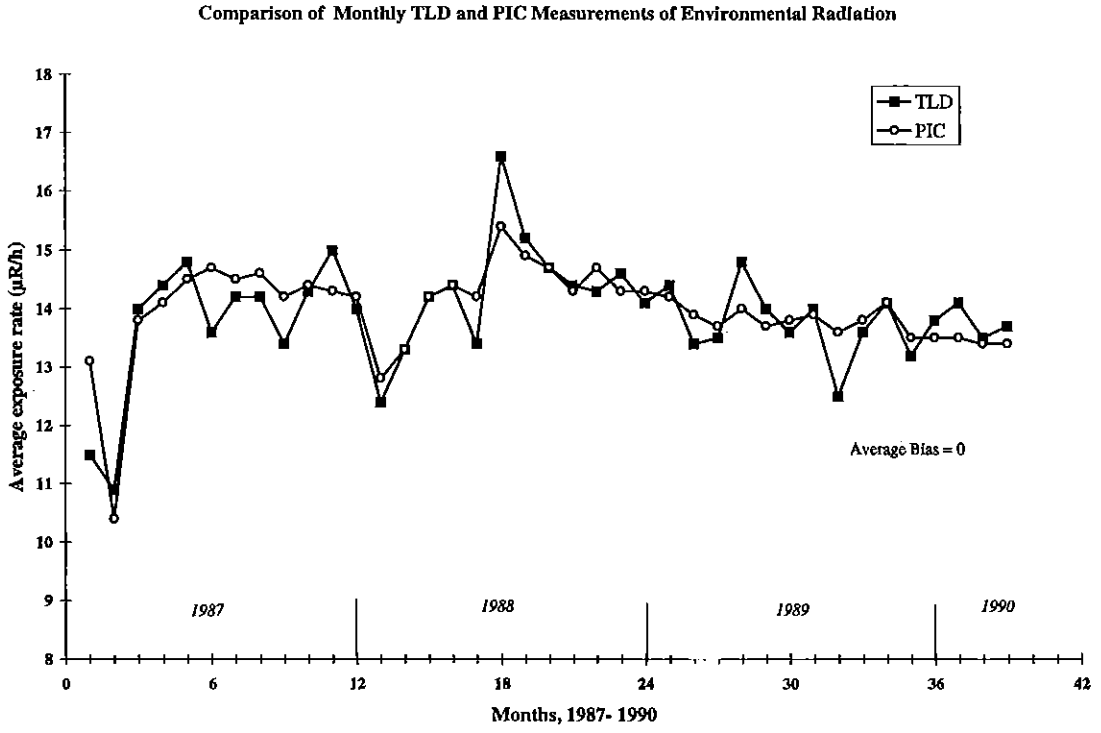

Figure 8.1: Comparison of monthly TLD and PIC measurements of the environmental radiation, [CHI94].

The TLD measurements tend to have larger fluctuations than the PIC results, but overall the two sets of data track each other rather well. The statistical uncertainty associated with the PIC measurements is small (<<1%) since it is the average of a large number of one minute readings (n»40000). For TLD measurements it tends to be higher (~5-10%) due to variations between chips and possible changes in reader conditions as well as the expected poorer statistics resulting from averaging over a small number of chips per dosimeter (n»15). This is probably the reason for larger variations observed in the TLD results. There does not seem to be any strong systematic difference between the two data sets, and on average the percent bias (defined as 100% x (TLD Result - PIC Result),PIC Result) for the 39 comparisons is -0.4%.

8.3 Data from International Intercomparisons of Environmental Dosemeters

The International Intercomparisons of Environmental Dosemeters were begun in 1974 to access the performance of environmental dosemeters by comparing the overall distribution of results with reference measurements of the delivered doses and generally accepted performance standards. Participants submit dosemeters for irradiation at an outdoor field site and in the laboratory. Reference measurements in the field are obtained with EML PICs.

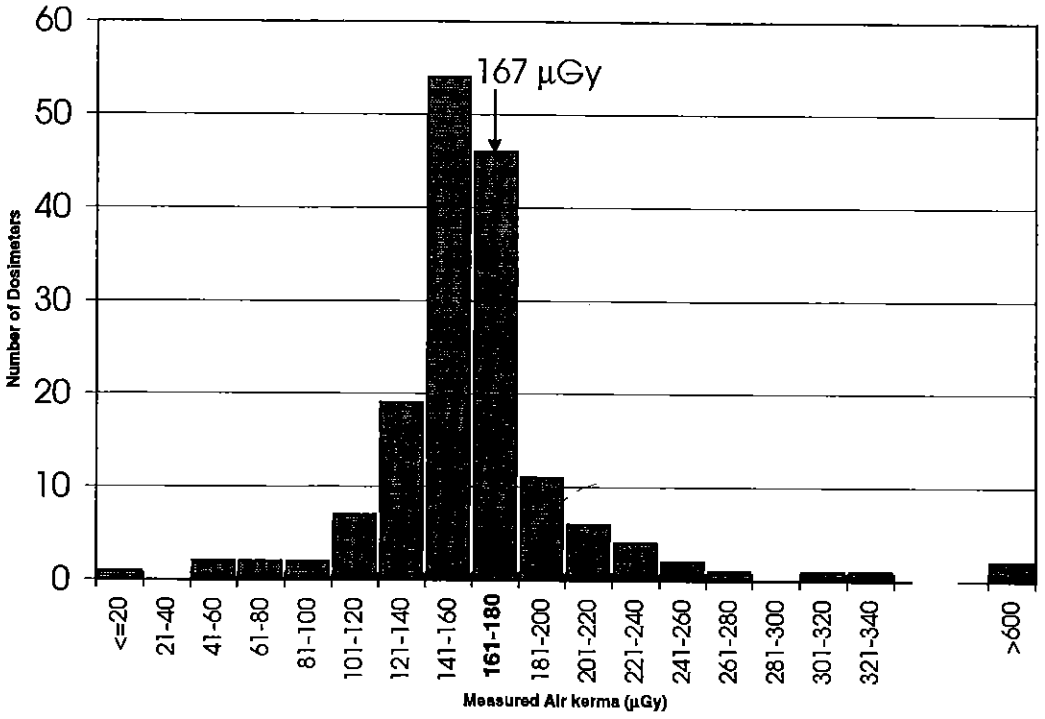

Figure 8.2: Results of eleventh international environmental dosemeters intercomparison programme organised by US-DOE Environmental Measurements Laboratory, [KLE99].

The eleventh and most recent intercomparison was held at the Brookhaven National Laboratory (BNL), in the summer of 1996 and included 174 sets of passive dosemeters from 121 participants in 31 countries. Eleven of the dosemeter sets were non-TL materials (film, electret, phosphate glass and Geiger-Müller device) and there were 11 different types of TLDs in all. Field dosemeters were deployed outdoors at fenced, secure area at BNL located on Long Island, New York, about 110 km east of EML in New York City.

The distribution of results is shown in a frequency histogram in Figure 8.2. The x-axis is dose measured by participants' passive dosemeters, and the y-axis is the number of dosemeters with results in each dose range. The vertical line is the PIC result, with the estimated uncertainty represented by the horizontal bar. The mean of the passive dosemeters' results is 166 μGy, in good agreement with the PIC result of 167 ± 10 μGy. The standard deviation of the distribution is 70 μGy, or about 42% of the mean. There are few outliners, but overall the passive dosemeters' results are clustered around the ionisation chamber result, with 90% within 30% of the PIC measurement. This is typical of the results for most of the previous intercomparisons.

8.4 CEC Intercomparisons

8.4.1 Intercomparisons 1984 to 1991

From 1984 to 1991 the Commission of the European Communities sponsored a series of intercomparison experiments investigating the response of several different types of detectors to a variety of background environments and for comparing different calibration techniques. An earlier Nordic intercomparison (1980) of detector systems for background radiation monitoring revealed large variations of detector responses when instruments were identically exposed. It concluded that internationally standardised calibration procedures should be established to secure an equal interpretation of measuring results, [BØT81].

In the CEC intercomparisons an average of 18 scientists from 10 European laboratories participated with 22 different environmental gamma-ray monitoring instruments in each study. The detector types used during the intercomparison were high-pressure ionisation chambers, plastic scintillators, G M counters and proportional counters. The experiments investigated the response of these detectors to cosmic radiation, both in the North Sea and at Roskilde Fjord in Denmark , [BØT85,CEC89 and CEC90].

The inherent response of each detector was also determined from measurements organised by the Physikalisch-Technische Bundesanstalt (PTB), Germany and made at 775 m depth in the Asse salt mine near Braunschweig where the background is approximately 1 nGy/h. This mine was also used to provide measurement's linearity using ^{137}Cs collimated and uncollimated sources to give air kerma rates of 10 to 2200 nGy $^{-1}$, for the determination of the detector's energy response using ^{241}Am, ^{57}Co, ^{137}Cs, and ^{60}Co sources; and measurements of the air kerma rate from mixtures of radionuclides which were not known by the participants.

Further experiments were made at Risø National Laboratory, Denmark, where the earlier PTB calibrations were compared with shadow-shield calibrations using ^{137}Cs sources and free-field calibrations from ^{137}Cs, ^{60}Co, and ^{226}Ra sources with corrections applied for ground albedo and air build-up.

Environmental measurements were made at several locations where the magnitude of the terrestrial components of the air kerma rates were significantly different. The measurements demonstrated that to make accurate measurements it is necessary to have a prior knowledge of an instrument's photon energy response, its response to cosmic radiation and its inherent background. A summary of the measurements made at two different field sites and measurements of the cosmic radiation component at sea are listed in Table 8.1. The terrestrial air kerma rates are those obtained by subtracting the sea air kerma rates from these for the field.

Table 8.1: Air kerma rate results (mean) of environmental measurements at two different field sites and measurements of the cosmic radiation component obtained on board boats at sea, [BØT89].

DETECTOR	PTB			RISØ		
	Field (nGy h^{-1})	Sea (nGy h^{-1})	Terrest. (nGy h^{-1})	Field (nGy h^{-1})	Sea (nGy h^{-1})	Terrest. (nGy h^{-1})
Ion chamber	38.4±0.9	35.0±0.6	3.5±0.9	69.2±1.5	39.5±1.4	29.7±1.1
Plastic scint.	20.8±8.4	18.7±9.5	2.0±0.9	58.2±13.3	29.7±12.2	28.5±4.0
G M + prop. Counter	53.9±14.0	50.5±15.7	3.4±2.1	87.8±10.8	54.8±11.5	32.9±3.4

Note: All results are the mean air kerma for the participants ±1 standard deviation.

During 1987 a further experiment at Risø used a special set-up with various lead shielding round a ^{137}Cs source to increase the environmental air kerma rate by between 3% to 35 % in steps that were unknown, regarding their duration and magnitude, to the participants. For these step type changes most commercially available environmental monitors could measure the 3% increase above the background level.

It should be noted, however, that all the participants were aware that the radiation levels were to be changed several times during the duration of two separate runs of an hour each. Thus even an instrument with only a meter indication, or hand-operated scaler, was able to observe the changes.

Although these experiments gave some indication of the ability of instruments to detect and quantify radiation emanating from nuclear installations, clearly in situations where even the date of such an increase would not be known, continuous reading and automatic recording of the measurement would have to be made. Therefore as part of the fourth CEC study, continuous measurements were made, from 6 November 1990 to 7 March 1991 at a location close to Hinkley Point Power Station in England, of the air kerma rates from the gamma radiation arising from the direct 6MeV radiation produced in the CO_2 coolant gas and from the routine discharge of ^{41}Ar from the 'A' Station, [THO93].

Four environmental dose rate instruments having different detectors, a high pressure ionisation chamber, a Geiger-Müller counter, a proportional counter and a scintillation counter, were used to make continuous measurements. Over a two months period TL dosemeters were also exposed at the same position as the detectors of the dose ratemeters.

Comparison of the estimated values of the integrated air kerma from the different radiation components given in Table 8.2 shows that considerable differences exist between three of the dose rate instruments. The standard deviations, expressed as a percentage of the mean values for the three instruments, for these components lay between 13% and 18%. Significant differences also exist between the total integrated air kerma values for the three dose rate instruments and those of the TLDs, shown in the last column of Table 8.2, the standard deviation being 20%.

Table 8.2: Integrated air kerma for the period B, 11 January to 7 March 1991, for the different radiation components, calculated from the dose rate instrument and TLD readings.

Doserate instruments or TLD	**Air kerma (μGy)**			
	Cosmic + terrestrial $\dot{K}_c + \dot{K}_t$	**^{41}Ar** $\dot{K}_{Ar}$	**Direct (6MeV)** $\dot{K}_{dir}$	**Total** $\dot{K}_{Total}$
Proportional counter	145	36.3	494	675.3
High pressure ionisation chamber	117	31.4	340	488.4
Geiger Counter	101	28.0	423	552.0
LiF TLD-100				422.0
$CaSO_4$:Tm				410.0
Discriminating dosemeter				452.0
Mean value for dose rate instruments (and TLDs for Total)	121	31.9	419	(500.0)
Standard deviation (% of mean value)	22.3 (18%)	4.2 (13%)	77.0 (18%)	100.0 (20%)

The corrected estimates of the air kerma over the two months period for the different radiation components and for the total air kerma are given in Table 8.3. Comparing the uncorrected values of the air kerma from the different radiation components given in Table 8.2 with the corresponding corrected values in Table 8.3 shows the significant improvements in dose estimations that result from correcting the measurements by accurately determined detector responses. For each radiation component much closer agreement is obtained between different detector types following such corrections. The standard deviations are reduced from 18% to 6% for the cosmic plus terrestrial radiation, from 13% to 10% for the ^{41}Ar radiation, from 18% to 7% for the 6 MeV photon radiation and from 20% to 5% for the total from all these radiation components.

The standard deviations for all the corrected components, and for the total air kerma are within the range 6% to 10%.

Table 8.3: Values of integrated air kerma for the period B, 11 January to 7 March 1991, for the different radiation components corrected for each dose rate instrument and TLD response to the different radiation components.

Doserate instruments or TLD	**Air kerma (μGy)**					
	Cosmic $\dot{K}_c$	**Terrestrial** $\dot{K}_t$	**Cosmic + Terrestrial** $\dot{K}_c + \dot{K}_t$	**^{41}Ar** $\dot{K}_{Ar}$	**Direct (6MeV)** $\dot{K}_{dir}$	**Total** $\dot{K}_{Total}$
Proportional counter	44.4	66.1	110.5	28.9	302	441.4
High pressure ionisation chamber	43.2	70.5	113.7	31.4	283	428.1
Geiger Counter	43.0	69.8	112.8	26.4	253	392.5
LiF TLD-100 [a)]	50	76	126	27	269	423
$CaSO_4$:Tm [a)]	49	62	111	33	263	406
Discrim. dosemeter						452
Mean value for dose rate instruments and TLDs	45.9	68.9	114.8	29.3	274	423.8
Standard deviation (% of mean value)	3.3 (7%)	5.2 (8%)	6.4 (6%)	2.8 (10%)	19.1 (7%)	22.0 (5%)

a) To Estimate the TLD values corresponding to the different radiation components the percentage of the total dose as estimated by the active dose rate instruments was used for each component.

Table 8.4: Results of source calibration, dose rate instruments, spectrometers and TLDs.

Detector Type	Free Field [1]			Shadow Shield [2]
	Ra^{226}	Co^{60}	Cs^{137}	Cs^{137}
HPI				
Eml/Spicer	0.955*	0.956	0.974	0.960
EML/PIC	0.975*	0.976	0.974	0.985
IRD/RS PIC	0.971	0.981	0.991*	1.000
Risø/RS	0.983	0.992	0.994*	0.990
Scintillators				
PTB/P1.Sc	1.016	1.021	0.992*	0.968
PTB/P1.Sc	0.987	1.030	0.974*	1.000
IRD.P1.Sc	1.023	1.049	1.008*	1.023
IRD/P1.Sc	0.993	1.016	0.991*	0.977
GM				
UK/GEC	0.972*	1.033	0.839	0.822
Spectrometer				
EML/Ge	-*	-	-	0.959
IRD/NaI	0.994	1.002	1.012*	0.978
IRD/NaI (diff. response)	0.964	0.949	0.931*	0.862
TLDs				
Krak/MCPN	0.921	0.940*	0.947	-
CIEMAT/MCP-n	0.957	0.993*	0.963	-
CIEMAT/GR-200	0.995	1.048*	1.008	-
BUD/Al_2O_3				
CIEMAT/Al_2O_3	1.032	0.996*	0.892	-
	1.153	1.056*	1.093	-
BUD/$CaSO_4$	0.995	0.964*	1.017	-

1) Mean response of calibration at 3, 5 and 10 m.
2) Mean response of calibration at 3. 4 and 5 m.
* Radionuclide source used for "home" calibration.

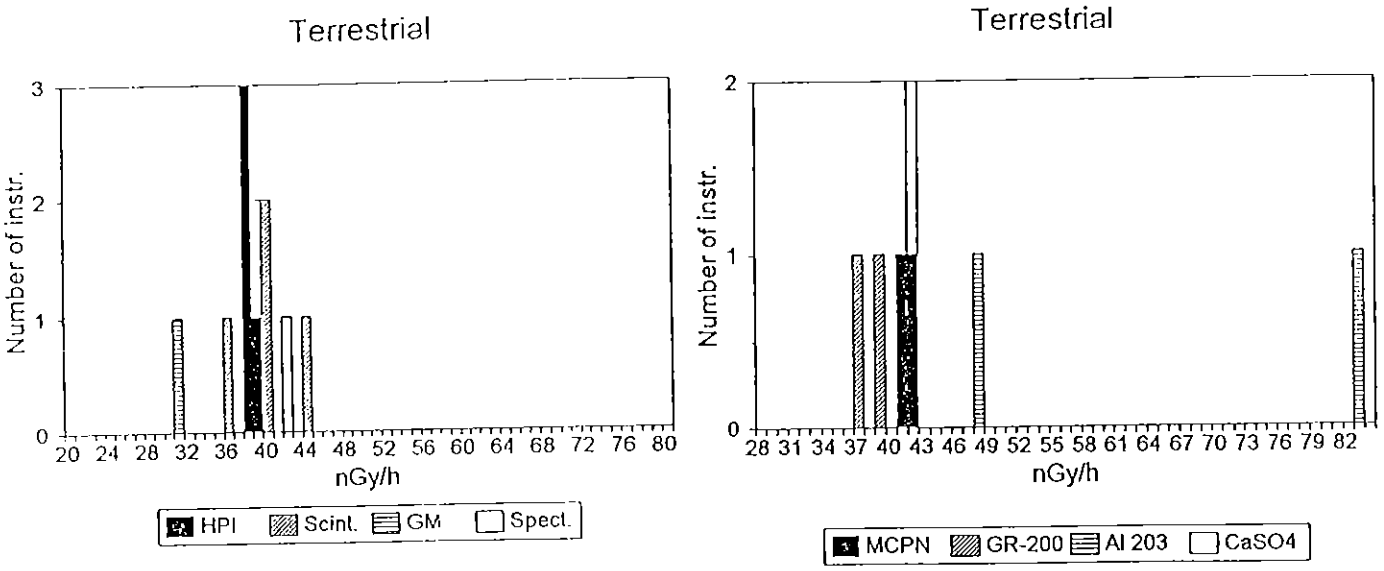

Figure. 8.3: Histogram showing the distribution of the measured terrestrial radiation component, taken as the field measurement subtracted the cosmic measurement, for the participating dose rate meters and TL dosemeters.

8.4.2 CEC intercomparisons 1994

8.4.2.1 Intercomparison experiments at Risø, [BØT95].

In the week 12-18 June 1994 an International intercalibration experiment was performed at Risø with participants from USA, Eastern Europe (PECO), and EU. One aim of the experiments was to intercompare the home calibration of detectors and dosemeter responses of environmental radiation measurement systems used in the USA, Eastern Europe, and EU and to try to make a link between the different reference standards used. A total of 12 active dose ratemeters and 8 different TL materials participated in the experiments which included:a) free-field calibrations using certificated Cs ^{137}, Co ^{60}, and Ra ^{226} sources, b) measurement of the natural radiation at the terrestrial field-site, c) measurement of the cosmic ray component both at a platform at sea and on a boat at sea, and d) shadow-shield calibration experiments (only dose rate meters) using a certificated Cs ^{137} source.

The USA was represented by Environmental Measurement Laboratory (EML), New York, who participated in the experiments with two of their new high pressure ionisation chambers and one Ge.Li gamma spectrometer. Eastern Europe was represented by 1) Institute of Nuclear Physics in Krakow who participated with their own developed highly sensitive LiF:Mg,Cu,P TL material, 2) Institute of Isotopes/Atomic Energy Research Institute in Budapest who participated with LiF:Mg,Cu,P and Al_2O_3 TL materials, and 3) Institute of Radiation Dosimetry in Prague who participated with plastic scintillators, high pressure ionisation chambers, and NaI gamma spectrometers. EC was represented by 1) PTB who participated with two new plastic scintillator systems, 2) The UK who participated with a GM environmental monitoring system and electronic dosemeters, 3) CIEMAT who participated with a variety of new TL materials (LiF:Mg,Cu,P and Al_2O_3), and 4) Risø as the host who participated with ionisation chambers and TL materials.

A summary of the preliminary results of the measurements for the doserate instruments and the TLDs is given in Table 8.4 and for the electronic dosemeters in Table 8.5. For an easy overview the data are presented as the ratios of measured-to-reference values where the reference values include the air and ground scatter contributions calculated by Monte Carlo calculations. It should be noted that most of the TL data are obtained over very short integration times, typically from 6 to 16 hours indicating a completely new scope of short term evaluation of the environmental radiation levels using TL techniques. As seen from the table an excellent overall agreement was found between most of the participating detector systems.

Table 8.5 gives the mean values and standard deviations for each detector type used with these electronic dosemeters as well as results for active detectors and different TLD's. The high standard deviations for the electronic dosemeters using solid state detectors are due to high readings of one type of dosemeter at the field and cosmic pier locations. This can be explained as being due to this detector's results not being normalised to its response to Ra^{226}.

Table 8.5: Summary of mean results or air kerma rate from field, cosmic and terrestrial radiation for each detector type.

Detector type (Dosemeter type)	Field, cosmic + terrestrial ($nGy.h^{-1}$)	Cosmic (sea) ($nGy.h^{-1}$)	Terrestrial=field-cosmic (sea) ($nGy.h^{-1}$)
HPICs (Dose rate meter)	74.4 ± 1.9	36.4 ± 1.6	38.0 ± 0.8
Pl. Scintillators (Dose rate meter)	71.4 ± 7.8	31.5 ± 6.5	39.8 ± 3.4
GM (Dose rate meter)	68.7	37.8	30.9
Spectrometers (NaI)	45.9 ± 1.9	5.7 ± 1.1	39.9 ± 2.2
TLDs, MCPN	70.0 ± 0.3	28.7 ± 0.1*	41.4 ± 0.4
TLDs, GR-200	67.9 ± 3.6	29.8 ± 1.6*	37.7 ± 1.4
TLDs, Al_2O_3:C	102.5 ± 34.6	37.2 ± 9.6	65.3 ± 25.0
TLDs, $CaSO_4$:Dy	72.0	30.4*	41.6
Electronic dosemeters (GM)	130.7 ± 22.4	96.7 ± 19.1*	34.0 ± 4.8
Electronic dosemeters (Solid state)	96.3 ± 62.5	61.0 ± 53.7*	35.3 ± 12.7

*Estimated from measurements made at the Cosmic Pier Station. N.B.
The ± values represent 1 SD.

The natural radiation was measured at the Terrestrial Measurement Station using the different participating detectors. Both active dose rate meters and TL dosemeters measured the natural background whenever the sources were removed from the field. The TL dosemeters were exposed to the natural radiation over different periods from 6 to 16 hours. The detector responses of the terrestrial radiation component, taken as the difference between the field measurements and the cosmic measurements, are given in column 4 of Table 8.5, and are shown in Figure 8.3.

8.4.2.2 Intercomparison experiments at PTB

a) Measurements of the inherent instrument background.

The inherent background of different types of electronic dose meters was determined. However, their indication of the environmental background radiation is often used as a test of their correct operation. For determination of their inherent response the instruments were exposed in the

underground laboratory UDO [LAU95]at an environmental dose rate level lower than 0.7 nGy h^{-1}. Several dose rate meters seemed to have a threshold at a fixed count rate below which they are internally switched off stating an error. Nevertheless, they may have an inherent background which is not directly measurable in a nearly radiation free environment. Future measurements in photon fields of different well known dose rates just above this threshold are expected to yield values of their inherent background. This method was applied during the reporting period for the dose rate meters as described below.

The dependence of the reading R_{Tot} of an instrument on the air kerma rate $\dot{K}_{ref}$ in the photon field of the collimated beam facility in the UDO laboratory is given by equation (8-1) where r_{ref} is the response to the photons of the reference field and B is given by equation (8-2).

$$R_{Tot} = r_{ref}\,\dot{K}_{ref} + B \qquad (8\text{-}1)$$

$$B = r_B\,\dot{K}_B + R_i \qquad (8\text{-}2)$$

R_i is indicated inherent background and r_B the response to the photons of the background radiation field in UDO with the air kerma rate $\dot{K}_B$.

Applying the linear relationship of equation (8-1) on calibration measurements with the collimated beam facility using different reference dose rates the slope yields the response r_{ref}. If the response to the background radiation field is known the inherent background R_i can be derived from B. The air kerma rate $\dot{K}_B$ is given as 0.7 nGy h^{-1}

In Table 8.6 a summary of these measurements is presented. Besides the calibration measurements and their evaluation by applying equation (8-1) the background reading of each instrument is given in the last column. The correlation coefficient r is a measure of the goodness of the linear fit.

Table 8.6: Results of Calibration Measurements for Dose Rate Meters with ^{137}Cs Sources

Instrument	Detector	Institute	Response r_{ref}	Interception B $(nGy\ h^{-1})$	Corr. Coefficient r	Inherent background r_i $(nGy\ h^{-1})$	Background reading B_m $(nGy\ h^{-1})$
Spicer	Ionisation chamber	EML[1)]	1.00	1.82	1.000	1.13	
Rs-11	Ionsiation chamber	EML[1)]	0.96	1.17	1.000	0.48	1.58
Rs-112	Ionisation chamber	IRD[2)]	0.99	0.52	1.000	(-0.17)	1.25
MAB 500(1)	Scintillator	PTB[3)]	0.90	11.2	0.999	10.5	12.5
MAB 500(2)	Scintillator	PTB[3)]	0.85	5.74	0.999	5.04	5.39
DLM 7908	Scintillator	PTB[3)]	0.91	1.86	0.999	1.17	0.88

1) US Dept. of Energy, Environmental Measurements Laboratory, 376 Hudson Street New York, New York 10014, USA.
2) Institute of Radiation Dosimetry, Na Truhlarce 39/64, 180 86 Prague, Czech Republic.
3) Physikalisch-Technische Bundesanstalt, Bundesalle 100, 38116 Braunschweig, Germany.

The participants used their home calibration of the instruments. The ionisation chambers of the EML were calibrated using ^{226}Ra sources. The determined responses for all ionisation chambers showed very satisfactory results. The scintillation dose rate meters used by the PTB were calibrated by the manufacturers. Their responses in the order of 0.85 up to 0.91 show the difficulty of a reliable calibration for air kerma rates of this order.

The correlation coefficients in the order of 1 confirm a good linear relationship for all investigated instruments between the air kerma rate and the reading.

The interception B should be comparable with the background radiation levels measured by each instrument, B_m. There are unexplainable discrepancies which need further investigation.

b) Determination of the response of the dose rate meters to 6 MeV - photons

The 6 MeV facility in the PTB generates a beam of 6 MeV photons using a nuclear reaction with accelerated protons. The air kerma rates at the measuring points were well known for the time of

each measurement. The experiments comprised measurements at various distances for the determination of the response to the 6 MeV photons as well as measurements with build-up material (perspex) in order to discover if the secondary electron equilibrium is already achieved by the instrument's material around the detectors. The detectors of the dose rate meters are GM counters, scintillators and ionisation chambers.

Table 8.7 shows the results of the responses for the dose rate meters. The probe with the GM counter shows the highest values of the response.

Table 8.7: Response of Dose Rate Meters to 6 MeV Photons

Instrument	Radio-scope	MAB 500	NB3201	RS-111	RS-112
Manufacturer	MAB	MAB	TESLA	REUTER-STOKES	REUTER-STOKES
Detector	GM counter	Scintillator	Scintillator	Ionisation-chamber	Ionisation-chamber
Response to 6 MeV photons without build-up material related to the response to 0.661 MeV photons	1.71	1.05	1.04	1.26	0.94

N.B. the two ionisation chambers were expected to have nearly the same response, but they differ by 32%.

9. MEASUREMENT OF ENVIRONMENTAL FIELDS AND INTERPRETATION OF RESULTS

9.1 Introduction

When choosing instrumentation the energy and kerma rate range of radiation to be measured should be taken into account. In order to correctly interpret any measurements of environmental radiation it is crucial that the energy response of the detector be known. For environmental monitoring the ideal detector response should be constant for the quantity of interest over the environmental spectrum. In practice, this is achieved through the use of an instrument having a good energy response, using energy compensating filters and/or appropriate calibration corrections. Thus in order to properly calibrate for environmental applications it is necessary to account for differences between the response of the detector to the calibration spectrum used and its response to the environmental spectrum. (See Chapter 6 on calibration.) The calculated air kerma response of a PIC relative to the response to a radium source plotted against energy shows that if this detector is calibrated with radium, it would be expected to over-respond to radiation of a few hundred keV, slightly under-respond over 1 MeV, and not detect photon radiation having energies below 50 keV. When the PIC is exposed to a typical terrestrial spectrum however, the overall response is quite similar to that of radium, differing only by 3%. Thus for routine environmental use, it is usually sufficient to apply this correction to the radium calibration factor.

The air kerma rate range of natural gamma radiation is relatively narrow. The lower limit can be as low as 10 nGy h^{-1}, the upper one for places with extremely elevated natural background 10 μGy h^{-1}. Some detectors used at early warning environmental monitoring systems are capable to measure the dose rates up to 1 to 10 Gy h^{-1}, i.e. levels which meet the emergency situation requirements as well.

The choice of a proper location for environmental dose measurement has the same importance as calibration of the measuring equipment. For mapping the most important requirement for location of measurement is that it should be representative for a given area. It means that the soil composition should be typical, the surface should be undisturbed and nearly horizontal with balance of precipitation water. The site with natural grass cover usually is optimal for measurements. Large trees or building disturb the measurement so their distance from the measuring point should be more

than ten times their height. Use of numbered wooden post is useful for periodic measurements monitoring purposes. The standard height of measurements is mostly 1 metre but it may be increased up to 2 metres if the surface is not homogeneous (e.g. mixture of stone and soil).

The choice of location of detectors for early warning purposes is more simple as it should be representative only for man-made radiation. The soil composition has importance but for compatibility of different sites the ground below the detector should be horizontal and preferably covered with short cut grass. The location of detectors on the roof of houses or above asphalt covered areas leads to erroneous results especially for doses due to deposition.

The mentioned requirements belong to the micro environment of a measuring site. The location of different measuring points for control purposes can be chosen as:

(i) source centred

(ii) area centred

(iii) population centred.

(i) Source centred. The source centred location of environmental monitoring points is justified for the control of large nuclear facilities (nuclear research centres, nuclear power plants). The monitoring points usually are located along circles around the installation. The first circle can be the fence line of the installation, the most far distance at neighbouring populated areas. For long term monitoring (determination of annual doses) 8 to12 passive detectors per circle are sufficient. For early warning purposes one circle should be equipped with on-line connected active detectors. The sequence number of detectors and their location can be determined by analysing the radiation consequences of possible incidents or accidents. To obtain characteristic measured data for decision making at any meteorological situation the number of measuring points should be in the range from 15 to 25 detectors.

(ii) Area centred. The area centred location (i.e. distributed in quadratic grid points) of detectors for early warning provides a calculation database for the determination of isodose distribution with a minimum number of detectors in case of far contamination sources (continental or world-wide scale contamination). The location of detectors along a state border accelerates the proper early warning requirement.

(iii) Population centred. The population centred location (near towns) gives the best result for the determination of population doses, both from natural and man-made components of external environmental radiation, but due to geometrically unsystematic distribution of measuring points extrapolation of measured data to the whole country is less correct. As the meteorological stations usually are located near a large town, they can also be used as monitoring sites.

9.2 Type of Measurement

Measurements of environmental radiation are usually performed for the purposes of either monitoring or for the characterisation of a site. Monitoring involves continuous recording of the ambient radiation to determine natural background exposure levels as well as to detect potential increases that could be due to man-made activities. Site characterisation is a more detailed study performed to identify sources of radiation and their spatial distribution for purposes such as accident assessment or clean-up.

The most common active detectors used for environmental monitoring are pressurised ionisation chambers (PICs), Geiger-Müller (GM) counters, proportional counters and plastic scintillators. Other instruments such as germanium or sodium iodide detectors are required for site characterisation. The most information can be obtained by combining data from different types of detectors.

9.2.1 Spot check

The single environmental kerma rate measurement for control purposes can be done using portable, battery operated instruments. The goal of such a measurement is the determination of the kerma rate at a given location. The usual kerma rate range to be measured is the background one up to several times the background value. This means that the sensitivity of the instrument should be enough to measure e.g. 100 nGy h^{-1} with a precision ±10% in several minutes. The instrument should have digital indication of the kerma rate. The energy dependence should be within ±30% over the range from 50 keV to 1.5 MeV and within ±50% at 6 MeV. (See details in Chapter 5)

The most convenient instruments for spot checks are based on organic scintillators, inorganic scintillators or on high sensitivity GM counters, such instruments are also portable.

High pressure or atmospheric pressure ion chambers as well as proportional counters are less convenient as portable instruments due to their greater weight.

In the event of a nuclear or radiological accident the main tasks of the measuring team are to carry out [DRA94]:

(a) rapid monitoring of large contaminated areas to find places with high levels of contamination;

(b) rapid monitoring at selected locations mainly aimed at determining the doses from radionuclide deposition.

The instrumentation for such a task may consist of e.g.:

- dose rate meter (high pressure ionisation chamber, combined scintillation detector, GM counter);
- spectrometer NaI(Tl) and/or HPGe to obtain the contribution of different radionuclides to the total kerma rate.

The *in situ* gamma spectrometry technique, with its ability to sample large areas and average local inhomogeneities, proved especially useful for fallout studies where source distribution tended to be uniform. Other applications such as the remediation of contaminated sites may require the ability to detect a "hot spot" or a limited area of high activity.

Characterising a large site with *in situ* measurements typically involves making a series of somewhat overlapping measurements on a grid. It is possible that a hot spot could be located between grid points and therefore have a relatively small contribution to the total flux seen by the detector. One solution being explored is to apply a method called maximum entropy which is often used in imaging problems where only incomplete, noisy information is available.

The maximum entropy deconvolution method tends to flatten the baseline and sharpen peaks, and has been useful in situations with excessively noisy data. Reginatto, [REG96], demonstrated that this method could be useful to test for hot spots in surveys of decommissioned sites to be released for public use.

9.2.2 Monitoring and early warning

Environmental radiation monitors keep a time record of the exposure or kerma rate, with

some capable of recording measurements every few minutes and storing from 1 week to several months of data. Alternatively, networks of many such monitors have been established which transmit data to a central location via direct wire, radio waves, or satellite.

An extensive and updated status of networks operating in several European countries can be found in the frame of the European Union Radiological Data Exchange Platform (EURDEP), [DeC96].

In case of early warning systems the most important requirement is the sensitivity of the detector. The data collection time should not exceed 10 minutes. The detector statistical error (3σ) should be less than 10 to 30% at usual environmental kerma rates. Long term stability (several percents per year) is a basic parameter. Small changes in sensitivity can be corrected using changeable sensitivity parameter in evaluation software. The same method can be used for correction of differences in individual sensitivity.

Another important parameter is good temperature stability. In the temperature range from -10°C to +40°C the change of the detector sensitivity should be in less than ±20%. Electrical shielding of the instrument may be required to reduce the instruments response to electrical and magnetic fields, (See Chapter 5).

The energy and directional dependence of the detector are also important, (see Chapter 5), and should be determined during the type testing at the instrument, the data so produced may be used for estimating correction factors that can be applied to measurements made in the environment.

For long term control both active and passive detectors can be used. The active detectors can provide time dependent data of the kerma rate between two sequential read-outs by the operator. The active detectors usually are based on GM counters or semiconductor radiation detectors. The passive detectors integrate the kerma rate between locating and collection of the detector. The most widely used passive detectors are based on TL dosemeters but RFL detectors can be used as well.

The installed systems (usually used for early warning purposes) can be used for the detection and evaluation of the accident severity. In the early phase of an accident the kerma rate measured by installed detectors is proportional to the local contamination of the air and ground and sometimes to the direct radiation in a plume. After the passing of a radioactive cloud the remaining excess (above natural background) kerma rate is caused by deposited activity.

Kerma rate measured continuously by installed systems gives an overall characterisation of the local radiation situation. From this value the external dose outside buildings (open air dose) can be calculated directly, especially if the detector is calibrated in dose equivalent rate. For other pathways of dose (e.g. ingestion) the external dose rates can be used only as relative figures.

To obtain correct results special care should made for any contamination of the detector surfaces as its unavoidable contamination will cause an overestimation of the dose rate.

In the case of active detectors a local data acquisition system is required. Earlier printers and/or recorders were used, but recently different semiconductor or magnetic recording systems are used. Some types of memories require local read-out (e.g. built-in battery operated RAMs) through a RS-232 port, another type have removable memory (e.g. memory card) which is subsequently evaluated at a computer.

The passive detectors need read-out devices, i.e. readers. Usually the reader is a laboratory type automatic or manual reader but portable readers can also be used for on site read out of dosemeters. In the latter case the result of the measurement is available within a few minutes after reaching the site of dosemeter location (SZA86 and SZA90). Such a solution has two advantages, the first is avoiding the errors due to transit doses, the second the immediate availability of measured dose. The second advantage is a very valuable feature for monitoring around reactors or other radiation facilities during an emergency situation, when the time factor for obtaining information on the radiation conditions can be very important. The measured results can be transmitted to an evaluation/emergency centre by radio link. Electronic dosemeters can also be used in place of or in conjunction with passive detectors. Compared to passive detectors they have the advantage of providing direct readout , no resetting is required, (for example annealing of TLDs) and they usually are more sensitive

9.2.3 Mapping

The presence of characteristic peaks in the spectrum quickly identifies radionuclides in the soil. However the count rate of the peaks can be used to quantify the concentration (activity per mass) or inventory (activity per area) as well as to infer information about the depth distribution, if the detector is appropriately calibrated. This technique is referred as *in situ* gamma spectrometry or

field gamma spectrometry, (See Chapter 7),and it will provide important information by the evaluation of dose rate components due to different radionuclides. This method helps to obtain a more complex database on environmental gamma radiation, connection between soil types and dose rates. It should be mentioned that for man-made contamination (plane surface source) and natural radiation (semi-infinite volume source) different peak count rate to dose rate conversion coefficient should be used. This is because in the case of a surface source the relative number of uncollided photons to scattered ones is significantly higher than for a volume source.

The instrument's detector should be positioned facing the ground, usually on a tripod, one metre from the soil. Gamma photons emitted by radioactivity located throughout a large region of soil will be incident on the detector. The dimensions of this "soil sample" depend on the distribution of the emitters in the soil and the energy of the gamma photons, as well as the height of the detector. For uranium distributed uniformly throughout the soil, 80-85% of the 93 keV photons that reach a detector one metre above the ground come from sources within the top 3 cm of soil and inside a radius of 5 metres. In contrast most of the 1000 keV photons reaching the detector represent emitters contained in a 9 cm depth. For radionuclides deposited mainly on the surface, the radius of the sampling area is of the order of 10 m.

The range of radii (5-10 m) for typical sampling can be used as a common figure for all detectors of gamma radiation detectors. This means that for correct measurement of the gamma dose rate the diameter of the undisturbed natural flat soil surface should be above 20 meters, with no buildings within 20 meters from the detector.

The terrestrial component of the air kerma rate determined by the *in situ* method may be used along with a PIC result to determine the cosmic component of the radiation field. If the PIC has the same response to environmental gamma photons as it does to cosmic radiation, this is a straightforward subtraction. If the response is different, then it will be possible to correct for this difference and find the total air kerma rate as well as the cosmic component. In this case, the cosmic component is given by:

$$(M_{display} - M_{terr})(r_g/r_c) \qquad (9\text{-}1)$$

where $M_{display}$ is the reading of the PIC, assuming the environmental gamma response was used for calibration, M_{terr} is the terrestrial component determined by *in situ* technique, and (r_g/r_c) is the ratio of the detector's response for environmental gamma to that for cosmic radiation.

The total air kerma rate is then the sum of derived cosmic and terrestrial kerma rates. A quality control check can be provided by comparing this value with documented cosmic radiation values for a particular latitude, atmospheric pressure, and solar cycle.

In some cases the soil activity concentrations of natural radionuclides are available. From these data the external gamma radiation kerma rate due to terrestrial sources can be evaluated by use of the following equation:

$$\dot{D} = 0.010\ A_1 + 0.506\ A_2 + 0.284\ A_3 + 0.421\ A_4 + 0.045\ A_5 \qquad (9\text{-}2)$$

where $\dot{D}$ is the absorbed dose rate in nGy h^{-1} and A_1, A_2, A_3, A_4 and A_5 are the specific activities (in Bq kg^{-1}) of the radionuclides ^{238}U, ^{226}Ra, ^{228}Ra, ^{228}Th and ^{40}K respectively.

The theoretical evaluation of the of the external kerma rates due to natural radionuclides is a preferable alternative to direct (e.g. PIC or TLD) dosimetry where the Chernobyl accident resulted in considerable contamination of soils with ^{137}Cs.

The relative concentration of terrestrial radionuclides can vary with geographical location as can the cosmic ray intensity, so that the total environmental spectrum may differ between locations. Depending on the energy response of the detector it may be necessary to adjust the calibration to get an accurate measure of the total kerma at a particular site. For example, in some locations approximately one third of the total kerma is due to cosmic rays, while at others it could be more than half of the total. If the response of the detector (i.e. the calibration factor) is different for cosmic rays than for terrestrial gamma photons, corrections should be made for proper interpretation of results.

Mobile laboratories. Mobile units capable of monitoring the radiological impact at any selected location in the field play an important role in emergency preparedness, [AND91]. These mobile units can also be used both for mapping of normal environmental radiation and for the monitoring of defined routes.

Fully equipped mobile units are usually based on medium size vehicles, preferably having four wheel drive. Kerma ratemeters are the basic instruments, they can be of different types having

high sensitivity and short measuring time (e.g. high pressure ionisation chamber, GM detector, scintillation type).

For detailed measurement of the kerma rate spectral components determined by the *in situ* spectrometer are used. The global positioning system (GPS) were also used with the basic instrumentation. For data collection laptop PC systems are preferred. Using an on-line connection with a kerma rate meter and GPS a precise and detailed dose rate map can be generated during a trip.

An initial survey of an environmental site may be performed with a PIC or GM detector to locate elevated regions, or check the field uniformity. A spectrometer is then needed to identify photon energy and thus the source of the radiation. High purity Ge detectors with portable dewar cooling system provide the best energy resolution and are well suited for field use.

Air contamination due to gamma emitting radionuclides can be measured with a vertically orientated germanium detector, laterally shielded by a lead ring. Assuming a semi-infinite space of constant activity concentration, calibration factors (air activity and dose rate) and detection limits of a number of fission products were determined by Sowa [SOW90]. The possibility of separate measuring of the kerma rate due to simultaneously existing air and soil contamination can be achieved by measurements with and without a lead shield.

By these means measuring equipment so far used for direct measurement of radionuclides deposited on the ground can be used, at small additional expenditure (a lead shield with frame) and preparatory work (angular calibration with and without lead shield up to 180°), to determine the kerma rate due to radioactivity in air.

Aerial Survey. The aerial survey provides an excellent possibility to rapidly measure the averaged contamination over large areas. For measurement of kerma rates due to natural background or contamination, any instrument can be used having high sensitivity and low energy dependence, e.g. HPIC, combined scintillation counter, package or GM counters. The use of large NaI(Tl) spectrometers gives the highest capacity for survey including a limited spectrometric database as well, but the cost of such equipment with proper fast on-line data evaluation system is rather high. The HpGe spectrometers have relatively low sensitivity for flight measurements and their resolution usually decreases due to vibrations on board helicopters.

Use of relatively large (3"x3") NaI(Tl) detectors in simple count rate mode requires both calibration of the detector in kerma rate units and measurement of height dependence of count rate for typical contamination over homogeneously contaminated area.

The actual background of the equipment can be measured over large water surfaces (rivers, lakes) at low height. In case of possible contamination of the detector this data should be frequently determined.

The dosimetric information should be combined with geometric type (horizontal co-ordinates and height over the terrain). The height over the terrain is a very important correction factor of the measured kerma rate (flux etc.) and should be measured with an accuracy of 10 meters as the kerma rate decreases from unity measured at 10 meters to 0.65 at 50 meters and to 0.33 at 100 meters as shown in Figure. 9.1, [DRA94].

In the case of the NaI(Tl) spectrometer an unfolding process is required to obtain the kerma rate. An example of a measured NaI(Tl) spectrum and the spectral distribution of the kerma rate in air gained with the spectrum unfolding are given in Figure. 9.2. The spectral distribution can be used for energy dependence correction of the gamma kerma ratemeter measurements.

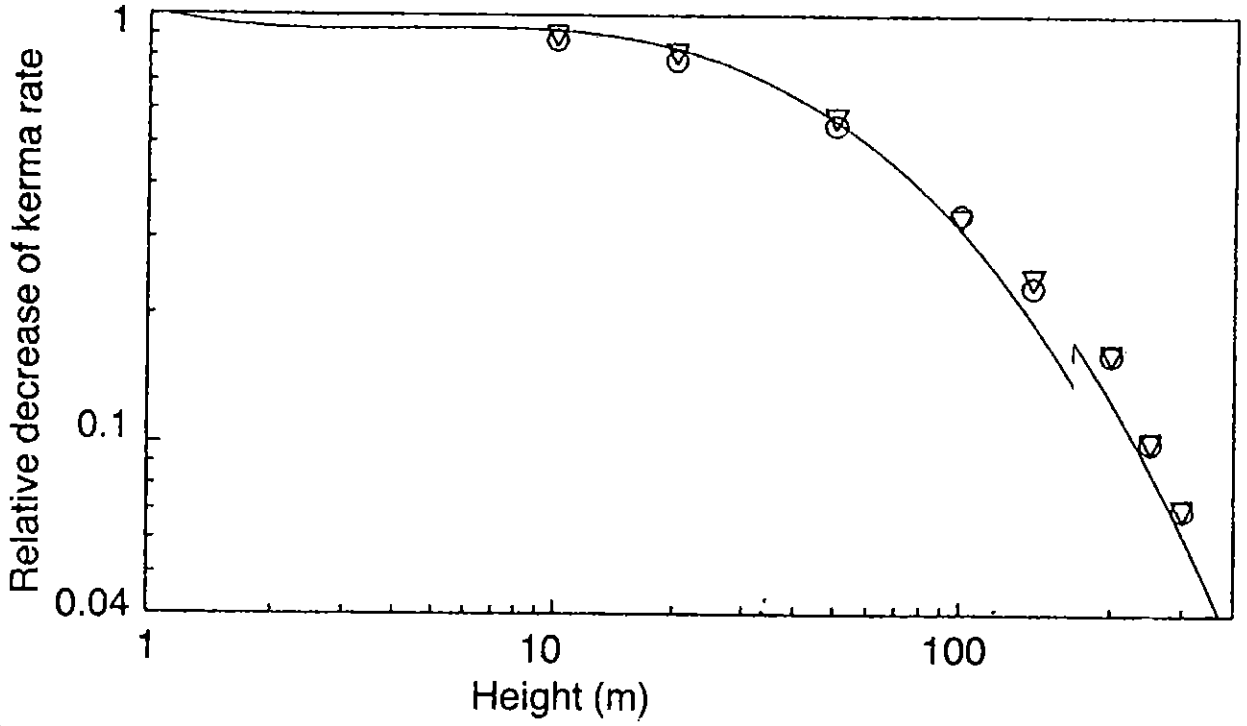

Figure 9.1: Variation of kerma in air with height above terrain – comparison of theoretical and experimental values at Chudjany, Belorus (the decrease of kerma rate in air relative to one metre value). (--) theoretical value. Experimental: (o) RSS 112 ion chamber, (∇) NB 3201 scintillation spectrometer [DRA94].

Snowfall is one of the most important factors altering terrestrial gamma ray fields, During winter periods the northern regions at many places are covered with heavy snow, often 2-3m in thickness even in residential areas. Consequently, the intensity of terrestrial gamma rays is greatly reduced by the shielding effects of snow.

In the paper of Saito [SAI91] the attenuation of the air kerma by snow cover was determined for snow water equivalent 0-50 cm at heights up to 250 m (Figure. 9.3)

In addition to the improvement of dose evaluation in the natural environment the above data can be applied to the determination of snow water equivalent from the detection of terrestrial gamma rays. The water equivalent of snow cover is essential for evaluating the amount of water resources stored during winter periods, and also for the regulation of watercourses and flood protection. The measurement of snow water equivalent over wide areas by use of terrestrial gamma ray observation with an aircraft has been extensively carried out. These measurements utilise the attenuation of terrestrial gamma rays by snow cover, and usually the total or partial counts of a pulse height spectrum from NaI(Tl) detector are converted to the snow water equivalent.

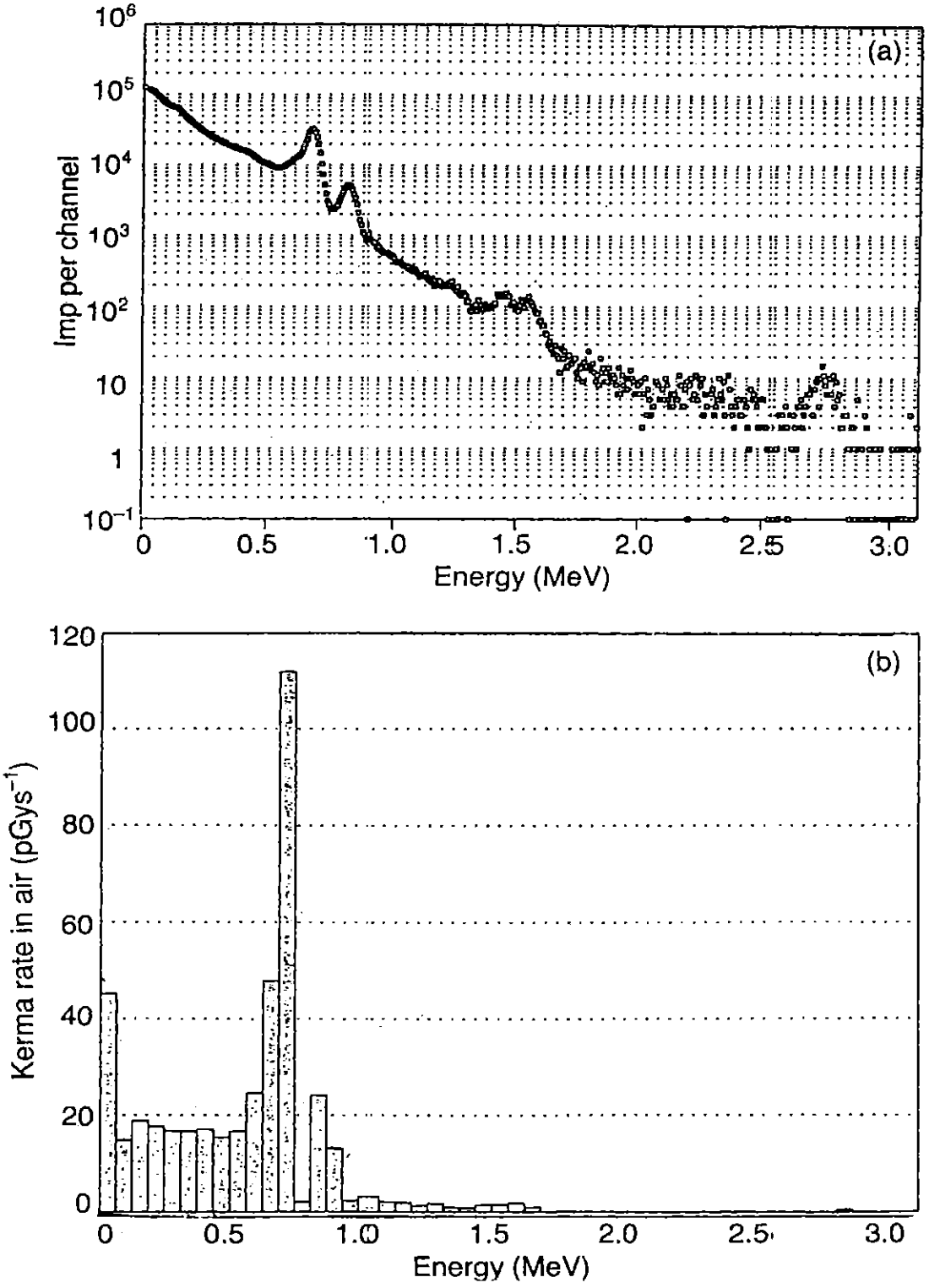

Figure 9.2: (a) Spectrum measured by NaI(Tl) spectrometer and (b) spectral distribution of kerma rate in air resulting from its unfolding, [DRA94].

9.3 Ancillary Equipment

Additional Radiation Measurements. Besides equipment for measurement of external environmental radiation (spectrum, dose rate, dose) some additional measurements and accessories may be necessary. In case of increased dose rate additional measurement of alpha/beta activity of the aerosols helps to identify the origin (natural or man-made) of the deviation.

The increase of environmental radiation dose rate may be caused by either an increase of natural radiation or to the appearance of a man-made radiation source. To determine the origin there is a possibility to use spectrometric analysis. However,by measuring the alpha and beta activity of the aerosol samples it is possible to asses the situation as in case of natural aerosols (radon daughter elements) the ratio of alpha to beta activity of aerosols is rather constant whereas the aerosols due to a nuclear accident are predominantly beta emitters (fission products).

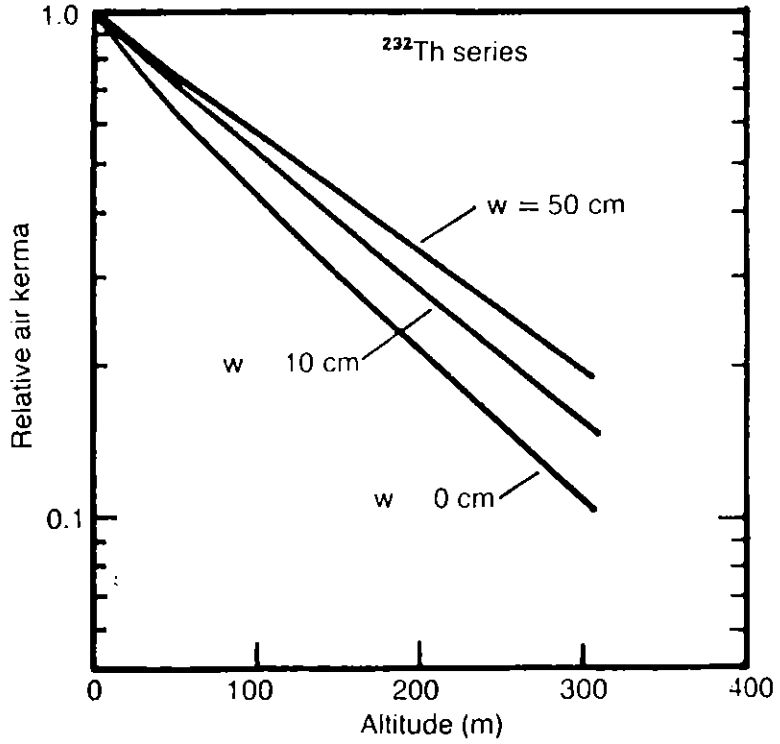

Figure 9.3: Attenuation of air kerma with height above the snow-covered ground for the three different water equivalents, [SAI91].

In cases of elevated environmental dose rate the sample measurement can serve for identification of source of excess radiation. If an *in situ* gamma spectrometer is not available a sample should be taken and its spectrum analysed.

Check Sources. A calibration check source should be used when making *in situ* measurements as this checks the stability of the equipment and permits corrections to be made, if required. For environmental measurements the use of check calibration sources are particularly important as due to transport and temperature shocks the working performance of the equipment may be altered.

Calibration or check sources serve only for local testing of the detector. They are usually small activity gamma radiation sources used at fixed, usually touching, very short distance from the detector. Such sources should have a lifetime of a minimum of several years and medium/high energy of gamma radiation (e.g. ^{137}Cs). It is very important to use the same check source both at the laboratory following calibration and then during field use of the instrument.

Meteorological Measurements. Meteorological measurements can be used for different purposes. One is for the application of corrections to measurements due to the environmental changes in response of a system, the other is for the identification of sources of excess radiation.

Barometric and temperature measurements may be necessary for the correction of measurements made by atmospheric pressure ionisation chambers. The temperature measurement can also be used for any required correction of the temperature dependence of measuring equipment.

A decrease in the barometric pressure causes an increase of radon emanation from the soil also precipitation leads to an enhanced deposition of radon daughter elements. Wind direction measurement in the vicinity of a nuclear installation gives additional information on possible source of contamination (upwind and downwind detectors).

Global Positioning Systems. The global positioning systems are a new, very effective tool for automatic identification of a measuring site, even in the case of continuous monitoring by a moving vehicle (car, aeroplane etc.)

The measurement of environmental radiation includes identification of the location of the measurement. Usually it is done using maps and visual identification of position. In the case of

periodic monitoring the identification of the measuring points can be made using fixed marking of the site.

The most up to date method for identification of measuring position is the application of Global Positioning System (GPS). GPS is a satellite-based radio navigation system. The system ultimately will be a constellation of 21 active satellites and 3 spares in orbits around the earth. This system will ensure World-wide operation with 24 hour, all-weather coverage. Each satellite transmits data that enables a GPS receiver to provide precise position and time. Systems are capable of measuring the position with an accuracy of the order of 10 m (see e.g. [TRA91]).

The GPS Personal Navigator is suitable for mobile laboratories, even for simple measurements with portable devices. It is a hand held, battery powered, navigation system that receives data from GPS satellites and calculates and displays position, velocity, time, and navigational information. Three dimensional fixes are obtained when tracking four or more satellites; two dimensional fixes can be obtained from three satellites plus user-entered altitude.

A GPS receiver has different functions and the user can select a wide variety of navigation functions including: position and altitude, range and bearing, cross-track error, velocity, and time to go.

The combination of a dose rate meter with short measuring time and a GPS system both connected to a computer based data acquisition system enables very fast and efficient measurement along a route used by a car. The proper software provides the possibility to draw a route on a map using e.g. colour coding of kerma rate.

Data Acquisition and Transfer. The primary data acquisition and evaluation systems are mainly used with early warning systems and recently they are based on digital principles. The measured data are compared to previous, or to a mean value, and in case of a significant increase the evaluation system generates an alarm signal. Both the measured data and/or alarm signal are transmitted or transferred to a control centre.

The communication system can be either a public or dedicated one. The simplest solution of the communication is the use of public telephone lines. This is usually the cheapest but less reliable as especially in the case of an accident the telephone lines may well be blocked by other users. The

use of a dedicated/leased telephone or other data transfer line is more economic where measuring station/sub center/centre structures are used.
The communication line between sub center/centre should have high transfer capacity (speed) and back-up communication.

9.4 Interpretation of Results

Proper interpretation of environmental radiation requires a knowledge about features of the environmental natural radiation and its fluctuations with time and location as well as consideration of the response characteristics of the detector used (see Chapter 4).

The environmental radiation consists of natural and man-made radiation. The nature of environmental radiation is described in detail in Chapter 2.

The most typical characteristics of man made gamma radiation emitting radionuclides are given in Table 9.1. In the case of an atmospheric release of radionuclides their concentrations decrease along the trajectory and some radionuclides (except noble gases) may be deposited on the ground surface due to dry and wet deposition processes.

The gamma air kerma rate due to radionuclides in the ambient atmosphere and deposited on the ground can be calculated using a semi-infinite volume source for the radioactive cloud and an infinite plane source for the deposited activity, using data given in Table 9.1.

The air kerma rate at a grid point is then calculated using the formula:[JAC90]

$$\dot{K}_g = \sum_{i=1}^{n} 0.0619 E_\gamma C$$

where

E_γ is the energy release in MeV/decay of given nuclide

C the activity concentration of nuclide in air [Bq m^{-3}]

9.4.1 Primary data evaluation

To correct for any variations in the cosmic ray component of the measured environmental air kerma rates due to atmospheric pressure the atmospheric pressure should be measured. Table 2.1 shows the typical correction factors for an ionisation chamber.

For detectors based on counting or spectrometry the cosmic ray correction factor should be measured experimentally. It is also possible from a knowledge of the height above the sea level of the measurement to use the height mean barometric pressure relationship given in Table 2.1. This relationships is shown in graphical form in the NCRP report, [NCRP77].

There is a possibility to compare the calculated and the measured dose rates. A model has been developed to calculate the absorbed dose rates caused by gamma emitters of both natural and artificial origin distributed in the soil [ORT91]. The model divides the soil into five compartments corresponding layers situated at different depths, and assumes that the concentration of radionuclides is constant in each one of them.

In order to calculate the response of a detector to the gamma radiation coming from a source distributed in the soil, the energy spectrum of the photons incident on the detector has to be known. Figures 9.4, 9.5 and 9.6 [ORT91] show the relative contribution of the direct and scattered photons to the total flux that intercept a detector as a function of the initial energy of the photons.

The calculations, based on the concentrations of the radionuclides in the different compartments, give as a result the dose rate at a height of one metre above the ground caused by each radionuclide and the percentage this represents with respect to the total absorbed dose rate originating from this soil.

Table 9.1: Characteristics of some significant man-made radiation sources (gamma radiation emitting only).

Nuclide	Half life (1)	Plane source air kerma rate (2)	Energy release in MeV/decay for energy range in MeV				
			≤.35	>0.35 ≤0.75	>0.75 ≤1.5	>1.5	full range
^{41}Ar	1.8+3 h	-	0	0	1.28	0	1.28
^{85m}Kr	1.83 h	-	0	0	0	0	1.56E-1
^{87}Kr	76.3 m	-	0	2.14E-1	9.36E-2	4.63E-1	7.71E-1
^{88}Kr	2.84 h	-	5.70E-2	1.57E-2	2.17E-1	1.62+0	1.91
^{89}Rb	15.4 m	5.54	0	0	1.15+0	7.43E-1	1.89
^{95}Nb	35.1 d	2.30	0	0	7.66E-1	0	7.66E-1
^{110m}Ag	255 d	8.03	0	9.30E-1	1.59+0	2.16E-1	2.74
^{131}I	8.04 d	1.18	2.06E-2	3.58E-1	0	0	3.79E-1
^{131m}Xe	11.8 d	-	2.00E-2	0	0	0	2.00E-2
^{132}I	2.3 h	6.66	0	1.01+0	1.15+0	5.64E-2	2.22
^{132}Te	78.2 h	7.09E-1	2.31E-1	0	0	0	2.31E-1
^{133}I	20.8 h	1.84	0	4.85E-1	1.10E-1	0	5.94E-1
^{133}Xe	5.25 d	-	4.60E-2	0	0	0	4.60E-2
^{133m}Xe	2.19 d	-	4.07E-2	0	0	0	4/07E-2
^{134}Cs	2.06 a	4.68	0	7.32E-1	8.23E-1	0	1.56
^{134}I	52.0 m	7.49	1.47E-2	3.32E-1	1.90+0	0	2.24
^{135}I	6.68 h	4.32	0	6.65E-2	9.91E-1	4.74E-1	1.53
^{135}Xe	9.14 h	-	2.26E-1	1.99E-2	0	0	2.64E-1
^{135m}Xe	15.6 m	-	0	4.28E-1	0	0	4.28E-1
^{137}Cs (^{137}Ba)	30.17 a	1.82	0	5.63E-1	0	0	5.63E-1
^{137}Xe	3.9 m		0	1.37E-1	7.23E-3	6.96E-3	1.51E-1
^{138}Xe	17.5 m		1.00E-1	1.29E-1	5.06E-2	7.99E-1	1.08

(1) s – seconds, m – minutes, h – hours, d – days, a – years.
(2) Kerma rates in air at 1 m above ground for infinite plane sources in the ground at a depth of 5 mm (density of soil: 1 g cm^{-3}) in nGy h^{-1} per kBq m^{-3}, [JAC90].

9.4.2 Detection of man-made radiation

One of the most important goals of external environmental gamma radiation dose measurements (dose rate) is to differentiate between the dose from natural and that from man made components.

As the simple dose measurement provides only the sum of doses from natural and man-made radiation some additional parameter, different for natural and man-made radiation, should be used for evaluation of the data. Such a parameter can be the time characteristics of the dose rate.

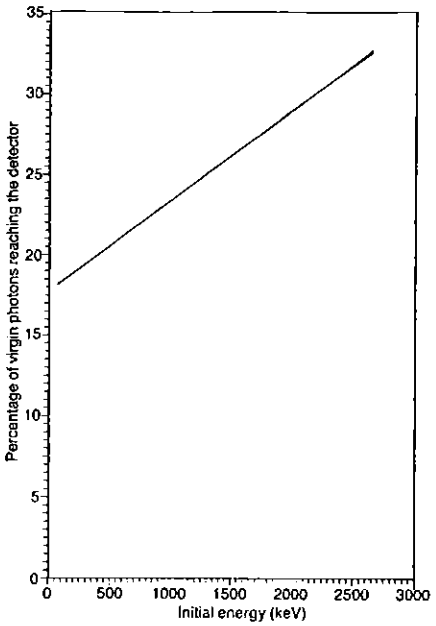

Figure 9.4: Percentage or original photons reaching a detector situated 1 m above ground level proceeding from a source uniformly distributed in the soil, as a function of initial energy of the photons, assuming a depth range of 0 – 40 cm.

Using a spectrometric type detector (NaI or HpGe) the composition of the spectrum can give the dose rate components due to different radionuclides. In some cases additional (independent) measurement of the airborne alpha/beta activity can support the exclusion of man-made radiation as a contribution to the measurement. For measurements made in the environment around a given source (e.g. nuclear installation) the wind direction measurement can be used to confirm an increase in dose rate.

Dependence Analysis. Background radiation can include natural perturbations typically of the order of 20% in the course of a few hours. In fact scavenging of radon progeny can cause increases as high as two or three times the baseline level. Such variations must be taken into account in any attempt to assess a potential increases due to man made sources. The task is complicated by the possibility that the man-made perturbations may be of lower magnitude than natural fluctuations. Frequently it is necessary to measure other parameters in conjunction with a PIC or GM counter in order to able to attribute increases to man made causes.

Spectral Analysis. In comparison with pure gamma dose rate measurement spectral analysis (*in situ* gamma spectrometry) has the advantage of the ability to determine the dose rate due to a single nuclide from a single transport calculation for different energies and radionuclide distribution in the soil.

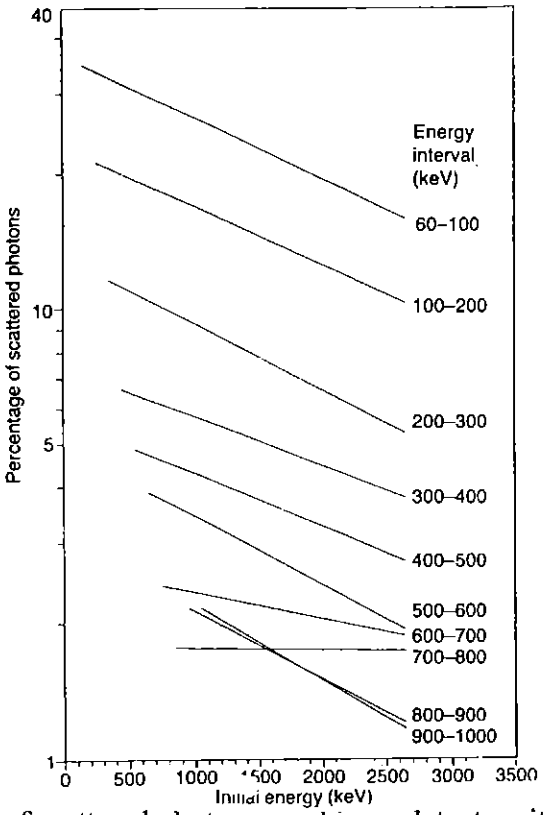

Figure 9.5: Percentage of scattered photons reaching a detector situated 1 m above ground level (each line corresponds to the energy interval shown at the end), proceeding from a source uniformly distributed in the soil, as a function of initial energy of photons, assuming a depth range of 0-40 cm.

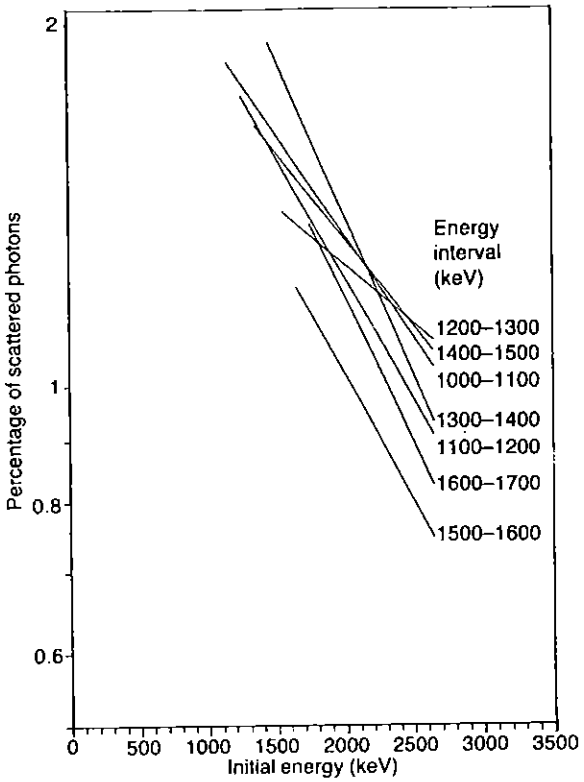

Figure. 9.6: Percentage of scattered photons reaching a detector situated 1 m above ground level (each line corresponds to the energy interval shown at the end), proceeding from a source uniformly distributed in the soil, as a function of initial energy of the photons, assuming a depth range of 0- 40 cm

Measurements that permit the separation of natural and artificial radioactivity and the nuclide specific result of *in situ* gamma spectrometry allows improvements in predicting the radiation exposure to the population. The method is therefore particularly applicable in emergencies that cause environmental contamination.

A disadvantage of this method is that it requires the determination of some input parameters (radionuclide distribution in soil and some soil parameters) by sample measurements or the adoption of certain assumptions concerning these parameters. The investigation of the sources of uncertainty shows that this method gives good results for the activity concentration in/on soil and the resulting dose rate, even if general mean or estimated values are accepted for some parameters [SOW89]. Investigations of the variation of deposition in limited areas have shown that measurements could be considered to be representative for areas with a diameter up to 200 m. Further reduction of the uncertainty of one measurement (e.g. by better determination of parameters) should not improve the results, because of variation of contamination in an area characteristic of a population group would be certainly greater than the uncertainty of measurement.

Use of Additional Measurement Data. Analysis of time dependence of the environmental dose rate can be accompanied with analysis of meteorological data. Sudden decrease of barometric pressure increases the emanation of radon from the soil. Precipitation causes wash out of radon daughters from the atmosphere. Ground level inversion leads to very shallow mixing layer and increased near surface concentration of radon and radon daughters. Wind direction measurement can be used for identification or exclusion of some man-made radiation source.

Continuous measurement of aerosol alpha activity can be used as indicator of concentration of radon daughter elements in the atmosphere. Such data can be used for evaluation of environmental gamma dose rate only together with a precipitation measurement as the deposited radon daughter elements should be taken into account as well.

Soil sample activity data can be used for comparison of dose rates directly measured and calculated from sample activity.

9.5 Examples of Measurements

Description of some typical measurements are given as illustrations of practical solutions for different tasks.

9.5.1 Measurements of natural radiation using pressurized ionisation chambers

Routine monitoring of the penetrating component of the environmental radiation field (gamma plus cosmic) has continued since 1976 at the Environmental Measurements Laboratory (EML) regional baseline station at Chester, New Jersey, USA, EML-580, 1995 Annual Report [EML96]. Figure 9.7 shows a plot of the eighteen-year record from 1976 to 1995. This plot illustrates the overall magnitude and daily variations in the dose rate, the temporal variations result primarily from snow cover, soil moisture and atmospheric scavenging of radon progeny. An analysis of the data by season indicated that the winter months exhibited the largest variation and lowest dose rate.

9.5.2 Measurements of external photon air kerma rate in the vicinity of nuclear power stations

a) Estimates of the Ar^{41} gamma dose rate around Hinkley Point Power Station in the U.K. were made using many automatic recording GM detector systems at distances of 300, 600 and 900 metres from the 'A' Station. The results were compared with estimates made from calculations using standard plume dispersion and cloud-gamma integration models. The measurements were also supported by a series of chemical tracer measurements as well as by wind tunnel simulations. The complete study enabled the annual radiation doses due to the Ar^{41} discharges to be evaluated at all the local population centres in the environs of the Hinkley point Power station. Estimated values of the effective dose equivalent were in the range from 4.2 to 14.7 μSv per year, [Mac89].

b) As part of the CEC intercomparison described in Section 8.4, the measurements of air kerma rate from a high pressure ionisation chamber, a Geiger-Müller counter, a proportional counter and a scintillation counter were intercompared over a four month period at a location close to Hinkley Point Power Station in England, [THO93]. The measured, uncorrected variations in air kerma rate

for the four detector system over the complete four month measurement period are shown in Figure 9.8. All four systems measured and automatically recorded the air kerma rate every five minutes over this four month period. It should be noted that data were not obtained for the scintillation detector over the complete period due to an interface failure. The variation in total power levels for the two reactors over this same period are also shown in Figure 9.8.

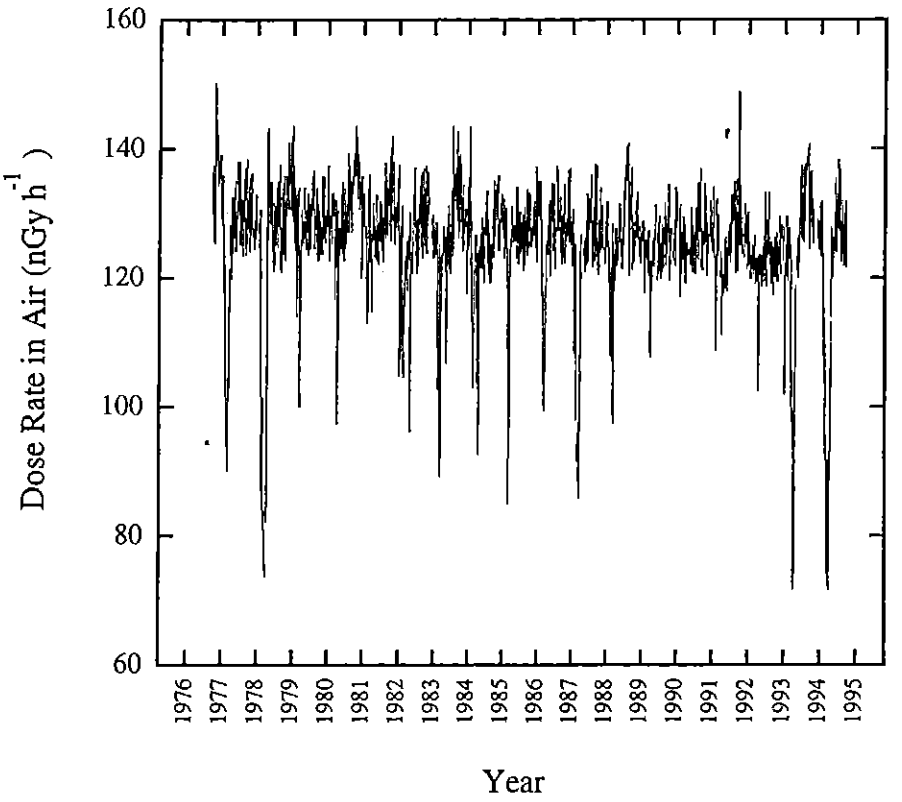

Figure 9.7: Average daily dose rate in air at EML's regional baseline station in Chester, NJ, from 1976 to 1995, [SHE96].

The time-dependent dose rates obtained over the whole measurement period show two principal but differing structures. Constant dose rates of different magnitudes are caused by the natural background and the high energy ^{16}N radiation at different power steps of the reactor. The peak shaped variations riding on the constant dose rates have their origin in the changes of the wind direction blowing the ^{41}Ar plume from the station above the dose rate meters. These peaks corresponded to recorded wind directions from the NE, the direction of the station. The dose rate value during the 7th of January represents the natural background level since the reactors were shut down completely.

Comparison of the results from the four detectors shows that though they all very closely followed the variations in air kerma rate with time, they did not agree with each other on the magnitude of the different radiation components.

A more detailed analysis of these measurements was made over the two month period of time from 11 January to 7 March 1991 in which corrections were made for the responses of the detectors to the different radiation components. This analysis is discussed in detail in Section 8.4.

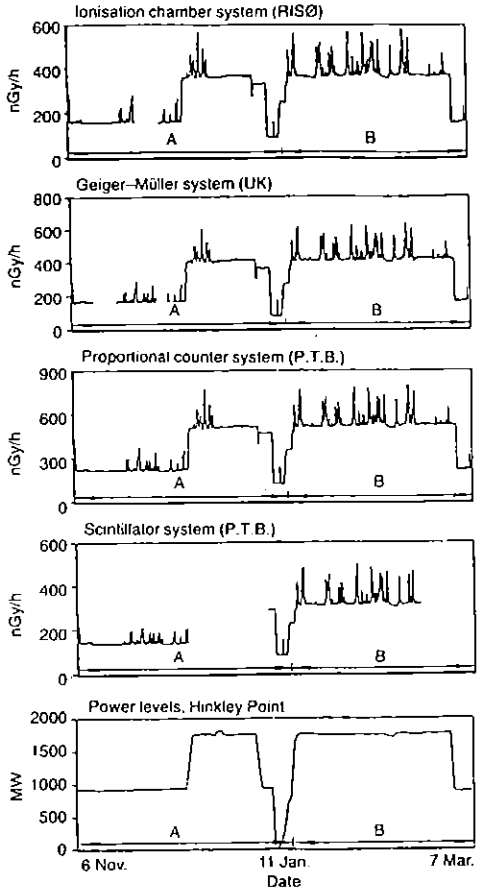

Figure 9.8: The uncorrected variations in air kerma rate as measured by the four active detector systems as well as the reactor power levels over the period 7 November 1990 to 7 March 1991 (periods A and B).

9.5.3 Mobile laboratories

Measuring ranges of dose rate meters used at different mobiles laboratories are given in Figure 9.9 [AND91]. Most of the laboratories are equipped with two or more dose rate meters to cover the dose rates from the usual background up to dose rates that might occur during severe accidents.

Following the Chernobyl accident in April 1986, the Finnish Centre for Radiation and Nuclear Safety initiated assessment of the environmental gamma radiation levels by means of sensitive Geiger counters, a high pressure ionisation chamber and a gamma spectrometer placed in motor vehicles, [ARV90].

The total exposure rate was measured using an efficient Geiger-Müller tube and a high pressure ionisation chamber (HPIC). The GM tube, provided with a digital counter, was located above the car at a height of 2.5 m from the road surface. The HPIC was inside the vehicle continuously recording the exposure rate with a strip chart recorder. During journeys the instruments were continuously taking measurements, the results thus representing average radiation levels for each section of the route. The HPIC continuously gave information about changes in kerma rate levels. The results gave a more representative survey of the radiation levels compared with single measurements made at various points of each route.

The exposure level were recorded in units of mR h^{-1}, the results being presented as dose rates in units of mSv h^{-1}. A conversion factor of 1 mR h^{-1} = 0.01 mSv h^{-1} was used. The following factors affecting the calibration were considered: (a) point source calibration, using ^{137}Cs, and calculated response to both natural and fall-out radiation; and (b) attenuation of the radiation by the car. The HPIC was specially designed for environmental measurements; it is sensitive and its angular response is isotropic. Comparison measurements between the GM counter and the HPIC were used for controlling the GM counter calibration. For measurements made solely with the GM counter the dose rate caused by the Chernobyl fall-out was calculated by subtracting the natural background radiation level from the dose rate measured. The accuracy of the dose rate increments measured solely with the GM tube is 0.03-0.05 mSv h^{-1} for levels of 0-0.3 mSv h^{-1}. The measurements with both the GM counter and the spectrometer gave much more accurate results for dose rate increments (0.5nSv h^{-1}).

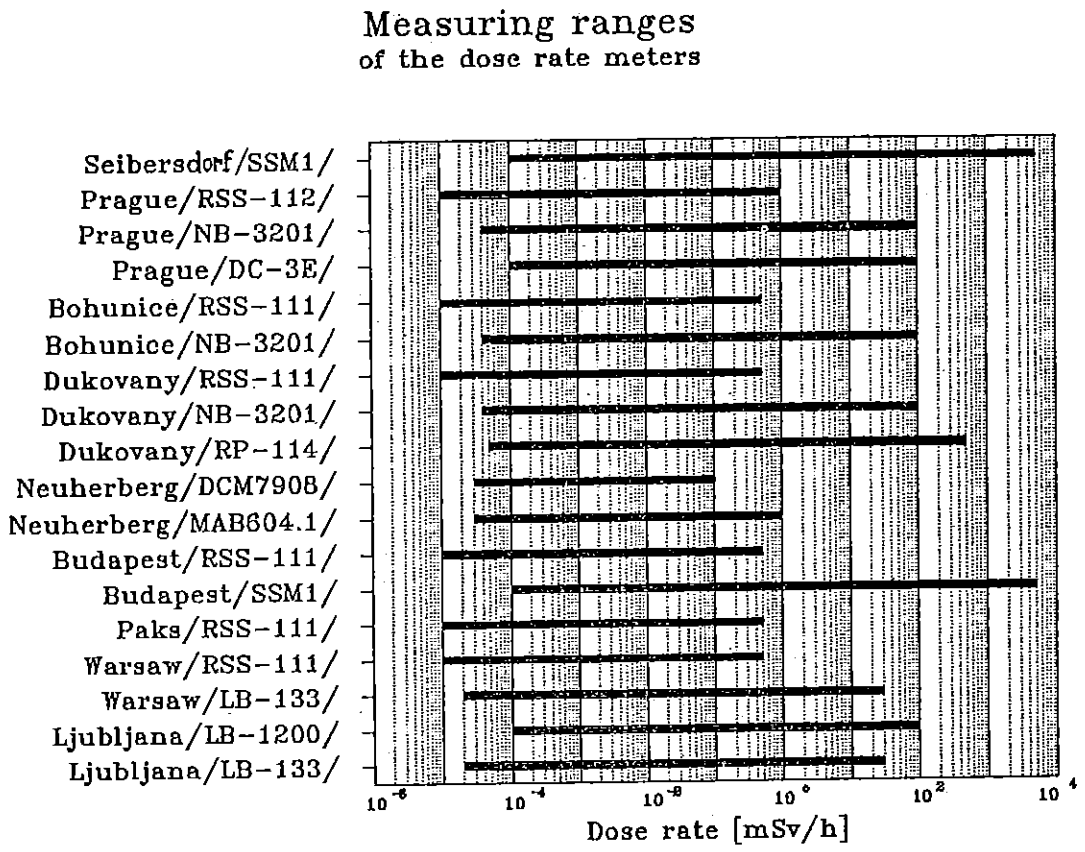

Figure 9.9: Measuring ranges of dose rate meters used by different mobile laboratories [AND91].

Examples of environmental radiation mapping in Hungary are given in Table 9.2 [ZOM94]. The measurements were made with HpGe spectrometer to obtain the dose rate components and with RSS-111 type Reuter-Stokes high pressure ionisation chamber using a mobile laboratory.

Table 9.2: Gamma dose rate components and full dose rates measured with HpGe *in situ* gamma spectrometer at different locations in Hungary [ZOM94].

Pos. no.	Location	Dose rate components					Full dose rate[1]	
		^{40}K	U-Ra	Th	^{137}Cs	^{134}Cs	HpGe	RSS-111
		[nGy/h]						
1	Ajka	9.3	8.0	6.3	4.6	1.0	29.2	33
2	Baja	13.4	8.9	11.0	3.8	1.0	38.2	38
3	Balassagyarmat	14.8	7.8	11.5	3.9	1.3	39.3	43
4	Békéscsaba	21.8	14.6	19.7	0.8	<0.4	56.9	56
5	Budapest	13.0	8.0	11.4	7.3	1.8	41.4	40
6	Cegléd	13.1	8.2	13.8	0.4	<0.4	35.5	47
7	Csorna	15.5	8.8	10.5	1.6	0.8	37.2	48
8	Debrecen	15.6	11.4	17.2	1.0	<0.4	45.2	48
9	Dombóvár	18.7	19.0	23.5	0.6	<0.4	61.8	66
10	Dunaújváros	11.6	34.3	18.5	3.7	<0.4	68.0	58
11	Eger	15.4	10.5	21.0	2.1	0.9	49.9	53
12	Esztergom	11.3	5.9	9.2	5.2	1.1	32.6	35
13	Gödöllö	16.9	9.1	15.9	4.8	1.4	48.2	48
14	Gyöngyös	17.2	9.7	19.3	2.7	1.0	49.9	45
15	Györ	11.5	9.5	12.1	4.8	1.9	39.8	33
16	Hajdúböszörmény	18.8	12.2	21.6	1.1	0.7	54.5	55
17	Hatvan	18.6	9.3	11.8	11.4	2.8	53.9	52
18	Hódmezövásárhely.	19.9	11.8	18.1	2.8	0.8	53.4	54
19	Jászberény	17.2	10.6	16.6	2.9	0.8	48.2	48
20	Kalocsa	18.0	15.4	16.8	0.6	0.8	51.6	48
21	Kaposvár	19.3	12.9	24.2	1.7	1.2	59.3	57
22	Karcag	21.4	11.1	19.4	1.2	<0.4	53.2	59
23	Kecskemét	12.1	8.2	10.5	3.1	0.8	34.6	36
24	Keszthely	15.8	16.0	17.3	1.9	0.9	52.0	49
25	Kékestetö	12.8	6.7	13.0	3.9	1.3	37.6	51
26	Kiskunfélegyháza	13.1	11.7	15.2	0.8	0.5	41.3	40
27	Kiskunhalas	17.8	10.3	19.0	5.3	0.8	53.1	52
28	Komárom	11.6	11.0	10.8	15.1	3.5	52.0	52

[1]Typical error is ±2 nGy h^{-1+}

9.5.4 Measurement of dose with TL dosemeters

The TLD detector shown in Figure 9.10 uses a measuring probe consisting of a plastic rod containing, at 1 m height, a dosemeter capsule of aluminium with a proper filter to reduce the energy dependence of the $CaSO_4$:Dy TLD.

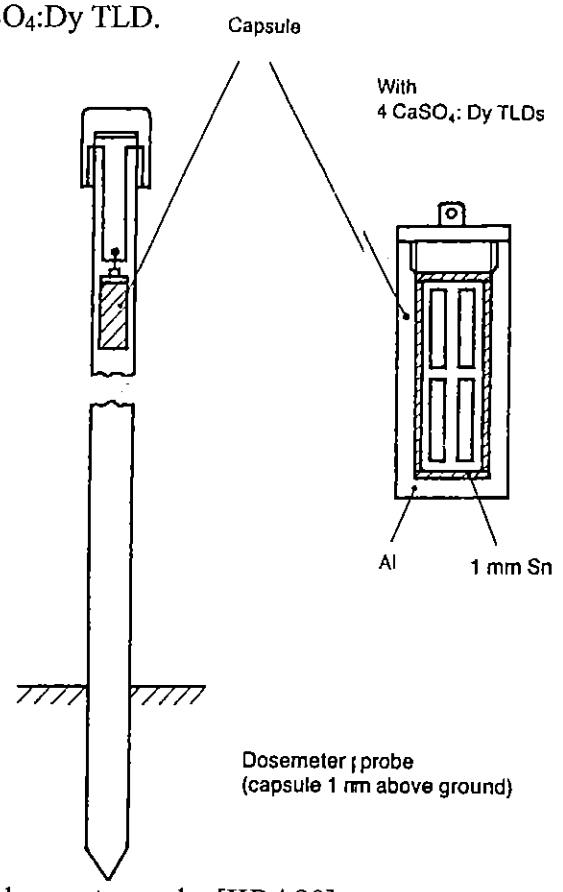

Figure 9.10: Environmental dosemeter probe [KRA90].

Kraus, [KRA90] describes the application of $CaSO_4$:Dy dosemeters for environmental monitoring. The measuring probe consists of a plastic rod containing, at 1m height, a dosemeter capsule of aluminium with a 1 mm tin filter to reduce energy dependence. In this capsule there are four polyethylene packets, each containing 50 mg $CaSO_4$:Dy powder, three for dose measurement and one for calibration. Corrections were made for fading (5%. a^{-1}) and self-irradiation effects due to natural radioactive contamination in the detector material (30 μGy a^{-1}). For a site with several measuring probes and a half-yearly surveillance period , 50 μGy a^{-1} above the natural radiation level can be detected with an error of ±50% at the 95% confidence interval.

Delgado [DEL90] has shown that the simplified glow curve analysis (GCA)

evaluation method permits one to extend in a reliable way the TLD-100 effective dose range towards lower doses than when conventional evaluation systems are employed. In particular, the good measurement ability exists for doses of 10-20 μGy is not only convenient, but strategically interesting. For example, it permits one to measure ambient doses, with a nearly tissue-equivalent material such as TLD-100, integrating over only one week. This permits a more reliable dosimetry, identifying, when necessary, short duration contributions to the environmental doses that would otherwise be masked by longer integration period.

The $CaSO_4$:Dy TLD badge designed for individual monitoring can be used for environmental monitoring as well. A method for estimating the ICRU quantity, ambient dose equivalent, $H^*(10)$, K_a and H_E from environmental radiation using a combination of the TL responses under metal filters and Perspex has been developed, [LAK90]. This can, in turn, be used to estimate, H_E, the effective dose equivalent, and K_a, the air kerma from a typical natural terrestrial radiation. $H^*(10)$ can be estimated for environmental dosemeters, using $CaSO_4$:Dy TLDs by the proposed method even when the photon spectrum deviates significantly from that normally expected in the environment.

Several examples of elevated recordings are given in Figures 9.11, 9.12, 9.13 and 9.14. In all figures the solid line indicates the warning level of 162 nSv h^{-1}. Figure 9.11 shows rainout or washout of radon progeny. Similar recordings usually have a definite spatial correlation. Figure 9.12 illustrates the increase arising from the using of a strong gamma radiation sources for the control of welding near to the location of the radiation detector. In Figure 9.13 the elevated dose rates were caused by an enhanced level of natural radioactivity (^{226}Ra and decay products) due to the unloading of freighters with cargo destined for a nearby fertiliser plant. In Figure 9.14 appears an unexplained recording of dose rate, conceivably caused by equipment failure.

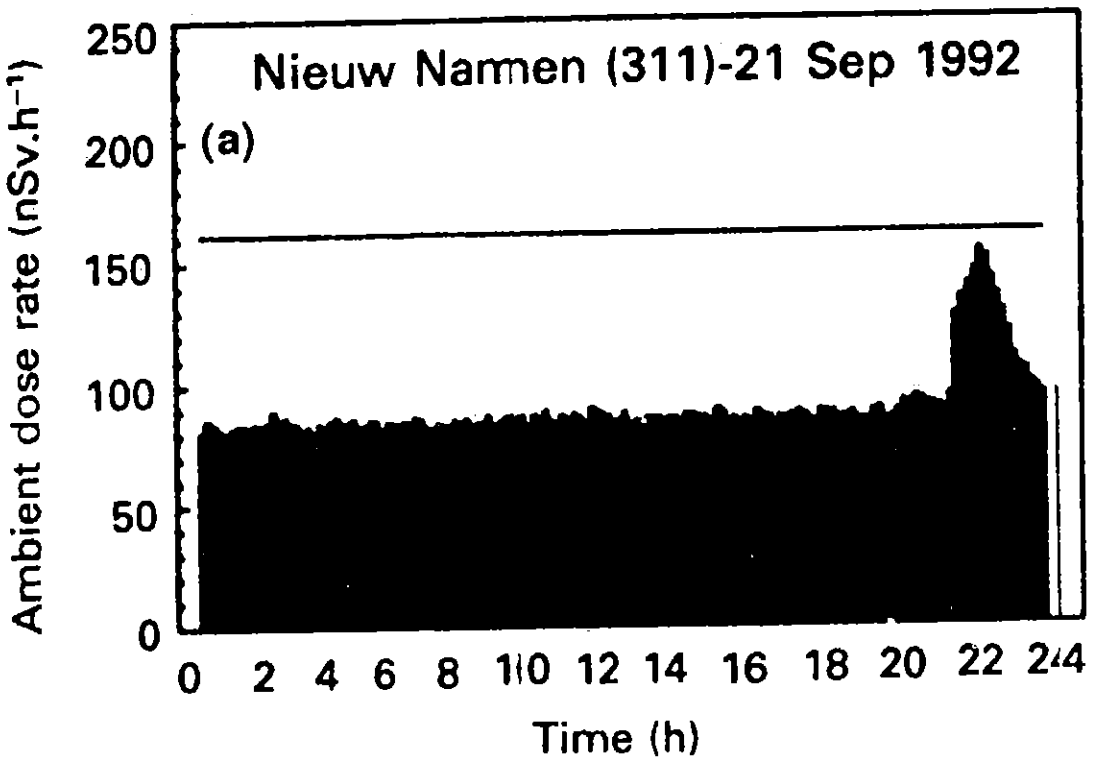

Figure 9.11: Increase in ambient dose equivalent due to rainout or washout of radon progeny.

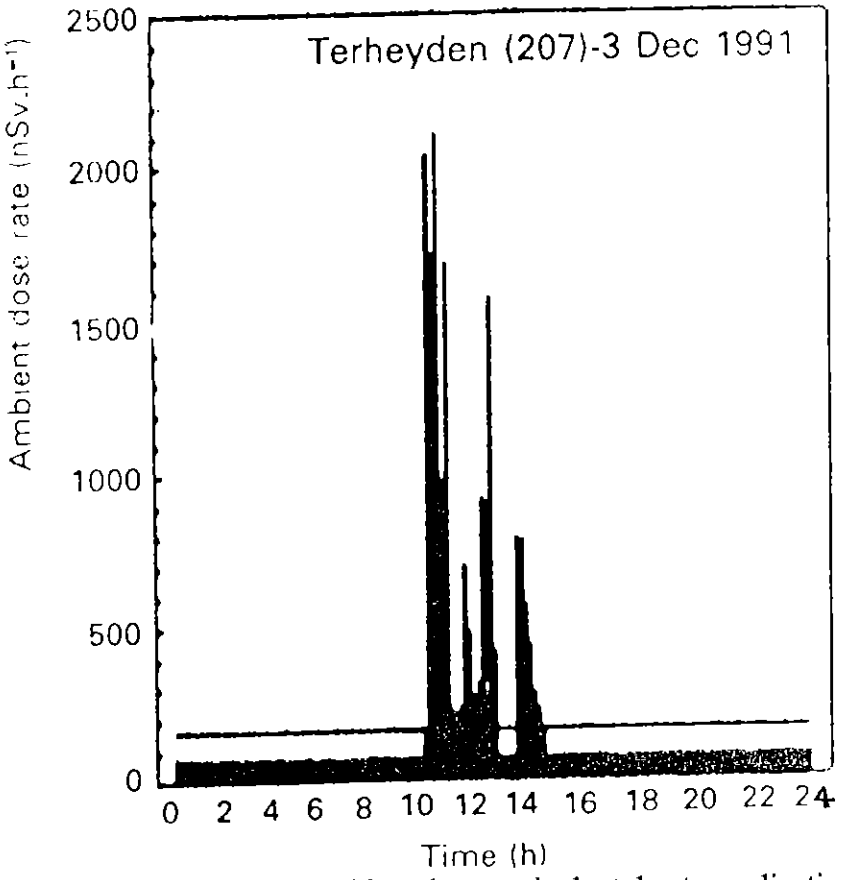

Figure 9.12: Elevated recording of ambient dose equivalent due to application of strong gamma radiation sources for the control of welding.

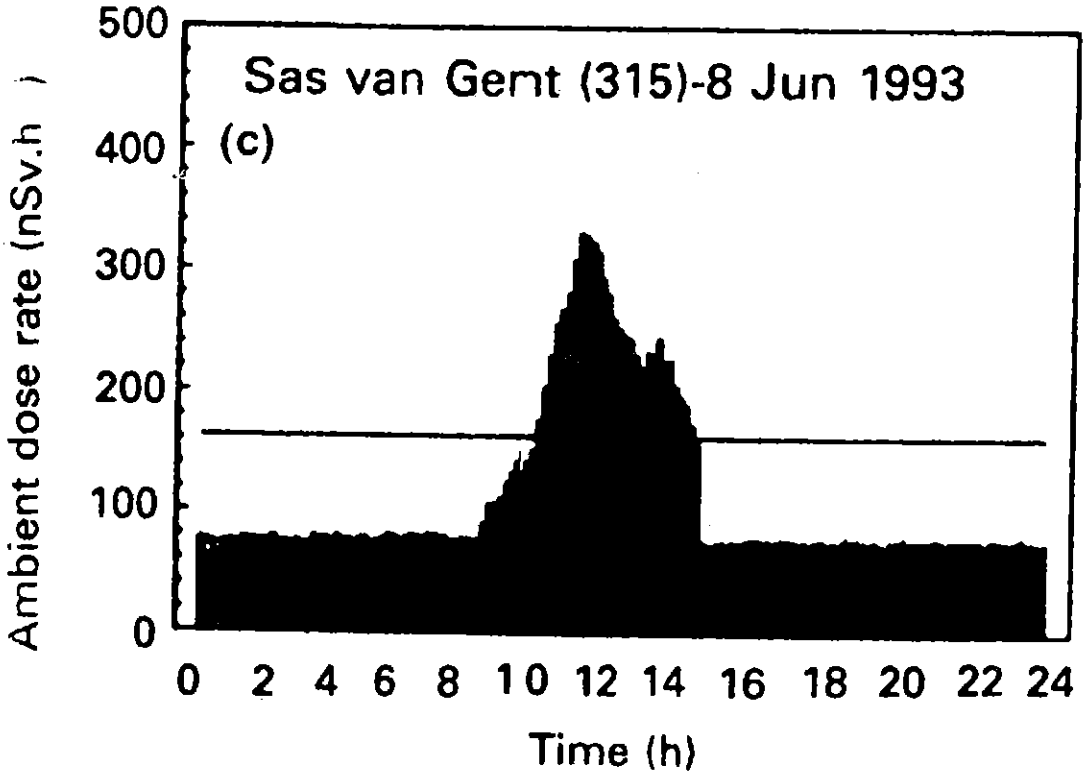

Figure 9.13: Increase in ambient dose equivalent is caused by enhanced levels of natural radioactivity (^{226}Ra and decay products) due to unloading of freighters with cargo destined for a nearby fertilizer plant.

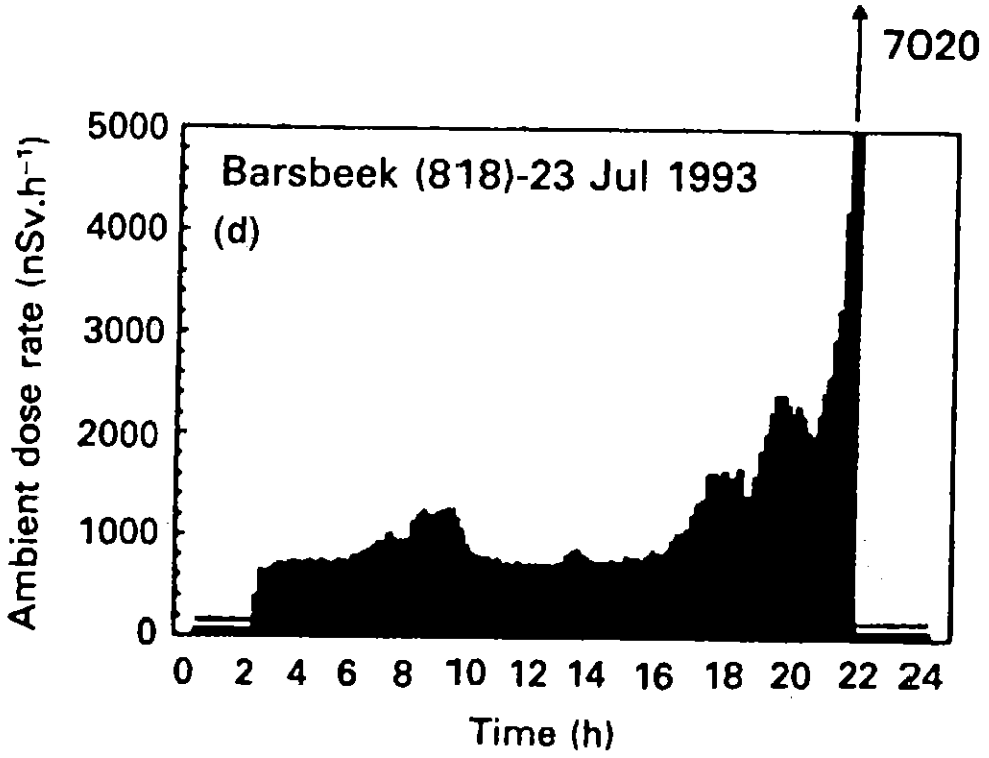

Figure 9.14: Increase in ambient dose equivalent conceivably caused by equipment failure.

9.5.5 Early warning systems

After the Chernobyl accident, most European countries established or further improved their on-line radiological monitoring networks and started bilateral exchange of the information obtained. EURDEP was set up as a feasability study to explore the technical possibilities of exchanging this information at European level. Technical details on the different national networks can be found in the EURDEP Manual [DeC96]. In this Section some networks are breifly presented as examples.

a) The National Radioactivity Monitoring Network (NRM) for nuclear incidents in Netherlands consists of 58 measuring sites, of which all contain a proportional counter tube for determination of external irradiation levels, [SME94]. Recordings initially expressed in exposure rate in $mR.h^{-1}$ are converted to the quantity ambient dose-equivalent rate, [H*(10)]in $nSv\ h^{-1}$ (henceforth abbreviated to 'ambient dose rate') using a conversion factor of 10.8 $mSv\ R^{-1}$.

At so-called 'principal stations', an airborne activity monitor determines the natural gross alpha and artificial gross beta activity concentration in air.

b) The United Kingdom Government system for response to overseas nuclear accidents RIMNET (Radioactive Incident Monitoring Network) has 92 gamma radiation dose rate sites located throughout the UK, [JAC93]. Most of the sites are meteorological office stations which also report meteorological data on a regular basis.

The monitors are housed in weatherproof containers, built to withstand extremes of weather. The detectors are mounted at a height of 1 m above the ground, wherever possible over open grass at least 10 m from any building or trees. Their latest readings are routinely polled every hour by the Central Database Facility. They can be interrogated more frequently should the need arise.

Each monitor has a battery back-up power supply to help ensure continuous operation in the event of mains power supply failure. The majority of sites are manned and are also provided with local hard copy facilities for recording readings to cover the eventuality of communications system failure.

In the event of any abnormal increases in radiation levels being detected, alarms sound in the continuously manned Department of the Environment offices. The alert level used is normally 1.8 times normal site background, but this factor can be adjusted downwards to increase sensitivity

if any form of radioactive incident has been reported. The system allows for extension of both the number of monitoring sites and the forms of monitoring undertaken.

c) Czech Republic. Gamma radiation monitoring system calibrated in photon dose equivalent consists of 44 measuring points at the stations of State Office for Nuclear Safety and observatories of the Czech Hydrometeorological Institute, [SON97].

d) Spain. The Spanish Environmental Surveillance Radiological Network (REVIRA) has 25 automatic stations to measure air activity concentration and the dose rate. These stations are located in the same places as some National Weather Institute automatic stations, so the meteorological parameters are also determined, [DeC96].

e) Denmark's on-line early warning radiation monitoring network [WAL88] was established after the Chernobyl accident to assess fluctuations of 10% or more of the ambient background level. The monitoring system consists of 10 stations located around the country, each equipped with a PIC, rain intensity gauge, and a sodium iodide spectrometer. All data are sent to a central computer at Risø National Laboratory where a health physicist can evaluate all the data to determine if there is evidence that any such fluctuations could result from other than natural causes.

f) The continuous NaI(Tl) spectrometry can be used as a relatively simple method for early detection of artificial fall-out, [KOR94]. For this purpose the ambient gamma ray background due to natural radioactivity is measured outdoors with a 76 mm x 76 mm NaI(Tl) crystal and a 256 channel analyser. A computer continuously updates the background count rates of 10 windows for reference purposes. The influence of atmospheric radon daughters washed out during precipitation is eliminated by stripping using 3 energy windows for measurement of ^{214}Bi activity as shown in Figure. 9.15. In the given case some peaks of the ^{135}I coincidence with the Bi windows and delay the alarm. Examination of the stripped gamma ray spectrum every 12 minutes reveals the presence of artificial radioactive nuclides. The detectable exposure level for fission products is in the range of 2.4 - 6.1 nGy h^{-1}, which is 4% to 9% of the average natural background. It should be mentioned that the exposure rate due to natural radioactivity can double due to radon daughter washout during heavy rain.

In the system described by Paatero [PAA94] the external gamma-radiation is measured with two 76 mm x 76 mm NaI(Tl) detectors. They are separated by a lead shield 25 mm thick situated

1.5 m above the ground. This counting geometry causes the lower detector to be more sensitive to gamma radiation from the ground and deposited gamma emitters, while the upper gamma detector is more sensitive to gamma radiation from air-suspended gamma emitters. Coincidence pulses are generated when muons produced by cosmic radiation travel through both detectors. The count rate of the coincidence is used as a criterion for proper operation of the instrument.

All pulses of NaI(Tl) detectors exceeding the lower level of discrimination are counted by the data logger in 10 minute intervals. The gamma analyser incorporates one programmable single-channel analyser (SCA) for each detector. These SCA measurements are made independently from the total gamma count rate measurements in photon energy ranges of important gamma nuclides (e.g. ^{131}I and ^{137}Cs). This counting arrangement allows comparisons between defined energy regions and total gamma count rate.

The detector arrangement allows the system to distinguish whether the increased gamma activity is air suspended or deposited on the ground. In the first case the increase in count rate of both detectors is about the same. In the latter the count rate of the lower detector increases two or three times more than the count rate of the upper detector.

In the case of deposited activity with an associated occurrence of precipitation, it is possible to deduce whether the increase of external gamma radiation is due to natural or artificial gamma emitters. If the gamma activity is due to ^{222}Rn progeny it should start decaying with a half-life of about 40 minutes as soon as the precipitation ceases. An increase of external radiation corresponding to 0.01 mSv h^{-1} caused by artificial radionuclides can therefore be distinguished from radon progeny. No such simple analysis can be made in the case of suspended activity.

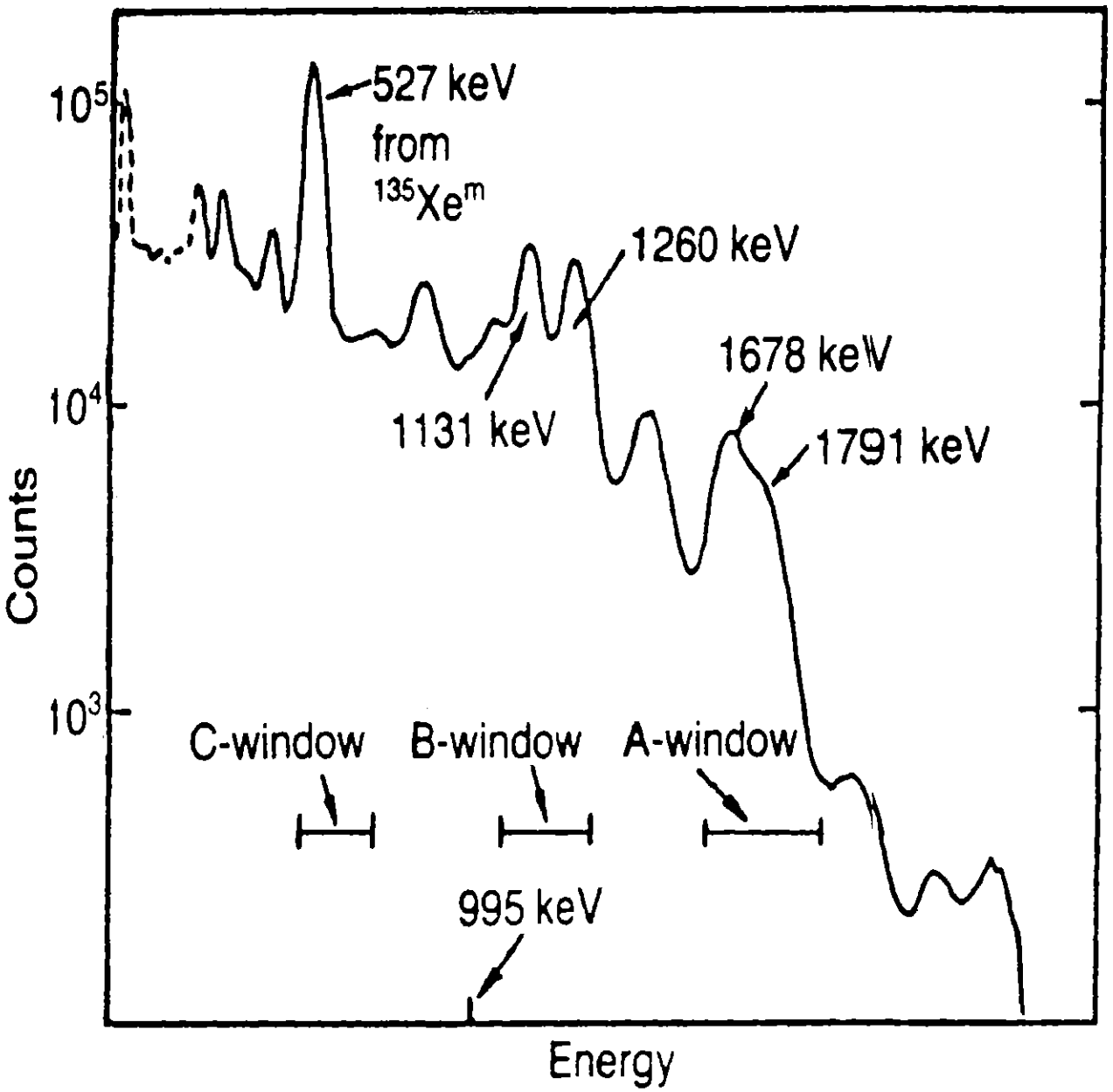

Figure 9.15: ^{135}I spectrum measured with a 76 mm x 76 mm NaI(Tl) crystal and the three 'Bismuth windows' (A-, B- and C- windows).

10. UNCERTAINTY ANALYSIS FOR ENVIRONMENTAL RADIATION MONITORING

10.1. General

In the past, the terms 'error' and 'uncertainty' were used interchangeably. The more modern approach is to distinguish between the two concepts as outlined by the CIPM where the concepts of true value and error no longer appear in the practical evaluation. Briefly, errors can be divided into two groups: random errors and systematic errors. An error is the difference between the measured value and the 'true' value. Therefore, it has both a numerical value and a sign. It can be seen that if the errors were known exactly, the true value could be determined and there would be no other problem. Unfortunately, this is not the case and one must estimate the errors in the best possible way and make corrections for them. Once these corrections have been made, however, errors need no further consideration.

Uncertainties can also be divided into two groups: type A uncertainties and type B uncertainties which have no direct relationship to the previously mentioned random and systematic errors. These uncertainties are defined in Section 10.2 and either type can be comprised of values that result from random error corrections or systematic error corrections. An uncertainty is a parameter that characterizes the dispersion of values that could reasonably be attributed to the measurand. This is normally an estimated standard deviation and as such carries no known sign and is usually assumed to be symmetrical. An uncertainty is the measure of the lack of exact knowledge after all recognized effects have been eliminated through applied corrections.

Development of the algorithm is the most crucial step in dosimetry. There should be corrections for all errors which contribute significantly to the reported value. Careful analysis of errors should be performed as some errors are automatically covered within the scatter of data and should not be accounted for in a separate correction. The extent to which errors should be included should be governed by the level of precision that one is trying to achieve.

Ideally, all uncertainties would be determined as independent type A uncertainties - through statistical analysis. Unfortunately, this is not always possible, but that aim should be kept in mind. Covariance among values is a topic which is beyond the scope of this document and it is recommended that a statistician be consulted for such cases.

The values reported for environmental radiation monitoring (air kerma, absorbed dose, etc.) are not measured directly, but are derived from measurements and calculations of other quantities. This can be expressed as $Y = f(X_1, X_2, X_3, ..X_n)$, where the X_i are parameters such as reader values, air kerma or dose conversion factors, fading corrections, etc. The estimated value of X_i, noted as x_i ,used for each input quantity i has an uncertainty, $u(x_i)$, that generates a corresponding uncertainty in the estimated value of Y, *noted as* y. The equation:
$u_i(y) \equiv |\delta y/\delta x_i| * \mu(x_i)$
is called a component of combined uncertainty of y. Since the result to be reported is an estimate based on these x_i values, that result is only complete when accompanied by an analysis of the uncertainty of that estimated value.

The goal is to evaluate each x_i and each $u_i(y)$, and then combine these $u_i(y)$ in a way to obtain the total uncertainty of y. According to the ISO Guide to the Expression of Uncertainty in Measurement, [ISO93],(further referred to as the ISO Guide), "it is imperative that the method for evaluating and expressing uncertainty be uniform throughout the world so that measurements performed in different countries can be easily compared". The reader is referred to that document for further discussion on this subject. Further advice on the treatment of uncertainties is given in a European document " Expression of Uncertainty of Measurement in Calibration", [EAL97].

10.2. Definitions

The terms and definitions below are reproduced directly from the ISO Guide, but are listed here for the benefit of those who are not in possession of that document.

uncertainty - doubt about the validity of the result of a measurement

standard uncertainty - uncertainty of the result of a measurement expressed as a standard deviation

type A evaluation of uncertainty - method of evaluation of uncertainty by statistical analysis of series of observations

type B evaluation of uncertainty - method of evaluation of uncertainty by means other than the statistical analysis of series of observations

combined standard uncertainty - standard uncertainty of the result of a measurement when that result is obtained from the values of a number of other quantities, equal to the positive square root of a sum of terms, the terms being the variances or covariances of these other quantities weighted according to how the measurement result varies with changes in these quantities

expanded uncertainty - quantity defining an interval about the result of a measurement that may be expected to encompass a large fraction of the distribution of values that could reasonable be attributed to the measurand

coverage factor - numerical factor used as a multiplier of the combined standard uncertainty in order to obtain an expanded uncertainty

10.3 Procedure for Uncertainty Analysis, Passive Detectors

To help the reader follow this procedure, a simple example has been prepared. It involves the use of environmental dosemeters comprised of 5 TLD chips placed in some type of packaging for use in the environment. Several assumptions have been made for this example for purposes of simplification: 1) field, calibration and storage dosemeters are all constructed in the same manner and from the same selection and anneal batch, the

field dosemeters being placed in additional packaging for placement in the environment; 2) the field, calibration and storage dosemeters remain together at all times except when the field dosemeters are stationed in the field and when the calibration dosemeters are irradiated; 3) the field, calibration and storage dosemeters are read out at the same time; and 4) all values in the algorithm are independent of each other.

10.3.1 Write out *y* as a function of the x_i and determine the contributory variances.

The algorithm to be used is:

$$y = [(x_1 * x_2) - x_3] * x_4 * x_5 \qquad (10\text{-}1)$$

where:

x_1 =	the field dosemeter reading	$c_1 = \frac{\delta y}{\delta x_1} = x_2 x_4 x_5$
x_2 =	packaging correction	$c_2 = \frac{\delta y}{\delta x_2} = x_1 x_4 x_5$
x_3 =	storage dosemeter reading	$c_3 = \frac{\delta y}{\delta x_3} = x_4 x_5$
x_4 =	dosemeter calibration factor	$c_4 = \frac{\delta y}{\delta x_4} = (x_1 x_2 - x_3) x_5$
x_5 =	fading factor	$c_5 = \frac{\delta y}{\delta x_5} = (x_1 x_2 - x_3) x_4$

Factors such as temperature dependence, angular dependence, etc. should be factored in if significant, but in this example are presumed negligible and represented within the scatter of data.

Note: This example is by no means meant to imply that this is the way to analyse environmental dosemeters. This is only one of many possible algorithms that may be used, and the authors express no endorsement of this one – it is only an example.

10.3.2 Evaluate the standard uncertainty $u(x_i)$

10.3.2.1 Uncertainty of the dosemeter response, $u(x_1)$

The experimental standard deviation characterizing the dosemeter response was determined from the responses of the five TLDs within the dosemeter. The mean of this example dosemeter is 9.1 nC with a percent standard deviation of 5.00 %.

10.3.2.2 Uncertainty of the packaging correction, $u(x_2)$

A test was conducted in which 40 dosemeters were irradiated to a given level. Half of these dosemeters were placed in the special environmental packaging for irradiation while the other half were irradiated in the standard calibration configuration. The means and standard deviations, s, of the two batches were calculated using standard techniques. The standard uncertainty was then calculated as:

$$u^2(x_2) = u^2\left(\frac{\overline{w}}{\overline{v}}\right) = u^2(\overline{w})\left(\frac{\delta x}{\delta w}\right)^2 + u^2(\overline{v})\left(\frac{\delta x}{\delta v}\right)^2$$

$$= u^2(\overline{w})\left(\frac{1}{\overline{v}}\right)^2 + u^2(\overline{v})\left(\frac{\overline{w}}{\overline{v}^2}\right)^2$$

or:
$$u(x_2) = \sqrt{\frac{s_w^2}{n_w}\frac{1}{\overline{v}^2} + \frac{\overline{w}^2}{\overline{v}^4}\frac{s_v^2}{n_v}} \qquad 10\text{-}2$$

The ratio for this example was 1.02 with an uncertainty of 0.35 %. An additional uncertainty of 0.50 % is added due to observations of some angular dependence of the packaging configuration. This has not been measured directly, but is based on the experience of the operator.

10.3.2.3 Uncertainty of the storage control response, $u(x_3)$

Determined by the same methods as 10.3.2.1 above, the mean response of the storage controls was 6.01 nC with a standard deviation of 7.52 %.

10.3.2.4 Uncertainty of the calibration factor, $u(x_4)$

The TLD response calibration factor is usually obtained from a report generated to transfer the calibration data. The uncertainty statement may look similar to that shown in Table 1. If exact knowledge of the calibration process is known, the components may be

listed on the environmental dosemeter uncertainty statement in both the Type A and Type B columns. When calibrations are performed by an outside service or group, the exact process is generally unknown to the final user and therefore the uncertainty associated with the calibration factor would be listed as a Type B. For this example, the same personnel responsible for the environmental measurements performed the calibration and the result was 2.92×10^{-5} Gy/nC ± 3.06 %. Note how the values transfer from Table 10.1 into Table 10.2.

Table 10.1: Summary of relative combined uncertainty components of the calibration factor. All values are listed as percent standard deviations.

Source of uncertainty	Type A	Type B
Exposure rate	0.15	0.72
Timing		0.10
Distance		0.10
Beam uniformity		0.20
Variance in dosemeter readings	3.00	
Quadratic summation	3.00	0.76
Relative combined standard uncertainty	3.06	

10.3.2.5 Uncertainty of the fading factor, $u(x_5)$

A set of dosemeters is irradiated at the beginning of a field deployment cycle. A second set (of equal size) is irradiated to the same level at the mid-point of the field cycle. All of the dosemeters are read out at the same time, shortly after the irradiation of the second set. The fade factor is the ratio between the means of the two sets of dosemeters and is 1.02 with a standard deviation of 0.25% determined by the method of 10.3.2.2. An additional factor of 1.00 % is added due to uncontrollable influences in the environment, such as heat, which would effect the field dosemeters, but not those used for the test.

10.3.3 The combined standard uncertainty

The combined standard uncertainty is calculated as:

$$u_c^2(y) = c_1^2 u^2(x_1) + c_2^2 u^2(x_2) + c_3^2 u^2(x_3) + c_4^2 u^2(x_4) + c_5^2 u^2(x_5) \qquad 10\text{-}3$$

The layout of the uncertainty analysis can be seen in Table 10.2. Please note that the uncertainties have been listed as a percentage at the 1σ level, or $u_i(y) = |c_i|u(x_i)$.

Table 10.2: Summary of standard uncertainty components for environmental dosemeter reading.

Source of uncertainty	Type A	Type B
Average of TLD readings	1.52×10^{-4}	
Packaging	9.49×10^{-5}	1.36×10^{-4}
Average of control readings	2.24×10^{-4}	
Calibration factor	10.02	2.54
Fading	2.39×10^{-5}	9.55×10^{-5}
Quadratic summation	10.02	2.54
Combined standard uncertainty	10.34	
Coverage factor, k	2.00	
Expanded standard uncertainty	20.68	

10.3.4 The expanded uncertainty

The additional measure of uncertainty that provides an interval about the measurement result that may be expected to encompass a large fraction of the distribution of values is termed *expanded uncertainty*. The expanded uncertainty is obtained by multiplying the combined standard uncertainty by a *coverage factor k*:

$$U = ku_c(y) \qquad 10\text{-}4$$

The result of the measurement is then conveniently expressed as $Y = y \pm U$. If the uncertainties were only of Type A, a coverage factor of 2 offers a level of confidence of 95% (be definition). When Type B uncertainties are involved, however, it only carries the significance of a 95% level of confidence. For this example, one would report the dosemeter result as 265.7 μGy ± 22.08 %.

10.4 Example Calibration of Active Detectors.

In this example the calibration factor of an air kerma rate meter is determined. The calibration is performed with a reference instrument and no monitor chamber is required.

a) Specification of the instrument (as stated in the manufacturer's manual).

- Measurement quantity: Air kerma rate in nGy h^{-1}.
- Detector: Geiger-Müller counter.
- Photon energy range: 30 keV to 1.3 MeV.
- Reference point: Cross point between GM counter axis and line mark
- Reference direction: Perpendicular to GM counter axis.
- Warm up time: 50 s.
- Measuring range: 10 nGy h^{-1} to 1 mGy h^{-1}.

b) Measurement conditions.

- Reference radiation ^{226}Ra source used in a shadow shield facility
- Distance from source to point of test: 3 m.
- Environmental conditions: 23^0C, 102 kPa.
- Reference instrument: LS10 Ionisation chamber, unsealed and calibrated at a primary laboratory with ^{226}Ra.
- Reference instrument ^{226}Ra calibration factor, $N_R = 0.971$ (from primary calibration certificate).
- reference instrument correction factor for 10 μGy h^{-1} range, $k_r = 0.992$ (from primary calibration certificate).
- reference instrument warm up time: 2 minutes.

c) Procedure for determining the conventional true value of the air kerma rate.

Place the reference ionisation chamber, with its appropriate build-up cap on, with its reference point at the point of test and in its reference orientation relative to the reference source. Switch the reference instrument on and wait at least 2 minutes for the instrument to

warm up. Perform the setting up procedures given in the manufacturer's manual, e.g. electrical zero test, battery and polarity tests. Switch the instrument to the 0-10 μGy h^{-1} measuring range. Expose the ^{226}Ra source and take ten readings, separated by sufficient time to be independent of each other and exceeding the time constant for the instrument.

Readings:- $R_{RI,bare.}$:-2.16, 2.13, 2.19, 2.20, 2.15, 2.23, 2.17, 2.20, 2.19, 2.21. μGy h^{-1}.
Mean value R_{RIbare} = 2.18 μGy h^{-1}, standard deviation of the mean=0.03 μGy h^{-1}

Cease the source exposure and place the LS10 shadow shield in its correct position between the source and the ionisation chamber. Expose the source and take ten independent readings.

Readings:- $R_{RIshield}$:-0.56, 0.58, 0.52, 0.59, 0.57, 0.52, 0.56, 0.53, 0.54, 0.56. μGy h^{-1}
Mean value $R_{RIshield}$ = 0.55 μGy h^{-1}, standard deviation of the mean=0.02 μGy h^{-1}

Cease the exposure of the source.

The conventional true value of the air kerma rate $\dot{K}$, is given by the following equation:-

$$\dot{K} = N_R \, k_r (R_{RIbare} - R_{RIshield}) k_{pr} \, k_T \qquad (10\text{-}5)$$

where :-k_{pr} is the correction from pressure test conditions to standard conditions for pressure

k_T is the correction from temperature test conditions to standard condition for temperature

$$\dot{K} = 0.971 \times 0.992 \, (2.18\text{-}0.55) \times 101.3/102 \times 296.15/293.15$$

$$\dot{K} = 1.58 \text{ μGy } h^{-1} = 1580 \text{ nGy } h^{-1}$$

d) Calibration of field instrument.

Remove the standard instrument's ionisation chamber and its shadow shield and replace the ionisation chamber with the GM counter. The GM counter should have its reference point at the point of test and be in its reference orientation. Switch the instrument on and wait at least 50 s for the instrument to warm up, then ensure that the battery test is satisfactory. Expose the reference ^{226}Ra source and take ten independent readings.

Readings:- M_{bare} :- 2070, 2058, 2088, 2073, 2048, 2052, 2073, 2080, 2075, 2035. nGy h^{-1}
Mean value M_{bare} = 2065 nGy h^{-1}, standard deviation of the mean = 16 nGy h^{-1}

Cease the exposure of the source and place the GM shadow shield in its correct position between the source and the GM counter. Expose the source and take ten independent readings.

Readings:- M_{shield} :- 480, 473, 498, 470, 452, 448, 467, 488, 481, 475. nGy h^{-1}
Mean value M_{shield} = 473 nGy h^{-1}, standard deviation of the mean = 15 nGy h^{-1}

Instrument reading due to direct radiation, $M_I = M_{bare} - M_{shield} = 2065\text{-}473 = 1592$ nGy h^{-1}

The instrument calibration factor $N_{INST} = \dot{K}/M_I = 1580/1592 = 0.992$.

10.5 Estimate of Uncertainty of Calibration of Active Detector.

The calibration factor for the field instrument is given by the equation :-

$$N_{INST} = N_R\, k_r \{(R_{RIbare} - R_{RIshield})/ (M_{bare} - M_{shield})\}\, k_{pr}\, k_T \qquad (10\text{-}6)$$

The relative combined uncertainty of the calibration factor, $S(N_{INST})/N_{INST}$ is given by :-

$$\{(u(N_R k_{pr})/N_R k_{pr})^2 + (s[R_{RIbare}-R_{RIshield}]/[R_{RIbare}-R_{RIshield}])^2 + (s[M_{bare}-M_{shield}]/[M_{bare}-M_{shield}])^2+(u(k_T)/k_T)^2 +(u(k_{pr})/k_{pr})^2\}^{1/2} \quad (10\text{-}7)$$

$u(N_R k_r)/N_R k_r = 1\%$ as given in the calibration certificate of the primary laboratory.

Type A uncertainty of $(R_{RIbare}-R_{RIshield})$ is calculated according to :-

$$s(R_{RIbare}-R_{RIshield})=\{s^2(r_{RIbare}) + s^2(R_{RIshield})\}^{1/2} = \{0.03^2 + 0.02^2\}^{1/2} \approx 0.036\ \mu Gy\ h^{-1}$$

Therefore:- $s = 0.036/1.63 = 0.022$.

Likewise the type A uncertainty of $M_{bare} - M_{shield} = \{s^2(M_{bare}) + s^2(M_{shield})\}^{1/2}$

$$=.\{16^2 + 15^2\}^{1/2} = 21.9\ nGy\ h^{-1}$$

Therefore:- $s = 21.9/1592 = 0.014$.

The air pressure p varied between 99 kPa and 105 kPa during the calibration, but was not measured separately for every indicated value. The extreme deviations from the mean pressure, ± 3 kPa, have been divided by the conventional factor to obtain $u(k_{pr})/k_{pr}$:

$$u(k_{pr})/k_{pr} = \{(3/2.5)/102\}\div 0.993 = 0.012$$

The air temperature varied between 295.2 K and 297.2 K during the calibration, and $u(k_t)/k_T$ was obtained by

$$u(k_T)/k_T = \{(1/2.5)/296.15\}\div 1.01 = 0.0013$$

The distance between the reference source and the reference points of the instruments was positioned at the nominal distance of 300 cm.. It is estimated that the distance was set within

0.5 mm with 2 cases out of 3. Therefore the error due to positioning = 0.5/3000 = 0.00017 and so errors due to the positioning of the instruments can be neglected.

The separate type A and B uncertainties are summarised in Table 10.3. In this example the degrees of freedom are the number of measurements minus one. The combined uncertainty, or standard deviation is 3.04%. An overall estimated uncertainty of 7.6% is then obtained by multiplying the overall combined uncertainty by a factor of 2.5 introduced for type B uncertainties: Table 10.3

Table 10.3: Summary of the type A and B uncertainties

Quantities	**Relative Standard Deviation in %**	**Type of uncertainty**	**Degrees of freedom**
$(R_{RIbare} - R_{RIshield})$	2.2	A	9
$(M_{bare} - M_{shield})$	1.4	A	9
$N_R k_r$	1.0	B	-
k_{pr}	1.2	B	-
k_T	0.001	B	-
N_{INST}	3.04		

The instrument calibration factor is therefore = 0.992 ± 0.03 (3.04%).

N.B. The same procedures have to be applied if other air kerma rates are used for the calibration.

10.6 Estimate of Uncertainty of Field Measurements with Passive and Active Detectors

The above calculation of the calibration factor and its uncertainty only applies to the calibration of the instrument and cannot be used to reflect the accuracy with which the instrument will perform measurements in the environmental field. This is very clearly demonstrated in Section 9.5.2 where. different instrument types, which had been extremely carefully calibrated many times at the same calibration facility and had then been subsequently intercompared, gave field measurements at the same location and time which differed by about 20%.

Uncertainties associated with field measurements have been discussed in the BCRU Guide, [GIB93]. The accuracy with which one can measure environmental gamma radiation with active and passive detectors depends on many factors.

Factors to be carefully considered in the uncertainty estimation include;

- Radiation field

  Natural terrestrial component (soil content)

  Artificial component (between soft sky shine and direct photons from a nuclear power station)

  Cosmic ray component (depending on altitude)

- Dosemeter type

  Energy and directional dependence for the whole measurement range

  Response to cosmic radiation

  Intrinsic background

  Environmental influence parameters on reading (temperature, humidity, pressure, shock etc.)

  Variation in response between individual detectors of the same type

- Calibration procedures in low dose range and methods of estimating correction factors

The highest uncertainty, which may exceed a factor of two, is expected in the worst case for just taking the uninterpreted reading of any dosemeter in an unknown radiation field. The uncertainty can be considerably reduced by applying reasonable correction factors

which reflect the knowledge of the operator about the radiation field being measured, the characteristics of the instrument used and the technique that was used to calibrate the dosemeter.

In Table 10.4, [GIB93], estimates are given of type B uncertainties for different active and passive detector types weighted for typical variations in the soil content of uranium, thorium and potassium

Table 10.4: Estimated component type B uncertainties for different types of detector

Source of uncertainty	**GM counter (%)**	**Ion chamber (%)**	**Scintillator (%)**	**TLD (%)**
Energy dependence	±2	±2	±2	±2
Calibration	±6	±6	±6	±6
Internal background	±0.6	±0.1	±10	±2
Cosmic ray contribution	±1	±2	±2	±2
Dead time correction	±4	----	----	----
Directional dependence	±2	±1	±1	±0.1
Total uncertainty(1)	±8	±7	±7	±7

(1) Individual components weighted for typical variations in soil content and then added in quadrature

Thus a total air kerma rate of 77 nGy h^{-1} could be determined to $\pm 7\%$, (± 5 nGy h^{-1}) if type A uncertainties are excluded. This is equivalent to ± 50 μGy per year on a total air kerma rate of 680 μGy per year.

The user of Table 10.4 should be aware that the values for energy and directional dependence as well as the cosmic ray contribution given in the table may be significantly higher for some radiation fields encountered, particularly if no field dependent correction factors are applied. To be able to properly compare measurements made with different types of detectors at the same location it is essential that a correct estimation of the uncertainty for each measurement be made.

11. CONCLUSIONS

This chapter summarises the main conclusions and proposes recommendations to encourage good practice and harmonisation of the measurement of external environmental gamma radiation doses.

The natural radiation comprises cosmic radiation from outer space and terrestrial radiation fom the rocks and soil. The photon energy spectrum is complex, with ^{40}K, ^{238}U and its daughter products and ^{232}Th and its daughter products all contributing to the terrestrial air kerma rate. Likewise the composition of the cosmic radiation is complex with about 25% of the air kerma rate being produced from soft radiation from electrons and photons, and the remaining 75% being produced from a hard component, mostly from mu mesons. The natural air kerma rate can also be significantly different from one location to another even when they are close to each other. The interpretation of measurements is made even more difficult since the kerma rate also varies with time at any fixed location and the magnitude of these variations can often exceed the kerma rate arising from a nuclear installation.

The air kerma rate range of natural gamma radiation is, however, relatively narrow. The lower limit can be as low as 10 nGy h^{-1}, the upper one for places with extremely elevated natural background being as high as 10 mGy h^{-1}. Some detectors used at early warning environmental monitoring systems are capable to measure the dose rates up to 1 to10 Gy h^{-1}. The last figure fits the emergency situation requirements as well.

The selection of measuring equipment and the choice of measurement site has to be very carefully assessed, taking into account the purpose of the measurement and their required accuracy. The characteristics and performance of passive and active detectors are discussed in Chapter 4. For on the spot measurements only active detectors can be used but for long term measurements either, or combinations of both, active and passive detectors may be utilised. Passive detectors will only provide an integration of the air kerma for the measurement period and if in addition short term variations of the air kerma rate over extended measurement periods are required then installed active detectors with repeated sampling and storage of data are necessary. For emergency applications many active detectors will have to be used in a net work with their data being transmitted to a central decision making facility.

To ensure that measurements can be accurately made it is necessary to have a prior knowledge of an instrument's or detector's photon energy response, its angular response to photons, its response to cosmic radiation and its inherent background. Without such information, and correcting the measurements for these responses, different designs of instruments will yield significantly different values for the air kerma rate at the same location and time. Advice on the determination and correcting for a detector's photon energy and angular response, its response to cosmic radiation and its inherent background are given in Chapter5. It is recommended that for instruments whose energy reponses vary by more than ± 25% over the range of photon energies to be measured, the energy spectrum of the radiation field should be determined and appropriate correction factors applied to the instruments readings. This is particularly important if the instrument is to be used within a kilometer of a nuclear facility producing 6 MeV radiation. If thereis asymmetry in the detector structure that affects its directional dependence, this should be investigated and a 2π or a 4π weighted calibration factor determined and applied to the measurement.

Proper calibration of equipment is essential, see Chapter6. Annual calibrations of equipment should be made using a reference source of ^{137}Cs or of ^{226}Ra.The shadow–shield calibration method gives more precise results than a free field calibration method, particularly at larger distances where the scatter contribution is more significant. However, uncollimated calibrations made at distances of less than 2 meters are equally as accurate as shadow-shield calibrations. Free-field calibrations, although less accurate, are particularly well suited for the calibration or intercomparison of large numbers of instruments at the same time. The annual calibration should be traceable to secondary or primary standards. In addition to annual calibrations spot check calibrations should be undertaken. It is unlikely that these calibrations will be traceable but the technique should ensure that the geometry of calibration ensures reproducible dose rates so that the stability of equipment remains adequately constant between its annual calibrations.

A quality control program should also be implemented in order to guarantee the correct and consistent measurement program and dose evaluation. As a very important part of a dosimetry systems, written procedures and formats should be implemented and reviewed periodically to assure the regular operation, solve the problems that have been found and to continuously improve the systems capabilities.

The Working Group strongly encourages participation in national and international intercomparisons. Recent international intercomparisons have been described in Chapter 8. Such intercomparisons provide unique opportunities for participants to check the adequacy of their home

calibrations and field measurements. To ensure that there would be harmonisation of measurements made by national network systems following a major nuclear accident the working group advises that such systems should be intercompared. This should help to ensure that results reported by different counties would be consistent and comparable. It is important that the overall results show no increments or decrements at national boundaries in the plume doses or contamination levels due to. inadequate calibration or different measurement quantities being used for different systems.

The techniques for using spectrometers to determine the radionuclide composition of the photon environment are given in Chapter 7.

Advice on the choice of a proper location for environmental dose measurement is given in Chapter 9. The location has the same importance as calibration of the measuring equipment. For mapping the most important requirement for location of measurement is that it should be representative for a given area. It means that the soil composition should be typical, the surface should be undisturbed and nearly horizontal with balance of precipitation water. The site with natural grass cover usually is optimal for measurements. Large trees or building disturb the measurement so their distance from the measuring point should be more than ten times their height. The standard height of measurements is mostly 1metre but it may be increased up to 2 metres if the surface is not homogeneous (e.g. mixture of stone and soil).

Choice of location of detectors for early warning purposes is more simple as it should be representative only for man-made radiation. The soil composition has importance but for compatibility of different sites the ground below the detector should be horizontal and preferably covered with short cut grass. The location of detectors on the roof of houses or above asphalt covered areas leads to erroneous results especially for doses due to deposition.

The mentioned requirements belong to the micro environment of measuring site. The location of different measuring points for control purposes can be chosen as: source centered, area centered or population centered.

REFERENCES

[AKS90] Akselrod, M.S., Kortov, V.S., Kravetsky, D.J., and Gotlib, V.I., 1990: "Highly Sensitive Thermoluminescent Anion-defect α-Al_2O_3:C Single Crystal Detectors". Radiat. Prot. Dos. 33, pp119-122 (1990).

[AMA92] Amaral, E.M., Alves, J.G., and Carreiro, J.V., 1992: "Doses to the Portuguese Population due to Natural Gamma Radiation". Radiat. Prot. Dosim. 45 (1-4), pp541-543 (1992).

[AND91] Andrási, A., Németh, I., Zombori, P., and Urbán, J., 1991: "Report on a Workshop on Mobile Laboratories for Monitoring Environmental Radiation". KFKI-1991-41/K (Budapest: Central Research Institute for Physics) 31 (1991).

[ARV90] Arvela, H., Markkanen, M., and Lemmelä, H., 1990: "Mobile Survey of Environmental Gamma Radiation and Fall-Out Levels in Finland after the Chernobyl Accident". Radiat. Prot. Dosim. 32, (3) pp177-184 (1990).

[ASH79] Ashton, T., and Spiers, F.W., 1979: "Attenuation Factors for Certain Tissues when the Body is Irradiated Unidirectional". Phys. Med. Biol. 24, pp950-953 (1979).

[BCRU89] British Committee on Radiation Units., 1989: "Quantities for Environmental Monitoring". Br. J. Radiol. 62, pp482-483 (1989).

[BEC72a] Beck, H.L. 1972: "The Physics of Environmental Radiation Fields. The Natural Radiation Environment, II". Edited by J.A.S. Adams et al., Washington, DC, US Energy Research and Development Administration, Report No. CONT-72085, Vol. 1, pp101-133 (1972).

[BEC72b] Beck, H.L., DeCampo, J., and Gogolak, C.V., 1972: "In-situ Ge(li) and NaI(Tl) Gamma-ray Spectrometry". US Atomic Energy Commission Health and Safety Laboratory, Report HASL-258, New York (1972).

[BER72] Berger, M.J., and Seltzer, S.M., 1972: "Response Functions for Sodium Iodide Scintillation Detectors". Nucl. Instr. and Meth. 104, pp317-332 (1972).

[BIL94] Bilski, P., Olko, P., Burgkhardt, B., Piesch, E., and Waligorski, M., 1994: "Thermoluminiscence Efficiency of LiF:Mg,Cu,P (MCP-N) Detectors to Photons, Beta Electrons, Alpha Particles and Thermal Neutrons". Radiat. Prot. Dos., 55, 1 (1994).

[BØT81] Bøtter-Jensen, L., and Nielsen, S.P., 1981; " A Nordic Intercomparison of Detector Systems for Background Radiation Monitoring". Risø Report M-2266 (1981).

[BØT82] Bøtter-Jensen, L., 1982: "Calibration and Standardization of Instruments for Background Radiation Monitoring", SRP, Third International Symposium, Radiation Protection Advances in Theory and Practice. Inverness (1982).

[BØT85] Bøtter-Jensen. L. and Nielsen, S.P., 1985: "A Multi-Laboratory Testing of Calibration Methods for Environmental Dose Rate Meters". Risø Report M-2542 (1985).

[BØT89] Bøtter-Jensen, L., Lauterbach, U., Pessara, W., and Thompson, I.M.G., 1989: "Multi-Laboratory Testing of Environmental Gamma Dose-Rate Meters". Proceedings of the 4th International Symposium, Radiation Protection Theory and Practice. Malvern, U.K. (1989).

[BØT92] Bøtter-Jensen, L., and Hedemann-Jensen, P.H., 1992: "Determination of Scattered Gamma Radiation in the Calibration of Environmental Dose Rate Meters". Radiat, Prot. Dosim., 42, 4, pp291-299 (1992).

[BØT95] Bøtter-Jensen, L., and Thompson, I.M.G., 1995: "An International Intercomparison of Passive Dosemeters and Dose Rate Meters used for Environmental Radiation Measurements". Radiat. Prot. Dosim. 60,3, pp201–211 (1995).

[BUD96] Budzanowski, M., Burgkhardt, B.; Olko, P.; Peßara, W.; Waligorski, M.P.R.,1996: "Long-Term Investigation on Self-irradiation and Sensitivity to Cosmic Rays of TL Detector Types TLD-200, TLD-700, MCP-N and New Phosphate Glass Dosemeters". Radiat. Prot. Dosim 66, pp135-138 (1996).

[BUR78] Burgkhardt,B.,and Piesch, E., 1978; "The Effect of Post-Irradiation annealing on the Fading Characteristics of Different Thermoluminescent Materials: PartI- Experimental Results". Nucl. Instr. Meth., 155, pp293-298, (1978). and PartII- Optimal Treatment and Recommendations". Nucl. Instr. Meth., 155, pp293-298, (1978).

[BUR84] Burgkhardt, B., and Piesch, E., 1984: "Fading Characteristics of LiF and $Li_2B_4O_7$ TLD Systems Dependent on the Ambient Temperature, the Monitoring Periods and the Interval between Irradiation and Readout". Radiat. Prot. Dosim., 6, pp.338-340 (1984).

[BUR96a] Burgkhardt, B., Festag, J.G., Piesch, E.,and Ugi, S., 1995: "New Aspects of Environmental Monitoring using Flat Phosphate Glass and Thermoluminescence Dosemeters". Proceedings in Radiation Protection Dosimetry, Solid State Dosimetry Conference, Radiat. Prot. Dosim., 66 pp187-192 (1996).

[BUR96b] Burgkhardt, B., Ugi, S., Vilgis, M., Piesch, E., 1995: "Experience with Phosphate Glass Dosemeters in Personal and Area Monitoring". Proceedings in Radiation Protection Dosimetry, Solid State Dosimetry Conference, Radiat. Prot. Dosim.,66, pp83-88 (1996).

[CAN97] Canberra Industries, Inc.., Edition Ten Product Catalogue, Meriden, CT, U.S.A. (1997).

[CEC89] Commission of the European Communities, (CEC.), 1989: "Intercomparison of Environmental Gamma Dose-Rate Meters, A Comprehensive Study of Calibration Methods and Field Measurements, Part 1, 1984 and 1985 Experiments". Report EUR 11665 EN, Radiation Protection-41 (Luxembourg: CEC) (1989).

[CEC90] Commission of the European Communities, (CEC.), 1990: "Intercomparison of Environmental Gamma Dose-Rate Meters, A Comprehensive Study of Calibration Methods and Field Measurements, Part 2, 1987 to 1989 Experiments",
Report EUR 12731 EN, Radiation Protection-48. (Luxembourg: CEC) (1990).

[CHI94] Chieco, N.A., Bogen, D.C., and Knutson, E.O., (Eds.), 1994: "EML Procedures Manual", Report No. HASL-300, 28th ed., Vol 1, Section 3; (New York, NY: US Department of Energy) (1994).

[CLA93] Clark, M.J., Burgess, P.H., and McClure, D.R., 1993: "Dose Quantities and Instrumentation for Measuring Environmental Gamma Radiation during Emergencies". Health Phys., 64, 5, pp491-501(1993).

[CLE72] Clements P.J.,1972: "A Discussion of Variations on the Scofield-Gold Iterative Deconvolution Technique". Materials Physics Division, U.K.A.E.A. Research Group, Atomic Energy Research (1972).

[DeC72] DeCampo, J., Beck, H., and Raft, P., 1972: "High Pressure Argon Ionization Chamber Systems for the Measurement of Environmental Radiation Exposure Rates". HASL-260 (New York, NY: US Atomic Energy Commission) (1972).

[DeC96] De Cort, M., and De Vries, G.,1996: " EURDEP Reference Manual and European Automatic Monitoring Systems". report EUR 16415EN, Joint Research Centre, Ispra, Italy (1996).

[DEL90] Delgado, A., and Gomez-Ros, J.M.. 1990: "A Simple Method for Glow Curve Analysis Improving TLD-100 Performance in the Dose Region below 100 μGy". Radiat. Prot. Dosim. 34 (1/4) pp357-360 (1990).

[DEL95] Delgado, A., Sáez-Vergara, J.C., Gómez Ros, J.M., and Romero, A., 1995: "Intrinsic Self-dosing and Long Term Stability of LiF TLD-100 and GR-200 TL Detectors". Radiat. Prot. Dosim. 58, pp211-215 (1995).

[DeP80] de Planque, G., Julius, H. W., and Verhoef, C. W., 1980: "Effects of Storage Intervals on the Sensitivity and Fading of LiF TLDs". Nucl. Instr. Meth. 175, pp177-179 (1980).

[DeP86] de Planque, G., and Gesell, T.F., 1986: "Environmental Measurements with Thermoluminescent Dosimeters - Trends and Issues". Radiat. Prot. Dosim. 17, pp193-200 (1986).

[DIN95] DIN Standard 25483, "Environmental Monitoring Using Integrating Solid-state Dosemeters". DIN, completely revised in 1995, to be published in 1996.

[DRA94] Drábová, D., Cešpírová, I., and Tranecek, R., 1994: "Measurement of Post Chernobyl Contamination in Mogilev Region, Byelorussia". Radiat. Prot. Dosim. 51(3) pp217-223 (1994).

[DRI88] Driscoll, C.M.H., 1998: " Report on the Results of the third Intercomparison Study of Thermoluminescenct Dosimeters for Environmental Measurements". Report EUR 11870EN, CEC Luxembourg (1998).

[EAL97} "Expression of the Uncertainty of Measurements in Calibration, European Co-operation for Accreditation of Laboratories". Publication EAL-R2, Edition 1, April, (1997).

[EGG97] EG&G Ortec Catalogue, "Modular Pulse-Processing Electronics and Semiconductor Radiation Detectors". EG&G Ortec, Oak Ridge, TN, U.S.A. (1997).

[EML92] Environmental Measurement Laboratory, 1992: "EML Procedures Manual". 27-th Edition, Volume 1, Environmental Measurements Laboratory, U.S. Dept. of Energy, New York, U.S.A. (1992).

[EML96] Environmental Measurement Laboratory, 1996: "1995 Annual Report", EML-580. Environmental Measurement Laboratory, U.S. Dept. of Energy, New York, U.S.A. (1996).

[FEH96] Fehrenbacher, G., Meckbach, R., Jacob, P., 1996: " Unfolding the Response of Ge Detector used for In-situ gamma Ray Spectometry". Nucl. Instr. and Meth.. A383, pp454-462 (1996).

[GIB93] Gibson, J.A.B., Thompson, I.M.G., and Spiers, F.W., 1993: BCRU. ".A Guide to the Measurement of Environmental Gamma radiation", British Committee on Radiation Units and Measurements, London. HMSO. (1993).

[GOL93] Goldfinch, E.P., McKeever, S.W.S., and Scharmann, A., 1993: "Proceedings of the 10th International Conference on Solid State Dosimetry", Radiat. Prot. Dosim. 47,1-4 (1993).

[GRA74] Grasty, R.L., and Charbonneau, B.W., 1974: "Gamma-ray Spectrometer Calibration Facilities". Geological Survey of Canada Paper 74-1B pp69-71 (1974).

[HEL88] Helfer, I.K., and Miller, K.M., 1988: "Calibration Factors for Ge Detectors used for Field Spectrometry". Health Phys. 55, pp15-29 (1988).

[HOR84] Horowitz, H.S., 1984 "Thermoluminescence and Thermoluminescent Dosimetry". CRC Press, Boca Raten (1984).

[HUF94] Huffert, A.M., Meck, R.A., and Miller, K.M., 1994: "Background as a Residual Radioactivity Criterion for Decommissioning", U.S. – DOE, Environmental Measurements Laboratory, Report NUREG-1501 (1994).

[HUL80] Hull, A. P., 1980: "A Critique of Source Term and Environmental Measurement at Three Mile Island", IEEE Transactions on Nuclear Science, Vol. NS-27, No.1, pp664-668 (1980).

[IAEA91] International Atomic Energy Agency, 1991: "Airborne Gamma Ray Spectrometer Surveying". Technical Report Series No.323, Vienna (1991).

[IAEA99] International Atomic Energy Agency, 1998: "Calibration of Radiation Protection Monitoring Instruments". Technical Report Series, to be published (1999).

[ICRP77] International Commission on Radiation Protection, Annals of the ICRP 1977: "Conversion Coefficients for use in Radiological Protection against External Radiation". ICRP Publication 74,Oxford: Pergamon Press (1977).

[ICRP87] International Commission on Radiation Protection, Annals of the ICRP 1987: "Data for Use in Protection against External Radiation". ICRP Publication 17, Oxford: Pergamon Press (1987).

[ICRU85] International Commission on Radiation Units and Measurements, 1985: "Determination of Dose Equivalents from External Radiation Sources". ICRU Report 39, Bethesda, MD: ICRU Publications (1985).

[ICRU92] International Commission on Radiation Units and Measurements, 1992: "Measurement of Dose Equivalent from ExternalPhoton andElecton Radiations". ICRU Report 47, Bethesda, MD: ICRU Publications (1992).

[ICRU94] International Commission on Radiation Units and Measurements, 1994: "Gamma-Ray Spectrometry in the Environment". ICRU Report 53, Bethesda, MD: ICRU Publications (1994).

[IEC91a] International Electrotechnical Commission, 1991: "Portable,Transportable or Installed X or Gamma Radiation Ratemeters for Environmental Monitoring, Part 1: Ratemeters.". IEC Standard 61017-1 (1991).

[IEC91b] International Electrotechnical Commission, 1991: "Thermoluminiscence Dosimetry Systems for Personal and Environmental Monitoring". IEC Standard 61066 (1991).

[IEC94] International Electrotechnical Commission, 1994: "Portable,Transportable or Installed Equipment to Measure X or Gamma Radiation for Environmental Monitoring, Part 2: Integrating Assemblies.". IEC Standard 61017-2 (1994).

[ISO93] International Standards Organisation, 1993: " Guide to the Expression of Uncertainty in Measurement". ISO (1993).

[ISO96] International Standards Organisation, 1996: "X and Gamma Reference Radiations for Calibrating Dosimeters and Doserate Meters and for Determining their Response as a Function of Photon Energy, Part 1, Characteristics of the Radiations and their Methods of Production". ISO 4037 Part 1 (1996).

[ISO97] International Standards Organisation, 1997: "X and Gamma Reference Radiations for Calibrating Dosimeters and Doserate Meters and for Determining their Response as a Function of Photon Energy, Part 2, Dosimetry of X and Gamma Reference for Radiation Protection over the Energy Range from 8KeV to 1.3MeV and from 4MeV to 9MeV". ISO 4037 Part 2 (1997).

[ISO99] International Standards Organisation, 1999: "X and Gamma Reference Radiations for Calibrating Dosimeters and Doserate Meters and for Determining their Response as a Function of Photon Energy, Part 3 Reference Photon Radiations for the Calibration of Area and Personal Dosemeters and for the Determination of their Response as a Function of Energy and Angle of Incidence". ISO 4037 Part 3 (1999).

[JAC90] Jacob, P., Meckbach, R., Müller, H.M., and Meimberg K., 1990: "Abnahme der Abgelagerten Kunstlichen Radioaktivitat in Stadtischer Umgebung". GSF-Bericht 17/90 (GSF Forschungszentrum fur Umwelt und Gesundheit, D-8042 Neuherberg, Germany) (1990).

[JAC93] Jackson, R. L., 1993: "RIMNET: The United Kingdom Government System for Response to Overseas Nuclear Accidents". Radiat. Prot. Dosim. 50(2-4) pp171-176 (1993).

[KAR90] Karlberg, O., 1990: "In-situ Gamma Spectrometry of the Chernobyl Fallout on Urban and Rural Surfaces". Studsvik Nuclear, Report NP-89/108, Sweden (1990).

[KLE99] Klemic, G., Shobe, J., Sengupta, S., Shebell, P., Miller, K., Carolan, P.T., Holeman, G., Kahnhauser, H., Lamperti, P., Soares, C., Azziz, N., and Moscovitch, M., 1999: " State of the Art of environmental Dosimetry: 11th International intercomparison and Proposed Performance Tests". To be published in Radiat. Prot. Dosim. Vol. 83-84 (1999).

[KLU90] Kluso, J., 1990: "Calculation of the Field Spectrometer Response and Calibration for the Operational and Accidental Monitoring of Nuclear Power Plant Neighbourhood" Progress in Nuclear Energy, 24, pp377-383 (1990).

[KNO79] Knoll, G.F., 1979: "Radiation Detection and Measurement". John Wiley & Sons, New York, U.S.A. (1979).

[KOL74] Kolb, W., and Lauterbach, U., 1974: "The Improved Scintillation Dosemeter PTB 7201". Radiation Protection and Environmental Protection: Proceedings of Eighth Annual Meeting of the Fachverband für Strahlenschutz, AED-CONF-74-715-000, 2, pp662-690 (1974)

[KOR94] Korsbech, U., and Nielsen, K. G., 1994: "A Simple Method for Early Detection of Fall-out". Radiat. Prot. Dosim. 40(2), pp103-109 (1994).

[KRA90] Kraus, W., Will, W., Buchröder, H., Edelmann, B., and Schwedt, J., 1990: "Use of Thermoluminescence Detectors in National Radiation Protection Monitoring Programmes". Radiat. Prot. Dosim. 34(1/4), pp353-356 (1990).

[KRE91] Krey, P. W.,and Freeswick, D. C., 1991: EML Regional Baseline Station at Chester, NJ -1987-90. EML Report 538 (1991).

[LAK90] Lakshmanan, A. R., Popli, K. L., and Kher, R. K., 1990: "Estimation of Ambient Dose Equivalent from Environmental Radiation using a $CaSO_4$:Dy Thermoluminescent Dosemeter". Radiat. Prot. Dosim. 32(2) pp127-130 (1990).

[LAU95] Lauterbach, U., and Pessara, W., 1995: " Investigation of Environmental Dosemeters in the Ultra Low Background Facility 'UDU'". Radiat. Prot. Dosim. 61 (1-3), pp71-72 (1995).

[LOV84] Lovborg, L., 1984: "The Calibration of Portable and Airborne Gamma-ray Spectrometers - Theory, Problems and Facilities". Rep. Risoe-M-2456 Calibration Blocks, GJBX-59(78), Bendix Field Engineering Corp., Grand Junction, CO. (1984).

[LOW66] Lowder, W.M., and Beck, H.L.,1966: "Cosmic-Ray Ionisation in the Lower Atmosphere". J. Geophys. Res. 71, pp4661-4668 (1966).

[Mac89] Macdonald, H.F., Thompson, I.M.G., Foster, P.M., and Robins, A.G., 1989: "Improved Estimates of Ar^{41} gamma Dose Rates Around Hinkley point Power Station, Proceedings of 4^{th} International Symposium, Radiation Protection Theory and Practice". Malvern, U.K. pp379-382 (1989).

[McC87] McClure, D.R., 1987: "Instrument Evaluation No. 33, Automess Szintomat 6134, Radiation Survey Meter". NRPB Report IE33, HMSO. Publications (1987).

[McK85] McKinlay, A.F., 1985: "An Intercomparison Study of Thermoluminescent Dosemeters for Environmental Measurements". Report EUR 10330EN, CEC, Luxembourg (1985).

[McK95] McKeever, S.W.S., Moscovitch, M., and Townsend, P.D., 1995: " Thermoluminescence Dosimetry Materials: properties and Uses". Nuclear Technology Publishing (1995).

[MIL84] Miller, K.M., 1984: "A Spectral Stripping Method for a Ge Spectrometer used for Indoor Gamma Exposure rate Measurements". USDOE Report EML-419, New York (1984).

[NCRP77] National Council on Radiation Protection and Measurements., 1977: "Environmental Radiation Measurements". NCRP Report ??,Bethesda, MD (1977).

[NUC80] Nuclear Enterprises., 1980: "Scintillators for the Physical Sciences". Brochure 126P,Nuclear Enterprises Ltd., Sighthill, Edinburgh, Scotland (1980).

[OBE81] Oberhofer, M., and Scharmann, A., 1981: " Applied Thermoluminescence Dosimetry". ISBN, 0-85274, 544-3, EUR 6990 EN (1981).

[OBR78] O'Brien, K., 1978: "The Response of LiF Thermoluminescence Dosemeters to the Ground-level Cosmic-ray Background". Appl. Rad. Isot. 29, pp735-739 (1978).

[OLK93] Olko, P., Bilski, P., Ryba, E., and Niewiadomski, T., 1993: "Microdosimetric Interpretation of the Anomalous Photon Energy Response of Ultra-Sensitive LiF:Mg,Cu,P TL Dosemeters". Radiat. Prot. Dosim. 47, pp31-35 (1993).

[OLK94] Olko, P., Bilski, P., and Michalik, V., 1994: "Microdosimetric Analysis of the Response of LiF Thermoluminescent Detectors to Radiations of Different Qualities". Radiat. Prot. Dosim. 52, pp405-408 (1994).

[ORT91] Ortega, X., Rosell, J. R., and Dies, X., 1991: "Validation of a Model for Calculating Environmental Doses Caused by Gamma Emitters in the Soil". Radiat. Prot. Dosim. 35(3), pp187-192 (1991)

[PAA94] Paatero, J., Hatakka, J., Mattson, R., and Lehtinen, I. *A., 1994:"* Comprehensive Station for Monitoring Atmospheric Radioactivity. Radiat. Prot. Dosim.,54,1, pp33-40 (1994).

[PER96] Pernicka, F., and Kluson, J., 1996: "Variations of Natural Radiation Background and their Effect on Detector Responses". Environmental International 22 (Suppl. 1), S 85-91 (1996).

[PET96] Peto, A., and Uchrin, Gy., 1996: " Proceedings of the 11th International Conference on Solid State Dosimetry". Radiat. Prot. Dosim.,65-66 (1996)

[PIE83] Piesch, E., and Burgkhardt, B., 1983: "A Review of Environmental Monitoring using Solid State Dosemeters and Guidelines for Technical Procedures". Radiat. Prot. Dosim., 5,(2), pp79-94 (1983).

[PIE84] Piesch, E., and Burgkhardt, B., 1984: "Environmental Monitoring - European Interlaboratory Test Programme for Integrating Dosemeter System". Report EUR-8932-EN (1984).

[PIT90] Piters, T.M., and Bos, J.J., 1990: "Influence of the Cooling Rate on Repeatability of LiF:Mg,Cu,P thermoluminescence Chips". Radiat. Prot. Dosim. 33, pp91-94 (19900.

[QUI92] Quindos, L. S., Fernandez, P. L., Rodenas, C., and Soto, J., 1992: "Estimate of External Gamma Exposure Outdoors in Spain", Radiat. Prot. Dosim. 45 (1-4), pp527-529 (1992).

[RAD87] Radford, D.C., Ahmad, I., Holzmann, R., Janssens, R.V.F., and Khoo, T.L., 1987: "A Prescription for the Removal of Compton-Scattered Gamma Ray Spectra.". Nucl. Instru. Meth. Phys. Res., A258, 111 (1987).

[REG96] Reginatto, M., Shebell, P., and Miller, K. M., 1996: "Application of the Maximum Entropy Method for Assessments of Residual Radioactivity at Contaminated Sites", In: Proceedings of the IEEE Nuclear Science Symposium (1996).

[RYB92] Rybáèek, K., Jacob, P., and Meckbach, R., 1992: "In Situ Determination of Deposited Radionuclide Activities: Improved Method Using Derived Depth Distributions from the Measured Photon Spectra". Health Phys. 62, Nos. 6, pp519-528. (1992).

[SAE96a] Sáez-Vergara, J.C., and Romero A.M.,1996: "The Influence of the Heating System on the Hypersensitive Thermoluminescence Material LiF:Mg,Cu,P. (GR-200)". Proceedings in Radiation Protection Dosimetry, Solid State Dosimetry Conference, Radiat. Prot. Dosim. 66,pp431-436 (1996).

[SAE96b] Sáez-Vergara, J.C., Romero, A.M., Olko, P., and Budzanowski, M., 1996: "The Response of the New Hypersensitive Thermoluminescence Material to High Energy Photons (0.6 - 6 MeV)". Proceedings in Radiation Protection Dosimetry, Solid State Dosimetry Conference, Radiat. Prot. Dosim. 65, pp167-172 (1996).

[SAI91] Saito, K., 1991: "External Doses Due to Terrestrial Gamma Rays on the Snow Cover". Radiat. Prot. Dosim. 35(1) pp31-39 (1991).

[SAI95] Saito, K., and Jacob, P., 1995: " Gamma Ray Fields in the Air due to Sources in the Ground". Radiat. Prot. Dosim. 58, pp29-45 (1995).

[SCO63] Scofield N.E., 1963: NAS - NS - 3107,108 (1963).

[SHA63] Shambon, A.W., Lowder, W.M., and Condon, W.J., 1963: "Ionisation Chambers for Environmental Radiation Measurements2", New York, US Atomic Energy Commission Health & Safety Laboratory, Report No. HASL-108, New York (1963).

[SHE96] Shebell, P., and Miller, K.M., 1996: "Analysis of Eighteen Years of Environmental Monitoring Data"" Environmental International, 22, (Suppl. 1), pp575-583 (1996).

[SIE52] Sievert, R.M., and Hultquist, B., 1952: "Variations in the Natural Gamma Radiation Background in Sweden",.Acta. Radiol., 37, pp388-398 (1952).

[SME94] Smetsers, R. C. G. M., and van Lunenburg, A. P. P. A., 1994: "Evaluation of the Dutch Radioactivity Monitoring Network for Nuclear Emergencies over Period 1990-1993". Radiat. Prot. Dosim. 55(3), pp165-172 (1994).

[SON97] State Office for Nuclear Safety, 1997: "Annual Report 1997". Prague (1997).

[SOW89] Sowa, W., Martini, E., Gehrcke, K., Marschner, P., and Naziry, M.J., 1989: "Uncertainties of In Situ Gamma Spectrometry for Environmental Monitoring". Radiat. Prot. Dosim. 27, pp93-101 (1989).

[SOW90] Sowa, W., 1990: "Direct Measurement of Homogeneously Distributed Air Contamination with Germanium Detector". Radiat. Prot. Dosim.,. 32(3), pp171-176 (1990).

[SPU73] Spurny, Z., Kovar,Z., Koci, J. and Sulcova, J., 1973: "Analysis of Mean Exposure to Population in CSR from Environmental Radiation", (in Russian). Kernenergie 18,pp 260-262 (1973)

[SPU77] Spurny, Z., Kovar, Z. and Minarik, F., 1977: "Dose to Population of SSR from Environmental Radiation", (in Czech). Nuclear Energy 23,pp98-100 (1977).

[SZA86] Szabó, P. P., Fehér, I., Deme, S., Szabó, B., and Vágvölgyi, J., 1986: "Dosimetric Properties of the 'Pille' Portable, Wide Dose Range TLD Reader2. Radiat. Prot. Dosim. 17(1-4), pp279-281 (1986).

[SZA90] Szabó, P. P., Fehér, I., and Germán, E., 1990: "Environmental Monitoring Around Nuclear Installations Using TL Dosemeters2. Radiat. Prot. Dosim. 34(1/4) pp191-194 (1990).

[THO93] Thompson, I. M .G., Bøtter-Jensen, L., Lauterbach, V., Peßara, W., Saez-Vergara, J. C., and Delgado, A. 1993: "The Assessment of External Photon Dose Rate in the Vicinity of Nuclear Power Stations: an Intercomparison of Different Monitoring Systems". Radiat. Prot. Dosim. 48, (4) pp.325-332 (1993).

[TRA91] TranspackII GPS Personal Navigator with I/O. Technical Description. Trimble Navigation, Sunnyvale, California (1991).

[UNSC77] United Nations Scientific Committee., 1977: "Sources and Effects of Ionizing Radiation". Report of the United Nations Scientific Committee on the Effects of Atomic Radiation, General Assembly 32nd Session, Supplement 40 (A/32/40), New York, United Nations (1977).

[UNSC82] United Nations Scientific Committee on the Effects of Atomic Radiation. 1982: "Sources, Effects and Risks of Ionising Radiation", UNSCEAR 1982. Report to the UN General Assembly with Scientific Annexes, United Nations, New York (1982).

[UNSC88] United Nations Scientific Committee on the Effects of Atomic Radiation. 1988: "Sources, Effects and Risks of Ionising Radiation", UNSCEAR 1988. Report to the UN General Assembly with Scientific Annexes, United Nations, New York (1988).

[VAN93] Van Steveninck, W., 1993: "A Pressurized Ion Chamber Monitoring System for Environmental Radiation Measurements Utilizing a Wide-Range Temperature-Compensated Electrometer". IEEE Nuc. Sci. Symp. Proced. (1993) in press.

[WAL88] Walmod-Larsen, O., and Ryder, H. P., 1988; "Denmark's Planned Nationwide Warning System for Fallout from Nuclear Accidents". Nucl. Eur., 3-4, 27 (1988).

[WOO83] Woods, M.J., Callow, W.J., and Christmas, P., 1983: " The NPL Radionuclide Calibrator Type 271 ". J. Nucl. Med. Biol., 10, pp127-132 (1983).

[ZHA93] Zha, Z., Wang, S., Shen, W., Zhu, J., and Cai, G., 1993: "Preparation and Characteristics of LiF:Mg,Cu,P Thermoluminescent Material". Radiat. Prot. Dosim. 47, pp111-118 (1993).

[ZOM92] Zombori, P., Andrási, A., and Németh, I., 1992: "A New Method for the Determination of Radionuclide Distribution in the Soil by In Situ Gamma-ray Spectrometry". KFKI-1992-20/K (Science, Central Academy of Hungarian Research Institute for Physics, Budapest) (1992).

[ZOM94] Zombori, P., Personal communication (1994).

European Commission

Radiation protection 106 — Technical recommendations on measurement of external environmental gama radiation doses

Edited by I.M.G. Thompson, L. Bøtter-Jensen, S. Deme, F. Pernick and J.C. Sáez-Vergara

Luxembourg: Office for Official Publications of the European Communities

1999 — VIII, 191 pp. — 21 x 29.7 cm

ISBN 92-828-7811-2

Price (excluding VAT) in Luxembourg: EUR 29.50

These recommendations provide guidance and information on the measurement of the air krema rate in the environment arising from photo radiation both from natural sources and from man made sources. During the past decade there has been significant interest in the levels of radiation to which the general public is exposed.
The purpose of this Technical Report is to disseminate considerable experience and expertise and to give practical advice on all aspects of environmental photon dose monitoring. The report starts by describing the nature and variability of environmental gamma radiation within Europe and then discusses the quantities that should be used for measurements. The characteristics and performance of both passive and active detectors as well as spectrometry systems are discussed. Type testing and calibration methods are recommended which will enable the response of the monitoring equipment to the different radiation components to be properly determined. Techniques for assessing the uncertainties associated with both calibration and measurement are described. Examples are given of the early warning systems installed within the European countries.